Epstein-Barr virus and multiple sclerosis:

investigating EBV antigen-induced

T-cell cross-recognition of central nervous system proteins

Olivia Grace Thomas

A thesis submitted to the University of Birmingham for the degree of

DOCTOR OF PHILOSOPHY

Institute of Cancer and Genomic Sciences

College of Medical and Dental Sciences

University of Birmingham

July 2017

Abstract

Multiple sclerosis (MS) is a debilitating disease in which the immune system aberrantly targets the central nervous system (CNS). There is compelling evidence that Epstein-Barr virus (EBV) is associated with MS development but the pathogenic mechanisms are unknown. The molecular mimicry hypothesis suggests the immune response to EBV, which normally would restrain the virus infection, mistakenly targets CNS components. This thesis characterised humoural and cellular responses to the virus in healthy controls (HC) and MS patients, increasing the range of EBV and CNS proteins investigated and seeking evidence of cross-reactivity as predicted by the hypothesis.

Compared to HC, patients had elevated EBNA1 and virus capsid antigen-specific antibody responses. EBNA3-specific antibody responses were also more frequently detected in patients, a previously undescribed observation. Both groups had similar frequencies of circulating T-cells specific for autologous lymphoblastoid cell lines (LCL) or EBNA1, although minor differences in cytokine profile were detected.

LCL-specific T-cell cultures established from both patients and HC exhibited cross-reactivity to CNS antigens. This result supports a role for molecular mimicry but also suggests that other unknown or more complex factors must influence MS development. While such T-cells are a necessary prerequisite for the molecular mimicry hypothesis, their presence in HC suggests other factors must influence MS development. Identification of these factors must be a priority for future studies.

Dedication

For my Nan,

Acknowledgements

First and foremost, I would like to thank my supervisors Jill and Graham, your guidance over the years has been invaluable and I could not have achieved this without you. Jill, thank you for giving the opportunity to carry out this PhD – I have thoroughly enjoyed working with you and thank you for your help every step of the way. Graham, your optimism got me through many months of worrying about failed experiments and disappointing data, one meeting with you would always set me back on track with fresh ideas and put everything back into perspective. Thank you both.

I would also like to thank Tracey for always being there to answer my endless questions and for first teaching me in the lab when I was a fresh-faced student, working with you has been a pleasure and I will miss you. Alison, thank you for all of your help over the years, Cancer Sciences has not been the same since you left! Thank you also to Heather who gave me my first taste of lab work way back when I was at school, without you I would not have been inspired to pursue a career in research.

Thank you so much to all members of the T-cell group (past and present) and to all of my friends in Cancer Sciences, I have thoroughly enjoyed working with you and you have made my time in Birmingham a wonderful one.

Thank you to the Multiple Sclerosis Society who funded this work and also to the University of Birmingham for supporting me these past 4 years.

Finally, and most importantly, I would like to thank my incredible parents and sisters for everything. This year has been so hard for all of us and I would not have got through it without your constant support and encouragement. Thank you.

Contents

List of Figures

List of tables

Abbreviations

APC – antigen presenting cell

ATCC – American Type Culture Collection

β2m – β2 microglobulin

BBB – blood-brain barrier

BCR – B-cell receptor

BHK21 – baby hamster kidney fibroblast 21

BMI – body mass index

BZLF1 - BamHI Z Epstein-Barr virus replication activator

CCR7 – C-C motif chemokine receptor 7

CD – cluster of differentiation

CD40L – cluster of differentiation 40 ligand

CEF – chicken embryo fibroblast

CIS – clinically isolated syndrome

CLP – common lymphoid progenitor

CMP – common myeloid progenitor

CMV – cytomegalovirus

CNP – 2',3'-Cyclic-nucleotide 3'-phosphodiesterase

CNS – central nervous system

CPE – cytopathic effect

CRYAB - αB-crystallin

CSF – cerebrospinal fluid

DAMP – damage-associated molecular pattern

DC – dendritic cell

DNA – deoxyribonucleic acid

EAE – experimental autoimmune encephalomyelitis

EBER – Epstein-Barr virus-encoded small RNA

EBNA – Epstein-Barr nuclear antigen

EBNAc – Epstein-Barr nuclear antigen complex

EBNA-LP – Epstein-Barr nuclear antigen leader protein

EBV – Epstein-Barr virus

ELISA – enzyme-linked immunosorbent assay

FACS – fluorescence-activated cell sorting

FoxP3 – forkhead box protein 3

GM-CSF – granulocyte-macrophage colony stimulating factor

GWAS – genome wide association studies

GzmB – granzyme B

HEV – high endothelial venule

HHV-6 – human herpesvirus 6

HINGS – heat-inactivated normal goat serum

HLA – human leukocyte antigen

HNRNPL – human heterogeneous ribonucleoprotein L

HSC – haematopoietic stem cell

HSCT – haematopoietic stem cell transplant

ICS – intracellular cytokine staining

Ig – immunoglobulin

IF - immunofluorescence

IFNβ – interferon-β

IFNγ - interferon-γ

IL-2 – interleukin-2

IL-17 – interleukin-17

IM – infectious mononucleosis

KO – knock out

LCL – lymphoblastoid cell line

MAG – Myelin associated glycoprotein

MAIT-cells – mucosal-associated invariant T-cells

MBP – myelin basic protein (variant 1)

MBP V8 – myelin basic protein variant 8

MHC – major histocompatibility complex

miRNA - microRNA

MLA – monkey leukocyte antigen

MOBP – myelin oligodendrocyte basic protein

MOG – myelin oligodendrocyte glycoprotein

MOI – multiplicity of infection

MPP – multipotent progenitor

MRI – magnetic resonance imaging

MS – multiple sclerosis

MVA – modified Vaccinia Ankara

NK cell – natural killer cell

OCB – oligoclonal bands

PAD2 – peptidylarginine deiminase 2

PAMP – pathogen-associated molecular pattern

pDC – peripheral dendritic cell

PI – polyfunctionality index

PLP – proteolipid protein

PML – progressive multifocal leukoencephalopathy

PPMS – primary progressive multiple sclerosis

PRR – pattern recognition receptor

RA – rheumatoid arthritis

RNA – ribonucleic acid

RRMS – relapsing-remitting multiple sclerosis

RT – room temperature

SEB – Staphylococcal enterotoxin B

SLE – systemic lupus erythematosus

SNP – single nucleotide polymorphism

SPMS – secondary progressive multiple sclerosis

STAT3 – signal transducer and activator of transcription 3

TACE - TNFα-converting enzyme

TAL-H – transaldolase-H

TAPI-0 - TNFα processing inhibitor-0

TCR – T-cell receptor

T_{FH} – follicular helper T-cell

TNFα - tumour necrosis factor α

T_{reg} – regulatory T-cell

VCA – viral capsid antigen

1 Introduction

The immune system is a highly specialised and dynamic system of cells, tissues and organs which work together to protect against disease. It is critical in defending against pathogens and cancerous cells, however these mechanisms are not perfect and when dysregulated can damage tissues and cause disease. This system can be roughly divided into two main arms: the innate and the adaptive immune responses.

1.1 Innate immunity

The ability to guard against pathogenic invasion is a highly-conserved trait which can be traced back to the evolution of multicellular organisms, and it has evolved to protect hosts against a multitude of infections such as viruses, bacteria, fungi and helminths. The innate immune system is the oldest in evolutionary terms and forms the first line of defence against invading pathogens. Innate immune mechanisms form a somewhat non-specific protection and consist of a network of barriers and cells generally considered to have no element of memory, forming a rapid and non-specific responses against infection through a variety of mechanisms.

The innate immune defence comprises three barriers to infection: physical barriers such as the skin, an impenetrable layer of keratinised cells which acts to prevent pathogen entry (Friedman, 2006), epithelial surfaces which form a resilient barrier due to tight junctions connecting the cells (Citi and Cordenonsi, 1998), and internal epithelia sustain a flow of mucus over their surfaces via cilia or peristalsis which physically removes pathogens and debris from the body (Sheehan et al., 2006). Epithelial membranes also produce a wide variety of antimicrobial chemicals that protect from invasion, for example the upper gastrointestinal tract produces

hydrochloric acid as well as digestive enzymes, lysolipids and many other components which protect the body from ingested pathogens (Dann and Eckmann, 2007).

The second barrier comprises complement proteins, a family of large, soluble molecules in the plasma that coat bacteria and other foreign particles in a process called opsonisation, enabling them to be taken up by phagocytic cells (Sarma and Ward, 2011).

The third barrier is formed by a range of innate immune cells. These are produced in the bone marrow from pluripotent haematopoietic stem cells (HSCs), first differentiating into common myeloid progenitors (CMPs) which can then either differentiate into granulocytes (eosinophils, basophils, neutrophils and mast cells) or monocytes (dendritic cells and macrophages) (Cowland and Borregaard, 2016).

Innate immune cells primarily act by recognising molecules that do not naturally occur under normal physiological conditions in the host organism. These can be derived from infectious agents, termed pathogen-associated molecular patterns (PAMPs), or molecules which are normally “hidden” from immune cells and are only accessible upon tissue damage, termed damage-associated molecular patterns (DAMPs). Recognition of PAMPs and DAMPs by innate immune cells is achieved via pathogen recognition receptors (PRRs) on their surface. Once PRRs are activated, a cascade is triggered in the cell which both induces production of inflammatory mediators and attracts other immune cells to the area (Thompson et al., 2011).

Dendritic cells of the innate immune system perform a critical role, alerting and directing adaptive immune responses to incoming pathogens.

1.2 Adaptive immunity

In addition to innate immunity, vertebrates have also evolved an adaptive immune system to provide a more sophisticated level of defence (Hirano et al., 2011). Adaptive immune mechanisms establish immunological memory upon first exposure to an antigen, resulting in an enhanced response to pathogens upon subsequent exposures. Evolution of adaptive immune cells to randomly recombine their pathogen receptor gene segments and produce a diverse receptor repertoire enables their recognition of an almost infinite number of epitopes (Laydon et al., 2015). However, this vast repertoire, whilst invaluable in guarding against pathogens, can also generate responses with reactivity to self-tissues, and as such systems to prevent autoreactivity have evolved alongside these defences.

The ability to maintain a population of antigen-specific cells which can expand rapidly upon subsequent exposure to antigen is fundamental to forming a memory response, and enables protection from re-infection with previously encountered pathogens. Adaptive immunity in vertebrates can be broadly subdivided into two main categories: cellular which is predominantly arbitrated by T-cells, and humoural which is mostly mediated by antibodies produced by B-cells.

1.2.1 Overview of B-cell biology

T- and B-cells were first identified in the 1960s by Good, Peterson and Cooper when observations from chickens following removal of either the thymus or bursa of fabricus – the site of haematopoiesis in birds – caused animals to develop two very different forms of immune deficiency (Gitlin and Nussenzweig, 2015, Cooper et al., 1965). These observations were then

applied to immune insufficiencies in humans and eventually led to the discovery of the bone marrow as the site of human haematopoiesis 10 years later (Gitlin and Nussenzweig, 2015).

Bone marrow resident haematopoietic stem cells (HSCs) first divide to give multipotent progenitors (MPP) which then go on to produce common lymphoid progenitors (CLP) which are the precursors to all lymphoid lineages, including immature B-cells.

Naïve B-cells undergo somatic recombination of their immunoglobulin (Ig) genes in the bone marrow, generating receptor diversity and giving each cell a different antigen specificity. It is here that B-cells undergo rounds of selection to prevent autoreactive B-cells from leaving the bone marrow (Shlomchik, 2008). Maturation and proliferation of B-cells is dependent on the nature of the antigenic challenge, and can have direct downstream implications for the type of response generated. Immature B-cells migrate to the spleen and lymph nodes where, if they encounter their cognate antigen, they mature to become short-lived plasma cells and produce pentameric IgM antibodies with moderate affinity for their ligand (Melchers et al., 2000, Fagarasan and Honjo, 2000).

B-cells can become activated in two main ways. The first is by antigen alone in a thymus-independent manner; these antigens tend to be larger, often containing repeated structures in their surface which cross-link B-cell receptors (BCRs) on the B-cell surface, inducing activation and low affinity antibody production (Mond et al., 1995).

Most antigens, however, require CD4+ T-cell help to induce an antibody response with high affinity. In this process BCRs first bind antigen and are internalised, delivering the foreign antigen to lysosomes where it is processed and re-expressed on the cell surface bound to major histocompatibility complex (MHC) class II molecules. TCRs on the CD4+ T-cell surface recognise specific peptides presented by MHC Class II molecules alongside co-stimulatory interactions. TCR engagement causes cytokine production in the T-cell and sends strong signals to the B-cell inducing activation and proliferation. BCR and co-receptor ligation

strongly amplifies the antibody response to antigen and is essential for creating both memory B-cell and long-lived plasma cell repertoires (Radbruch et al., 2006).

Following activation, B-cells migrate to germinal centres in lymph nodes where they undergo a number of important changes through germinal centre reactions. Somatic hypermutation in the variable (V) regions of immunoglobulin genes introduces single point mutations in specific areas and leads to a process called affinity maturation. This process can change the receptor's affinity for its antigen, and B-cells bearing receptors with an increased affinity for their cognate antigen survive, mutated B-cells with decreased affinity receptors die by neglect (Eisen, 2014). These selected, high affinity B-cells then undergo class switching of their immunoglobulin heavy chains before differentiating into either memory B-cells or into long-lived plasma cells. Memory B-cells reside in the periphery and can rapidly divide and differentiate into plasma cells upon re-exposure to antigen. Plasma cells produce large quantities of higher affinity antibodies, and these are capable of three main functions: opsonising bacterial or viral components to facilitate phagocytic uptake, neutralising soluble antigen and activation of the classical complement pathway (Forthal, 2014).

1.2.2 T-cell receptor generation and structure

Interminable variation in pathogens and their constant evolution provides an immense challenge for the immune system, which must be able to respond to every theoretical or real antigen it may encounter. Using a finite genome, T-cells have met this need by evolving a repertoire with an almost infinite number of specificities produced from one section of the genome termed the T-cell receptor gene locus. The locus is made up from a large number of contiguous segments of three types, named the variable (V), joining (J) and diversity (D) regions which are joined together in random genetic recombination events to form a T-cell

receptor (TCR) (Figure 1.2.1). These recombination events are similar to those used for rearrangement of immunoglobulin genes in B cells, and are directed by DNA recombinase and flanking regions upstream of the TCR locus leading to the insertion of non-germline nucleotides between segments to create greater diversity (Gellert, 2002).

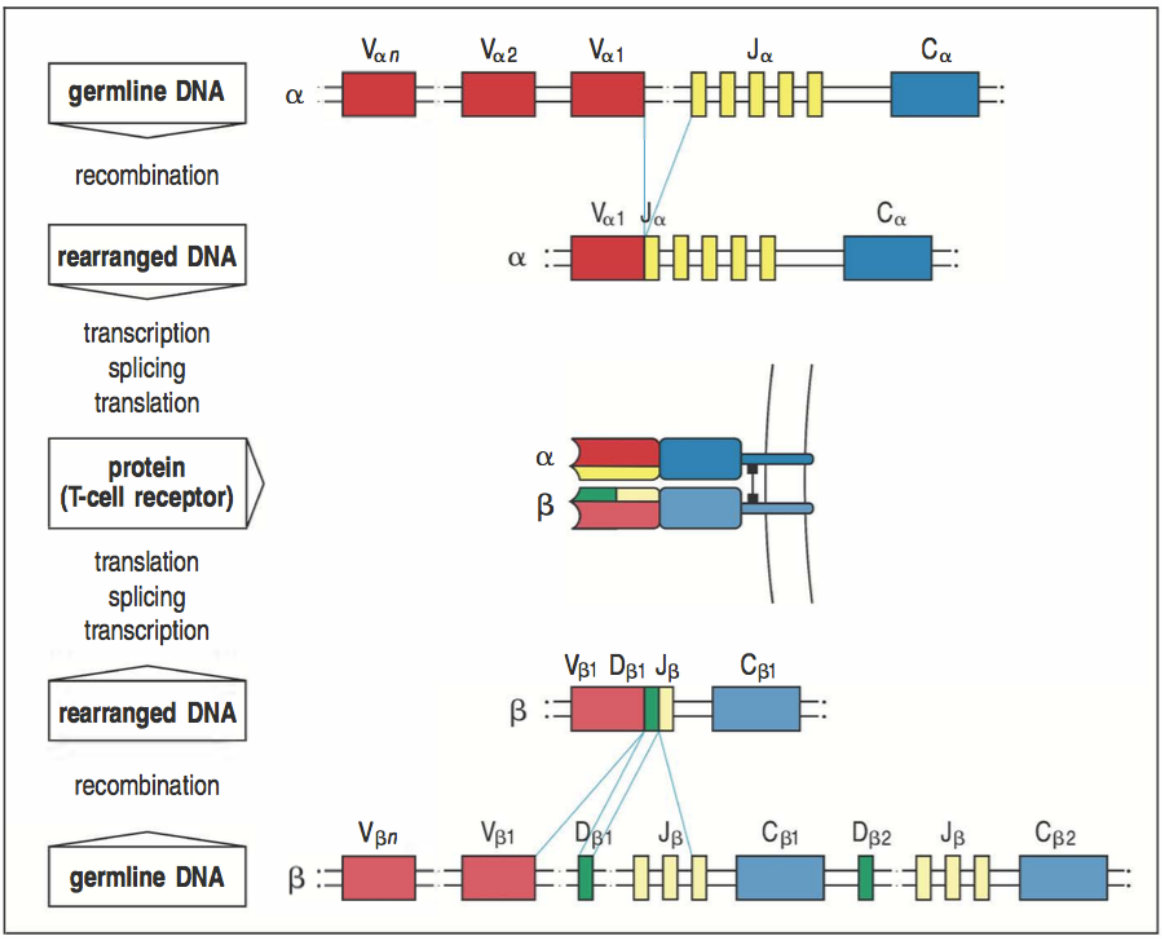

Figure 1.2.1 TCR rearrangement and expression. αβ TCR are made up from two discrete chains, and are expressed from gene segments that are rearranged during somatic recombination events in the T-cell. These events are homologous to those that generate immunoglobulin chains in B-cells. **Top** The α chain V_α segment is joined to a J_α segment to form the variable region of the TCRα chain. The VJ_α region is then joined to a C_α, forming the mRNA that encodes the functional TCRα chain. **Bottom** The β chain variable domain is formed by three different gene segments: V_β, D_β and J_β. These segments are rearranged and form the functional variable β chain exon, before being spliced to the C_β region, forming a functional TCRβ locus that is then transcribed and translated to form the TCRβ chain. α and β chains bind each other soon after their synthesis to form a functional αβ-TCR heterodimer. Adapted from Janeway's Immunobiology 8th Edition.

Each αβ T-cell has approximately 30,000 identical T-cell receptors on its surface, each made up from a single α and β chain joined by a disulphide bond, termed the α:β TCR (Figure 1.2.2). T-cells expressing α:β TCRs make up the majority of T-cells, however a subset express γ:δ TCRs which have different antigen recognition properties and are not thought to be MHC restricted (Brenner et al., 1986, Lew et al., 1986). These events create an enormous TCR repertoire with an equally large number of specificities. Each T-cell has its own, distinct T-cell receptor, making it genetically traceable and the association of the α and β chains on the cell surface provides an added layer of complexity.

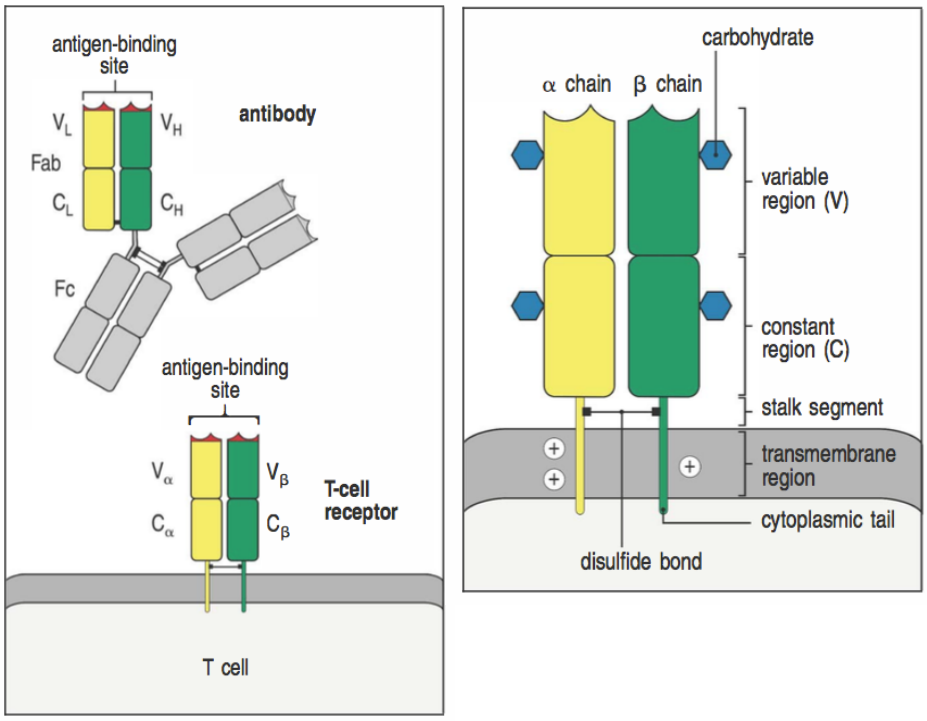

Figure 1.2.2 Similarities in α:β T-cell receptor and immunoglobulin structure. Left The Fab fragment of an antibody is made up from a heavy and a light chain, each containing a constant (C) and a variable (V) region which are linked by a disulphide bond. The variable regions make up the antigen-binding site of the antibody; each antibody molecule contains two of these sites. **Right** Like the Fab fragment, the T-cell receptor (TCR) is also a heterodimer linked by a disulphide bond, containing regions termed immunoglobulin-like C and immunoglobulin-like V domains with the V regions forming the antigen-binding site. T-cell receptor structure is formed from two homologous transmembrane glycoproteins chains which are termed α and β. Each domain has a carbohydrate side residue, and a disulphide bond in the stalk of each chain connects the two molecules. Transmembrane helices contain basically-charged residues with the cytoplasmic tail projecting into the cell and mediating cytoplasmic signalling. Figure adapted from Janeway's Immunobiology 8th Edition.

TCR recombination produces almost inexhaustible variation in TCR structure, however not all of receptors produced will be immunologically effective, as some will not recognise self-MHC molecules or will have a high affinity for self-antigens and be autoreactive (discussed further in chapter 1.3).

1.2.3 T-cell development and central tolerance

As with B-cells, T-cells are named after the organ in which they mature – the thymus. Soon after their production, lymphoid progenitors migrate from the bone marrow to the thymus after which they can be referred to as "thymocytes". The thymus is a primary lymphoid organ in the upper chest, and has an essential role in the adaptive immune system as the site of all major stages in T-cell development.

T-cell progenitors first enter the thymus from the blood via venules and localise to the cortico-medullary junction, where they interact with thymic stroma via Notch1 and begin their commitment to T-cell lineage (Radtke et al., 2013). At this stage cells are termed "double-negative" as they still lack expression of CD3 and the two main subtype markers CD4 and CD8. As double-negative thymocytes migrate through the cortex to the subcapsular region they undergo T-cell receptor gene recombination, first rearranging the β chain locus (Nitta et al., 2008). Following β chain recombination, double negative thymocytes begin to proliferate and become "double-positive", expressing both CD4 and CD8 receptors. Double-positive thymocytes make up the majority of T-cells in the thymus, and following the rapid division phase their expansion slows down. They reduce in size and they begin the rearrangement of their α chain locus, which continues until a productive chain which pairs efficiently with the β chain already expressed on the surface is produced (Petrie et al., 1993). Once double-positive thymocytes have a functional TCR expressed on their cell surface, they continue their

migration back through the cortex towards the medulla where they undergo rounds of positive selection by interacting with medullary epithelia.

Rounds of positive selection occur in the thymus to ensure that only thymocytes with a TCR that can engage peptide:MHC complexes are maintained. T-cells with no binding or too high affinity for peptide:MHC complexes displayed by medullary epithelial cells do not survive long-term. Negative selection ensures that immature T-cells with a TCR that strongly recognises self-peptide:MHC on specialised antigen presenting cells (APCs) in the thymus die by apoptosis. This ensures ineffective or autoreactive T-cells are removed from the T-cell repertoire before they exit the thymus or mature. Binding with moderate affinity of a TCR to self-MHC:peptide complexes causes T-cells to receive survival signals and these cells go on to lose expression of either CD4 or CD8 to become single positive CD4 or CD8 naïve T-cells.

A subset of cells with TCRs that bind to self-peptide:MHC with high avidity – but not high enough to initiate cell death – survive, turning on the expression of the transcription factor FoxP3 and receiving signals to become natural T regulatory cells (T_{reg}), characterised by CD4 and CD25 expression (Li and Zheng, 2015). Through this, positive selection has a role in influencing expression of cell surface receptor expression, as most thymocytes with TCRs that recognise peptides bound to MHC class I molecules will differentiate into CD8-expressing immature T-cells; likewise, most cells that recognise MHC class II become CD4+ T "helper" cells.

Specialised stromal cells called medullary thymic epithelial cells (mTEC) express the transcription factor AIRE (autoimmune regulator) which interacts with transcriptional machinery and increases protein transcript length from the promoter. AIRE elongates transcripts which would otherwise have terminated at an earlier point, and through this mechanism mTECs are able to express proteins that would normally be found in peripheral tissues (Zumer et al., 2013). Peptides from AIRE-synthesised proteins are presented on MHC

molecules, and interaction of a TCR with peripheral self-peptide:MHC complexes causes apoptosis in the bound T-cell. This process occurs alongside positive selection in the thymic cortex and medulla and prevents self-reactive immature thymocytes from exiting the thymus and maturing into potentially autoreactive T-cells.

Once T-cells have undergone rounds of positive and negative selection they end their migration through to the cortico-medullary region via acquisition of the CCR7 receptor, exiting into the blood to be carried to peripheral lymphoid tissues as naïve T-cells (Forster et al., 2008). Once in the circulation, these cells first home to secondary lymphoid organs using receptors such as L-selectin (CD62 ligand) and CCR7 to bind proteins on the high endothelial venule (HEV) which enables them to pass into lymph nodes (Forster et al., 2008). CCR7 is also expressed on peripheral dendritic cells (pDC) and these cells traffic to the lymph nodes where they present processed antigens to naïve T-cells via MHC class I and II molecules in the T-cell zones of the lymph node (Itano and Jenkins, 2003).

1.2.4 MHC and antigen presentation

MHC class I and II molecules have distinct structures but share many similarities in function, and both present peptide fragments to be recognised by TCRs on the surface of T-cells.

MHC class I molecules are expressed on all nucleated cells and are formed from the MHC heavy chain and β2 microglubulin (β2m) making a heterodimer. Two extracellular domains in the heterodimer form the peptide binding groove, creating a closed pocket into which peptides of approximately 8-11 amino acids in length can bind (Garrett et al., 1989). HLA class I molecules have three main types, termed A, B and C, with the chains being highly polymorphic; heterozygous individuals can express up to 6 different alleles, allowing a wide range of peptides to be presented (Lund et al., 2004). Peptides presented by MHC class I

molecules are mostly endogenous to the cell, and MHC class I:peptide complexes are engaged by T cells expressing the CD8 co-receptor.

MHC class II molecules are only expressed on antigen presenting cells (APC) and structurally resemble MHC class I but are formed from two homologous, transmembrane glycoprotein chains, termed the α and β chains. The tops of both chains form the peptide binding groove which, unlike MHC class I, is not a closed space, meaning that the length of peptides able to bind into the groove is not constrained and peptides of varying length (usually between 12 and 22 amino acids) are able to bind MHC class II molecules. The overhanging amino acids from these interactions are termed the peptide flanking region and these domains have been shown to affect TCR interactions with peptide:MHC class II (Moudgil et al., 1998). Analogous to class I, MHC class II are highly polymorphic, allowing extensive variation in the peptides displayed on the molecules, which are mostly exogenous and derived from proteins taken up by the cell. MHC class II molecules present peptides to helper T-cells which express CD4 as the TCR co-receptor.

As previously discussed, T-cell function is reliant on their capacity to recognise infected cells or those that have internalised foreign proteins. Generally surface MHC class I and II molecules present internally processed peptide fragments for recognition by CD8+ and CD4+ T-cells respectively.

Classically MHC class I molecules present peptides derived from endogenous proteins, whilst MHC class II proteins present fragments of proteins that have been phagocytosed by APCs – exogenous antigens. However, MHC class II proteins have also been shown to present endogenous peptides on the surface (Rammensee et al., 1999), and likewise, MHC class I proteins are also known to be able to present exogenous peptides to CD8+ T-cells (Huang et al., 2005). CD4+ T-cells have also been shown to exhibit direct cytotoxic activity as well as

their classical role providing immunological help to CD8+ T-cells and B-cells, affording another way in which the immune system can directly recognise and remove infected cells.

1.2.5 T-cell responses

Naïve T-cells migrate through the blood and secondary lymphoid tissues, sampling peptide:MHC complexes displayed on the surface of DCs that have migrated from peripheral tissues. Naïve T-cells not able to stably bind to the peptide:MHC complex via their TCR are quickly released from the interaction and go on to interact with other DCs displaying alternative peptides until they either bind with high affinity or migrate back into the circulation. If a T-cell engages a peptide:MHC complex able to bind strongly to its TCR it also needs to receive co-stimulatory signals to become activated: binding of CD28 on T-cells to CD80 (B7.1) ligand expressed on DCs induces expression of IL-2 , up-regulation of high affinity IL-2 receptor (IL-2R) and clonal expansion of the T-cell (Lin and Leonard, 1997).

This stimulation of naïve T-cells also triggers their differentiation into effector phenotypes. Differentiation allows T-cells to carry out their function upon subsequent exposure to cognate antigen without the need for co-stimulatory signals; differentiated T-cells are primed for response and are able to dock onto MHC:peptide complexes on target cells and carry out their function without needing co-stimulation (Lanzavecchia and Sallusto, 2001, van Stipdonk et al., 2001, Kaech and Ahmed, 2001).

There are two main groups of T-cell defined by their effector phenotype and function, and classified into subsets by the expression of CD4 and CD8 markers. Differentiated CD8+ T-cells are cytotoxic lymphocytes (CTLs), exhibiting direct killing activity on target cells after docking their TCR with a cognate peptide:MHC complex and forming an immunological synapse. The immunological synapse is enriched for TCR and co-stimulatory molecules, and

target cells are killed through release of perforin and granzymes (Cullen and Martin, 2008). Naïve CD4+ T-cells become "helper" cells and have a number of different effector subsets each with subtly distinct roles in directing adaptive immune responses.

CD4+ T-cells differentiate into effector cells upon antigen encounter, and it was previously accepted that they can be broadly divided into two main groups based on their cytokine secretion. T_H1 CD4+ T-cells produce IFNγ and IL-2 and differentiate following priming by a DC in the presence of IL-12 (Nizzoli et al., 2013); T_H1 cells provide help to cytotoxic cells such as macrophages and CD8+ T-cells and produce stimulatory cytokines (eg. IL-2) to aid killing of intracellular pathogens such as viruses and bacteria (Mosmann and Coffman, 1989). T_H2 cells are harnessed to target extracellular bacteria and helminths, and are primed by DCs in the presence of IL-4 to produce IL-4, IL-5 and IL-13, also providing help for B-cells (Mosmann et al., 2005, Geginat et al., 2014).

However, it is now clear that there are several more subsets, including T_H17 cells which are marked by their production of IL-17 and IL-22 and perform essential roles in inflammatory responses to extracellular pathogens by recruiting innate cells such as macrophages and neutrophils (Veldhoen et al., 2006). Follicular helper T-cells (T_{FH}) are characterised by expression of the transcription factor Bcl-6 and their production of IL-4 and IL-21. T_{FH} cells have a range of effector functions, including the provision of help to follicular B-cells for their maturation and antibody production (Qi, 2016). A summary of CD4+ T-helper subsets with transcription factors controlling their differentiation, cytokines produced and effector function is shown in Figure 1.2.3.

Classical reports of CD4+ T-cells describe them as helpers with no direct cytotoxic function, however this is no longer the case and CD4+ T-cells have been shown to be able to target virally-infected cells directly via recognition of MHC class II molecules up-regulated on the surface of infected cells (Debbabi et al., 2005). CD4+ T-cells now have a widely-recognised

role in antiviral defences and have been shown to help control infections such as measles and gammaherpes viruses as well as for many other viruses (Reich et al., 1992, Sparks-Thissen et al., 2004).

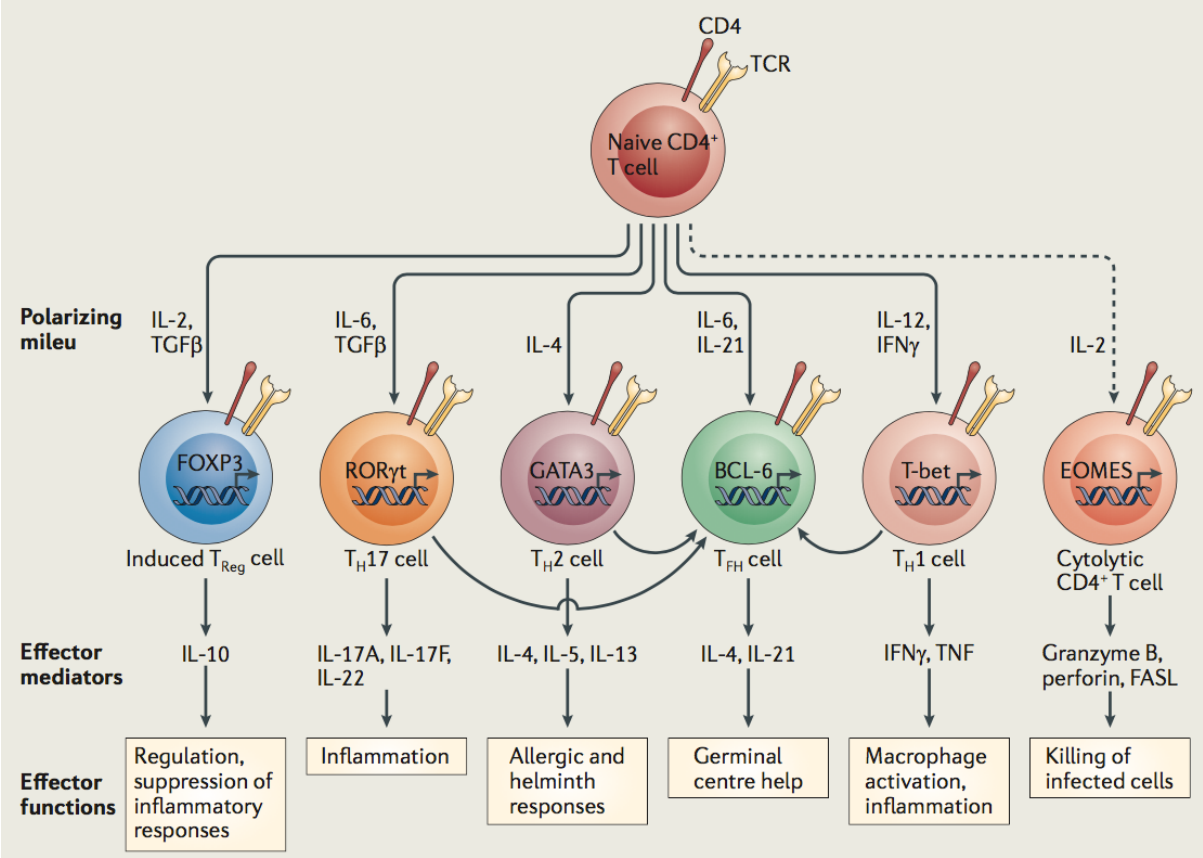

Figure 1.2.3 CD4+ T-helper cells have adapted to perform many different roles. Differentiation of CD4+ T-cells into subsets occurs after recognition of cognate antigen, and is regulated by transcription factors and soluble cytokines in the local environment which determine effector lineage. Whilst CD4+ T-cells are classically divided into subgroups via their markers and function they are also plastic and are able to adapt their function to the pathogen encountered *in vivo*. Classically T_H1 cells are primarily thought to be responsible for clearance of viral pathogens but it is now apparent that multiple subsets are involved. Cytolytic CD4+ T-cells have been shown to be able to directly kill virus-infected cells *in vitro*. T_{FH} cells have a key role in priming B-cells to produce neutralising antibodies and also those specific for viral proteins. T_H17 cells are defined by their production of IL-17 and their function is primarily pro-inflammatory, recruiting neutrophils and macrophages to infected tissues. T_H17 cells have also been implicated in chronic inflammation and autoimmunity. Following re-stimulation memory CD4+ T-cells are able to rapidly produce effector cytokines and provide helper functions to other immune cell subsets. Adapted from Swain *et al.*(Swain et al., 2012).

1.3 Peripheral immune tolerance and T-cell anergy

Peripheral tolerance acts to maintain a balance between protective T-cell responses which clear infection and self-recognition, preventing damage to tissues by removing autoreactive TCRs from the repertoire. However, mechanisms of tolerance deleting self-reactive T-cells from the repertoire are not perfect and some autoreactive cells can survive, and this is evident from the development of autoimmune diseases.

As previously described, TCRs recognise peptides expressed by MHC class I or II molecules, and all nucleated cells in peripheral tissues express HLA class I; HLA class II molecules are mainly expressed on APCs and on activated cells. APCs, such as dendritic cells (DCs), migrate to peripheral lymphoid tissues to present exogenously derived peptides on HLA class II to T-cells and B-cells.

As previously described, to amount a T-cell response co-stimulatory molecules are needed in addition to TCR interaction with peptide:MHC complexes. Under normal, uninfected conditions, peripheral tissues and DCs do not express these co-stimulatory molecules which are needed to efficiently activate T-cells engaging their TCR. Interaction of a cognate TCR with peptide:MHC complexes without co-stimulation results in the T-cell being rendered anergic, a state in which a T-cell becomes unresponsive to stimulation. Anergic T-cells are unable to respond to their cognate antigen upon subsequent exposure, even in the presence of co-stimulatory signals.

The two-checkpoint model for efficient T-cell activation requires two separate signals for the cell to become activated. However, anergy is only one possible outcome of T-cells receiving antigen-specific signals without co-stimulation, and they may also undergo apoptosis or differentiate into induced CD25+ regulatory T-cells. This feature, in addition to central

tolerance, provides another layer of protection against autoimmunity by removing or silencing cells that can potentially target self-tissues.

1.4 Multiple sclerosis

Multiple sclerosis is a chronic, debilitating condition of the central nervous system (CNS), characterised by inflammation which causes damage to the brain and spinal cord over time. Clinical presentation is extremely heterogeneous, with symptoms depending largely on the area of the CNS where inflammatory lesions have formed. Over time, damage to the CNS can become more severe and progress to secondary progressive multiple sclerosis (SPMS) which is characterised by increased neurological dysfunction and fewer definite periods of clinical remission. Average age of diagnosis for the relapsing-remitting form of MS (RRMS) is 20-40 years, and, after trauma, MS remains the second most common cause of neurological disability in young adults in the UK affecting approximately 130,000 people (Mackenzie et al., 2014).

The first clinical episode in patients is termed clinically isolated syndrome (CIS), and a definitive diagnosis of conversion to MS is only made following the patient experiencing a second episode (Filippi et al., 2016). It is also possible for lesions to be detected in a patient's CNS by magnetic resonance imaging (Koini et al.) without experiencing symptoms, and this is termed radiologically isolated syndrome (RIS). Approximately 85% cases of MS present with RRMS form of disease. A minority of cases present with a more insidious syndrome without periods of remission named primary progressive MS (PPMS). The majority of RRMS patients go on to develop SPMS after a variable number of years. SPMS patients still undergo relapses and these are characterised by continual accumulation of disability with pathology showing persistent microglial activation and demyelination.

Despite extensive research, very little is known regarding MS disease pathogenesis and progression, and as worldwide prevalence of MS increases it is more important than ever that we are able to understand and develop treatments to slow or prevent progression of disease.

1.4.1 History of multiple sclerosis

Numerous reports of neurological conditions with symptoms consistent with modern observations of MS are apparent throughout history, with the earliest dating back to the fourteenth century (Murray, 2009). However, it was only in the mid-nineteenth century that observations from many physicians throughout Europe were brought together by a French neurologist named Jean-Martin Charcot and subsequently published in a series of books and lectures describing symptoms and post-mortem observations, naming the condition "sclérose en plaques" (Murray, 2009).

The late 1800s marked a surge of interest in MS, and for the first time epidemiological aspects of disease distribution were considered and published by Sir Byron Bramwell, who reported an increased prevalence of MS at higher latitudes (Murray, 2009). Genetic contribution towards disease development also began to be investigated, however these avenues required much larger study cohorts and in-depth analysis of heredity was not possible until the 1970s and 1980s.

In the 20th century several epidemics of MS broke out in different European locations, most notably in the Faroe Islands, which had previously not had any diagnosed cases between 1900 and 1943 (Kurtzke, 2013). After the Islands' 5-year occupation by British forces during the Second World War, many MS cases emerged and for several decades researchers have speculated whether an infectious agent was introduced to the islands at this time and caused the epidemic. However, this hypothesis is not widely accepted and much speculation still surrounds the cause of this sudden rise in disease incidence around this time (Kurtzke and Heltberg, 2001, Poser et al., 1988).

The modern view of MS is that of an autoimmune-mediated disease affecting the CNS which is brought about in some genetically pre-disposed individuals by a series of unknown

environmental triggers. Our understanding and attitudes to MS have changed with the advent of MRI to image the brain in high definition and availability of immunomodulatory treatments which can ameliorate disease, and these will continue to change as our knowledge of disease becomes more comprehensive.

1.4.2 Diagnosis and prognosis

Onset of RRMS can be insidious, with many individuals only experiencing mild symptoms years before they seek medical help, by which time the disease may no longer be in the early stages. Classic symptoms of RRMS begin as mild neurological deficits and it is common for patients to experience sensory occlusion, such as vision disturbances or changes to touch, hearing, taste and smell. These symptoms are caused by specific parts of the brain becoming inflamed and impeding neuronal function in that precise area. A neurological episode is defined as lasting for 24 hours or more, but the attacks can last for up to several weeks (Figure 1.4.1). Patients are assessed using the revised McDonald Criteria (Filippi et al., 2016) which uses neurological evaluation, presence of brain and spinal cord lesions over time as pictured by MRI, and presence of oligoclonal bands (OCB) in cerebrospinal fluid (CSF) to confirm MS diagnosis. OCB are bands of immunoglobulins which indicate antibody production, they can be found in sera or CSF and are used in diagnosis of MS as their presence in CSF is indicative of an intrathecal immune response. OCB are also present in other diseases, such as infections, and observed on their own are not diagnostically conclusive for MS.

Amongst RRMS cases there is a stark gender bias towards females reported in many developed countries across the world including Canada, Australia, the United States of America (Larsen et al.) and Japan (Orton et al., 2006, Wallin et al., 2004, Barnett et al., 2003, Houzen et al., 2003), with the ratio of women developing MS relative to men being calculated as high as

~3.2:1 (Orton et al., 2006). It is not clear what is driving this increase but it is apparent that this trend is only becoming stronger. A study of Canadian patients showed the ratio of male:female patients to be increasing each year, further supporting findings that prevalence of MS is increasing in women (Orton et al., 2006).

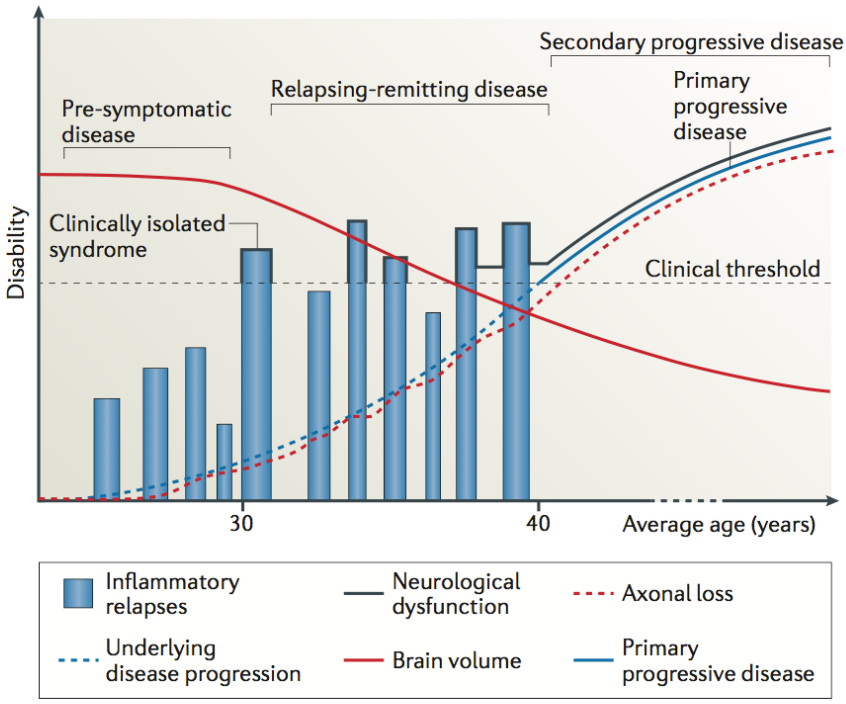

Figure 1.4.1 Disease progression of relapsing-remitting multiple sclerosis is heterogeneous. RRMS disease course is characterised by a first clinical episode which resolves and generally leaves no long-term disability. Subclinical episodes may occur with brain lesion formation but with no obvious neurological dysfunction. Remission is interspersed with periods of relapse, becoming more severe over time with eventual accumulation of disability as neuronal injury becomes greater. Approximately 80% of RRMS patients eventually develop the secondary progressive form of disease (SPMS) which is characterised by gradual loss of brain volume and atrophy. 10% of patient present with the primary progressive (PPMS) form, which is disease that accumulates without apparent remission from symptoms (blue line in graph). Figure adapted from Dendrou *et al.* (Dendrou et al., 2015).

1.4.3 Clinically isolated syndrome and early disease

85% of people who develop MS present with a single neurological disturbance named clinically isolated syndrome (CIS), caused by a single or multiple lesions in cerebral white matter (Maurer et al.). Symptoms vary greatly between patients, and a review of CIS presentation reported that 46% of patients had spinal cord symptoms, 10% had disease affecting the brainstem, 21% with optic neuritis and 23% with multiple areas affected (Miller et al., 2005). Presenting symptoms were not predictive of conversion rate to MS but number of lesions and volume correlated moderately with progression and future disease severity (Brex et al., 2002). Early disease is thought to be pathologically different to late disease, and the exact triggers for immune infiltration into the CNS are unclear; it is also not known whether the pathogenic T-cells attacking myelin are activated in the periphery or within the CNS itself. Early disease is characterised by immune infiltration into the brain parenchyma via direct entry from meningeal blood vessels, subarachnoid space or via the CSF and the choroid plexus. Immune cells, including innate and adaptive cells, accumulate in the perivascular space surrounding parenchymal tissue where they mediate damage either via cell contact-dependent mechanisms or through secretion of inflammatory mediators. T-cells, B-cells, DCs and macrophages may be involved in these processes, with CNS-resident microglia and astrocytes becoming activated in an environment that promotes inflammation and demyelination. Early in disease the damage is often reversible in the sense that there are no lasting clinical symptoms. However, damage can accumulate with ongoing inflammatory processes leading to late stage disease and permanent disability.

1.4.4 Late disease and neurodegeneration

Late stage disease is marked by lower immune cell infiltrate from the circulation, and it has been speculated that this may be due to exhaustion of adaptive immune cells due to chronic antigen exposure over time. However, astrocyte secretion of chemokines such as GM-CSF and CCL2 can promote immune cell infiltration of the CNS perpetuating the inflammatory environment and preventing resolution of inflammation (Mayo et al., 2014).

Lingering inflammation in brain tissues promotes loss of axons that accumulate and compromise tissue function. Neuroaxonal damage interrupts the extremely metabolically demanding transport of cellular components, such as mitochondria, down axons. Disruption to energy transport in neurones leads to metabolic stress and further damage to the cell, compromising function.

In SPMS tertiary lymphoid structures form in meningeal spaces. These structures consist of aggregates of immune cells that form in different sites under conditions of chronic inflammation, and are made up from a mixture of T-cells, B-cells, plasma cells and follicular DCs. Aggregates form inflammatory loci in the meninges and contribute towards long-term cortical injury; formation of these structures has also been observed for other conditions such as infectious diseases and those involving chronic brain inflammation (Howell et al., 2011).

Lesion formation is a very complex process and is still not fully understood in MS due to early inflammatory events often being subclinical and therefore impossible to sample and the inability to biopsy brain tissue. Post-mortem samples, whilst informative, only give an end stage picture of disease and provide very little insight into early MS pathogenesis. Observations from the CSF during inflammatory events may provide more answers regarding initial disease processes in the MS brain.

1.4.5 Immunology of MS

The initial triggers of CNS attack in early MS are not known, and it is thought that a complex interplay between genetic predisposition and environmental factors are responsible for the first inflammatory events which progress into clinical disease. However, difficulties in obtaining samples from early MS mean that only immunological processes in later disease have been investigated in humans, and it is only based on these finding that potential mechanisms for disease initiation have been developed.

Without a clear picture of the exact triggers, it is not known whether initial immunological events driving MS disease are derived from the periphery or from inside the CNS itself. In the externally-primed model, T-cells are thought to become activated in peripheral tissues and migrate to the CNS alongside other immune cells such as B-cells and macrophages. It is not known how these cells may become activated to target neuronal tissue, and potential mechanisms include molecular mimicry, bystander activation or co-expression of TCRs on individual T-cells with different specificities (Olson et al., 2001, Ji et al., 2010). The second model suggests that primary events are initiated in the CNS, with influx of immune cells from the periphery as a secondary phenomenon. These initial intrinsic triggers are so far unknown, but suggested mechanisms include potential viral infections of the CNS or from primary neurodegenerative mechanisms similar to those observed in Alzheimer's or Parkinson's disease (Heneka et al., 2014).

The blood-brain barrier (BBB) and anatomical separation of the CNS from the lymphatic system provides a certain level of protection for the brain and spinal cord by limiting entry of leukocytes, and for many years the CNS was considered an immune privileged site. However, recent studies have shown that this is not the case, and immune surveillance by memory T-cells has been observed in healthy neuronal tissues; the discovery of CNS lymphatic vessels in mice

has further challenged this view (Ransohoff and Engelhardt, 2012, Shechter et al., 2013, Louveau et al., 2015). Natural surveillance of CNS tissues by adaptive immune cells therefore indicates the potential for a T-cell to become activated in the CNS without the need for permeabilisation of the BBB, triggering an inflammatory event with further recruitment of immune cells.

T-cells in MS brain lesions are detectable in early disease but despite this their autoantigenic targets are still not known. Autoreactive targets are thought to be derived from myelin antigens and predominantly influenced by HLA type of patients, with disease progression leading to epitope spreading and greater variation between patient responses. CD4+ T-cells specific for CNS antigens have been detected in peripheral blood of MS patients but no consensus has been reached regarding their frequency, avidity or role in disease due to their additional detection in healthy individuals (Bielekova et al., 2004, Hellings et al., 2001). Lack of a candidate autoantigen in MS reflects the heterogeneity between patients and warrants the further investigation of this area to assess contribution of CNS-specific T-cells in disease initiation and progression.

Much of what is known about MS immunopathology comes from observations in the murine model of disease, experimental autoimmune encephalomyelitis (EAE), and from administration of disease modifying therapies to patients. In EAE models, disease is induced by adoptive transfer of autoreactive CD4+ T-cells which are reactivated in the CNS by antigens presented by DCs. Activated autoreactive CD4+ T-cells produce pro-inflammatory cytokines which recruit innate cells (such as monocytes and macrophages) to the CNS and activation of naïve T-cells, leading to epitope spreading and perpetuation of the inflammatory environment (McMahon et al., 2005).

CD4+ T-cells are thought to be key orchestrators in MS development, and T_H1 and T_H17 cells are implicated by various studies as the predominant pathogenic subsets in patients (Frisullo et

al., 2008, Tzartos et al., 2008). Disease modifying therapies have therefore aimed to target T_H1 and T_H17 subsets with the aim of skewing them towards a T_H2 (and potentially less pathogenic) phenotype, and this is thought to be how several licenced drugs are able to ameliorate MS disease: glatiramer acetate (Miller et al., 1998), dimethyl fumarate (Zoghi et al., 2011) and IFNβ (Kozovska et al., 1999). However, a role for T_H1 and T_H17 cells in MS is not completely clear, and a failed clinical trial in RRMS of ustekinumab, which targets the p40 shared subunit of IL-12 and IL-23, sheds doubts on their involvement (Segal et al., 2008). IL-12 and IL-23 are involved in the differentiation of T_H1 and T_H17 cells respectively and blockade of these pathways was hypothesised to prevent generation of these pathogenic subsets.

CD8+ T-cells, though thought to have a lesser role in disease initiation, are present in MS brain lesions at higher numbers than CD4+ T-cells and their numbers have been found to correlate with axonal damage (Frischer et al., 2009). EAE models have also shown CD8+ T-cells specific for myelin antigens become activated by epitope spreading via cross-presentation of antigens by DCs (Ji et al., 2013). Studies of human active brain lesions have shown a quarter of CD8+ T-cells to be IL-17 producing mucosa-associated invariant T-cells (MAIT-cells) (Willing et al., 2014), and prolonged depletion of these cells following haematopoietic stem cell transplant (HSCT) indicates their potential role in MS pathogenesis (Abrahamsson et al., 2013). More research is needed to elucidate the exact contribution of CD8+ T-cells towards disease development and progression.

T_{reg} cells have been implicated in many autoimmune diseases, and alterations in this key subset have been shown to contribute to breakdown of immune tolerance. The role of T_{reg} cells (CD4+FoxP3+) in CNS-mediated autoimmunity are not fully understood, and studies have varied in their reports of decreased frequency or function of T_{reg} cells in MS patients compared to controls (Venken et al., 2008, Feger et al., 2007, Fletcher et al., 2009). Other studies suggest that, rather than impairment of frequency or function, it is pathogenic T-cells themselves that

are resistant to suppressive mechanisms. Impairment of the signal transducer and activator of transcription 3 (STAT3) signalling pathway via IL-6 and granzyme B (GzmB) has been shown to contribute towards resistance of MS patient derived effector T-cells to T_{reg} suppression *in vitro* (Schneider et al., 2013, Bhela et al., 2015).

Arguments against a role for T_{reg} cell dysregulation in MS come from observations from a primary immunodeficiency affecting function of regulatory CD4+ T-cells. Patients with IPEX syndrome (immunodysregulation, polyendocrinopathy, enteropathy, X-linked syndrome) suffer from a severe, rare genetic disease caused by mutations in the transcription factor FoxP3 resulting in the inability to generate T_{reg} cells. Patients with this deficiency however do not develop CNS-directed autoimmunity, indicating that dysregulation of these cells are not solely responsible for autoimmune attack on the brain and spinal cord seen in MS (Bennett et al., 2001).

Therapeutic efficacy of B-cell-depleting monoclonal antibodies in MS, such as rituximab and ocrelizumab, in reducing relapse rates suggest that these cells contribute towards MS pathology (Hauser et al., 2008, Kappos et al., 2011). However, these immunomodulatory drugs specifically deplete CD20-positive cells, a marker which is not expressed on antibody-secreting plasma cell subsets. This therefore suggests that efficacy anti-CD20 therapies is due to other effector functions of mature B-cells, such as antigen presentation or promotion of inflammation via IL-6 secretion (Barr et al., 2012).

Heterogeneity between patients and conflicting data in literature make it difficult to draw conclusions regarding immunological processes of MS, and much of what we know is derived from observations from EAE models, therapeutic trials in humans and aetiological data.

1.4.6 Aetiology

Development of MS is thought to be complex and influenced by a combination of environmental factors in genetically predisposed individuals, and these factors are discussed in sections 1.4.6.1 and 1.4.6.2.

1.4.6.1 Genetics

The genetic risk of developing MS has been previously estimated by studies of twins from British and Canadian cohorts which found a 5% chance of both dizygotic twins developing disease, but this increases to 25% in monozygotic twins (Willer et al., 2003, Mumford et al., 1994). Studies of adopted children brought up in families with a history of MS show a similar risk of developing disease to the rest of the population but also show that biological relatives remain at increased risk, indicating a role for genetic factors in MS development (Ebers et al., 1995, Dyment et al., 2006).

The search for genes associated with MS revealed links to the MHC locus in the 1970s, with the HLA-DR15 haplotype being found to confer increased risk (Compston et al., 1976, Terasaki et al., 1976); this search has since been narrowed down to a single nucleotide polymorphism (SNP) (International Multiple Sclerosis Genetics et al., 2007). Subsequent investigations searching for MS risk alleles have been less fruitful, and HLA-DR15 remains the genetic factor conferring highest risk. Other reports have found further variants in the MHC locus which affect susceptibility, with the MHC class I allele HLA-A2 and HLA-C5 found to be negatively associated with MS (Yeo et al., 2007, Link et al., 2010). A recent study of

Goodpasture disease, an autoimmune condition driven by autoreactive HLA-DR15-restricted CD4+ T-cells, showed HLA-DR1 to be dominantly protective and to shape the immune repertoire by skewing autoreactive T-cell responses towards a T_{REG} phenotype (Ooi et al., 2017). Similar mechanisms of immune repertoire skewing by protective alleles may exist in MS but these have so far not been investigated.

In addition to variants of the MHC locus affecting risk, genome wide association studies (GWAS) have identified other associated gene polymorphisms, with most having roles in immune regulation and function.

The IL-2 receptor α (IL-2Rα) chain is part of the IL-2 receptor (IL-2R) which forms a complex with IL-2β and IL-2Rγ chains to form the high affinity IL-2R complex. Components of the high affinity IL-2R are up-regulated to the cell surface upon T-cell stimulation and act to perpetuate the immune response and aid T-cell proliferation (Minami et al., 1993). SNPs in the IL-2Rα gene have been associated with an increase in susceptibility to MS (Wang et al., 2011b) (Cavanillas et al., 2010).

Polymorphisms in other receptor genes have been associated with MS. The cytokine receptor for IL-7 (IL-7R) is expressed on T- and B-cells and polymorphisms have also been shown to confer increased risk of developing MS (Gregory et al., 2007). SNPs in the TNFα gene have been linked to MS, alongside other immune conditions such as TNF receptor-associated periodic syndrome (Caminero et al., 2011).

Polymorphisms in alleles which encode for co-stimulatory molecules and their ligands have also been associated with MS, including CD28, CD80, CD86 and CTLA-4, with the SNPs also found to influence age of disease onset (Wagner et al., 2015). Despite influencing age of disease onset, the effects of polymorphisms in these loci on risk were more modest when compared with those of the MHC gene locus.

Approximately 10-15% of MS cases are thought to have a predominantly hereditary component, and a recent Canadian study identified a variant in the receptor NR1H3 (nuclear receptor subfamily 1 group H member 3) which confers a 70% chance of individuals developing disease (Wang et al., 2016). The study documented two families with multiple members initially diagnosed with RRMS that rapidly developed into progressive disease with significant morbidity. Such studies investigating functional significance of SNPs in genes linked to MS could give an insight into some of the mechanisms underlying development, as there is currently no universally accepted model of pathogenesis.

Epigenetics have increasingly been recognised for the role they play in MS, and several studies have investigated the environmental and hereditary impact of gene modifications on disease development. One of the most striking effects of epigenetic modification impacts the MHC gene locus, with reports that the HLA-DR15 haplotype is carried by more women than men and daughters being more likely to inherit the allele from their mother than from their father (Chao et al., 2010).

Researchers have investigated effects of epigenetic changes to the enzyme peptidylarginine deiminase (PAD2) on brain lesion pathology, and higher levels of citrullinated myelin basic protein (MBP) were found to be the result of epigenetic changes to the PAD2 gene promoter causing increased expression of the PAD2 enzyme in MS patient brains (Mastronardi et al., 2007).

MicroRNA (miRNA) have also been implicated in MS pathogenesis, with altered expression of miRNAs between active and dormant lesions of RRMS patients indicating a role for epigenetic regulation of CD47 in MS brain lesions (Junker et al., 2009). Differentially expressed miRNAs in T_H17 cells from MS patients have been shown to influence pathogenic T-cell differentiation (Du et al., 2009).

Despite the excitement surrounding them, epigenetics may only have a modest influence on disease development, and one study showed that different concordance rates between identical twins were not attributable to epigenetic changes (Baranzini et al., 2010). Genetics account for ~30% of susceptibility to MS, but there is a greater role for environmental factors in development of disease.

1.4.6.2 Environment

Recent meta-analyses have established many factors that are involved in the complex interplay of MS disease initiation. Many of these factors involve lifestyle choices, as shown by large multicentric studies of healthy people which include those who go on to develop MS over time. For many years, it has been apparent that MS incidence increases with distance from the equator, with the highest number of people with MS residing in countries with relatively little sunlight. These observations have been backed up by analysis of serum vitamin D levels, and a study of 7 million people using the US military serum repository found that increased serum 25-hydroxyvitamin D in Caucasians had a protective effect and lowered risk of developing MS (Munger et al., 2006). Other studies have corroborated these findings (Duan et al., 2014, Pakpoor and Ramagopalan, 2015), and low vitamin D levels and reduced sunlight exposure are considered to be key risk factors in MS pathogenesis. Migration studies of individuals have also supported a role for sunlight exposure, with early reports of US military veterans from Northern states experiencing a lower incidence of MS after being deployed South (Kurtzke et al., 1985). Studies of adopted children have also shown MS risk to be conferred by where they spent the majority of their early years (Gale and Martyn, 1995).

One of the highest risk factors for developing MS identified only in recent years is smoking, with reports showing that it can increase risk by ~50% and has an even more pronounced effect in young adults (Handel et al., 2011, Salzer et al., 2013). It is not clear exactly what contribution smoking makes towards the development of MS, however it has been shown that nicotine increases permeabilisation of the blood-brain barrier in rats (Chen et al., 1995), which can potentially facilitate migration of pathogenic cells into the CNS. In addition to this it has also been shown that smoking increases citrullination of proteins by upregulation of the enzyme PAD2 in lung alveoli, which may in turn lead to synthesis of novel epitopes and autoimmunity

in some patients who are genetically susceptible (Makrygiannakis et al., 2008). As previously mentioned, the HLA DR15 haplotype is associated with increased risk of developing MS, however more recent studies investigating interaction of risk alleles with environmental factors have shown current smokers who possess the HLA DR15 allele to be 13.5 times more likely to develop disease, whereas non-smokers with the same genetic background only have an increased risk of 4.9-fold (Hedstrom et al., 2011). Smoking is now widely accepted to be a key risk factor for developing MS, although more research is needed to determine exactly what contribution smoking makes to disease development and progression.

Global obesity rates have increased significantly in the last 30 years, with an estimated 10.8% of males worldwide being classified as obese and 14.9% of women (Collaboration, 2016). Coincidentally, incidence of MS in the western world has also steadily increased in the 20th century, particularly RRMS in women (Grytten et al., 2015, Alonso et al., 2007). The first comprehensive study to investigate a relationship between MS development and obesity was the Nurses' Health Study in the USA which found women with a BMI of 30kg/m^2 or more to have a 2.25-fold increased risk compared to those of "normal" weight (Munger et al., 2009). A large population study from Sweden also calculated that individuals with a BMI of 30kg/m^2 or more had a two-fold increased odds ratio of developing MS, a finding which was significant in both men and women (Hedstrom et al., 2012). Other studies from Norway and Italy have also replicated this two-fold increased incidence of MS amongst overweight individuals (Wesnes et al., 2015).

High socioeconomic status has been suggested as a risk factor for MS with the hypothesis of greater hygiene leading to later exposure of individuals to pathogens and skewed or altered immune responses. However, this idea is not widely accepted with conflicting and varied studies not reaching any commonly accepted conclusion (Goulden et al., 2015). Low

socioeconomic status is associated with poor lifestyle and, in Western countries, accompanies smoking and obesity in groups with lower standards of living.

Infectious agents have also been implicated in MS development. The gram-negative bacterium *Chlamydia pneumoniae* (*C. pneumoniae*) was suggested as a potential trigger for disease after detection of bacterial DNA and antibodies in the CSF of MS patients (Sriram et al., 1999). However, after further analysis of intrathecal antibody production against *C. pneumoniae* levels were found to have no significant correlation with disease severity or duration, MRI disease activity or presence of OCB, and a potential link between MS and the bacterium is no longer considered (Krametter et al., 2001, Tsai and Gilden, 2001).

Human herpesvirus 6 (HHV-6) is a β herpesvirus which has been more frequently found in blood and CSF of MS patients than healthy controls, and virus reactivation has been put forward as a contributing factor in disease development. However, results from DNA and antibody analysis were mixed, with the virus reactivation detected only in a proportion of MS patients (Liedtke et al., 1995, Goldberg et al., 1999, Alvarez-Lafuente et al., 2002, Nielsen et al., 1997). It was concluded that HHV-6 DNA was only detected in a small proportion of MS patients and was also present in patients with other neurological diseases.

Human endogenous retroviruses have also been implicated in MS pathogenesis, and several studies have investigated a relationship between reactivation and disease development. However, the majority of studies found evidence of viral transcription in both healthy controls and patients; one report found transcripts of several endogenous retroviruses in the peripheral blood mononuclear cells (PBMC) of MS patients and controls (Rasmussen et al., 1997), and Hackett *et al.* reported no findings of retrovirus in serum, CSF or PBMC of MS patients (Hackett et al., 1996).

The most compelling evidence for an infectious role in MS disease development lies with EBV. Research in this area is discussed further in chapter 1.5.2.

1.5 Epstein-Barr virus

EBV is a gammaherpes virus containing a double-stranded DNA genome of ~192kbp, and formally known as human herpesvirus 4 (HHV4). It was first isolated over 50 years ago from a Burkitt's lymphoma sample by Anthony Epstein and Yvonne Barr, and became the first cancer-causing virus discovered to infect humans (Epstein, 2015). EBV DNA is enclosed in an icosahedral capsid, surrounded by a tegument layer rich in viral proteins and finally an outer layer derived from the plasma membrane of the host cell during virus budding (Brown and Newcomb, 2011).

EBV infects B-cells establishing a latent infection which cannot be fully cleared by the body's own defences. Latency is a state in which the virus down-regulates viral gene expression in order to avoid detection by immune cells and establish long-term infection of a cell. Most children are first exposed to the virus in infancy or early childhood, with most individuals becoming asymptomatic carriers.

EBV is listed as a group 1 carcinogen by the World Health Organisation due to its ability to transform B-cells, and it is a listed cause of a growing number of cancers, including Burkitt's lymphoma, Hodgkin's lymphoma, nasopharyngeal carcinoma and gastric carcinoma amongst others.

EBV is now increasingly recognised for its role in multiple sclerosis; associations with other autoimmune diseases (eg. rheumatoid arthritis (RA) and systemic lupus erythematosus (SLE)) have been put forward but are less well associated.

1.5.1 Life Cycle and primary infection

EBV is transmitted orally and first establishes a lytic infection of epithelial cells and local B-cells of the oropharynx. Large amounts of virus are shed in the throat, and newly infected B-cells migrate to local lymphoid tissue where they establish a growth-transforming infection of B-cells and enter a phase of gene expression termed latency III. Some EBV-infected B-cells

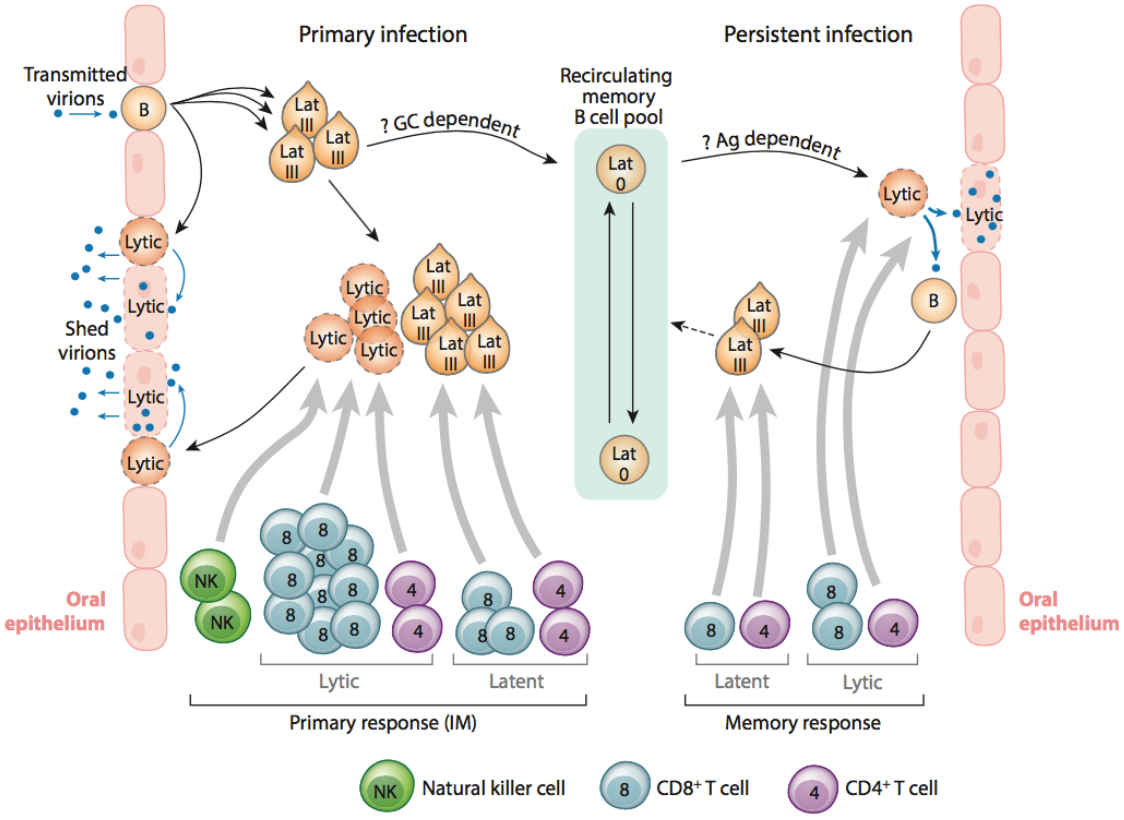

Figure 1.5.1 Epstein-Barr virus life cycle and establishment of latency in the immunocompetent host. EBV is transmitted orally, infecting B-cells and squamous epithelia of the oropharynx with some infected B-cells going on to down-regulate gene expression to avoid immune cell surveillance. Infected B-cells are targeted during primary infection (IM) by NK cells, CD4+ T-cells and large expansions of lytic protein-specific CD8+ T-cells; expansions shrink in the months following IM to leave low but stable levels of EBV-specific cells in the blood of carriers. Blue arrows indicate transfer of infectious virions, black arrows signal transfer or transformation of infected cells, wide grey arrows indicate targets of cellular immune responses. Abbreviations: Ag, antigen; EBV, Epstein-Barr virus; GC, germinal center; IM, infectious mononucleosis; Lat 0, Latency 0; Lat III, Latency III; NK, natural killer. Adapted from Taylor *et al.* (Taylor et al., 2015).

further down-regulating antigen expression to a latency 0 programme, or antigen-negative state, to avoid immune detection.

Latency 0 is maintained long-term in transformed memory B-cells and is characterised by expression of only viral micro RNA (miRNA) and EBV-encoded small RNAs (EBERs), allowing the virus to avoid detection by host CD4+ and CD8+ T-cells. Infected B-cells with latency I phenotype express only EBERs, viral miRNA and EBNA1. Newly infected B-cells and those transformed *in vitro* are characterised by a latency III phenotype and express EBNA 1, 2, 3A, 3B and 3C, LMP1, LMP2A and B proteins and miRNA and EBERs (Rowe et al., 1992, Rowe et al., 2014), making them more easily recognisable by host T-cells. *In vivo*, newly infected B-cells with latency III phenotype rapidly downregulate their latent antigen expression to a latency 0 program to avoid detection by the immune system.

Latently-infected B-cells occasionally become reactivated to produce infectious virions via mechanisms that are unclear but may be initiated by signals in the cellular environment or by differentiation into plasma cells, causing low-level foci of replication and virus production into the oropharynx. Levels of virus production are controlled by immune cells as lytic cells express viral proteins and are rapidly targeted and killed by T-cells and other effectors (Figure 1.5.1). Infected B-cells expressing a latency III program of gene expression are also rapidly killed by immune cells due to viral latent proteins being strong immunogenic targets.

Once acquired, EBV persists as a lifelong latent infection in the memory B-cell pool with restricted viral antigen expression. Latent infection transforms B-cells so that they are able to pass on EBV DNA in episomal form to both daughter cells upon cellular division via EBNA1 (Yates et al., 1985). EBV latency programmes describe the viral antigens expressed in infected B-cells, and this is dependent on many factors including the duration of infection or underlying disease.

B-cells transformed with EBV *in vitro* establish immortalised cell lines termed lymphoblastoid cell lines (LCLs) and are an important tool used to analyse T-cell responses to the virus. LCLs in culture typically have a latency III phenotype and reactivate into lytic cycle at low levels via mechanisms that are unclear. Induction into lytic cycle is triggered by expression of the transactivator protein BZLF1 and knock down of this protein maintains LCLs that are unable to reactivate into lytic cycle and produce virus (Sinclair, 2013, Murata, 2014). Persistence of latently infected B-cells in hosts maintains virus-specific CD4+ and CD8+ T-cell responses throughout life and these can be detected in the blood of virus carriers.

Infectious mononucleosis (IM) is the primary symptomatic infection with EBV, causing significant morbidity in most patients and characterised by four key symptoms which can last up to 6-weeks in duration: sore throat, cervical lymphadenopathy, fever and fatigue (Luzuriaga and Sullivan, 2010). However, the majority of virus conversions are asymptomatic and go unstudied, and most children whose exposure to the virus occurs early do not develop IM; incidence of symptomatic infection increases with age at first exposure (Balfour et al., 2013). Symptoms of IM are thought to be caused by large expansions of immune cells observed in the blood of patients, and these expansions include immune cell subsets such as NK cells (CD3-CD56+), CD4+ T-cells (CD3+CD4+) and CD8+ T-cells (CD3+CD8+).

The role for NK cells in IM remains unclear, but evidence from humanised mouse models of EBV infection have identified a population of early differentiated NK cells that expand and target virus-infected cells in the blood, appearing before expansions of CD8+ T-cells (Chijioke et al., 2013). Circulating numbers of this early, undifferentiated subset of NK cells have also been found by another study to reduce in number with age, indicating their potential role in protecting against EBV infection and IM in children (Azzi et al., 2014).

CD4+ T-cell responses during IM are significantly expanded but at much lower levels than seen in the CD8+ T-cell compartment, and with a greater proportion of responses directed

against latent proteins of EBV. CD4+ T-cell responses to the latent protein EBNA1 however have been showed to be delayed, and only become detectable 3-6 months following primary infection for reasons that are unclear; EBNA1-specific antibody responses also reflect this pattern (Long et al., 2013). Circulating EBV-specific CD4+ T-cell numbers have been shown to correlate with viral load over time in IM, and CD4+ T-cell expansions shrink to those of normal, low levels typical of long-term virus carriers following disease resolution (Long et al., 2013, Precopio et al., 2003). CD4+ T-cell responses to EBV proteins are maintained throughout life by the persistence of EBV-infected B-cells, and responses to a variety of antigens can readily be detected in the blood of virus carriers. A summary of CD4+ T-cell responses to EBV proteins can be found in Figure 1.5.2.

The expansion of CD8+ T-cell responses to EBV in IM is dramatic, with some lytic epitope-specific responses constituting up to 50% of peripheral CD8+ T-cells (Abbott et al., 2013). The majority of expanded CD8+ T-cells in IM are directed against lytic antigens; latent antigen specificities have been estimated to represent ~5% of the CD8+ T-cell pool during IM (Hislop et al., 2005). These responses, as for CD4+ T-cells, shrink over time to levels found in healthy virus carriers and continue to control reactivation of infected B-cells into lytic cycle throughout life. EBV-specific CD8+ T-cell responses are maintained following seroconversion throughout life; size and antigen specificity of responses are largely dependent on the HLA type of the host. A summary of CD8+ T-cell responses to EBV antigens can be found in Figure 1.5.2.

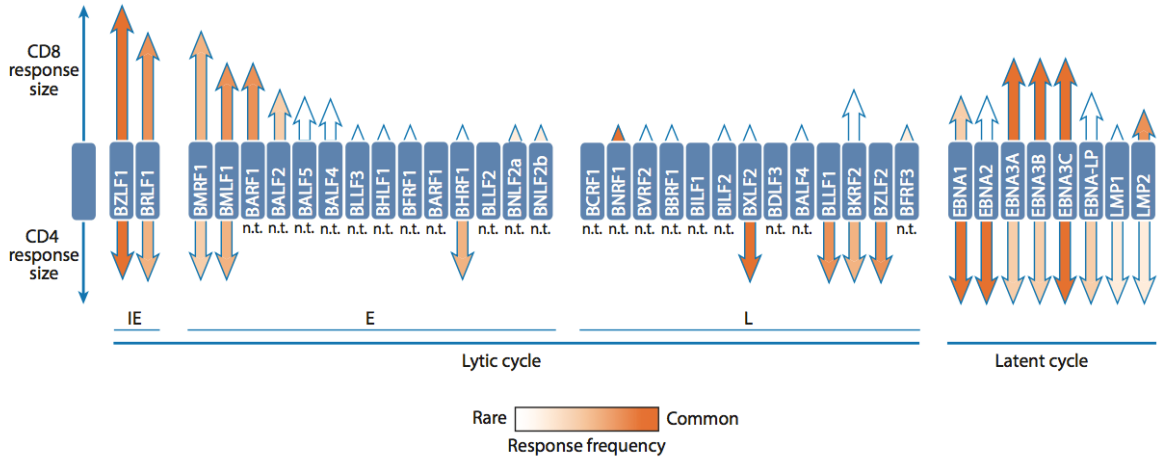

Figure 1.5.2 CD4+ and CD8+ T-cell responses to EBV latent and lytic proteins. Summary of known CD4+ (bottom) and CD8+ (top) T-cell responses to EBV proteins: 2 immediate early (IE), 14 early (E), 13 late (L) and to 8 latent proteins. Results from comparative studies of CD4- or CD8-depleted PBMC from >30 Caucasian donors screened against peptide pools spanning the sequence of each EBV protein using IFNγ ELISpot assays. Height and depth of arrows indicate mean size of response in CD8+ and CD4+ T-cells respectively relative to other proteins. Arrow shading indicates how common responses are amongst subjects in cohorts, with dark red indicating frequent responses and colourless arrows representing rare responses. CD8+ scale is larger than that of CD4+ responses and reflects the generally 10-20-fold difference in size between these subsets. E, early; EBNA, EBV nuclear antigen; EBV, Epstein-Barr virus; IE, immediate early; L, late; LMP, latent membrane protein; n.t., not tested. Figure adapted from Taylor *et al.* (Taylor et al., 2015).

1.5.2 Epstein-Barr virus and multiple sclerosis

EBV has long been known to be associated with autoimmune diseases, the most convincing evidence supporting an association with MS (Ascherio and Munger, 2010). MS is very rare in individuals not infected with the virus; almost 100% of MS patients are seropositive for EBV compared with ~90% of healthy, age-matched controls (Pakpoor et al., 2013). These findings are mirrored in paediatric cohorts where children with MS show significantly increased EBV infection rates compared to healthy controls (Pohl et al., 2006, Alotaibi et al., 2004, Banwell et al., 2007). Long-term study of seronegative individuals in one particular cohort showed no cases of MS development before acquisition of the virus (Levin et al., 2010), further supporting EBV's role as a causal factor.

In addition to EBV carriage increasing risk of MS, results from serology have shown a correlation with antibody IgG titres directed against the latent protein EBNA1 and EBNA complex with MS risk. EBNA complex consists of several viral proteins that associate to form a functional unit in the virus lifecycle, and includes EBNA1, EBNA2, EBNA3 proteins and EBNA leader protein (EBNA-LP). Results from the US military serum repository analysing large numbers of subjects have shown elevated anti-EBNA1 antibodies to increase risk of MS by 8-fold, and inflated anti-EBNA complex IgG to increase risk 36-fold compared to those with lower levels (Munger et al., 2011, Levin et al., 2005).

Studies investigating antibody responses to EBV antigens are numerous and have used several different MS patient cohorts, and it is widely accepted that elevated anti-EBNA1 IgG and anti-EBNA complex IgG titres are a feature of multiple sclerosis and have potential use as diagnostic markers (Ascherio et al., 2001, Sundstrom et al., 2004, Levin et al., 2005, DeLorenze et al., 2006). However, it is not clear whether these elevated antibody responses to EBV antigens in MS patients are involved in development of disease or are an effect of MS disease

itself, and without an accepted mechanism of how EBV contributes towards development it is difficult to draw conclusions.

Correlation of anti-EBNA antibody responses with increased risk has also been shown to be independent of risk conferred by the HLA-DR15 allele (De Jager et al., 2008), the strongest genetic predictor of MS, indicating that elevated EBNA1 IgG are not driven by this haplotype and suggesting that the two contributing factors influence development of MS separately.

Two studies investigating a relationship between EBV serology and disease activity in patients have been carried out with different results. Farrell *et al.* found the number of gadolinium-enhancing lesions and disability scores to be positively correlated with EBNA1 IgG titres but not with virus capsid antigen (VCA) IgG titres (Farrell et al., 2009). Zivadinov *et al.* showed that anti-VCA IgG titres were linked to loss of brain volume in a cohort of 50 MS patients over a 3-year period (Zivadinov et al., 2009). VCA is a complex made up from BALF4 (gp125) and p160 (Pearson, 1988), and antibody responses to VCA have been reported to be elevated in MS patient sera and CSF compared to controls (Castellazzi et al., 2010, Zivadinov et al., 2009).

The majority of one cohort's EBNA1 antibody responses were mapped to the glycine-alanine repeat, suggesting that this region has high immunogenicity (Ruprecht et al., 2014). Further mapping of antibody responses from paediatric cohorts to specific regions of the EBNA1 protein have revealed a broader specificity of responses with antibodies reacting to many regions (Lunemann et al., 2008a); this effect that has also been observed in CD4+ T-cell responses to EBNA1 of adult MS patients (Lunemann et al., 2006).

As well as extensive studies on EBNA1 and EBNA complex serology, other antibody responses to EBV proteins have been investigated in the context of MS, with early reports from the 1980s observing an elevation in anti-capsid antigen IgG titres among patients (Larsen et al., 1985, Sumaya et al., 1985). More recently, elevated IgG titres have also been found in patients against certain lytic protein antigens; Lindsey *et al.* found a broad increase in titres

with reactivity to EBV early antigens, but neutralising antibody responses to the virus capsid antigen gp350 were unchanged between MS patients and controls (Lindsey et al., 2010). A modest increase in IgG responses to the immediate early BZLF1 protein has been shown in one cohort (Massa et al., 2007), and a more in depth analysis by Dooley *et al.* screened MS patient sera for reactivity to 28 EBV latent and lytic proteins, with only three exhibiting an elevated titre compared to healthy seropositive controls. EBNA1 showed the strongest association, with BFRF3 – a major structural protein – and BRRF2 also showing increased responses compared to controls (Dooley et al., 2016).

Serology from the CSF is more difficult to analyse, and diagnosis often uses the presence of OCB which are present in 95% of MS patients. However, OCB are also present for other diseases affecting the CNS such as infections and their analysis is semi-quantitative, making them subject to interpretation. No consensus has been reached on the antigen specificity of OCB in MS patient CSF, with conflicting results from different research groups. A study using epitope mapping and a brain-tissue derived cDNA library mapped the two most frequent responses in MS OCB to EBNA1 and BRRF2 proteins of EBV (Cepok et al., 2005), and these findings agree with those previously found in a different cohort suggesting that CSF levels of anti-EBNA1 IgG are elevated in patients (Bray et al., 1992). In contrast a study from the Netherlands showed there to be no evidence of intrathecal anti-EBNA1 IgG synthesis in their cohort (Jafari et al., 2010).

Conflicting data regarding EBV serology in MS make it difficult to draw conclusions regarding the role of antibodies in disease development. However, differences between patient cohorts and variation in technique and sensitivity of experimental techniques may all contribute to this variation, and more standardised research is needed regarding EBV-specific antibody responses to address this. EBV infection rates and serology strongly implicate a role for EBV

in the development of MS, but despite this mounting aetiological and serological evidence no consensus has been reached regarding how this might occur.

1.5.3 T-cell responses to EBV in MS

Cellular responses to EBV have been extensively studied in MS patients, with the aim of correlating these with the serology of patients. There have been conflicting reports on whether cellular immunity to EBV is unchanged, increased or decreased in MS patient blood, and with an unclear picture surrounding virus-specific T-cell responses it is difficult to unravel EBV's contribution to disease development. However, elevated risk of developing MS following IM suggests a role for perturbation of immune responses to EBV in the disease process. As previously described, the EBV-specific T-cell compartment expands and becomes dysregulated during IM, and it is possible that T-cell events during this process contribute towards MS pathogenesis after disease convalescence.

Ex vivo T-cell responses to LCLs can be measured for cytokine production allowing frequency and phenotype of circulating cells specific for EBV antigens to be measured accurately. Early studies in the 1980s observed a reduced cytotoxicity of MS patient lymphocyte cultures as measured by their inability to control outgrowth of LCLs *in vitro*, suggesting an impaired control of viral replication in patient cells (Fraser et al., 1979, Craig et al., 1983). More recent studies investigating T-cell responses to LCL found no difference in cytokine production by CD4+ or CD8+ subsets between patients and controls. Lindsay *et al.* observed a reduced proliferative capacity in patient T-cells but these effects did not reach significance (Lindsey and Hatfield, 2010). However, patients in the study were on IFNβ or glatiramer acetate therapy which may confound results, and whilst these treatments do not have a direct immunosuppressive effect on T-cells they do have immunomodulatory properties (Dhib-Jalbut

and Marks, 2010, Racke et al., 2010). Cepok *et al.* also investigated T responses to EBV latent proteins in MS patients and found CD4+ responses to be unchanged between groups but an elevation in CD8+ T-cell responses (Cepok et al., 2005); studies from a Danish patient cohort showed increased T-cell responses to two MHC class I-restricted epitopes from EBNA3A and LMP2 proteins from EBV (Hollsberg et al., 2003).

Investigation of EBV-specific T-cell responses in the CSF is of key interest as this is closest to the tissue affected in MS. Several groups have reported a reduced T-cell response to LCL and have consistently shown circulating CD8+ T-cell responses to be decreased in MS patients (Pender et al., 2009, Pender et al., 2017, Jilek et al., 2012). However, other studies have shown CD8+ T-cell responses to be intrathecally enriched for EBV specificity, and some researchers argue that this suggests a lack of control of viral replication with infiltration of infected cells in the CNS (Jaquiery et al., 2010).

Higher frequencies of autologous LCL-specific CD4+ and CD8+ T-cells were also detected in the CSF of MS donors by van Nierop *et al.*, and CNS-derived CD8+ T-cells were further characterised to reveal oligoclonal expansions with specificity for EBV lytic proteins (van Nierop et al., 2016b).

Interestingly an increased frequency of EBNA1-specific CD4+ T-cells in MS patient blood was reported by Lunemann *et al.*, with responses also showing a broadened range of epitope specificities to the antigen with the majority of epitopes belonging to the C-terminal of the protein (Lunemann et al., 2006); these findings are interesting and tie in with widely accepted elevated EBNA1-specific IgG serology.

Cellular responses to EBV are still widely debated in the MS field, hindering development of a consensus mechanism for the virus's contribution to disease. However, five general theories exist which are described below.

1.5.4 Proposed mechanisms of EBV's role in MS

The first theory derives from data investigating post-mortem brain samples and suggests that immune cell attack on CNS-infiltrating EBV-transformed B lymphocytes causes bystander damage and inflammation to brain tissue. Serafini *et al*. described ectopic B-cell follicles formed in the meninges of post-mortem brains from SPMS samples, suggestive of specific CNS infiltration of EBV infected B-cells in MS as these structures were not found in the brains of patients with other neurological diseases (Magliozzi et al., 2007, Serafini et al., 2007, Serafini et al., 2017). Activation of innate immune mechanisms such as IFNα production by microglia and macrophages were also found in active MS lesions by Tzartos *et al.* and coincided in areas staining positive for EBERs (Tzartos et al., 2012). However, these results and theory of bystander activation in MS brain lesions are not accepted as consensus due to a lack of independent verification (Lassmann et al., 2011).

The second theory, based on reports of increased viral load in MS patients detected by some studies, suggests dysregulation of T-cell responses to EBV contributes towards disease development by allowing EBV-infected B-cells to gain access to the CNS (Lunemann et al., 2010). Viral load in PBMC is used as a crude measure of EBV reactivation in individuals, and those with a high copy number of virus genomes have generally either recently acquired the virus, are suffering from symptomatic primary infection (IM) or have ineffective control of virus replication. However, these reports of decreased EBV-specific T-cell responses are contradicted by other studies which found no difference compared to healthy controls (Cocuzza et al., 2014, Wagner et al., 2004, Lindsey et al., 2009, Santiago et al., 2010, Alvarez-Lafuente et al., 2006, Lucas et al., 2011).

Other autoimmune diseases such as systemic lupus erythematosus have been shown to have an increased EBV load. However, this is thought to be an effect and not a cause of disease, and is

attributed to activation of B-cells due to underlying autoimmunity and exhaustion of CD8+ T-cells, rather than a specific causal role for the virus in lupus pathogenesis (Moon et al., 2004, Larsen et al., 2011).

The third theory suggests that EBV-transformation rescues B-cells that are specific for autoreactive epitopes, ensuring their survival from tolerance mechanisms. These self-reactive B-cells have been hypothesised to survive tolerance mechanisms by EBV-transformation, and are able migrate to the CNS of MS patients in an environment with impaired EBV-specific CD8+ T-cell responses. It could also be argued that intrathecal enrichment of EBV-specific CD8+ T-cell responses is due to infiltration of EBV-infected B-cells in the CNS (Jaquiery et al., 2010). Research showing a diminished cellular response to EBV has been published since the 1980s but despite this the theory is not accepted as consensus (Pender et al., 2009, Pender et al., 2017, Jilek et al., 2012, Craig et al., 1983, Craig et al., 1988).

However, other research groups have found peripheral CD8+ T-cell responses to be unchanged or increased in frequency in MS patients (Lindsey and Hatfield, 2010, Jilek et al., 2008) and, combined with analysis of EBV-infected B-cell pools, provides no evidence for enrichment of autoantigen specificity (Tracy et al., 2012). Doubt has therefore been cast on EBV "rescue" of autoreactive B-cells a plausible mechanism for MS pathogenesis.

The fourth theory surrounds mistaken self, and suggests that EBV infection and transformation of B-cells causes the up-regulation of self-antigens, which in turn become the target of autoreactive CD4+ T-cell responses in MS patients. Supporting this theory is the observation that virally-infected B lymphocytes upregulate expression of αB-crystallin (CRYAB) *in vitro* (van Sechel et al., 1999). Further studies have gone onto confirm expression of CRYAB in active brain lesions of MS patients and as a target of T-cell responses (van Noort et al., 1995, van Noort et al., 2010, Bajramovic et al., 1997). CRYAB has been identified as the target of pathogenic CD4+ T-cell responses secreting T_H1-type cytokines (Chou et al., 2004).

However, reports of the effect of free CRYAB peptide on T-cell responses in MS have suggested a role for the protein in tolerisation of autoreactive responses, and a clinical trial administering "sub-immunogenic" amounts of intravenous CRYAB protein to RRMS patients have reported beneficial results after 9 months of therapy (van Noort et al., 2015). Experimental autoimmune encephalomyelitis (EAE) models also produced similar results of tolerisation when CRYAB administered to animals with a pre-established T-cell response to the autoantigen (Verbeek et al., 2007). Quach *et al.* reported CRYAB peptide to have a repressive effect on pathogenic CD4+ T-cell cytokine production *in vitro* (Quach et al., 2013), and this may be due to free peptide antigen inducing anergy in autoreactive T-cells. Further studies are needed to establish the effect of CRYAB epitope processing and presentation on MHC molecules.

As well as CRYAB, studies have shown other self-antigens to be up-regulated in B-cells upon EBV infection and these proteins have drawn interest from researchers in several different fields including autoimmunity and EBV-driven cancer. Long *et al.* showed that LCL-reactive CD4+ T-cells could not be mapped by specificity to any known EBV antigens, suggesting that they were specific for self-antigens up-regulated by EBV-transformation. The identified non-EBV antigen restricted CD4+ T-cells were also able to kill LCLs *in vitro* (Long et al., 2009). Despite lack of characterisation, previous studies have also shown CD4+ T-cells in LCL-stimulated polyclonal T-cell lines that have no known reactivity to EBV epitopes to have cytotoxicity against LCLs (Haque et al., 2002, Comoli et al., 2002), further supporting the presence of CD4+ T-cell responses generated against a host of self-proteins up-regulated upon EBV infection and transformation of B-cells.

The fifth theory suggests that molecular mimicry between virus and neuronal antigens is responsible for the CNS tissue damage observed in MS patients, and is discussed in detail in the following section.

1.5.5 Molecular mimicry in EBV-induced T-cell responses

The theories described above do not fully explain important epidemiological and clinical observations reported in recent studies of MS patients, which need to be taken into account when constructing a mechanism linking EBV to MS.

There are several arguments against the hypothesis that MS arises from uncontrolled EBV infection, the first being that MS is not a reported complication of patients undergoing immunosuppressive therapy after post-transplant lymphoproliferative disease (PTLD), and other conditions such as chronic active EBV or X-linked lymphoproliferative disease patients do not experience neurological symptoms or MS-like disease. Immunosuppression is in fact used to treat MS and, were uncontrolled infection the cause of MS, such therapy would exacerbate symptoms.

It is also apparent that MS symptoms take at least months or even years to develop following acquisition of EBV, findings demonstrated by Levin *et al*. (Levin et al., 2010) and supported indirectly by a lack of MS cases in individuals who have recently experienced IM (Yea et al., 2013). If uncontrolled infection were the cause of MS then at least a proportion of patients suffering from symptomatic primary infection would develop neurological symptoms upon acquiring the virus. In addition to this, studies of EBV load in serum or PBMC of MS patients have only reported a modest increase (Wagner et al., 2004, Buljevac et al., 2005, Lindsey et al., 2009), a contrast to the high viral loads observed during IM and viral reactivation in patients with PTLD (Gartner et al., 2002).

Natalizumab is a monoclonal antibody that prevents migration of T-cells into the CNS by blocking $\alpha 4\beta 1$ integrin and has been shown to be an effective immunomodulatory therapy for MS (Polman et al., 2006). Prevention of T-cell entry into the CNS would therefore exacerbate disease if uncontrolled EBV infection was one of the contributing factors of MS development.

Observations from the clinical efficacy of rituximab, a monoclonal anti-CD20 antibody, have also shown the role of B cells in MS to be more complex than just production of antibodies. Plasma cells are responsible for antibody production but no longer express the marker CD20, and are therefore are not directly depleted by rituximab therapy. Rituximab has been shown to reduce relapse rates in MS patients within a few weeks of treatment initiation and before antibody titres are reduced, suggesting that B-cells may contribute towards MS pathogenesis in other ways, such as antigen presentation or cytokine production (Hauser et al., 2008, von Budingen et al., 2011, Lisak et al., 2012). This clinical observation also implies that production of autoreactive antibodies is not the sole contribution of B-cells to MS development, and suggests that clinical efficacy of rituximab would be less rapid if rescue of autoreactive B-cells was one of the major mechanisms driving MS disease.

Elevated EBV antibody titres have also been strongly linked to risk of developing MS in young adults, such as those specific for EBNA complex and EBNA1 (Ascherio et al., 2001), and is an effect that has been confirmed by several independent studies (Sundstrom et al., 2004, Levin et al., 2005, DeLorenze et al., 2006, Munger et al., 2011). Elevated antibody titres are not immediately present in initial infection but take several months to become elevated, consistent with the delayed onset of MS after primary infection (Levin et al., 2010) and also delayed development EBNA1-specific antibody and CD4+ T-cell responses (Long et al., 2013). This delayed onset of MS symptoms following EBV infection and the strong genetic association with HLA-DR15 is suggestive of disease that is driven by the immune response to EBV, rather than uncontrolled viral replication.

Considering all of these arguments, we therefore sought to investigate an alternative mechanism linking EBV with MS development which is (so far) not strongly contradicted by clinical and epidemiological studies.

The most reasoned theory currently explaining EBV's role in MS development is molecular mimicry. Here, infection with EBV induces T-cell responses – most likely CD4+ – which recognise both EBV and CNS epitopes displayed by MHC molecules. Strong evidence for elevated anti-EBNA1 IgG in MS patient sera, coupled with work by Lunemann *et al.* describing an increased and broadened CD4+ T-cell response to the protein (Lunemann et al., 2006), has made EBNA1 the focus of most investigations into cross-reactivity of EBV-specific T-cell responses.

Lunemann *et al.* found a population of expanded T_H1 CD4+ T-cells with mixed central memory and effector memory phenotype in MS patients which were further characterised and revealed to have higher reactivity to a pool of myelin peptides and co-produce IFNγ and IL-2. CNS proteins included in the pool were myelin basic protein (MBP), proteolipid protein (PLP), myelin oligodendrocyte glycoprotein (MOG), and 2',3'-cyclic nucleotide 3'-phosphodiesterase (CNP) (Lunemann et al., 2008b). Increased polyfunctionality of this cross-reactive, EBNA1-specific CD4+ T-cell population suggests chronic antigen stimulation like that seen in controlled, latent viral infections.

Less work has been completed at the single cell level, however there are several examples of EBV antigen-specific CD4+ T-cells which also display reactivity to a specific myelin epitope. BALF5 is an EBV protein with DNA polymerase activity, and CD4+ T-cells specific for this protein have been shown by two research groups to cross-react with an epitope found in the neuronal antigen MBP. Lang *et al.* structurally modelled a TCR from an MS patient with reactivity to both MBP (85-99) and BALF5 (627-641), restricted by HLA-DR15 (HLA-DRB1*15:01) and HLA-DR51 (HLA-DRB5*01:01) respectively (Lang et al., 2002). This finding, coupled with the epitope restriction to the allele conferring highest risk for MS, supports a role for EBV inducing degenerate responses that are able to react with structurally similar peptide:MHC complexes from EBV and the CNS. Further work by Holmoy *et al*. found

BALF5/MBP-specific CD4+ T-cells to be specifically enriched in the CSF of a MS patient compared to a matched blood sample, indicating tissue specific homing of the cross-reactive T-cell to the CNS (Holmoy et al., 2004).

Despite evidence of cross-reactivity between EBV and neuronal epitopes from these studies no new examples of this phenomenon have been published in several years, and further investigation is warranted regarding this mechanism in the context of MS.

1.6 Scope of thesis

EBV's contribution to the development of MS is critical, as demonstrated by epidemiological and serological evidence. It is therefore of key clinical importance that we understand the immune mechanisms involved in disease pathogenesis in order to develop better therapies for MS. This thesis explores the broad immune responses to EBV in healthy controls, individuals with a recent history of IM and MS patients, investigating viral load, antibody responses, CD4+ and CD8+ T-cell responses to latently-infected B-cells. Cross-reactivity of cellular responses to EBV were investigated using a panel of novel modified Vaccinia Ankara (MVA) viruses which have been engineered to express CNS proteins.

2 Methods

2.1 Tissue Culture

2.1.1 Tissue culture media and reagents

RPMI-1640 – Roswell Park Memorial Institute-1640 medium supplemented with 2mM L-glutamine (Sigma)

DMEM – Dulbecco's Modified Eagle's medium (Sigma)

IMDM – Iscove's Modified Dulbecco's medium (Gibco)

B-cell blast media – IMDM, 10% HuS, IL-4 (100IU/mL), $5.5x10^{-7}$ cyclosporin A, 1% penicillin-streptomycin solution (Gibco), 2mM L-glutamine

T-cell media – RPMI 8% FCS, 1% HuS, 30% MLA-144 supernatant (filtered), IL-2 50IU/mL

Opti-MEM (Gibco)

Foetal calf serum (FCS) (Gibco)

Human serum (HuS) (Corning) derived from male, AB+ donors, virus and mycoplasma tested

Express Trypsin (Gibco)

Penicillin-Streptomycin 100x stock (Gibco) 500IU/mL penicillin and 5000µg/mL streptomycin

L-glutamine (Gibco) 100x stock (200mM)

Phosphate buffered saline (PBS) made up in house using 10xPBS tablet (Oxoid) per litre of distilled water (KCl 2.68mM, KH_2PO_4 1.47mM, NaCl 136.89mM, Na_2HPO_4 8.10mM), sterilised by autoclaving (20mins at 121°C)

MACS buffer – 0.5%, BSA, 2mM EDTA in distilled water and sterilised by autoclaving (20mins at 121°C)

Paraformaldehyde (PFA) (Sigma)

Saponin extract from quillaja bark (Sigma)

IL-2 – Recombinant interleukin-2 (Peprotech) stock made up in 1% BSA PBS at 10^5IU/mL

IL-4 – Recombinant interleukin-4 (Peprotech) stock made up in 1% BSA PBS at 10^5IU/mL

IL-7 – Recombinant interleukin-7 (Peprotech) stock made up in 1% BSA PBS at 10^5IU/mL

MLA-144 – Monkey Leukocyte Antigen-144 cell line supernatant, filtered, grown in-house and originally obtained from the ATCC

Lymphoprep (Cedar Wood)

Dimethyl sulphoxide (DMSO) (Sigma)

Staphylococcal enterotoxin B (Sargsyan et al.)

TNFα processing inhibitor (TAPI-0) (Enzo Life Sciences)

2.1.2 Peptides and peptide pools

Peptides were synthesised by Alta Biosciences and dissolved in DMSO to obtain a concentration of 5mg/mL and stored at -20°C. Overlapping peptide pools were obtained from JPT (PepMixes) and consisted of 15mers overlapping by 11 amino acids. Pools were reconstituted in DMSO at 250µg/mL and stored at -20°C.

2.1.3 PBMC isolation from whole blood and plasma collection

Peripheral blood was collected from donors into 9mL vacuum tubes containing Lithium heparin (Grenier Bio One) and diluted 1:1 with warm RPMI. 35mL blood/RPMI was then layered onto 15mL lymphoprep in 50mL falcon tubes and centrifuged for 30 minutes at 900G with brake off. Lymphocyte layer was aspirated off and the cells washed with RPMI twice. Cells were either used immediately or frozen down (Chapter 2.1.6). Plasma was harvested from above the lymphocyte layer as a 1:1 mix of plasma:RPMI and frozen down immediately for later use.

2.1.4 Generation of B-cell blast cultures from whole PBMC

L-CD40L cells (ATCC) were cultured in DMEM supplemented with 8% FCS to ~90% confluency before being trypsinised (0.00625% (w/v) Trypsin in EDTA), washed and irradiated (100 Grays) before being seeded into 6-well tissue culture plates and incubated for 6 hours at 37°C at 5% CO_2 to allow adhesion to plates. Donors' PBMCs were re-suspended in B-cell blast medium at a concentration of $1.7x10^5$ cells/mL. Supernatant was aspirated off irradiated L-CD40L cells and the re-suspended PBMCs were added dropwise onto the feeder layer (~$5x10^6$ cells/well). At 3 day intervals expanding B-cell blasts were layered onto fresh L-CD40L monolayer in fresh medium. At day 14 expanded B-cell blast populations were ready for use in further experiments or frozen in freezing medium and subsequently thawed at a later date (protocols as 2.1.6 and 2.1.7).

2.1.5 Generation of lymphoblastoid cell lines

Wild type LCL

$5x10^6$ PBMC were re-suspended in 5mL of filtered B95.8 cell line supernatant and incubated overnight at 37°C, 5% CO_2. The following day cells were washed and re-suspended in RPMI-1640 supplemented with 10% FCS and 1µg/mL cyclosporin A and put into one well of a 24-well plate; cells were monitored for B-cell transformation over 2 weeks. Cells were then bulked up until they could be maintained in a T25 tissue culture flask in RPMI-1640 8% FCS.

BZLF1 KO LCL

293 cells containing the BZLF1 KO construct were a gift from Henri-Jacques Delecluse and have been described previously (Feederle et al., 2000). Method was as described above for B95.8 LCL generation using supernatant from the 293-BZLF1 KO cells harvested after transfection with BZLF1 construct to induce lytic cycle in the replication deficient cell line.

2.1.6 Cryopreservation

Cells to be frozen in liquid nitrogen were centrifuged and re-suspended in freezing medium (RPMI-1640, 40% FCS, 10% DMSO) and transferred to cryovials (Nunc). "Mr Frosty" containers were used to gradually cool specimens by 1 degree per minute to -80°C before transferring samples to liquid nitrogen freezers.

2.1.7 Thawing of cryopreserved cells

Cryovials were placed into a 37°C water bath to thaw, washed twice with RPMI-1640 10% FCS before being re-suspended in appropriate media. Cells were then cultured in an incubator (37°C, 5% CO_2).

2.1.8 Mycoplasma testing

All cell cultures were routinely tested for mycoplasma using a Mycoalert kit (Cambrex) according to the manufacturer's protocol.

2.2 Generation of recombinant MVA virus panel

2.2.1 Construction of plasmids with central nervous system protein inserts

Plasmids containing CNS protein inserts under control of the bacteriophage T7 promoter were made prior to this project by Yolanda van Wijck (van Wijck, Y. (2011) *Construction of recombinant MVAs encoding CNS proteins and testing the MVA-T7 system with EBNA1-specific T-cells.* MSc internship unpublished thesis. Vrije Universiteit, Amsterdam, The Netherlands and the University of Birmingham, UK.) and Marye Hogenboom (Hogenboom, M. (2012) *Cloning of CNS proteins as cross-reactive targets for EBNA1-specofoc T-cells of MS patients.* MSc internship unpublished thesis. Vrije Universiteit, Amsterdam, The Netherlands and the University of Birmingham, UK.).

2.2.2 Recombination of MVA viruses with plasmids expressing CNS proteins

BHK21 cells were cultured to ~90% confluency and infected with wild type MVA at a MOI of 0.1 in PBS supplemented with 1% FCS; infected cells were incubated at 37°C, 5% CO_2 for 90 minutes, rocking every 30 minutes. Lipofectamine 2000^{TM} was used to transfect recombinant plasmid DNA (protocol as Lipofectamine 2000^{TM} guidelines) containing CNS protein sequences into wild type MVA-infected BHK21 cultures (protocol as Chapter 2.2.4) and incubated for 4 hours to generate recombinant virus. DMEM supplemented with 2.5% FCS was added and the cultures monitored for CPE for 48-72 hours. Once 90-100% CPE had been achieved the cells were harvested, freeze-thawed three times and sonicated. The virus preparations were then used to infect BHK21 cells at a MOI of 0.1 in 1%FCS PBS, and

infections were incubated for 4 hours at 37°C, 5% CO_2, after which 2.5% FCS DMEM was added to the cultures. After 3 days GFP-positive recombinant plaques were picked with a pipette tip under a fluorescent microscope and used to inoculate 250μL PBS (1% FCS). The inoculated PBS was used to infect a further monolayer of 80-90% confluent BHK21 cells, and successive rounds of plaquing were carried out until WT (GFP-negative) plaques were no longer observed. The purified recombinant virus plaques were then amplified in BHK21 cells by infecting confluent cultures at larger increments, freeze thawing and sonicating the virus between each stage. The final amplification step in BHK21 cells was used to produce virus stock reagents, which were used throughout this project for all experiments. A list of recombinant MVA viruses is listed in Table 2.1.

Table 2.1 List of generated recombinant MVA viruses

Recombinant CNS MVA	**Full name of recombinant protein inserts**
Empty vector	pYWK
CNP	2',3'-cyclic nucleotide 3' phosphodiesterase
Contactin-2	
MAG	Myelin associated glycoprotein
MOG	Myelin oligodendrocyte glycoprotein
PLP	Proteolipid protein
MBP	Myelin basic protein
MBP V8	Myelin basic protein variant 8
MOBP	Myelin-associated oligodendrocyte basic protein
CRYAB	Alpha-B crystalline
Claudin-11	
Tal-H	Transaldolase-H
EBNA1	Epstein-Barr virus nuclear antigen 1

2.2.3 Titration of MVA virus stock

Virus stocks were prepared as described in Chapter 2.2.2. Prepared virus stock was serially diluted from 10^{-2} to 10^{-9} in PBS 1% FCS and 500μL each dilution used to infect at least 2 wells (6-well plate) of 80-90% confluent BHK21 cells before incubating at 37°C, 5% CO_2 for 4 hours, rocking plates every hour to ensure cultures do not dry out. After 4 hours virus preparation was aspirated off and 3mL of semi-solid virus overlay was added slowly to each well (DMEM 2.5% FCS, 2.5% carboxymethyl cellulose), and plates were incubated at 37°C, 5% CO_2 for 3 days. After 3 days, infected BHK21 cells were observed under a fluorescent microscope and the GFP-positive virus plaques counted. The lowest dilution at which GFP-positive plaques could be observed was used to calculate titre for each MVA virus stock.

2.2.4 MVA infection of cells for use in Western blotting and stimulation assays

Cell lines were washed in 1% FCS media twice and re-suspended in residual volume. T7 polymerase MVA and CNS MVA were added to cells at a MOI of 10 and 5 respectively, before incubating at 37°C, 5% CO_2 for 4 hours, re-suspending cells every hour. For cellular stimulation assays, following incubation cells were washed twice with sterile 1% FCS medium and re-suspended in 8% media containing cells to be stimulated. For Western blots, infected cells were re-suspended in 2.5% FCS media and incubated for 24 hours at 37°, 5% CO_2, after which cells were washed twice in PBS and cell pellets prepared as Chapter 2.4.1.

2.3 Cellular and immunological assays

All tissues that required long-term culture were kept sterile with experiments performed in a microbiological safety cabinet (class II).

2.3.1 Intracellular cytokine staining of PBMC

PBMCs were washed in RPMI 8% FCS and re-suspended before being added to separate FACS tubes with various stimuli: Staphylococcal enterotoxin B (SEB) (0.2μg/mL), autologous wild type LCL (B95.8 LCL) (ratio 1:1), autologous BZLF1 KO LCL (ratio 1:1) or EBNA1 peptide mix (JPT) (1μg/mL). Brefeldin A (Sigma) (10μg/mL) was added after 1 hour and cells incubated overnight at 37°C, 5% CO_2. No overnight toxicity was observed from incubating cells with the concentration of Brefeldin A indicated. The following morning samples were washed twice in cold PBS and re-suspended in residual liquid. Surface stain antibodies (Table 2.2) were added and cells were mixed before incubating for 30 minutes on ice. Following incubation, cells were washed once with cold PBS and once with cold MACS buffer and re-suspended in residual volume. 0.4% paraformaldehyde (Sigma) was added to samples before cells were incubated at room temperature (RT) in the dark for 30 minutes. Samples were then washed twice with cold MACS buffer and 0.5% saponin (Sigma) was added to samples and they were incubated in the dark at RT for 5-10 minutes. Intracellular antibodies (Table 2.2) were added and samples were incubated for 30 minutes in the dark at RT. Samples were then washed twice with cold MACS buffer and run on a LSR II flow cytometer (BD Biosciences) that day.

Table 2.2 List of antibodies used in ICS of PBMC

Surface antibodies	
CD3 APC-Cy7	Cambridge Bioscience
CD4 PE-Cy7	eBioscience
CD8 PerCP-Cy5.5	eBioscience
CD14 PECF594	BD Biosciences
CD19 PECF594	BD Biosciences
Viability Live/Dead Red	Life technologies
Intracellular antibodies	
IFNγ FITC	Cambridge Bioscience
IL-2 PE	Cambridge Bioscience
IL-17 Pacific Blue	Cambridge Bioscience
GM-CSF APC	Cambridge Bioscience

2.3.2 Generation of polyclonal T-cell lines

PBMC were recovered from freezing and washed twice in RPMI 2% HuS. PBMC were then re-suspended in RPMI 8% HuS supplemented with IL-7 (1ng/mL) containing irradiated autologous wild type LCL (40:1) or autologous B-cell blasts infected with MVA EBNA1 (protocol as Chapter 2.2.4) (10:1). PBMCs were plated out at $2x10^6$ cells/well in 24-well plates and incubated for 7 days at 37°C, 5% CO_2. On day 7 cultures were re-stimulated with the same stimulus, re-suspended in T-cell medium at the same concentration and incubated at 37°C, 5% CO_2. Polyclonal T-cell lines were incubated for a total of 2 weeks before T-cell cloning or 4 weeks before screening by ICS against MVA CNS-infected B-cell blasts.

2.3.3 T-cell cloning techniques

All T-cell cloning methods used polyclonal T-cell lines generated according to the protocol outlined in Chapter 2.3.2.

Feeder cells were prepared by isolating PBMC from buffy coats (obtained from the Blood Transfusion Service, Birmingham, UK) from three separate donors by Ficol separation (Chapter 2.1.3). After separation, buffy coat cells were mixed together and rested overnight in RPMI 8% FCS containing phytohaemagglutinin (PHA) (10μg/mL). The following day buffy coat cells were washed five times in fresh medium, irradiated (40 Grays) and added to cultures as feeder cells.

Limiting dilution only cloning

Polyclonal T-cell lines (method Chapter 2.3.2) were re-suspended at differing concentrations of 3 cells/mL and 30 cells/mL in RPMI 8% HuS containing IL-7 (1ng/mL) with irradiated (40 Grays) autologous wild type LCL ($1x10^5$/mL) and feeder cells ($1x10^6$/mL). Polyclonal T-cell suspensions were then plated out using 100μL/well in 96-well plates (U-bottom), which gave final concentrations of 0.3 and 3.0 polyclonal T-cells per well. Plates were incubated at 37°C, 5% CO_2 for 5 days, after which 100μL T-cell media was added to each well. Plates were incubated for a total of 2 weeks, after which expanded microcultures started to become visible and could be screened for specificity.

IFNγ capture and limiting dilution cloning

IFNγ capture was performed using the human IFNγ secretion assay cell enrichment and detection kit (PE) from Miltenyi Biotech under sterile conditions. Autologous B-cell blasts were infected with selected MVA CNS viruses (protocol as Chapter 2.2.4) and incubated overnight in B-cell blast media at 37°C, 5% CO_2. The following day, infected B-cell blasts were washed 3 times and irradiated (40 Grays) before re-suspending in RPMI media (no supplements) with prepared polyclonal T-cell lines (protocol as Chapter 2.3.2) (1:1) for 3 hours at 37°C, 5% CO_2 re-suspending cells every hour. Following stimulation cells were washed twice in RPMI media, then once in cold MACS buffer after which the cell pellet was re-suspended in 80μL cold MACS buffer and 20μL catch reagent was added per $1x10^7$ cells, after which cells were incubated on ice for 5 minutes. 10mL warm RPMI media was then added per $1x10^7$ cells and tubes were incubated on a rotator at 37°C for 45 minutes. Cells were then washed with cold MACS buffer and the supernatant aspirated off, the pellet was then re-suspended in 80μL cold MACS buffer. 20μL IFNγ detection antibody (PE) was added per $1x10^7$ cells, vortexed and incubated on ice for 10 minutes. Cells were washed again in cold MACS buffer and the supernatant aspirated off. The cell pellet was then re-suspended in 80μL cold MACS buffer and 20μL PE microbeads were added, after which samples were vortexed samples incubated for 20 mins at 2-4°C. Samples were washed again with cold MACS buffer, the supernatant aspirated off and cells re-suspended in 0.5mL cold MACS buffer. MS columns (Miltenyi Biotech) were places into a magnetic separator and rinsed with 0.5mL cold MACS buffer, the effluent discarded. The now magnetically labelled cells were applied to the column and were allowed to pass through into a fresh tube by gravity flow. The column was washed a further 3 times with 0.5mL cold MACS buffer and the effluent collected as the negative fraction which was then discarded. The column was removed from the magnet and placed above a fresh tube. 1mL cold MACS buffer was then applied to the column to flush through the retained

cells, this was the positive fraction and contained the IFNγ-producing activated T-cells. Limiting dilution cloning technique was then used to plate out positively selected cells as described above but, instead of infected B-cell blasts, anti-CD3 antibody (OKT3 30ng/mL) (eBioscience) was added to T-cell media to provide non-specific stimulus. Plates were incubated at 37°C, 5% CO_2 for 5 days, after which 100μL T-cell media was added to each well. Microcultures were observed after two weeks and screened for antigen specificity.

TNFα capture and FACS cloning

Autologous B-cell blasts were infected with selected MVA CNS viruses (protocol as Chapter 2.2.4) and incubated at 37°C, 5% CO_2 overnight in B-cell blast medium. The following day infected B-cell blasts were washed 3 times, irradiated and re-suspended in RPMI 8% HuS containing IL-7 (1ng/mL) with prepared polyclonal T-cell lines (protocol as 2.3.2) at a ratio of 1:1. TAPI-0 (1μg/mL) and TNFα APC antibody (eBioscience) was added to stimulations and samples were incubated at 37°C, 5% CO_2 for 4 hours, re-suspending every hour to prevent clumping and aid stimulations. Surface staining of samples was performed under sterile conditions as and is described in Chapter 2.3.4. 96-well U-bottom plates were prepared for sorting and each well contained 100μL RPMI 8% HuS containing IL-7 (1ng/mL) with feeder cells ($1x10^6$/mL) and OKT3 (30ng/mL). After surface staining, cells were re-suspended in cold RPMI and run on a FACS Aria II machine (BD Biosciences). Single, live, CD19-, CD3+, TNFα+ cells were sorted into prepared 96-well U-bottom plates at 1 cell per well. Plates were incubated at 37°C, 5% CO_2 for 5 days, after which 100μL T-cell media was added to each well. After 2 weeks incubation microcultures were observed and screened for specificity.

2.3.4 TNFα capture staining and single cell sorting

Cells were stimulated with selected targets for 4 hours in the presence of TAPI-0 (1μg/mL) and TNFα APC antibody (eBioscience) and incubated at 37°C, 5% CO_2, re-suspending cells every hour. Samples were then washed twice in cold, sterile PBS before addition of surface stain antibodies (Table 2.3) and samples incubated on ice for 30 minutes. Cells were then washed once in cold PBS and once in MACS buffer, before re-suspending in cold RPMI (for cells run on cell sorter, see Chapter 2.3.3) or MACS (for cells run on flow cytometer). All samples were kept on ice and run immediately on a LSR II (BD Biosciences) flow cytometer.

Table 2.3 List of antibodies used in TNFα capture staining

Surface antibodies	
CD3 FITC	BioLegend
CD19 PECF594	BD Biosciences
Viability Live/Dead Aqua	Life Technologies
TNFα APC (added prior to stimulation)	eBioscience

2.3.5 IFN-γ ELISA

T-cell activation was measured by IFNγ production in an IFNγ enzyme-linked immunosorbent assay (ELISA). $1x10^4$ T-cells per well were incubated with target cells ($5x10^4$/well) or peptide (1μg/mL) and incubated overnight at 37°C, 5% CO_2 in RPMI 8% FCS. Supernatant was harvested the following day and IFNγ measured using the IFNγ ELISA kit as per the manufacturer's instructions. IFNγ antibody (clone 2G1, 1.01mg/mL, Thermofisher Scientific) diluted 1:7500 in ELISA coating buffer (carbonate-bicarbonate buffer 100mM) was used to

coat Nunc-Immuno MicroWell™ 96-well plates with MaxiSorp™ surface (50µL/well). Plates were incubated overnight at 4°C. The following day the antibody solution was flicked off, 100µL blocking buffer (PBS, 0.05% Tween-20, 10% BSA) was added to each well and plates were incubated for 1 hour at room temperature. Plates were then washed five times with wash buffer (PBS, 0.05% Tween-20) and then 50µL cell supernatant was harvested and added to the Nunc plates. Recombinant IFNγ (Peprotech) was used to make a standard curve by doubling serial dilutions from 20,000pg/mL down to 78.125pg/mL in RPMI 8% FCS; 50µL each dilution was added in triplicate to plates with plain media used as a negative control. Plates with supernatant and standards added were incubated for a minimum of 3 hours at room temperature. After incubation plates were washed 5 times with wash buffer and 50µL/well biotinylated IFNγ monoclonal antibody (clone B133.5, 0.5mg/mL, Thermofisher Scientific) diluted at 1:7500 in blocking buffer was added and plates incubated for 2 hours at room temperature. Following this, plates were washed five times in wash buffer and 50µL streptavidin-peroxidase (ExtrAvidin®-peroxidase, Sigma) diluted 1:5000 in blocking buffer was added to each well and the plates incubated for a further hour at RT. Plates were washed eight times in wash buffer and 50µL peroxidase substrate (3,3',5,5'-tetramethylbenzidine (TMB) solution, Tebu-Bio Laboratories) was added, the plates were then incubated at in the dark at RT for 20-30 minutes. The reaction was stopped with 50µL hydrochloric acid (1M HCl), after significant colour change to a blue solution in the top standards had occurred, resulting in a yellow solution. Plates were then read on an iMark™ Microplate Absorbance Reader at dual wavelengths of 450nm and 655nm. IFNγ in cell substrates was calculated by using the standard curve.

2.3.6 Detection of antibodies in human plasma

Blood collected from patients was separated using Ficol gradient separation (see protocol 2.1.3) and the plasma-RPMI fraction aspirated off and kept separately for further analysis of antibody responses by ELISA.

EBNA1-specific IgG

Levels of EBNA1 IgG in donor plasma were detected using the Diamedix™ Immunosimplicity™ EBNA1 IgG test kit (Fisher Scientific) according to manufacturer's instructions.

VCA-specific IgG

EBV IgG positive and negative cell lines – P3HR1 and Bjab respectively – were re-suspended in PBS at a concentration of 10^7/mL. 10μL of re-suspended cell lines were pipetted onto holes of microscope slides (SM011) and air dried in a warm room at 37°C. Slides were then fixed in cold acetone for 10 minutes, dried and stored at -20°C.

On day of staining, microscope slides were defrosted and blocked in PBS 10% HINGS for one hour at RT. Donor plasma was diluted down to 1:10, 1:20 and 1:40 in PBS 10% HINGS solution and 20μL of diluted serum was pipetted onto dried microscope slides before incubating for 1 hour at 37°C in a moist chamber. Slides were washed twice for 10 minutes in PBS using a magnetic stirrer, and the excess moisture wiped off around each hole. FITC-conjugated human IgG antibody (Sigma) was diluted 1:50 in PBS 10% HINGS and 20μL pipetted onto each hole of slides. Slides were incubated for 1 hour at 37°C in a moist chamber. Slides were washed twice for 10 minutes in PBS with magnetic stirring. Slides were mounted using DABCO mounting fluid and examined under a UV microscope.

CMV-specific IgG

Diluted mock lysate (1:4000) and virus-infected cell lysate (1:4000) was coated onto Nunc MaxiSorp™ plates and incubated overnight at 2°C. 100µL plasma samples (1:600 dilution) and appropriate standards (a mixture of 3 CMV-positive plasma samples) were added to the wells and the plate was incubated at RT for 1 hour, after which the plate was washed 3 times. 100µL anti-human IgG-HRP (horseradish peroxidase) secondary antibody was then added to the plate before incubating for 1 hour. The plate was washed 3 times and TMB (3, 3′, 5, 5′-tetramethylbenzidine) substrate was added. The plate was incubated in the dark at RT for 10 minutes before addition of 100µL 1M HCl to each well. Absorbance was read on a plate reader at 450 nm. To determine plasma CMV IgG titres, mock values were first subtracted from lysate values. The data were then analysed using GraphPad Prism (GraphPad Software, San Diego, CA, USA) and CMV IgG titres were calculated with reference to the standard curve. Values greater than 10 were considered to be seropositive. All samples were tested in triplicate and final titres were calculated as the average of these values.

Tetanus IgG detection

Plasma tetanus-specific IgG were measured by the staff at the Clinical Immunology Service, University of Birmingham using a Roche HITACHI Cobas®6000, with Roche IgG reagent kits as per the manufacturer's instructions. Plasma anti-tetanus IgG was measured using a previously described multiplexed bead based assay (Whitelegg et al., 2012). The definitions of protective antibody concentrations used have been previously characterised and published and are used as standards in the laboratory (Plotkin, 2001).

2.4 Western blotting

2.4.1 Preparation of type 1 and 2 EBV and EBNA3 protein cell lysates

The cord blood cell line C2 was infected with type 1 (OBA) and type 2 EBV (BL16) recovered from cell lines as described in the following publications (Rowe et al., 1989, Yao et al., 1996). For EBNA3A, B and C protein cell lysates, the EBV-negative cell line BJAB was infected with previously made MVA viruses containing EBNA3 genes separately (Long et al., 2009). BJAB cells were exposed to MVA viruses for 1 hour at a MOI of 10, before culturing in RPMI 2.5% FCS for 24 hours. After 24 hours cell lysates were prepared (method in Chapter 2.4.2).

2.4.2 Cell lysates

10^6 cells for each sample were washed in PBS and centrifuged. Pellets were then re-suspended 100μL urea buffer (9M) and the samples sonicated for 30 seconds at 40% intensity (probe sonicator). Samples were then spun at 8500g for 20 minutes and the supernatant transferred to a fresh tube. Lysates were then either used immediately (Chapter 2.4.2 and 2.4.3) or frozen at -80°C for future use.

2.4.3 Protein preparation for SDS-PAGE

β-mercaptoethanol was added to 2X Laemmli buffer (Bio-Rad) at a ratio of 1:20 in a fume hood, and the mixture was then used to dilute cell lysates. Diluted samples were then heated to 100°C for 5 minutes to denature proteins.

2.4.4 BCA protein determination assay

The bicinchoninic acid assay (BCA) was used to determine protein concentration of all cell lysates. Cell lysates (from Chapter 2.4.2) were diluted 1:5 in urea buffer (9M). Standards using bovine serum albumin (BSA) were diluted to a working range of 2ml/mL down to 0.125mg/mL, and 10µL diluted cell lysates and BSA standards were added in triplicate to a 96-well flat-bottomed plate. Working reagent was prepared by mixing reagents A and B (50:1) (Thermofisher Scientific) and adding 200µL to each well of the 96-well plate. The plate was incubated at 37°C for 30 minutes. After the plate had returned to RT, absorbance was read at 550nm, and protein concentration determined using the BSA standard curve.

2.4.5 SDS-PAGE

Commercially pre-made resolving gels of 4-15% acrylamide (Bio-Rad) were used to separate proteins in a Mini-PROTEAN® Tetra electrophoresis cell by SDS polyacrylamide gel electrophoresis (SDS-PAGE). Pre-cast gels were placed into the tank and submerged in running buffer (25mM Tris, 0.19M glycine, 0.1% SDS, pH8.3). 15µL of protein preparations were

loaded into each well with one lane Precision Plus Protein™ Dual Colour Standard (Bio-Rad). Gels were then run at 140V for ~1 hour.

2.4.6 Protein transfer

Resolved proteins were then transferred to PVDF membranes using the Trans-Blot® Turbo™ Transfer System according to manufacturer's instructions.

2.4.7 Staining of PVDF membranes

Presence of protein transfer to membranes was determined by Ponceau staining PVDF membranes for 30 seconds and subsequent washing with distilled water. Membranes were then blocked for a minimum of one hour at RT in 5% skimmed milk powder in PBS-Tween solution. Patient plasma was diluted 1:1000 in 5% skimmed milk powder PBS-Tween solution before being used to probe membranes by incubating them in the solutions overnight at 4°C with rocking. Membranes were washed a minimum of 5 times in PBS-Tween to remove primary antibody. Secondary anti-human IgG antibody conjugated with peroxidase (anti-human IgG Fc-specific peroxidase antibody produced in goats (Sigma)) was used to probe the membranes at a 1:2000 dilution in 5% skimmed milk powder in PBS-Tween solution for 1.5 hours at RT with rocking. Membranes were washed 5 times in PBS-Tween for one hour. Bound antibodies from donor sera were detected using ECL Western blotting detection reagent (Amersham) by chemiluminescence as per manufacturer's protocol.

2.5 Molecular techniques

2.5.1 Quantitative polymerase chain reaction for EBV genome load

DNA was extracted from ~1x10^6 PBMC using the Qiagen DNeasy commercial kit following the manufacturer's protocol and eluted in a total volume of 100µL. The DNA concentration was determined by UV-spectrophotometry at 260nm using a Nanodrop spectrophotometer.

Dilution of Namalwa Burkitt's Lymphoma (BL), which contains two copies of integrated EBV genomes per cell, were used to make DNA standards with the DNA being isolated as described above. The sample was adjusted to a final concentration of 132ng/µL and is equivalent to 40,000 EBV genome copies/µL; assuming that one cell contains 6.6pg DNA and each Namalwa BL cell contains two viral genomes. From this serial dilutions were made using PCR water.

Primers to detect EBV POL (BALF5) and the human β-2microglobulin (B2m) gene were used to probe EBV genome and serve as an endogenous control respectively. Primers were re-suspended at working stock concentrations of:-

POL F and R primers	2µM
POL probe	5µM
B2m F primer	3µM
B2m R primer	4µM
B2m probe	5µM

Test samples were run in triplicate. PCR master mix was prepared as followed for each well (total volume 25µL):-

Taqman Universal 2 x master mix	12.5µL

POL F primer (2μM)	2.5μL
POL R primer (2μM)	2.5μL
POL probe (5μM)	1μL
B2m F primer (3μM)	0.5μL
B2m R primer (4μM)	0.5μL
B2m probe (5μM)	0.5μL

20μL master mix and 5μL sample DNA was pipetted into each well of a 96-well PCR plate. The plate was run in an ABI7500 PCR machine (Thermo Fisher Scientific) and the data analysed using 7500 system v1.4 software (Thermo Fisher Scientific).

Table 2.4 Taqman primers and probes

EBV POL (BALF5)	
Forward primer	CTTTGGCGCGGATCCTC
Reverse primer	AGTCCTTCTTGGCTAGTCTGTTGAC
POL probe	(FAM)-CATCAAGAAGCTGCTGGCGGCC-(TAMRA)
β2m	
Forward primer	GGAATTGATTTGGGAGAGCATC
Reverse primer	CAGGTCCTGGCTCTACAATTTACTAA
β2m probe	AGTGTGACTGGGCAGATCATCCACCTTC-(BHQ)

2.6 Software and data analysis

2.6.1 Analysis of flow cytometric and combination gate data

All flow cytometry data was analysed using Kaluza flow cytometric software (Beckman Coulter). T-cell subsets were defined as single lymphocytes that stained as LiveCD14-CD19-CD3+ cells positive for either CD4 or CD8 markers. Tree plot analysis of cytokine production was used to determine percentage of T-cells in each combination gate set by the analysis software. Combination gate data was exported into the program Microsoft Excel and analysed using Funky Cells software. Background staining for analysis of *ex vivo* T-cell responses was set individually for each donor by the level of staining of each cytokine in the unstimulated control, and these values were deducted from all stimulated samples using Funky cells. Background staining for stimulations with MVA-infected B-cell blasts was set individually for each donor by subtracting level of staining in the MVA empty vector (pYWK)-infected B-cell blast control, allowing calculation of cytokines produced in response to CNS protein only. This normalisation of data allowed an unbiased comparison of cytokine staining for each donor and group. Funky cells also calculated the polyfunctionality index (PI) of each sample which was used as an arbitrary measure of the number of cytokines produced by cells in each stimulation (Larsen et al., 2012b). Combination gate data exported from Funky cells was analysed using SPICE (Simplified Presentation of Incredibly Complex Results, National Institute of Allergy and Infectious Diseases) software, which allows combination gates to be visualised in pie chart format with in depth multiple cytokine production analysis. Differences between data groups were calculated in SPICE using the Wilcoxon Signed Rank test and permutation test, P values below 0.05 were deemed to be significant.

2.6.2 Statistical analysis of data using GraphPad Prism software

Statistical significance of data was calculated using GraphPad Prism software (USA). The D'Agostino-Pearson omnibus normality test was performed to determine if data followed a Gaussian (normal) distribution and, with most data sets reporting a non-normal distribution, non-parametric tests were performed to determine statistical significance.

The Kruskall-Wallis test is a non-parametric test used for data sets with three or more categories that are not normally distributed. This test was used to compare variation in data from three cohort groups. The Mann-Whitney test is also a non-parametric test and was used to directly compare variation between two data sets.

Correlation of antibody responses and T-cell responses were calculated using the Spearmen's rank correlation coefficient (r) for non-normally distributed data.

The Fisher's exact test was used to compare categorical data, where data points were either positive or negative.

P values below 0.05 were deemed to be significant for all statistical tests used.

3 Cohort demographics

Our project aims were to investigate antibody and T-cell responses to EBV in MS patients, healthy controls (HC) and individuals with a recent history of IM. We recruited MS patients attending routine neurology clinics under the criteria that they were not currently suffering disease exacerbation or receiving immunomodulatory therapy for their condition. No prior administration of disease modifying therapy was of particular importance as this could potentially have impacted results.

Recruitment of healthy donors provided a control group with which to compare EBV-specific antibody and T-cell responses from MS patients. In addition to a control group, patients with a recent history of IM were recruited and their responses compared. As previously discussed, IM is a significant risk factor for the development of MS and we hoped to understand how these early EBV-specific responses after symptomatic infection compare to those of MS patients.

3.1 Ethics statement

All experiments were performed at the University of Birmingham in accordance with ethics approved by the West Midlands and Black Country NRES committee (ethics number 11/WM/0067 for MS and healthy control donors; ethics number 07/Q2702/94 for post-IM donors). All donors provided written informed consent for the collection of blood samples and their subsequent analysis.

3.2 Donor recruitment

All RRMS patients were recruited via the MS Research Clinic at the Queen Elizabeth Hospital, Birmingham and the Guest Hospital, Dudley, UK. Patients were diagnosed with RRMS and were currently not undergoing any immunomodulatory treatment at the time of blood donation. Blood was donated during routine follow-ups and patients were not currently undergoing any clinical relapse of disease.

IM patients were recruited from the Queen Elizabeth Hospital, Birmingham or from local general practice surgeries following a positive heterophile antibody test for IM. Blood was donated approximately 4-6 months following resolution of symptoms.

Healthy control (HC) donors were recruited from laboratory staff and postgraduate students at the University of Birmingham. All HC donors tested positive for VCA IgG staining by immunofluorescence, had no verbal history of IM and were age, gender and HLA-DR15 serotype matched as far as possible to MS donors in the study. Cohort demographics are shown in table 3.1.

Table 3.1 Cohort demographics

Donor group	No. of donors	Female	Gender (F:M)	Age (years MEAN +/- SD)	HLA-DRB1*15:01-positive	History of IM (%)
HC	33	23/33	2.3:1	35.67(+/-9.60)	15/33 (45.46%)	0/33 (0%)
MS	31	26/31	5.2:1	36.32 (+/-9.50)	13/31 (41.94%)	8/31 (25.81%)
IM	17	8/17	1:1.38	21.42 (+/-3.60)	6/17 (35.29%)	11/11 (100%)

Table 3.2 Individual patient demographics and HLA type

					HLA type									
Donor	Group	Gender	Age	IM*	A		B		DR				DQ	
MS1	MS	F	33	No	1	2	7	27	13	103	52a		6	7
MS2	MS	F	23	No	2	24	48	52	15	15(02)	51		6	
MS3	MS	F	49	No	2	3	15	35	1	103			5	
MS4	MS	F	39	No	2	11	7	40	4	15	51	53	6	8
MS5	MS	F	37	Yes	2	3	7	57	7	15	51		6	9
MS6	MS	F	45	No	2		15	27	13	103	52b		6	7
MS7	MS	M	45	Yes	1	3	8	39	8	17	52a		2	4
MS8	MS	F	60	No	1	2	8		4	17	52a	53	2	8
MS9	MS	M	30	Yes	11	29	15	35	12	16	51	52b	5	7
MS10	MS	F	27	No	1	3	7	8	15	51			6	
MS11	MS	F	47	Yes	2		15	35	1	4	53		5	8
MS12	MS	F	21	No										
MS13	MS	F	41	No	1		8	57	15	17	51	52a	2	6
MS14	MS	F	27	Yes	3		7		15		51		6	
MS15	MS	F	32	No	2	24	7	53	7	15	51	53	2	6
MS16	MS	F	53	No	1		8	37	4	14	52b	53	5	8
MS17	MS	F	37	Yes	1	3	8	51	17		52a		2	
MS18	MS	F	23	No	1		7	8	15	17	51	52a	2	6
MS19	MS	F	36	No	11	24	8	18	11	17	52a	52b	6	7
MS20	MS	F	31	No	3	24	8	35(08)	15	17	51	52a	2	6
MS25	MS	M	48	No	3	24	7	8	13	17	52a	52c	2	6
MS26	MS	F	37	No	1	2	15	39	4	8	53		4	8
MS27	MS	F	36	Yes	2	3	27	40	15		51		6	
MS28	MS	M	44	No	3	74	15	45	12	15	51	52b	6	7
MS29	MS	F	38	No	1	2	8	44(02)	4	17	52a	53	2	8
MS30	MS	F	40	No	1	3	7	8	15	17	51	52a	2	6
MS31	MS	F	30	No	2		13	27	7	103	53		2	7
MS32	MS	F	27	No	11	24	35	35(02)	1	17	52b		2	5

MS33	MS	F	41	No	2	26	14	15	4	7	53		2	7
MS34	MS	M	25	No	2	2(05)	7	50	4	15	51	53	6	7
MS35	MS	F	24	Yes	2	31	13	40	7	8	53		2	4
HC1	HC	F	33	No	2	3	7		15		51		6	
HC2	HC	M	42	No	2		22	40	7	16	51	53	2	5
HC3	HC	M	30	No	2	2(s)	40(s)		11	15	51	52b	6	7
HC4	HC	F	42	No	2	11	35	44	1	4	53		1	7
HC5	HC	F	30	No	26		44(02)	58	14	16	51	52b	5(02)	5(03)
HC6	HC	F	28	No	2	11	35	58	4	13	52c	53	6	7
HC7	HC	M	42	No	3	23	7	44(02)	4	15	51	53	6	7
HC8	HC	M	25	No	24	29	7	44	4	15	51	53	6	7
HC9	HC	F	46	No	2		40	41	8	103			4	5
HC10	HC	F	35	No	1		7	57	12	103	52		5	7
HC11	HC	F	34	No	1	24	8	18	17	7	52a	53	2	
HC12	HC	F	31	No	2	26	15	27	7	8	53			
HC13	HC	F	37	No	2	32	44		7	15	51	53	1	2
HC14	HC	F	49	No	29	30	7	45	4	15	51	53	6	7
HC15	HC	F	25	No	24	32	14	44	7	12	52b	53	2	7
HC16	HC	F	60	No	1	2	8	60	3	15	51	52a	2	6
HC17	HC	M	28	No	2		8	40	17		52a		2	
HC18	HC	F	48	No	1	2	44(02)		11	15	51	52b	6	7
HC19	HC	F	34	No	1	2	44	57	4	7	53		7	9
HC20	HC	F	25	No	1	24	8	15	13	17	52a	52c	2	6
HC21	HC	F	-	No	24	31	40	57	4	7	53		8	9
HC22	HC	F	53	No	2	11	8	44	13	17	52a	52c	2	6
HC23	HC	F	28	No	1	3	7	15	13	15	51	52b	6	6
HC24	HC	M	29	No	1	11	35	44(02)	13	103	52a		5	6
HC25	HC	F	37	No	1	3	7	2705	4	15	51	53	6	8
HC26	HC	M	24	No	3	23	15	58	15(03)	17	51	52b	2	6
HC27	HC	M	28	No	2	3	7	40	1	4	53		5	8
HC28	HC	M	53	No	2	24	39		8	15	51		4	6
HC29	HC	F	43	No	2	11	51	60	4		53		3	
HC30	HC	M	26	No	2	68	44	55	1	15	51		5	6

HC31	HC	F	22	No	2	11	15	51	4	15	51	53	6	8
HC32	HC	F	37	No	2	68	35	49	1	12	52b		5	7
HC33	HC	F	37	No	2		27		1	15	51		5	6
IM111.2	IM	M	18	Yes	1	3	8	39						
IM121.3	IM	M	20	Yes	2	33	8	44						
IM225.2	IM	F	20	Yes	2	3	7	27	15	17	52a	51	2	6
IM226.2	IM	F	19	Yes	2		40	50	7	13(02)	52c	53	2	6
IM230.2	IM	F	20	Yes	3	68	35	44	13	17	52a		2	6
IM231.2	IM	F	25	Yes	3	24	35	51	4	7	53		2	7
IM238.2	IM	F	18	Yes	1	24	18	35	1	15	51/N		5	6
IM239.3	IM	M	21	Yes	1	2	8	51	13	17	52a	52b	2	6
IM240.3	IM	F	20	Yes	2	11	18	44	1	17	52b		2	5
IM243.2	IM	M	20	Yes	1	23	8	44	7	15	51	53	2	6
IM253.3	IM	M	25	Yes	3	24	7	37/N	4	15	51	53	6	8
IM257.3	IM	F	21	Yes	1	68	40(02)	56	1	11	52b		5	7
IM265.7	IM	M	18	Yes	23	26	7	44	7	15	51	53	2	6
IM267.5	IM	F	20	Yes	26	31	27		4	13	52a	53	7	
IM269.3	IM	M	27	Yes	3	11	15	35	1	8			4	5
IM270.4	IM	M	21	Yes	3	26	14	38	12	13	52b	52c	6	7
IM279.6	IM	M	33	Yes	2	24	7	52	4	15/N	51/N	53	6	7

* Self-reported history of IM for HC and MS donors

/N Null allele

4 EBV viral load and antibody responses

Epidemiological data strongly implicates EBV in MS pathogenesis due to the almost universal seroprevalence and elevated anti-EBNA1 IgG antibodies prior to disease onset in patients (Pakpoor et al., 2013, Munger et al., 2011, Ascherio et al., 2001). However, despite over 30 years of research, little is known about the contribution of EBV towards MS development. Our aim for this part of the project was to investigate EBV viral load, EBNA1 and VCA IgG titres and other antibody responses to EBV which have not yet been characterised in our cohort.

4.1 EBV viral load

EBV resides latently in memory B-cells of the peripheral immune system, and viral genome load provides an indication of how many of these cells are infected and therefore the viral burden on an individual. Increased viral replication causes genome copy number to increase as more cells become infected, and this can be used as a measurement of EBV reactivation in patients. Several autoimmune diseases, such as systemic lupus erythematosus (SLE) and rheumatoid arthritis (RA) display an increased EBV viral load however this is still debated in MS, with reports of both unchanged and increased viral load in patients compared to healthy, EBV seropositive controls (Wagner et al., 2004, Cocuzza et al., 2014, Lunemann et al., 2010). Viral load was investigated in whole PBMC in our cohort by qPCR using primers specific for the BALF5 gene of EBV. EBV genome copy numbers in our cohorts were found to be unchanged between MS patients and HC, suggesting no increase in number of circulating B-cells infected with EBV in MS patients (Figure 4.1.1). Post-IM donors displayed an elevated viral load compared to other groups, indicative of a recent primary infection (Figure 4.1.1).

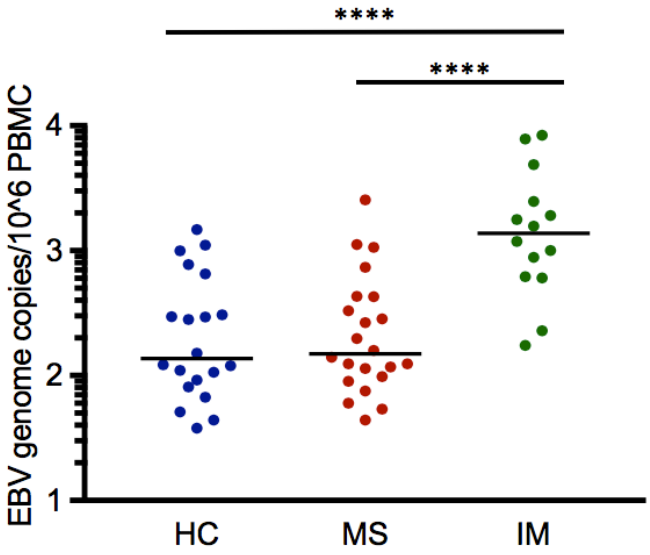

Figure 4.1.1 EBV load in PBMC. EBV genome load was determined from whole PBMC by q-PCR. No difference was seen between viral load of HC and MS donors. Post-IM donors had a significantly elevated EBV load compared to both HC and MS donors (HC:IM $p<0.0001$, MS:IM $p<0.0001$). Black line represents median of data set. Statistics calculated using the Mann-Whitney test (ns $p>0.05$, * $p\leq0.05$, ** $p\leq0.01$, *** $p\leq0.001$, **** $p\leq0.0001$).

4.2 EBV-specific antibody production

4.2.1 EBNA1 and VCA IgG titres

Plasma anti-EBNA1 IgG titres have been much investigated in MS literature, most notably using the US Military Serum Repository, and have shown antibody titres to be elevated in MS patients up to 5 years prior to disease onset (Munger et al., 2011). As anti-EBNA1 antibodies are known to be elevated and are a potential biomarker in MS, we investigated this in our cohort by ELISA to establish whether it was confirmed in our cohort.

Healthy EBV-seropositive donors had significantly lower levels of EBNA1-specific IgG antibodies in their plasma compared to MS donors, who also showed a strong increase when compared with post-IM donors (Figure 4.2.1A).

Antibodies specific for virus capsid antigen (VCA) have been studied previously with conflicting results, with reports of both elevated and unchanged VCA IgG titres in MS patients compared to seropositive controls (Farrell et al., 2009, Castellazzi et al., 2010). Semi-quantitative immunofluorescence was used to investigate levels in cohorts and MS patients were shown to have increased plasma anti-VCA IgG compared to HC and post-IM donors (Figure 4.2.1B).

VCA IgG titres were calculated using serial dilutions of donor plasma, however samples were not blinded for cohort group. This means that results may have been subject to human bias, and over-estimation of titres in a particular group might affect results. As donor titres were investigated at multiple dilutions and on different occasions we estimated any effect of bias to be minimal, however anonymization of patient numbers would prevent this influence in future.

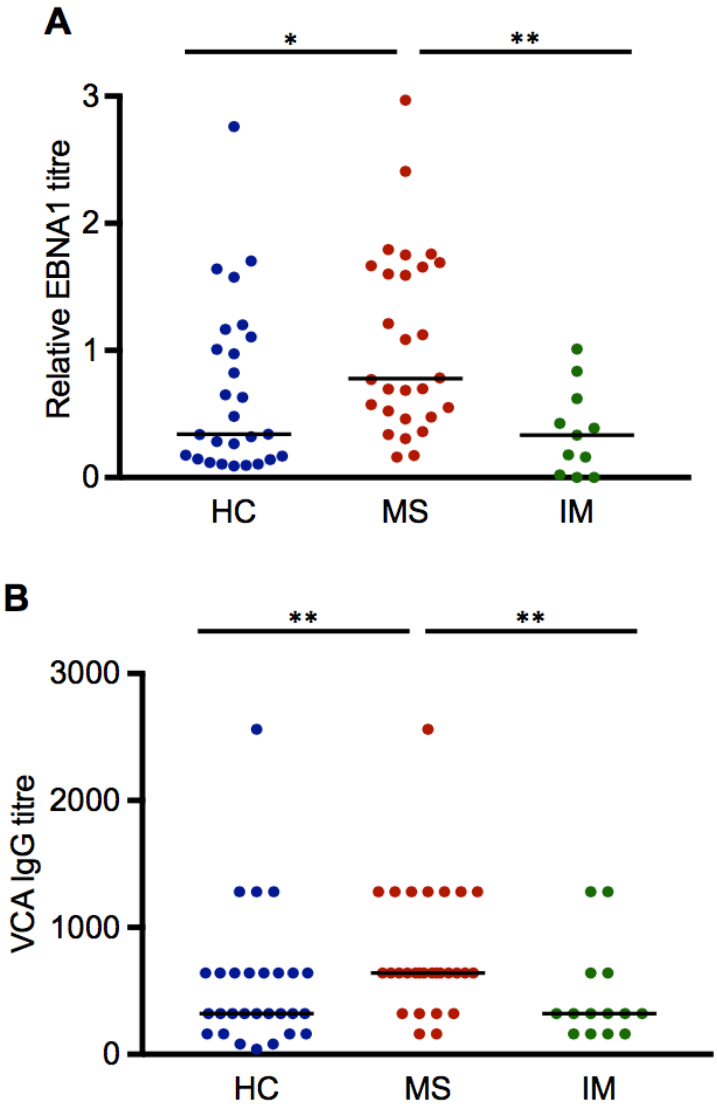

Figure 4.2.1 EBNA1 IgG and VCA IgG titres in peripheral blood. A. Semi-quantitative plasma anti-EBNA1 IgG titre was determined by ELISA. MS donors had significantly higher titres that HC or post-IM donors (HC:MS *p=0.0106*, MS:IM *p=0.0014*). **B.** VCA IgG titres from serum were investigated by immunofluorescence. MS donors had significantly increased serum anti-VCA IgG levels than HC and post-IM donors (HC:MS *p=0.0097*, MS:IM *p=0.0073*). Black line represents median of data set. All statistics performed using the Mann-Whitney test (ns $p>0.05$, * $p\leq0.05$, ** $p\leq0.01$).

4.2.2 Antibody responses to type 1 and 2 EBV

Research into EBV strains infecting MS patients has sought to investigate why an almost ubiquitous virus contributes towards disease in some individuals, and one theory suggests that a specific strain (or strains) could be responsible for disease development. Some studies have implicated that certain polymorphisms in EBNA1, EBNA2 and other EBV proteins are overrepresented in MS patients compared to HC (Brennan et al., 2010, Mechelli et al., 2015). An increased frequency of co-infections with type 1 and 2 virus was found in MS patients in one Spanish cohort (Santon et al., 2011), which may have an impact on pathogenesis and T-cell and antibody responses to the virus *in vivo*.

Type 1 and 2 subtypes of EBV are distinct from each other mainly in the sequence of their EBNA2 and EBNA3C proteins, and we investigated antibody responses to each virus in patient plasma by Western blot (Figure 4.2.2). Western blots were performed using lysates of cord blood cell lines infected with type 1 and 2 viruses separately, allowing us to see differences in antibody binding and protein size between the two strains and generating an "EBNA print" Western blot of latent protein serology. Position of EBNA1, EBNA2 and EBNA3C protein bands were identified using monoclonal antibodies (Yao et al., 1996) and are indicated on the blot (Figure 4.2.2).

EBNA print profiles of HC and MS donors were analysed and the frequencies of EBNA bands corresponding to each latent protein were compared between patient groups. Whilst this method was not quantitative, frequency of antibody responses could be detected and the intensity of bands are able to give an approximate indication of the amount of antibody present in donor plasma.

There were no observable differences in frequency of antibody responses to EBNA1 or EBNA2 proteins between HC and MS patients, and representative Western blots are shown in Figure

4.2.2. A band for an unknown small protein was observed in blots for some donors, however we were not able to identify which protein this belonged to using monoclonal antibodies. Table 4.1 shows all responses identified in cohort groups in EBV type I and type II Western blots and also to EBNA3 proteins, and a summary of responses is shown in Table 4.2.

Antibody responses to EBNA3 proteins showed the most notable difference. Plasma responses to EBNA3 were more frequently detected in MS patients with 72.41% (21/29) compared to 35.48% (11/31) of HC (Figure 4.2.2) (Table 4.1).

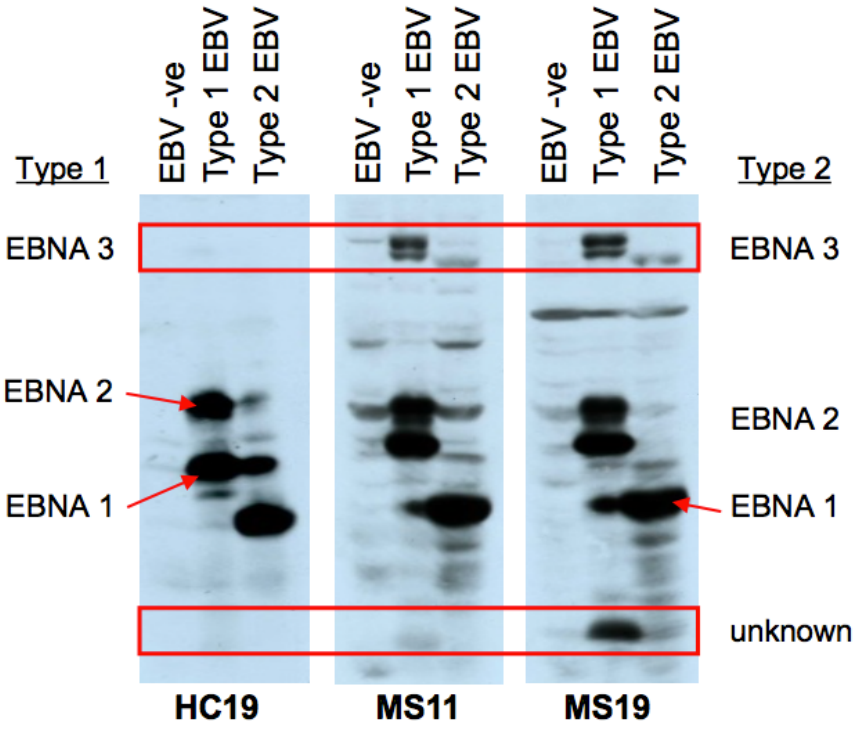

Figure 4.2.2 Antibody responses directed towards latent antigens of type 1 or type 2 EBV. Cell lysates were made from the EBV negative cell line BJAB, and cord blood cells infected with either type 1 or type 2 EBV separately and blotted onto nitrocellulose membrane. All patient plasma was diluted 1:1000 and used to incubate membranes, generating an "EBNA print" of antibody responses for each donor. Bands representing type 1 and type 2 latent proteins are labelled on representative blots from three separate donors. No significant differences were seen between responses to EBV type 1 and type 2 viruses between MS and HC donors, however responses to EBNA3 proteins were more common amongst MS donors than healthy controls.

Table 4.1 Antibody responses to EBV type I and II proteins and to EBNA3 proteins detected by Western blot

Donor	C2 cells infected with type I or II EBV								BJAB cells infected with MVA EBNA3A, B or C		
	EBNA1		EBNA2		EBNA3s		Unknown band		EBNA3		
	T1	T2	T1	T2	T1	T2	T1	T2	3A	3B	3C
HC1	+	+	-	-	-	-	-	-	+	-	-
HC2	+	-	-	-	-	-	-	-	-	-	-
HC3	-	-	-	-	-	-	-	-	+	-	-
HC4	+	+	-	-	-	-	+	-	-	-	-
HC5	+	+	-	-	-	-	-	-	+	-	+
HC6	+	+	+	-	+	+	+	-	+	+	+
HC7	-	-	-	-	-	-	-	-	-	-	-
HC8	-	-	-	-	-	-	-	-	-	-	-
HC9	+	+	-	-	+	-	+	-	+	-	+
HC10	+	+	+	-	+	-	+	-	+	-	+
HC11	+	+	-	-	-	-	+	-	-	-	-
HC12	+	+	-	-	-	-	-	-	+	+	+
HC13	+	+	+	-	-	-	-	-	-	-	-
HC14	+	+	+	-	-	-	-	-	-	-	-
HC15	-	-	-	-	-	-	-	-	-	-	-
HC16	+	+	-	-	-	-	-	-	+	+	+
HC17	+	+	-	-	-	-	-	-	-	-	-
HC18	+	+	+	-	+	-	+	-	+	+	+
HC19	+	+	+	+	-	-	-	-	+	+	+
HC20	+	+	+	-	+	-	+	-	-	-	+
HC21	+	-	+	-	+	-	-	-	+	+	-
HC22	+	+	-	-	-	-	-	-	-	-	-
HC23	+	+	-	-	+	+	+	-	+	-	+
HC25	+	+	+	-	+	-	-	-	+	+	+
HC27	-	-	-	-	-	-	-	-	+	+	+
HC28	+	+	+	-	+	-	-	-	+	-	+
HC29	+	+	+	+	+	+	+	-	+	+	+
HC30	-	-	-	-	-	-	-	-	-	-	-
HC31	+	+	-	-	-	-	-	-	-	-	-
HC32	+	+	+	-	-	-	-	-	+	-	+
HC33	+	+	+	-	+	+	-	-	+	+	-
MS1	+	+	-	-	-	-	-	-	+	-	-

MS2	+	+	-	-	-	-	-	-	+	+	-
MS3	+	+	+	-	+	+	-	-	+	+	-
MS4	+	+	+	-	+	-	-	-	+	+	+
MS5	+	+	+	-	+	+	+	-	+	+	+
MS6	+	+	+	-	+	+	+	-	+	+	+
MS7	+	+	-	-	-	-	+	-	-	-	-
MS8	+	+	+	-	+	-	+	-	+	-	+
MS9	+	+	-	-	+	-	-	-	-	+	+
MS10	+	+	-	-	-	-	-	-	+	-	-
MS11	+	+	+	+	+	+	+	-	+	+	+
MS13	+	+	-	-	+	-	+	-	+	+	+
MS14	+	+	-	-	-	-	-	-	+	+	-
MS15	+	+	+	-	+	+	-	-	+	+	+
MS17	+	+	+	-	+	+	+	-	+	+	+
MS18	-	-	-	-	-	-	-	-	+	+	+
MS19	+	+	+	-	+	+	+	-	+	+	+
MS20	+	+	+	-	+	+	+	-	+	+	+
MS25	+	+	+	-	+	-	+	-	-	-	+
MS26	+	+	+	+	+	-	+	-	+	+	+
MS27	+	+	+	+	+	+	-	-	+	+	-
MS28	+	+	+	+	+	+	+	-	+	+	+
MS29	+	+	+	+	+	+	+	-	+	+	-
MS30	+	+	+	+	+	+	+	-	+	+	+
MS31	+	+	+	-	+	+	+	+	+	+	+
MS32	+	+	+	-	+	-	+	-	+	+	+
MS33	+	+	+	-	-	-	-	-	-	-	-
MS34	+	+	-	-	+	-	-	-	+	-	-
MS35	+	+	+	-	-	+	-	-	+	+	+
IM225.2	+	+	+	-	+	+	+	-	+	+	+
IM226.2	-	-	+	-	+	-	+	-	+	+	-
IM238.3	+	+	-	-	-	-	-	-	+	-	-
IM239.3	+	+	+	-	+	-	-	-	+	+	+
IM240.3	+	+	-	-	-	-	-	-	+	+	-
IM243.2	-	-	-	-	-	-	-	-	+	+	-
IM253.3	+	+	+	-	+	+	-	-	+	+	+
IM257.3	+	+	-	-	-	-	-	-	+	-	-
IM265.7	+	+	-	-	-	-	-	-	+	+	-

IM267.5	+	+	+	-	-	-	-	-	+	-	-
IM269.3	+	+	+	-	+	+	+	-	+	+	+
IM270.4	+	+	-	-	-	-	-	-	+	-	-
IM272.2	+	+	-	-	-	-	-	-	-	-	-
IM275.3	+	+	-	-	+	+	-	-	+	-	-
IM279.6	+	+	+	-	+	+	-	-	+	+	+

Table 4.2 Summary of antibody responses to EBV type I and II proteins and EBNA3 proteins detected by Western blot

Donor Group	C2 cells infected with type I or II EBV							
	EBNA1		EBNA2		EBNA3s		Unknown band	
	T1	T2	T1	T2	T1	T2	T1	T2
HC	25/31 (80.65%)	23/31 (74.19%)	13/31 (41.94%)	2/31 (6.45%)	11/31 (35.48%)	4/31 (12.90%)	9/31 (29.03%)	0/31 (0%)
MS	28/29 (96.55%)	28/29 (96.55%)	20/29 (68.97%)	6/29 (20.69%)	21/29 (72.41%)	14/29 (48.28%)	16/29 (55.17%)	1/29 (3.45%)
IM	13/15 (86.67%)	13/15 (86.67%)	7/15 (46.67%)	0/15 (0%)	7/15 (46.67%)	5/15 (33.33%)	3/15 (20%)	0/15 (0%)

Donor Group	BJAB cells infected with MVA EBNA3A, B or C		
	EBNA3		
	3A	3B	3C
HC	18/31 (58.07%)	10/31 (32.26%)	15/31 (48.39%)
MS	25/29 (86.21%)	22/29 (75.86%)	20/29 (68.97%)
IM	14/15 (93.33%)	9/15 (60%)	5/15 (33.33%)

To identify which EBNA3 protein was differentially recognised, cell lysates were made from the EBV-negative cell line Raji after infection with MVAs expressing EBNA3A, 3B and 3C separately and the protein preparations then used to perform Western blots with patient sera (Figure 4.2.3A). The presence of bands of the correct size for each of the EBNA3A, 3B and 3C lysates indicated an antibody response to the proteins in donors, and example Western blots are shown in Figure 4.2.3A. Where there were clear bands each donor was marked as having a response, more faint bands were only considered a response if there was no background staining on the blot. For example, HC15 was scored as having no responses to all EBNA3 proteins and MS6 was scored as having a response to all 3 proteins, but MS29 only had antibody responses to EBNA3A and B (Figure 4.2.3).

EBNA3 antibody responses were more frequent amongst MS patients than HC, an effect that was strongest for EBNA3B (EBNA3A HC:MS *p=0.0220*, EBNA3B HC:MS *p=0.0009*, EBNA3C HC:MS *P=0.1239*) (Figure 4.2.3B). Responses to EBNA3C in MS patients were also significantly more frequent than in post-IM donors (MS:IM *p=0.0303*) (Figure 4.2.3B). Post-IM donor EBNA3A IgG responses were significantly higher than those of HC (HC:IM *p=0.0180*).

In addition to EBNA3A responses being more frequent in MS patients than healthy donors, bands formed by antibody responses in Western blots appeared to be larger and darker than those seen for responses in HC (Figure 4.2.3A). Whilst Western blots are only semi-quantitative, they do give an idea of the concentration of antibody when the same amount and concentration of cell lysate is applied to membranes between experiments. However, this observation would need to be measured using a quantitative method for these results to be verified.

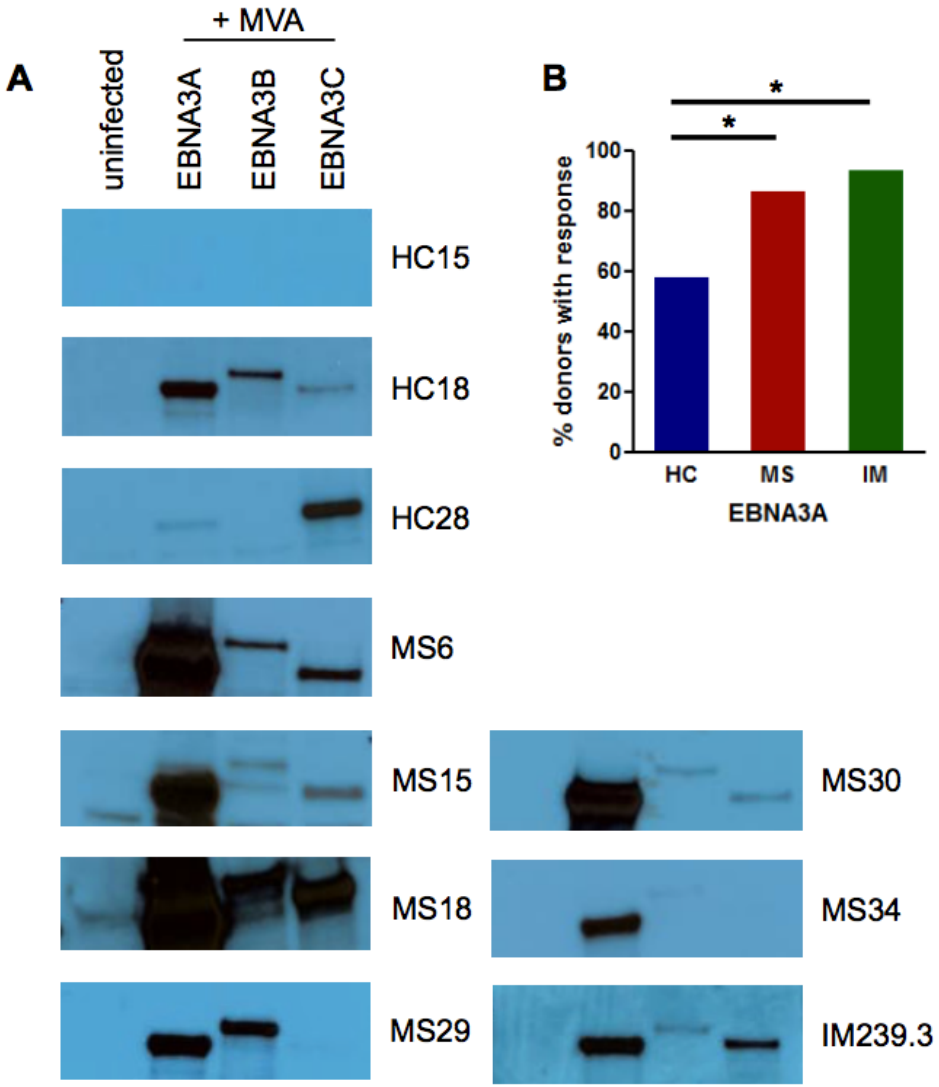

Figure 4.2.3 Antibody responses directed against EBNA3 proteins. A. Protein preparations were made from uninfected BJAB-cells and cells separately infected with MVAs containing EBNA3A, EBNA3B and EBNA3C proteins. Example blots are shown from HC, MS and post-IM donors. **B.** Percentage of donors with an IgG antibody response to each of the EBNA3 proteins. MS and post-IM donors were significantly more likely to have an EBNA3A response than healthy controls (HC:MS *p=0.0220*, HC:IM *p=0.0180*). MS donors were significantly more likely to have an EBNA3B response than HC (HC:MS *p=0.0009*). Responses in MS patients to EBNA3C were more frequent than in post-IM donors (MS:IM *p=0.0303*). All statistics were calculated using Fisher's exact test (ns $p>0.05$, * $p\leq0.05$, ** $p\leq0.01$, *** $p\leq0.001$).

4.3 CMV and tetanus toxoid antibody responses

Whilst EBV is thought to have a key role in MS development, other pathogens have been implicated in the disease process. Previous studies have investigated a role for CMV in MS and have reported that early infections with CMV are more common in MS patients (Djelilovic-Vranic and Alajbegovic, 2012). This suggests that CMV might have a role in disease development or progression, and evidence for this comes from reports that CMV also increases frequency of disease exacerbations in RRMS (Rainey-Barger et al., 2013, Buljevac et al., 2002).

Using a lysate of CMV-infected cells, an ELISA was performed on donors' plasma to determine both serostatus and CMV antibody titre of those who were positive for CMV-specific IgG. Frequency of CMV carriage was highest in post-IM donors, followed by MS and healthy controls respectively. There was an observable trend towards increased CMV infection in post-IM and MS donors, however when analysed using the Fisher's exact test of categorical data this observed difference did not reach significance (HC:MS $p=0.0716$, MS:IM $p=0.7507$, HC:IM $p=0.0615$) (Figure 4.3.1A). CMV IgG titre was compared between positive donors, and the highest titre was seen amongst MS patients, however this only reached significance when compared to post-IM donors (MS:IM $p=0.0261$) (Figure 4.3.1B); MS patient titres need to be compared with a greater number of HC positive for CMV in order to establish if this effect is real.

Tetanus toxoid-specific antibody responses were investigated in collaboration with the Clinical Immunology department at the University of Birmingham. Analysing tetanus toxoid responses allowed us to investigate whether elevations observed in antibody responses amongst MS patients were isolated to EBV or whether this effect was extended to other pathogens. Tetanus toxoid was selected as a control due to routine vaccination programs in the UK including the

antigen, and therefore donors in our cohort are all likely to amount an antibody response against the protein.

Anti-tetanus IgG was measured by ELISA and post-IM donors were found to have significantly higher titres than MS donors (Figure 4.3.2). No differences were observed in levels of anti-tetanus IgG between HC and MS donors (Figure 4.3.2).

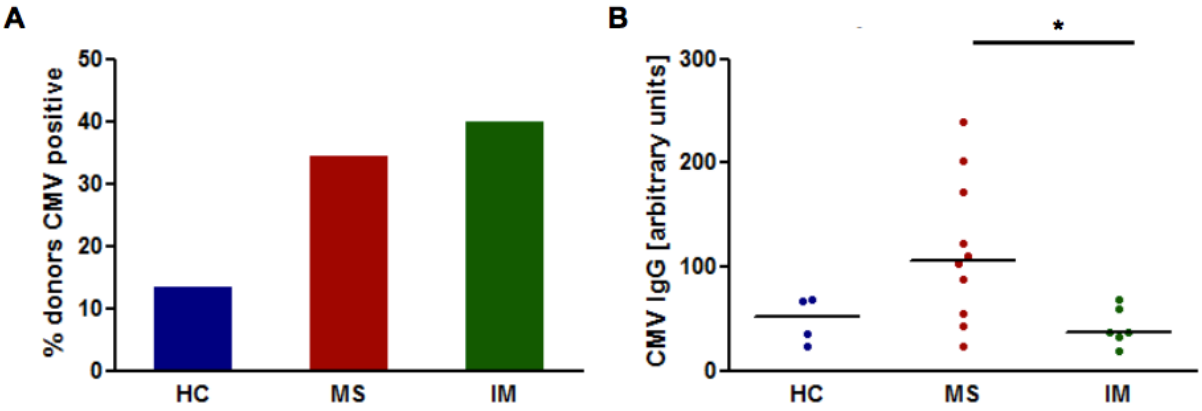

Figure 4.3.1 Anti-CMV IgG plasma titres. A. Donors were tested for carriage of cytomegalovirus using an in-house anti-CMV IgG ELISA, and number of donors positive for each group were as follows: HC 4/30, MS 10/29, post-IM 6/15. Frequency of CMV carriage was compared between groups using Fisher's exact test, with no significance found between groups (HC:MS *p=0.0716*, MS:IM *p=0.7507*, HC:IM *p=0.0615*). **B.** Levels of anti-CMV IgG from CMV-positive donors were compared using the Mann-Whitney test to determine significance (* *p≤0.05*). MS patients exhibited significantly higher titres than those of post-IM donors (MS:IM *p=0.0261*). HC and MS groups did not differ significantly (HC:MS *p=0.0893*). CMV IgG antibody titres are presented as arbitrary units, with the black lines representing the median of data sets.

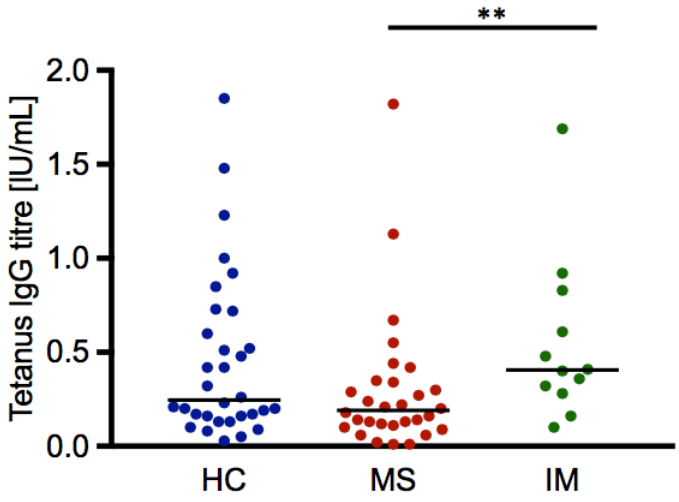

Figure 4.3.2 Plasma antibodies directed against tetanus toxoid in cohorts. Anti-tetanus toxoid IgG levels in plasma were analysed by multiplex bead assay, and levels between HC and MS donors were shown to be unchanged. However, post-IM donors had significantly elevated titres compared to MS patients (MS:IM *p=0.0092*), but this did not reach statistical significance when comparing HC to post-IM donors. All statistics performed using the Mann-Whitney test (ns *p>0.05*, * *p≤0.05*, ** *p≤0.01*).

4.4 Discussion

EBV viral load and serology in MS patients have been extensively researched over many years, establishing an epidemiological role for the virus in pathogenesis that is now widely accepted by researchers. However, despite this there are still many conflicting ideas regarding how EBV causes disease, advocating the need for more in-depth study of this area.

The work in this chapter sought to address some of the questions remaining surrounding serum parameters in previous MS literature, comparing MS patients with healthy donors and those with a recent history of IM with an aim to establish if these are unchanged, decreased or increased in our cohort from the West Midlands, UK. Post-IM donors have an increased risk of developing MS, and we analysed antibody responses to EBV proteins in these donors because they have not previously been investigated alongside MS patient samples. Analysis of EBV antibody responses in MS patients are of key importance due to the potential to develop markers for diagnosis and progression, as well as to understand the underlying immune mechanisms driving disease.

EBV viral load in circulating B-cells of long-term carriers is a broad measure of level of virus burden, and can be an indication of impaired immune control of infection and viral replication. EBV transformation of autoreactive B-cells and defective CD8+ T-cell control allowing their migration into the CNS is one potential mechanism put forward to explain EBV's contribution to disease, and this chain of events could potentially lead to an increased viral load in MS patients. However, only a few studies to date have reported an increased viral load in MS patients, including Lunemann *et al.* (Lunemann et al., 2010). A previous publication by Lunemann *et al.* found an elevated viral load amongst MS patients but the study did not have sufficient participants to determine significance (Lunemann et al., 2006). Pender *et al.* also reported an elevated viral load which has been used to argue that lack of control of EBV

replication in B-cells is due to ineffective CD8+ T-cell control of the virus allowing infected B-cells to enter the CNS of MS patients causing disease (Pender et al., 2014a, Pender et al., 2017). Evidence for an unchanged cellular viral load in MS patients when compared with healthy, seropositive donors is far more widespread and data from our cohort corroborates these findings (Figure 4.1.1) (Cocuzza et al., 2014, Alvarez-Lafuente et al., 2006, Lindsey et al., 2009, Lucas et al., 2011, Santiago et al., 2010, Wagner et al., 2004).

Plasma viral load is a measure of reactivation of latently-infected B-cells into lytic cycle producing free virus, however, as with cell-associated viral load, this has been shown to be unchanged in MS indicating no underlying chronic reactivation of EBV is driving disease in MS patients (Wagner et al., 2004), although Ramroodi *et al.* reported this to be elevated in one Iranian cohort (Ramroodi et al., 2013). However, plasma viral load is an unreliable measure of virus quantification as qPCR techniques are also able to detect fragments of viral DNA that are not part of infectious virus particles, and this measure is used as a biomarker in patients with nasopharyngeal carcinoma (Chan, 2014). For the purpose of our study we elected to test cellular DNA as it is a more consistent and reliable method of quantifying EBV load.

Viral load has also been studied in the context of other autoimmune diseases such as systemic lupus erythematosus (SLE) and rheumatoid arthritis (RA), with findings from these diseases showing it is elevated in these patients (Moon et al., 2004). However, this is thought to be due to autoimmune activation of the B-cell compartment driving increase in EBV load, and not related to EBV itself driving autoimmune disease in these patients (Larsen et al., 2011). This elevation in SLE and RA viral load contrasts with most findings in MS patients of an unchanged viral load, and supports evidence that MS pathology is predominantly T-cell-driven.

EBNA1 IgG antibody titres in MS patient serum are subject to less debate and are generally considered to be elevated in cohorts around the world (Ascherio et al., 2001, Sundstrom et al., 2004, Levin et al., 2005, DeLorenze et al., 2006), driving interest in the EBNA1 protein and

making it a potential marker of MS risk and diagnosis. Elevated EBNA1 antibody responses focussed attention onto a potential role for degenerate EBNA1-specific T-cell responses in patients.

Anti-EBNA1 IgG titres were analysed in our cohort by ELISA with MS patients shown to have significantly higher levels than HC and post-IM (Figure 4.2.1A). These results are concordant with published reports, showing our study cohort to have similar EBNA1 serology to those studied in many different countries and supporting potential use of humoural responses to this protein in calculating risk of developing MS. The commercial ELISA kit used to analyse EBNA1 IgG responses in our cohort is specific for the C-terminus of the protein. Other studies have shown the glycine-alanine (GA) repeat region to be the most immunogenic, and it has been shown to be the dominant region to which antibody responses are generated in IM (Rumpold et al., 1987). Autoantibodies in IM were also shown by Rhodes *et al.* to have specificity for the GA repeat region of EBNA1 (Rhodes et al., 1987). The EBNA1 GA repeat region has been shown to limit its own transcription and translation by reducing the number of *cis*-linked sequences to CD8+ T-cells (Apcher et al., 2009, Apcher et al., 2010, Tellam et al., 2012, Murat et al., 2014), but despite this T-cell responses to the protein can be detected in IM and healthy virus carriers (Blake et al., 2000). Analysis of antibodies to both the C-terminal and the GA repeat region of EBNA1 is needed in the same cohort to determine if these regions are similarly recognised in MS patients and IM donors.

The clinical significance of elevated antibody responses against EBNA1 in MS patients is not known, and debate surrounds what is driving the EBNA1-specific antibody and CD4+ T-cell responses which develop 3-6 months post infection (Long et al., 2013). It is unclear whether CD4+ T-cell responses are driving EBNA1 antibody responses to become elevated via providing 'help' to B-cells, or whether atypical EBNA1-specific CD4+ T-cells follow IgG responses in their emergence. EBNA1 is an interesting protein in that, unlike other EBNA

proteins, it is not shed from the cell or into the cytoplasm from the nucleus, meaning that autophagosome processing and presentation of the protein on MHC class II molecules on the surface of infected cells is restricted to very low levels (Leung et al., 2010). Due to this known restriction of antigenic source it is not clear how antibody and CD4+ T-cell responses are primed, and other studies identifying methods of intercellular antigen transfer are not able to fully explain this phenomenon (Taylor et al., 2006). More research is needed in this area to understand why these responses are elevated in patients compared to long-term healthy virus carriers, and identifying this pathway might help elucidate what contribution EBNA1 CD4+ T-cell and antibody responses are making to MS disease (Lunemann et al., 2006). Clues to their role come from observations that EBNA1 IgG antibodies correlate with disease activity as measured by MRI (Kvistad et al., 2014).

Investigations into the specificity of oligoclonal bands in CSF of patients has led to findings supporting intrathecal anti-EBNA1 IgG in MS (Pfuhl et al., 2015), and in several studies evidence was found for anti-EBNA1 IgG intrathecal production in a proportion of patients but at levels too low to support a key role in disease pathogenesis (Pohl et al., 2010, Castellazzi et al., 2014). Studies of cross-reactivity in EBNA1-specific antibody responses has revealed immunoglobulins able to recognise both EBNA1 and myelin basic protein (MBP) peptides (Mameli et al., 2014) and human heterogeneous ribonucleoprotein L (HNRNPL) (Lindsey et al., 2016), indicating that autoreactive EBNA1 IgG might directly contribute towards CNS damage in the early stages of MS and help to perpetuate inflammatory immune mechanisms in the CNS. It is likely that antibody responses detected in CSF are also synthesised in this compartment due to their inability to cross the blood brain barrier, therefore it is also apparent that the detected antibodies must be produced by B cells that have become activated within the CNS itself. However, intrathecal antibody responses have a limited clinical role in direct

damage of the CNS due to the controlled access of circulating immunoglobulins to the brain parenchyma (Pardridge, 2012).

VCA-specific antibodies are less well studied than those with reactivity to EBNA1, but are used routinely in the diagnosis of acute IM, with presence of low affinity anti-VCA IgM demonstrative of recent primary infection before a switch to IgG indicating longer term virus carriage. Kinetics of antibody responses to VCA are also very different from those of EBNA1; VCA IgG tend to be synthesised very quickly after primary infection and at high levels, gradually decreasing to a moderate level which is stable over time (Taylor et al., 2015). VCA antibody responses in multiple sclerosis are less well studied; our project investigated titres and found them increased (Figure 4.2.1B), consistent with previous reports finding anti-VCA IgG in MS patient sera and CSF to be increased (Castellazzi et al., 2010, Castellazzi et al., 2014, Simon et al., 2012). More research into viral capsid antigen humoural responses is needed to establish the contribution of these elevated VCA-specific antibody levels to disease, or to elucidate whether these elevated responses are secondary to MS disease itself.

Theories of an EBV strain specific to MS have been investigated for many years, with evidence from MS "epidemics" such as in the Faroe Islands lending credence to such hypotheses. However, after many sequencing studies, researchers have failed so far to identify a specific virus strain as the cause of MS (Lay et al., 2012), with single nucleotide polymorphisms in viral DNA also failing to explain why some individuals develop MS and others do not (Lindsey et al., 2008, Brennan et al., 2010). However, Santon *et al.* published an increased frequency of co-infection of patients with MS with type 1 and 2 strains of EBV (Santon et al., 2011), an effect that has so far not been observed by any other groups.

Patients within our cohort frequently showed antibody responses to proteins from type 1 EBV in our "EBNA print" analysis, with many also showing reactivity to the type 2 antigens but this may be due to sequence homology between proteins from different strains, as differences in

sequence mainly occur in the EBNA2 and EBNA3C loci (Rowe et al., 1989, Farrell, 2015). Sequencing would need to be performed on samples from our cohort to determine for certain whether co-infections are more common in MS patients, but no observable differences could be seen between groups to type 1 and type 2 EBV for Western blot analysis (Figure 4.2.2).

Antibody responses to EBNA3 protein have not so far been investigated in the context of MS, and following on from increased frequency of responses to the locus in "EBNA print" analysis we sought to characterise the differential responses to EBNA3A, EBNA3B and EBNA3C separately. To different extents, antibody responses to all three EBNA3 proteins were found to be more frequent amongst MS patients compared to healthy virus carriers (Figure 4.2.3). However, Western blots are only semi-quantitative and further analysis would be needed by ELISA or machine-measured chemiluminescence to verify these results. Prevalence of EBNA3B-specific antibody responses in MS patients was significantly elevated compared to controls, but again this would need to be confirmed by quantitative experiments.

The clinical significance of elevated EBNA3-specific antibody responses in MS is not known. Kinetics of latent antigen-specific T-cell responses following IM are generally lower than those for lytic proteins, however latent protein-specific CD8+ T-cells have been shown to make up to 5% of total CD8+ compartment in MS (Hislop et al., 2005). EBNA3A-specific CD8+ T-cell responses have been shown by one group to be elevated in MS patients during disease remission disease and lower during exacerbations, a contrast to the pattern observed for lytic protein T-cell responses in the same cohort (Angelini et al., 2013). CD4+ responses to EBNA3A in MS have so far not been studied but it is known to be a reasonably common EBV immune target in healthy virus carriers (Taylor et al., 2015).

Compared to EBNA3-specific T-cell responses relatively little investigation has been carried out into antibody responses to the proteins. Elevated EBNA3A, B and C antibody responses observed in MS patients from our cohort may indicate why increased EBNA complex IgG were

observed in MS cohorts, as these proteins are found in the complex (Munger et al., 2011). More research is needed in this area to study the kinetics of antibody responses to EBNA3 proteins to understand whether CD4+ T-cell responses follow those seen for antibodies, as is seen with EBNA1-specific immune responses, or vice versa (Long et al., 2013).

CMV is a β-herpesvirus which is less ubiquitous in the Western population, infection rates increase with age and approximately 80% of the over 65s population in the UK carry the virus (Vyse et al., 2009). CMV has been linked to MS but to a lesser extent than EBV; proposed mechanisms of the virus's involvement in disease are similar to those for EBV, however there is less epidemiological and serological evidence for an association of the two (Vanheusden et al., 2015). CMV has been shown to be able to cross the blood-brain barrier and MS plaques have been found to be positive for the virus (Olival et al., 2013, Smyk et al., 2014, Djelilovic-Vranic and Alajbegovic, 2012), with further evidence suggesting that CMV can contribute towards demyelination in immunocompromised patients (t Hart et al., 2009, Cermelli and Jacobson, 2000). Serological studies are fewer but it has been reported that CMV DNA and virus-specific IgG titres were higher in MS patients compared to HC (Sanadgol et al., 2011), and that MS patients at diagnosis are 86% more likely to have an early CMV infection, indicating that the virus may contribute towards disease development (Djelilovic-Vranic and Alajbegovic, 2012).

Our findings that MS patients have a higher frequency of CMV infection than HC fit with the literature and support a contribution of the virus towards development (Figure 4.3.1A). However, rates of CMV infection in MS patients did not reach significance when compared with healthy donors, but this may be due to the small number of HC with CMV in our cohort reducing the statistical power of the data (Figure 4.3.1A). Only a third of MS patients in our cohort were CMV positive, suggesting that it is not the sole cause, but multiple virus co-infections may contribute towards disease progression, as evidenced by previous studies

(Horakova et al., 2013, Wunsch et al., 2016). Prevalence of CMV infection has been shown to increase with age, but the mean age of healthy donors and MS patients in our study was 35.65 and 36.32 years respectively, indicating that this increased frequency of CMV infection in MS patients cannot be attributed to this (Table 3.1). Increased co-infection with EBV and CMV in our cohort corroborates findings from previous studies (Djelilovic-Vranic and Alajbegovic, 2012, Horakova et al., 2013, Wunsch et al., 2016), and indicates that dual infection with both viruses may contribute towards disease development and progression, and more research is needed to establish the contribution of immune responses to CMV in MS.

CMV-positive individuals were separately compared for CMV IgG titres, with MS patients appearing to have higher levels, but again this did not reach significance and is possibly due to the small number of CMV-positive HC in the cohort (Figure 4.3.1B). It is also likely that, due to similarities between EBV and CMV as herpesviruses, there might be some structural cross-reactivity of responses to viral antigens confounding results and further investigation is needed to establish CMV's direct contribution to disease (Grangeot-Keros and Cointe, 2001).

One interesting observation from our cohort was the high frequency of CMV infections in post-IM donors, despite the younger demographic of this group. 40.0% of post-IM donors in the cohort had anti-CMV IgG levels higher than background when tested in our study, a frequency that was higher than that observed in MS patients (34.48%) (Figure 4.3.1A). Post-IM donors were recruited after they received a positive heterophile test at diagnosis, and IgM antibodies detected by this test have been shown to cross-react with EBV antigens (Lang et al., 2001). Our analysis was conducted on plasma collected from individuals 4-6 months after onset of symptoms, by which time IgM antibodies have started to decline but low levels of cross-reactive antibodies may still be present in the blood (Taylor et al., 2015). However, all IM donors in our study were subsequently tested for VCA IgG responses which have been shown to not cross-react with antibodies directed against CMV, indicating that their IM was caused

by primary infection with EBV. Higher prevalence of early CMV infection in people who go on to develop EBV-driven IM has not been previously shown, and more research is warranted in a larger donor cohort to investigate these findings and their potential contribution to MS development.

Tetanus toxoid antibodies are almost ubiquitous in the UK population due to extensive vaccination programmes of all children, and thus we used these as a control marker of IgG antibody responses, finding them to be unchanged between healthy control donors and MS patients in our study (Figure 4.3.2). Post-IM donors were shown to have significantly higher titres of tetanus toxoid-specific antibodies when compared with MS patients, and this may be due to continued, low level dysregulation of the B-cell compartment following primary infection with EBV.

Statistics performed in our study used the Mann-Whitney test, a non-parametric test used to directly compare distribution of two groups of data. However, whilst this is sufficient for two groups, more appropriate statistical analysis of three data sets could be achieved using the Bonferroni correction (or similar). This would enable calculation of more accurate p values and provide a more robust evaluation of variation between cohort groups in future analysis.

Our study has confirmed previous studies' findings of elevated EBNA1 and VCA-specific IgG responses amongst MS patients, lending support to the hypothesis that EBV immune responses are dysregulated in patients and may contribute towards disease development. Lack of elevated viral load in patients compared to HC also suggests that there is no lack of control of viral replication, and this may indicate that it is EBV immune responses themselves driving disease rather than deficiency in anti-viral immunity. Increased frequency of CMV infections in MS patients reflects findings in previous reports stating that the virus can contribute towards disease exacerbations and progression. No increase in tetanus toxoid antibody responses in MS patients shows that elevations are specific to EBV. Taken together, these findings support a

role for EBV in MS development but further investigation of T-cell responses to EBV is needed to understand how this occurs.

5 *Ex vivo* EBV-specific T-cell responses in peripheral blood

T-cell responses to EBV in MS patients remain the subject of much speculation, and despite extensive research no consensus has been reached on whether they are altered in frequency or phenotype in patient peripheral blood. To address this question, we analysed CD4+ and CD8+ T-cell responses to EBV antigens in PBMCs from RRMS patients (MS), healthy EBV seropositive controls (HC) and patients with a recent history of IM, and analysed in depth the frequency, phenotype and polyfunctionality of these cells.

The antigens were selected carefully to allow detailed analysis of circulating EBV-antigen specific T-cells. B95.8 virus was originally isolated from an elderly patient with IM and is used in many laboratories as a type I EBV reference strain and is referred to in this thesis as wild type LCL (Skare et al., 1982, Baer et al., 1984). This virus was used to establish lymphoblastoid cell lines (LCLs) from each donor, and a minority of LCLs established with B95.8 virus spontaneously undergo lytic cycle, thus stimulating both latent and lytic antigen-specific T cells. A variant of B95.8 that lacks the transactivator protein BZLF1 required to initiate lytic cycle expresses only latent antigens (Feederle et al., 2000). Both viruses were used to establish LCLs from each donor allowing the total EBV and latent-specific EBV T-cell responses to be measured.

Given the interest in EBNA1 in MS patients, an EBNA1 peptide mix was used to examine T-cell responses to this antigen specifically, and we analysed *ex vivo* T-cell responses to the protein using a commercially sourced overlapping peptide mix.

Staphylococcal enterotoxin B (SEB) was used as a non-specific, positive control stimulus for cytokine production as it binds to particular V_β chains of TCRs to activate T-cells (Rodstrom et al., 2014). Levels of SEB stimulation can vary a lot between donors due to different V_β chain

usage of an individual's T-cell repertoire; SEB acts on specific TCR chains by cross-linking them with MHC molecules in a peptide-independent manner and producing a strong intracellular stimulus (Rodstrom et al., 2014). Due to restricted cell numbers some samples were not screened against SEB.

All experiments were performed with cryopreserved, whole PBMC from each donor which were recovered and stimulated overnight with different antigen sources. The next day the cells underwent intracellular cytokine staining (ICS) and flow cytometry.

5.1 Frequency of EBV-specific T-cell responses in peripheral blood

Ex vivo stimulation of PBMCs with LCL and EBV antigens allows the accurate measurement of the number of circulating EBV-specific T-cells an individual has in their blood, enabling comprehensive analysis of the function and phenotype of these cells between donor groups. Intracellular cytokine staining (ICS) was used to determine cytokine production by T-cells and to accurately measure the number of cells responding to each stimulus, and the unstimulated control was used to set the cut-off for positive cytokine production for each individual donor.

5.1.1 CD4+ T-cell responses

Whole PBMC from each donor were isolated and stimulated overnight with SEB, autologous wild type LCL, autologous BZLF1 KO LCL or EBNA1 peptide mix. ICS was performed on cells to determine production of interferon-γ (IFNγ), interleukin-2 (IL-2), interleukin-17 (IL-17) and granulocyte-macrophage colony-stimulating factor (GM-CSF) by CD4+ or CD8+ T-cell subsets.

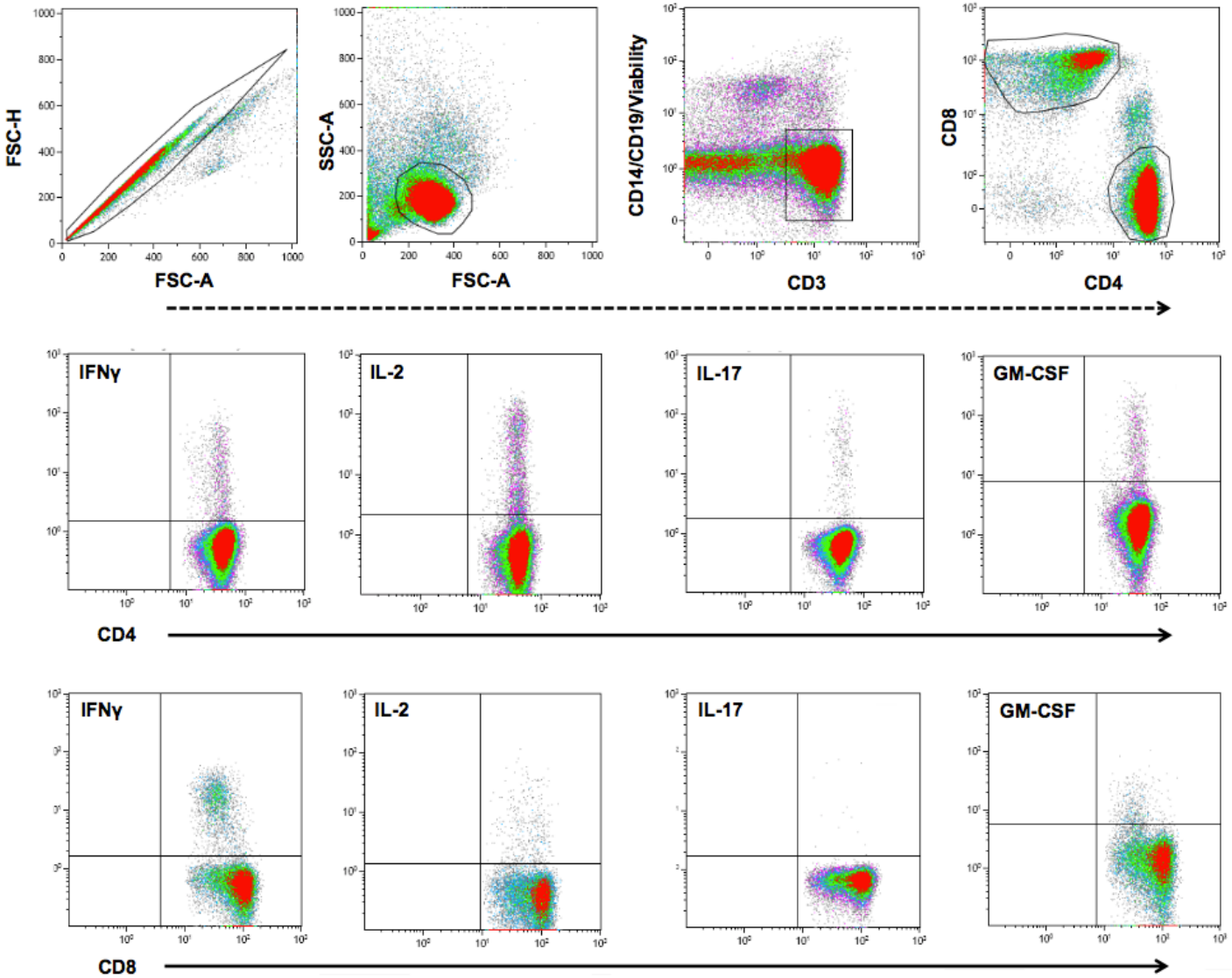

Figure 5.1.1 T-cell gating strategy for *ex vivo* PBMC stimulations. Example staining from MS11 PBMC stimulated with SEB (0.2µg/mL). Whole PBMC were stained for viability, CD14, CD19, CD3, CD4 and CD8. Cells were fixed with paraformaldehyde (4% in PBS) and permeabilised with saponin (0.5% in MACS buffer) before being stained intracellularly for IFNγ, IL-2, IL-17 and GM-CSF. Singlets were gated using FSC-H versus FSC-A. FSC-A and SSC-A were then used to gate the lymphocyte population. T-cells were defined as Live/CD14-/CD19-/CD3+ cells with CD4+ and CD8+ populations gated on separately for cytokine production. Dashed line represents direction of gating strategy, unbroken line represents cytokine staining for CD4+ and CD8+ subsets.

Gating strategy for *ex vivo* T-cell analysis is shown in Figure 5.1.1. Example staining from MS11 is shown in Figure 5.1.2 for IFNγ, IL-2, IL-17 and GM-CSF in unstimulated cells and those stimulated with SEB, autologous wild type LCL, BZLF1 KO LCL and EBNA1 peptide mix.

Background staining for all four cytokines in our panel was minimal, and allowed the antigen-specific and negative populations to be determined clearly in both CD4+ and CD8+ subsets (Figure 5.1.2 and 5.1.5).

The greatest *ex vivo* T-cell response was predictably seen in the positive control samples stimulated with SEB, with response to the toxin varying greatly between individuals due to the differing levels of circulating T-cells with particular V_β chains. These observed differences between donors in T cell repertoire V_β chain usage is greatly influenced by previous antigenic exposure and also other factors such as age, gender and lifestyle.

CD4+ T-cell responses to wild type and BZLF1 KO LCL were typically smaller than those seen for CD8+, and as with SEB size of response varied greatly between donors (Figure 5.1.3 and 5.1.6). IFNγ was generally the most frequent cytokine produced by donor T-cells in response to wild type and BZLF1 KO LCL, however a high proportion also produced IL-2 following stimulation (Figure 5.1.3). A small amount of GM-CSF production was observed in response to EBV antigens, with the lowest cytokine response observed for IL-17 (Figure 5.1.3). Numbers of circulating CD4+ T-cells producing cytokine in response to the different stimuli in all donors are shown in Figure 5.1.3.

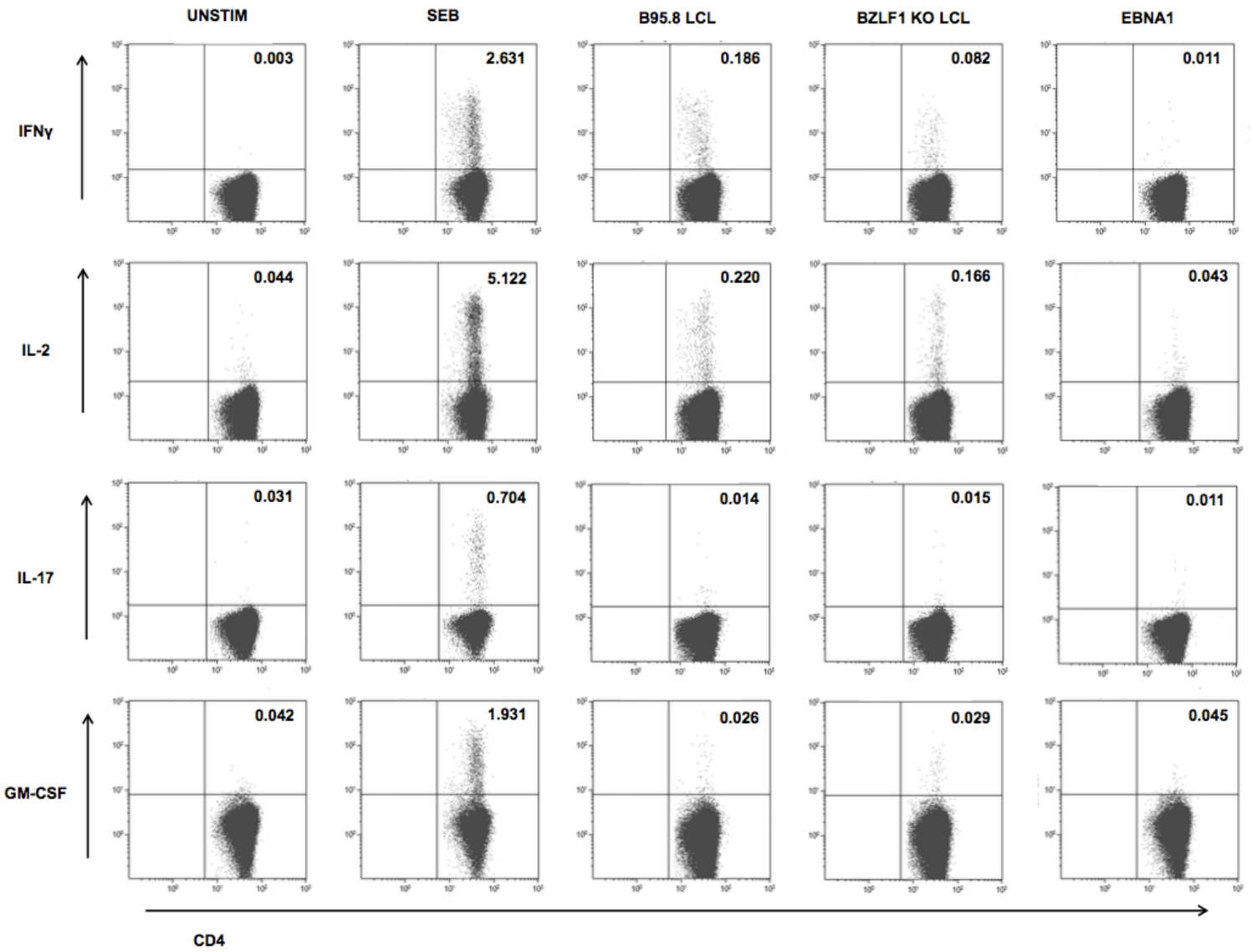

Figure 5.1.2 *Ex vivo* CD4+ T-cell responses to SEB and EBV antigens. PBMCs from an MS donor (MS11) were stimulated *ex vivo* with SEB, autologous wild type LCL, autologous BZLF1 KO LCL and EBNA1 peptides and their cytokine production measured by flow cytometry. Cells were gated as LiveCD14-CD19-CD3+CD4+ T-cells and then further gated for IFNγ, IL-2, IL-17 and GM-CSF. Values represent percentage of CD4+ T-cell population producing cytokine.

CD4+ T-cells from healthy donors and MS patients did not show any significant difference in cytokine response to SEB after overnight stimulation, with large variation in the size of response to SEB within the two groups (Figure 5.1.3A).

CD4+ T-cells from MS donors did not show any significantly changed levels of IFNγ, IL-2 or IL-17 production in response to autologous wild type LCL stimulation, however GM-CSF production was shown to be significantly higher in MS patient CD4+ T-cells compared to healthy donors (HC:MS *p=0.0138*, Mann-Whitney test) but not post-IM donors (Figure 5.1.3B).

IFNγ, IL-2 and GM-CSF production was not significantly different between HC, MS or post-IM donors after stimulation with autologous BZLF1 KO LCL (Figure5.1.3C), but IL-17 was produced at different levels between the groups in response to the latent LCL (*p=0.0352*, Kruskall-Wallis test). HC produced the highest amount of IL-17 but statistical comparison of HC and MS donor IL-17 responses using the Mann-Whitney test did not reach significance (Figure 5.1.1C).

EBNA1 is a key protein of interest in MS pathogenesis due to the elevated anti-EBNA1 antibody response in MS and post-IM patient blood (Long et al., 2013, Lunemann et al., 2006, Lunemann et al., 2008b). Analysis of CD4+ T-cell responses from our cohort to EBNA1 peptide mix revealed no overall difference in production of cytokines in our panel after stimulation (Figure 5.1.3D).

The median percentage of CD4+ T-cells producing IFNγ and IL-2 (represented by the horizontal black lines) is similar for both cytokines following stimulation with wild type or BZLF1 KO LCL, and shows that these are the two main cytokines produced in response to LCL stimulation (Figure 5.1.3). IL-17 and GM-CSF were produced at lower levels than IFNγ and IL-2 in response to LCL stimulation.

EBNA1 CD4+ T-cell responses were much lower than those for LCL, and cytokine production by responding cells was similar between all four cytokines, indicating a more varied functional response to the protein (Figure 5.1.3D).

The strongest genetic link with MS is the MHC class II allele HLA-DR15, and we therefore wanted to address whether having the HLA-DR15 allele influenced levels of circulating T-cells with reactivity to EBV or their phenotype. Using the same experimental data, we compared only donors that were HLA-DR15+ and the results are shown in Figure 5.1.4.

Pattern of cytokine production comparing HLA-DR15+ donors only did not alter the data significantly, however increases in the median of CD4+ T-cells responding to wild type LCL by producing IFNγ and IL-2 indicate that the allele may have a modest effect on responses (Figure 5.1.4B); more HLA-DR15+ donors would need to be analysed to determine if these results are significant. GM-CSF production in response to B95.8 LCL remained significantly higher in MS patients compared to HC after removal of HLA-DR15 donors (HC:MS $p=0.0454$, Mann-Whitney test) (Figure 5.1.4B). However, variation in IL-17 production after following BZLF1 KO LCL stimulation was no longer significant after removal of donors that were not HLA-DR15+ (Figure 5.1.4C) and this may be due to the low number of donors in the IM group causing a lack of statistical power in the analysis.

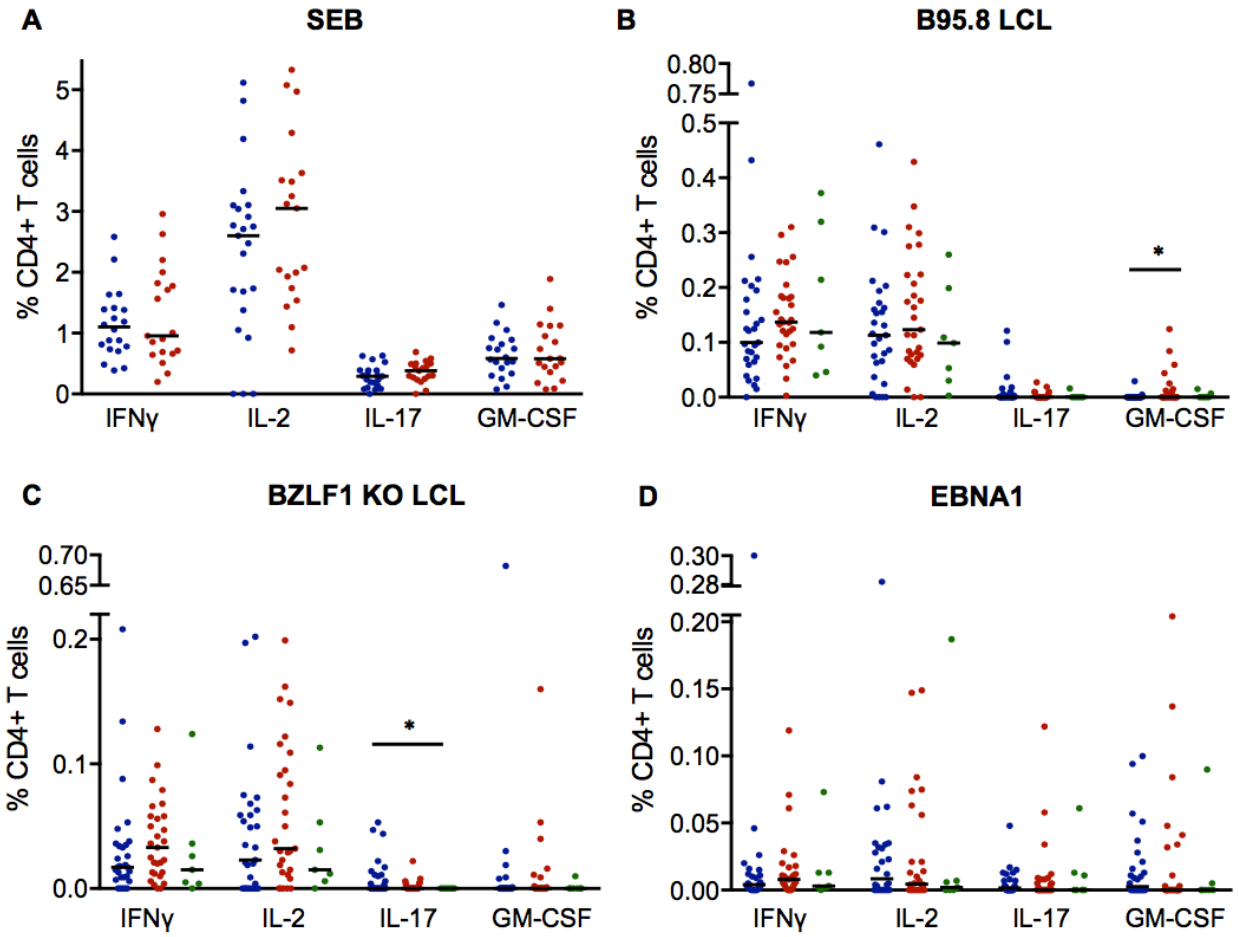

Figure 5.1.3 ***Ex vivo*** **EBV-specific CD4+ T-cell responses.** Whole PBMC were stimulated *ex vivo* and subjected to ICS. Responding CD4+ T-cells are presented as a percentage of the whole CD4+ T-cell population producing each cytokine in response to stimulation with: **A.** SEB **B.** wild type LCL **C.** BZLF1 KO LCL **D.** EBNA1 peptide mix. Colour of dots define patient group: blue=healthy control donors, red=RRMS patients and green=post-IM patients. Black bars represent median of data set (SEB stimulation: HC n=20, MS n=19, all other stimulations: HC n=29, MS n=29, post-IM n=7). Kruskal-Wallis test was used for comparison of three groups and the Mann-Whitney test for comparison of two patient groups (ns $p>0.05$, * $p\leq0.05$).

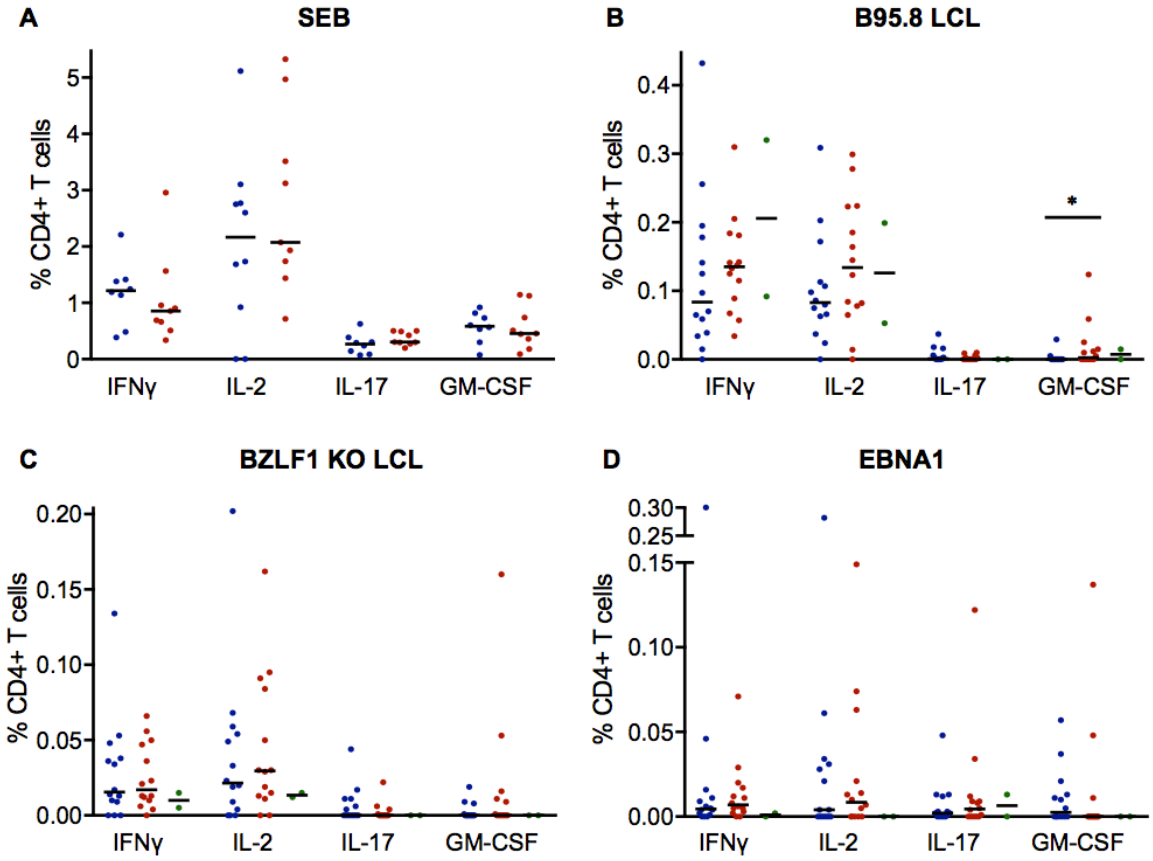

Figure 5.1.4 ***Ex vivo*** **EBV-specific CD4+ T-cell responses in HLA-DR15+ donors.** Whole PBMC from HLA-DR15+ donors were analysed separately to see if their responses were different in frequency or phenotype. Isolated cells were stimulated *ex vivo* and subjected to ICS. Responding CD4+ T-cells are presented as a percentage of the whole CD4+ T-cell population after stimulation with. **A.** SEB **B.** wild type LCL **C.** BZLF1 KO LCL and **D.** EBNA1 peptide mix. Colour of dots define patient group: blue=healthy control donors, red=RRMS patients and green=post-IM patients. Horizontal black line represents median of data set (SEB stimulation: HC n=8, MS n=9, all other stimulations: HC n=14, MS n=14, post-IM n=2). The Kruskal-Wallis test was used for comparisons of three groups and the Mann-Whitney test for comparison of two patient groups (ns $p>0.05$, * $p\leq0.05$).

5.1.2 CD8+ T-cell responses

Many studies have investigated CD8+ T-cell responses to EBV in MS but, as with many aspects of MS pathogenesis, there is currently no consensus reached on whether they are altered in patients. Conflicting reports of CD8+ T-cell immunity to the virus in peripheral blood highlight the need for more research in this area, and this was explored in our cohort.

The same stimulation experiments were used for analysis of both CD4+ and CD8+ T-cell responses to EBV antigens. As previously described for CD4+ T-cells, whole PBMC were stimulated overnight with SEB, autologous wild type LCL, autologous BZLF1 KO LCL and EBNA1 peptide mix and their T-cells analysed to understand whether there are any significant differences between frequency and phenotype of CD8+ T-cell responding to EBV antigens.

Example staining of CD8+ T-cell cytokine production in response to SEB, wild type LCL, BZLF1 KO LCL and EBNA1 are shown from a representative MS donor (MS11) in Figure 5.1.5. As with CD4+ T-cells, responses to SEB varied greatly between donors due to differences in TCR V_β chain usage in their repertoires. Minimal background staining was observed for IFNγ, IL-2 and IL-17; GM-CSF staining showing some background but this effect was removed using Funky Cells software analysis.

No significant differences were seen in the CD8+ T-cell SEB responses between HC or MS donors, despite there being a slight trend towards greater IL-2 and GM-CSF production in cells from MS patients (Figure 5.1.6A).

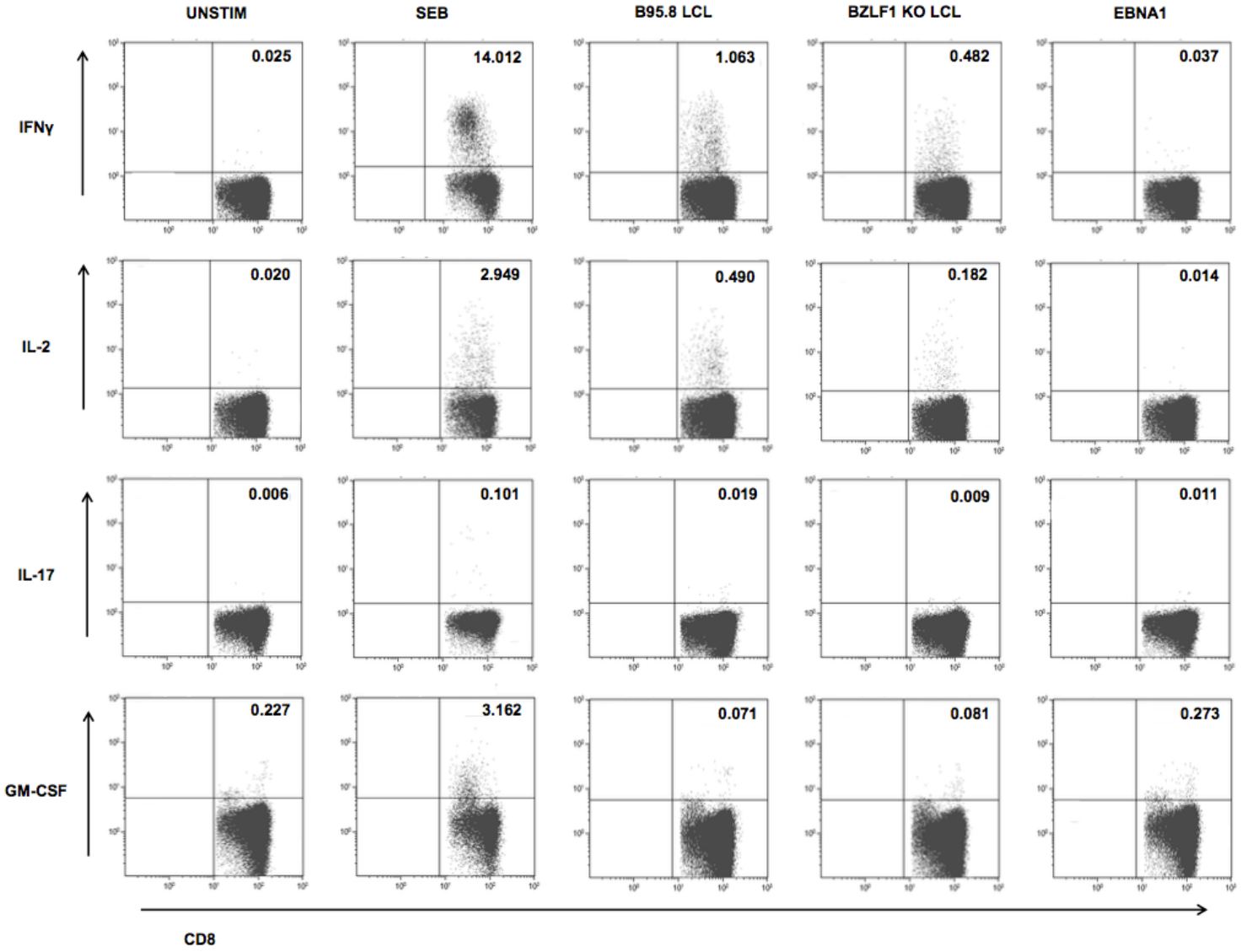

Figure 5.1.5 *Ex vivo* CD8+ T-cell responses to SEB and EBV antigens. Whole PBMC from one MS patient (MS11) was stimulated with SEB, autologous wild type LCL, autologous BZLF1 KO LCL and EBNA1 peptides separately and the intracellular cytokine responses analysed by flow cytometry. Cells were gated as LiveCD14-CD19-CD3+CD8+ cells and then further gated for IFNγ, IL-2, IL-17 and GM-CSF cytokine production. Values in top right corner of plots represents percentage of total gated CD8+ T-cells producing cytokine.

Lytic cycle proteins are major targets of EBV-specific CD8+ T-cell responses, and this is exaggerated during IM where CD8+ T-cells are massively expanded (Taylor et al., 2015). IM patients have elevated CD8+ T-cell responses directed against lytic antigens in their blood for several months following initial disease and this is evident in our cohort where up to 13% of post-IM donors' circulating CD8+ T-cells are IFNγ+ after *ex vivo* wild type LCL stimulation (Figure 5.1.6B). Healthy and MS donors showed much lower circulating frequencies of CD8+ T-cells specific for wild type LCL as shown by levels of IFNγ production; levels of IL-2 and GM-CSF were also unchanged between the two groups (Figure 5.1.6B and 5.1.6C). BZLF1 KO LCL stimulation showed responding CD8+ T-cells to be at much lower frequencies than for wild type LCL, and this reflects the high numbers of circulating CD8+ T-cells that are specific for EBV lytic proteins (Figure 5.1.6B and 5.1.6C). There were no significant differences between groups in cytokine production following autologous BZLF1 KO LCL stimulation (Figure 5.1.6C).

Interestingly, IL-17 production in response to both LCLs was significantly different across groups, with HC showing the highest cytokine production (B95.8 LCL: *p=0.0343*, BZLF1 KO LCL: *p=0.0212*, Kruskal-Wallis test) (Figure 5.1.6B and 5.1.6C). Cytokine production by CD8+ T-cells in response to EBNA1 peptide mix did not differ significantly between patient groups (Figure 5.1.6D).

CD4+ T-cells are key orchestrators of the immune response and many CD8+ T-cell responses are dependent on CD4+ T-cells for immunological help. We therefore investigated whether HLA-DR15 status of patients made a difference to the frequency or phenotype of CD8+ T-cell responses to EBV in HC or MS patients by comparing only data from patients who possessed the allele (Figure 5.1.7).

IL-17 production in HLA-DR15+ donors' CD8+ T-cells in response to wild type LCL remained very low but significantly higher in HC than MS donors (HC:MS *p=0.0323*, Mann-

Whitney test; all groups *p=0.0475*, Kruskal-Wallis test), but production in response to BZLF1 KO LCL lost significance (*p=0.1006*, Kruskal-Wallis test) (Figure 5.1.7C).

Production of GM-CSF in response to wild type LCL became significant between the three groups, however this may be skewed due to the high levels produced by the two HLA-DR15+ post-IM donors included in the analysis; levels between HC and MS donors were not different when statistically compared (*p=0.0363*, Kruskal-Wallis test) (Figure 5.1.7B).

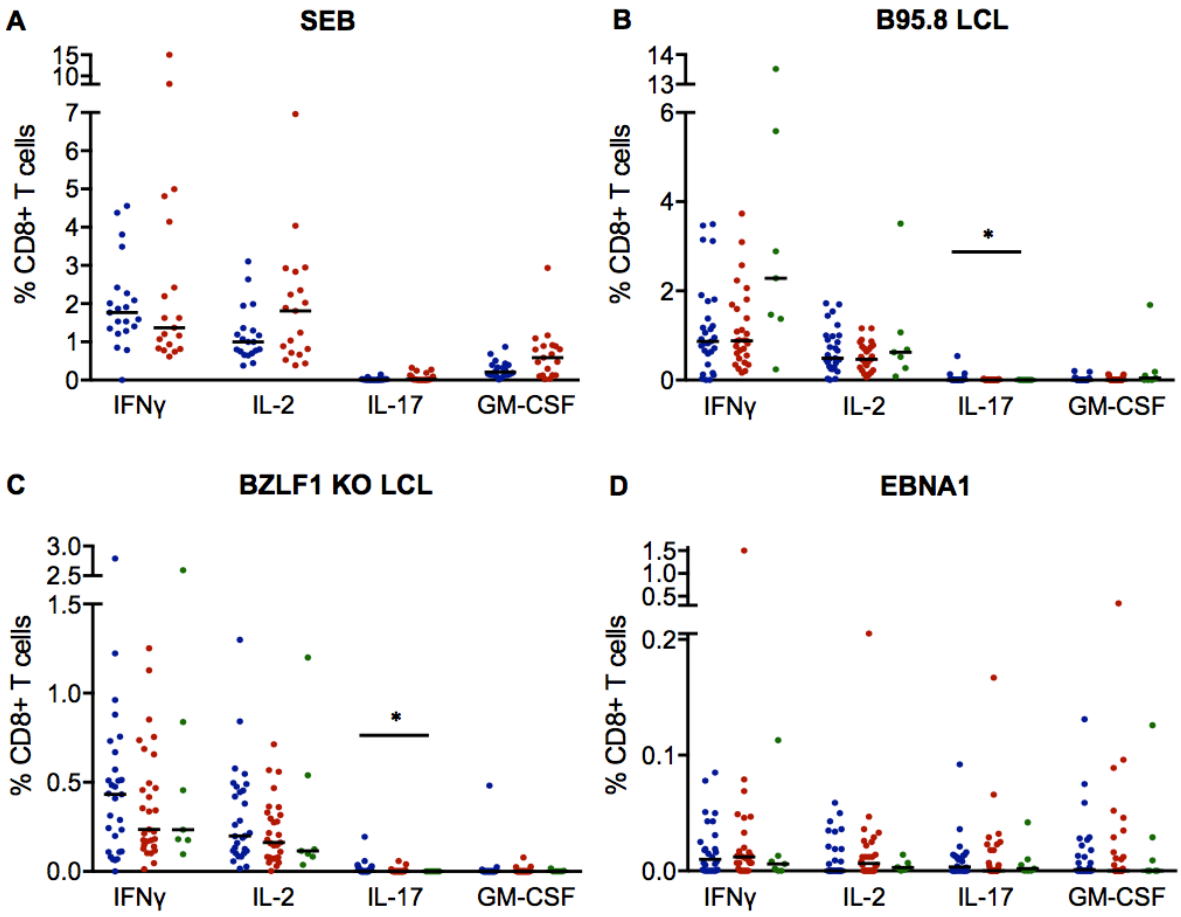

Figure 5.1.6 *Ex vivo* EBV-specific CD8+ T-cell responses. Whole PBMC were stimulated *ex vivo* and subjected to ICS. CD8+ T-cells are presented as a percentage of the whole CD8+ T-cell population responding to: **A.** SEB **B.** wild type LCL **C.** BZLF1 KO LCL and **D.** EBNA1 peptide mix. Colour of dots define patient group: blue=healthy control donors, red=RRMS patients and green=post-IM patients. Horizontal black line represents median of data set (SEB stimulation: HC n=20, MS n=19, all other stimulations: HC n=29, MS n=29, post-IM n=7). All statistics performed using the Kruskal-Wallis test for comparisons of three groups and the Mann-Whitney test for comparison of two patient groups (ns $p>0.05$, * $p\leq0.05$).

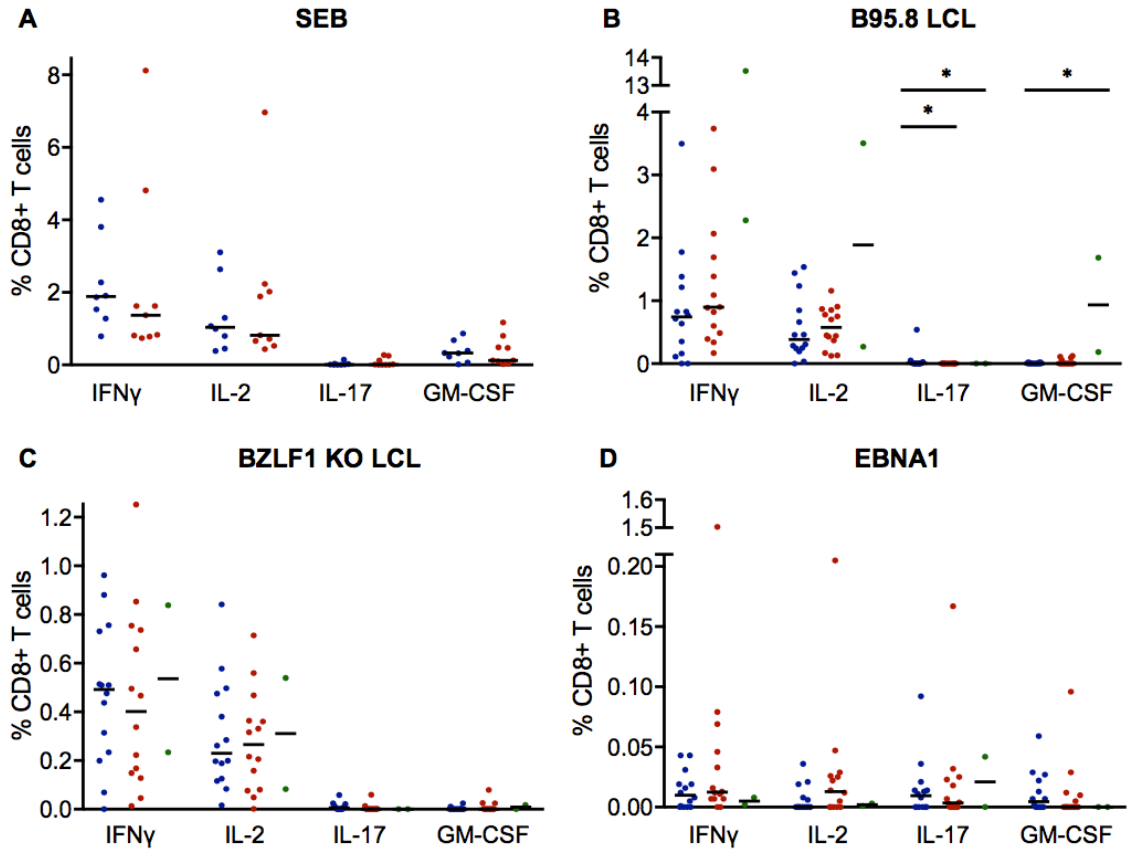

Figure 5.1.7 ***Ex vivo*** **EBV-specific CD8+ T-cell responses in HLA-DR15+ donors.** Whole PBMC from HLA-DR15+ donors were analysed separately for their reactivity to EBV antigens and their cytokine production. Responding CD8+ T-cells were presented as a percentage of the whole CD8+ population producing cytokine in response to: **A.** SEB **B.** wild type LCL **C.** BZLF1 KO LCL and **D.** EBNA1 peptide mix. Colour of dots define patient group: blue=healthy control donors, red=RRMS patients and green=post-IM patients. Horizontal black line represents median of data set (SEB stimulation: HC n=8, MS n=9, all other stimulations: HC n=14, MS n=14, post-IM n=2). All statistics performed using the Kruskal-Wallis test for comparisons of three groups and the Mann-Whitney test for comparison of two patient groups (ns $p>0.05$, * $p\leq0.05$).

5.2 Cytokine production of circulating EBV-specific T-cells

We observed no obvious difference in frequency of circulating EBV-specific CD4+ or CD8+ T-cells, however there were small phenotypic differences observed in cells responding to LCL in MS patients, and we characterised these in detail.

Ex vivo analysis of cytokine production in only responding T-cells was performed and compared between groups to gain a more detailed picture of function and phenotype of EBV-specific responses.

Responding cells were defined as CD4+ or CD8+ T-cells producing at least one cytokine in response to stimulation. Analysing only responding cells following EBV stimulation allows us to investigate the proportion of responding T-cells producing each cytokine in response to different stimuli, and through this interpret effector function or subset of T-cell responses to EBV antigens. It has been suggested that MS patients may have altered proportions of T_H1 or T_H17 CD4+ T-cells in their blood (Frisullo et al., 2008, Tzartos et al., 2008), and we sought to investigate whether EBV-responding T-cells showed different phenotype to those of HC or post-IM donors.

5.2.1 EBV-specific CD4+ T-cell responses

Figure 5.2.1 shows the overall percentage of responding CD4+ T-cells that produce each of the four cytokines. There were no significant differences in cytokine level produced following stimulation with SEB, autologous wild type LCL or EBNA1 peptide mix. However, there was a significant difference in IL-17 production between BZLF1 KO LCL-responding CD4+ T-cells from all three groups, with a higher proportion of CD4+ T-cells from HC producing IL-

17 than those from MS patients (HC:MS *p=0.0414*, Mann-Whitney test; HC:MS:IM *p=0.0355*, Kruskal-Wallis test) (Figure 5.2.1C).

This increased IL-17 production by CD4+ T-cells in response to LCL is in concordance with data shown earlier in the chapter (Figures 5.1.1 and 5.1.2), and indicates that fewer responding cells from MS patients produce IL-17 in response to LCL stimuli compared with those from HC.

A trend towards GM-CSF production in wild type LCL-specific CD4+ T-cells from HLADR15+ MS patients was observed compared to HC but did not reach significance. However, analysis of the whole cohort revealed the difference to be significant, and suggests that analysis of fewer subjects causes the data to lose power (Figure 5.1.1 and 5.2.1).

HLA-DR15+ donors were analysed separately to elucidate if the allele has any influence on cytokine production in responding cells, and results are shown in Figure 5.2.2. A higher proportion of CD4+ T-cells from DR15+ MS patients produced IL-17 compared to healthy donors following SEB stimulation (HC:MS *p=0.0315*, Mann-Whitney test), a contrast with BZLF1 KO LCL stimulation where healthy donors produced more IL-17 than MS patients (HC:MS *p=0.0100*, Mann Whitney test; HC:MS:IM *p=0.0058*, Kruskal-Wallis test) (Figure 2.2C). In the same analysis, MS patients were also shown to produce more GM-CSF than healthy controls in response to wild type LCL, a trend that did not reach significance when all donors were compared (Figure 5.2.2B; HC:MS *p=0.0036*, Mann-Whitney test) (Figure 5.2.1). Variation in GM-CSF production between groups in response to BZLF1 KO LCL stimulation was significant when only HLA-DR15+ donors were considered (Figure 5.2.2C; *p=0.0356*, Kruskall-Wallis test) (Figure 5.2.2B and C).

A difference in cytokine production when only analysing HLA-DR15+ donors may suggest that the allele affects phenotype of CD4+ T-cell responding to both SEB and EBV antigens, and this is interesting given that HLA-DR15 positivity is the strongest genetic link with MS.

Analysis of only HLA-DR15+ donors showed higher production of GM-CSF in response to wild type and BZLF1 KO LCLs (Kruskall-Wallis test), indicating that these donors produce more of this cytokine compared to patients that do not have the allele (Figure 5.2.1C and 5.2.2C).

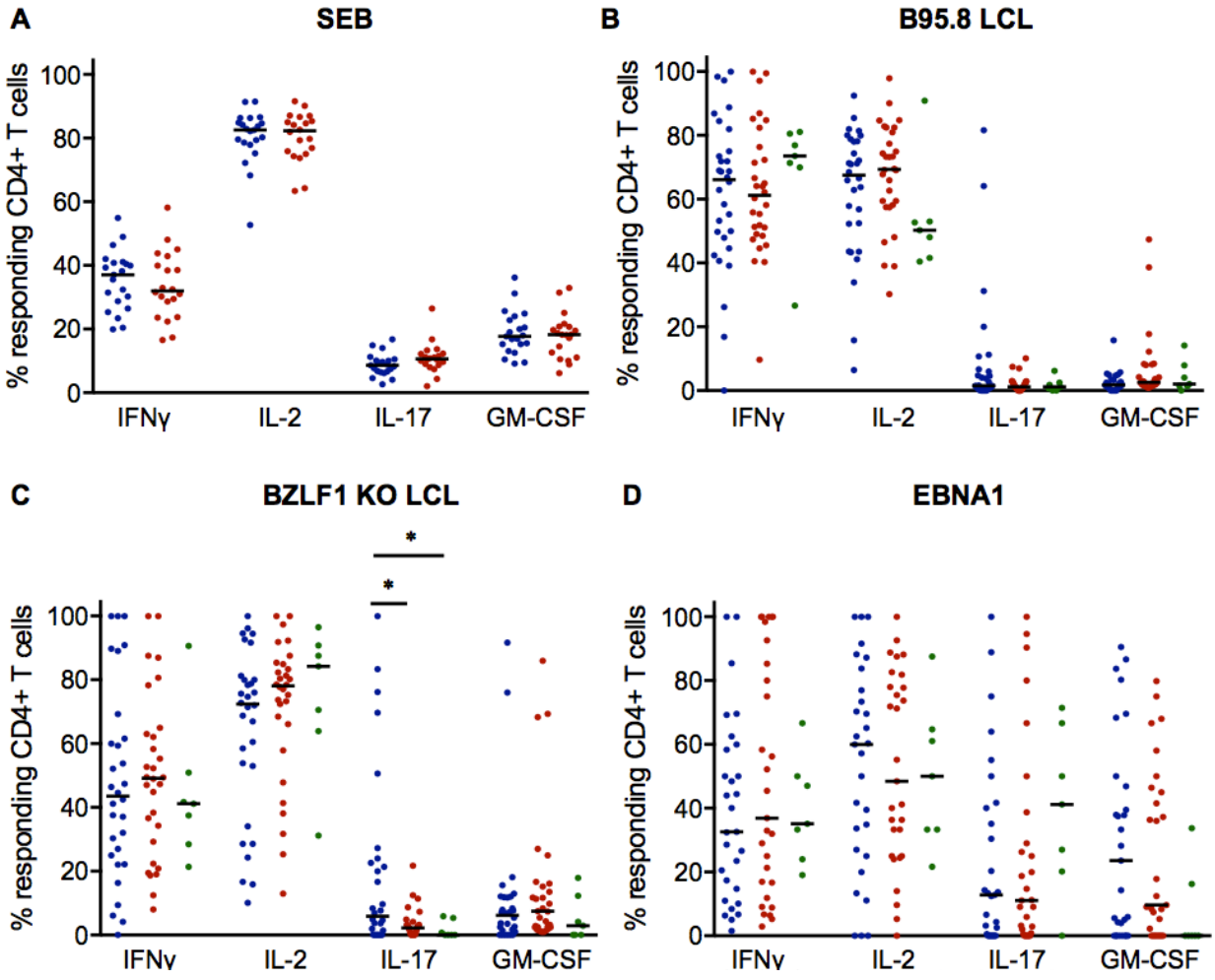

Figure 5.2.1 Function of EBV-specific CD4+ T-cells. Whole PBMC were stimulated and subjected to ICS. Responding CD4+ T-cells were defined as producing any combination of four cytokines in the staining panel. The proportion of responding CD4+ T-cells producing each of the cytokines are presented as a percentage of the total responding CD4+ T-cell population after stimulation with: **A.** SEB **B.** wild type LCL **C.** BZLF1 KO LCL and **D.** EBNA1 peptide mix. Colour of dots define patient group: blue=healthy control donors, red=RRMS patients and green=IM patients. Horizontal black line represents median of data set (SEB stimulation: HC n=20, MS n=19, all other stimulations: HC n=29, MS n=29, post-IM n=7). The Kruskal-Wallis test was used for direct comparison of variance between the three groups (long bar above data)and the Mann-Whitney test was used separately to analyse two patient groups (short bar above data) (*ns* $p>0.05$, * $p\leq0.05$).

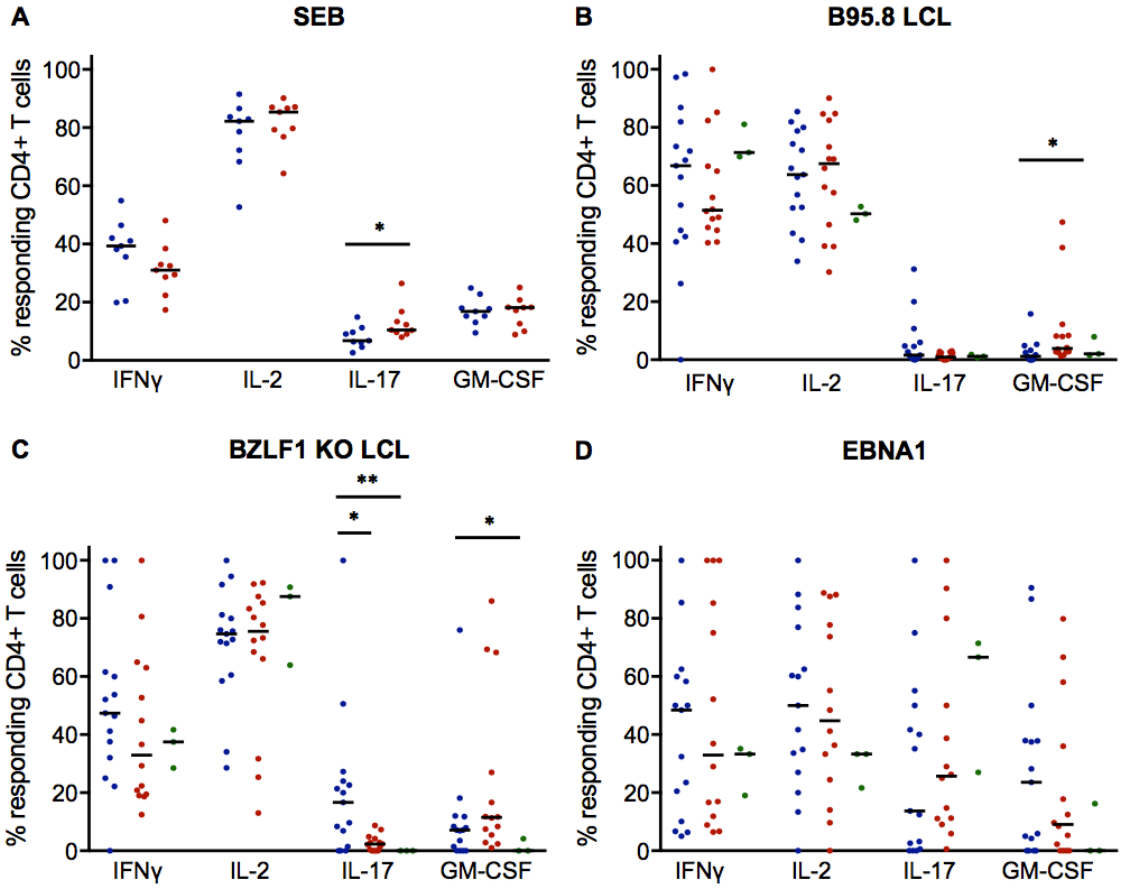

Figure 5.2.2 Function of EBV-specific CD4+ T-cells from HLA-DR15+ donors. Whole PBMC from HLA-DR15+ donors only were stimulated and subjected to ICS. Results from HLA-DR15+ donors only were compared. Responding CD4+ T-cells were defined as producing any combination of four cytokines in the staining panel. The proportion of responding CD4+ T-cells producing each of the cytokines are presented as a percentage of the total responding CD4+ T-cell population after stimulation with: **A.** SEB **B.** wild type LCL **C.** BZLF1 KO LCL and **D.** EBNA1 peptide mix. Colour of dots define patient group: blue=healthy control donors, red=RRMS patients and green=IM patients. Horizontal black lines represent median of data set (SEB stimulation: HC n=8, MS n=9, all other stimulations: HC n=14, MS n=14, post-IM n=2). The Kruskal-Wallis test was used for direct comparison of variance between the three groups and the Mann-Whitney test was used separately to analyse two patient groups (ns $p>0.05$, * $p\leq0.05$, ** $p\leq0.01$).

5.2.2 Boolean gate analysis of EBV-specific CD4+ T-cells

Further analysis of cytokine production from *ex vivo* T-cell stimulations was performed using Boolean combination gate analysis of Funky Cells transformed data using SPICE software. This data mining allowed further investigation of responding cells by calculating proportions of cells producing each of the sixteen possible combinations of cytokines in our staining panel and plotting them graphically. Annotation describing cytokine profile of T-cells is shown in table 5.1 and will be used throughout this thesis to refer to each of the sixteen Boolean gates (Table 5.1).

Table 5.1 Annotation for Boolean gating

IFNγ- IL2- IL17- GMCSF-	-	-	-	-
IFNγ- IL2- IL17- GMCSF+	-	-	-	+
IFNγ- IL2- IL17+ GMCSF-	-	-	+	-
IFNγ- IL2- IL17+ GMCSF+	-	-	+	+
IFNγ- IL2+ IL17- GMCSF-	-	+	-	-
IFNγ- IL2+ IL17- GMCSF+	-	+	-	+
IFNγ- IL2+ IL17+ GMCSF-	-	+	+	-
IFNγ- IL2+ IL17+ GMCSF+	-	+	+	+
IFNγ+ IL2- IL17- GMCSF-	+	-	-	-
IFNγ+ IL2- IL17- GMCSF+	+	-	-	+
IFNγ+ IL2- IL17+ GMCSF-	+	-	+	-
IFNγ+ IL2- IL17+ GMCSF+	+	-	+	+
IFNγ+ IL2+ IL17- GMCSF-	+	+	-	-
IFNγ+ IL2+ IL17- GMCSF+	+	+	-	+
IFNγ+ IL2+ IL17+ GMCSF-	+	+	+	-
IFNγ+ IL2+ IL17+ GMCSF+	+	+	+	+

Cytokine profile was first analysed in CD4+ T-cells responding to SEB stimulation with results shown in Figure 5.2.3. Cytokine profile of responding CD4+ cells was similar between groups,

with HC and MS donors both showing a response in which cells mostly produced IL-2 (Figure 5.2.3).

Following stimulation with autologous wild type LCL, post-IM patients showed a significant increase compared to HC in the proportion of responding cells that produce IFNγ only (HC:IM +--- *p=0.030*) and co-express IFNγ and GM-CSF (HC:IM +--+ *p=0.009*), and a reduced proportion of responding CD4+ T-cells in the IFNγ+IL-2+ subset (HC:IM ++-- *p=0.009*) (Figure 5.2.4).

MS patients' responding CD4+ T-cells showed a slightly different pattern of cytokine production after wild type LCL stimulation, with increased proportion of cells in the IFNγ+GM-CSF+ and IFNγ+IL-2+GM-CSF+ subsets compared to healthy controls (HC:MS +--+ *p=0.016*) (HC:MS ++-+ *p=0.034*) (Figure 5.2.4).

The proportion of responding CD4+ T-cells producing IFNγ only and co-expressing IFNγ and IL-2 were unchanged between all three groups, but a higher proportion of cells from post-IM donors produced IL-2 only compared to healthy controls (HC:IM -+-- *p=0.048*) (Figure 5.2.5). Healthy donors had a higher proportion of CD4+ T-cells producing IL-17 only but this did not reach significance when compared with other groups (Figure 5.2.5).

CD4+ T-cell responses to EBNA1 were more varied in their cytokine responses, with many subsets making up the overall response for each group and potentially skewed by the small numbers of responding cells in the populations. There were no significant differences in phenotype between groups' CD4+ T-cells responding to EBNA1 antigen (Figure 5.2.6).

Permutation tests were also used to compare contribution of cells in each combination gate to the responding populations as a whole, and the data for CD4+ T-cells are presented in pie chart format using SPICE software in Figure 5.2.7. SEB responding CD4+ T-cells did not show any difference in proportion of cells in each combination gate between healthy or MS donors. However, a difference was observed between MS and post-IM patients' CD4+ T-cells

responding to wild type LCL, with a higher proportion of cells from MS donors in the IFNγ+IL-2+ and IL-2+ subsets (MS:IM *p=0.0498*) (Figure 5.2.7B). No significant differences were seen in subset usage of CD4+ T-cells responding to BZLF1 KO LCL or EBNA1, however EBNA1 responses showed a very different subset usage compared to other stimuli indicating a strong phenotypic difference in cells responding to the antigen (Figure 5.2.7D).

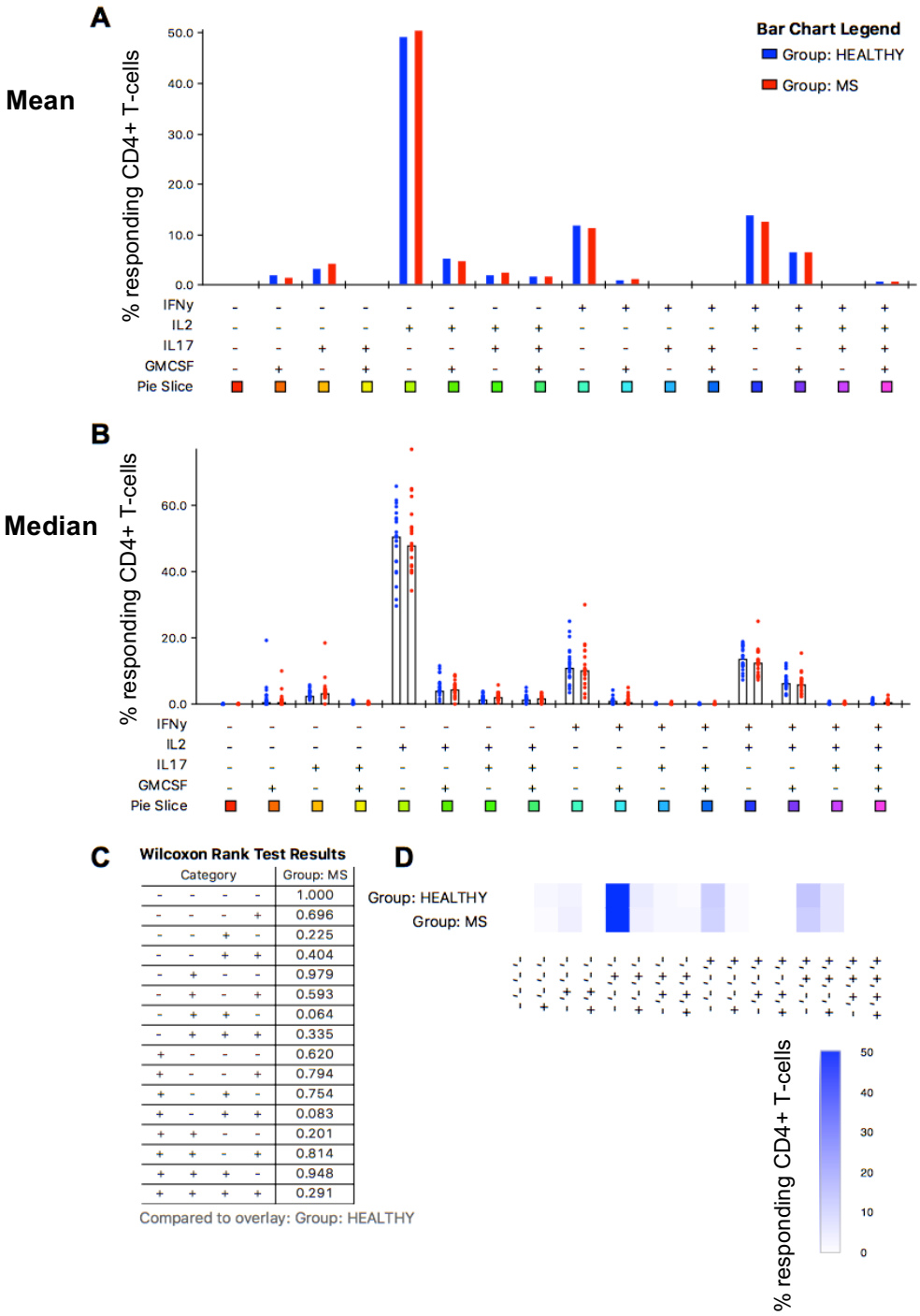

Figure 5.2.3 Cytokine profile of *ex vivo* SEB-specific CD4+ T-cells. Whole PBMC were stimulated *ex vivo* with SEB and ICS was performed (HC n=21, MS n=19). Responding CD4+ T-cells were defined as T-cells positive for any combination of cytokines. **A.** Graphical representation of responding cells in each combination gate with bars representing the mean of data set. Statistics were calculated using the Wilcoxon Signed Rank test. **B.** Scatter plot showing percentage of responding cells for each donor in combination gates. Black bars represent median of data set. **C**. Table shows results from the Wilcoxon rank test. **D.** Percentage of responding CD4+ T-cells shown in heatmap form. Combination gate data was processed using Funky Cells software and graphically displayed using the program SPICE.

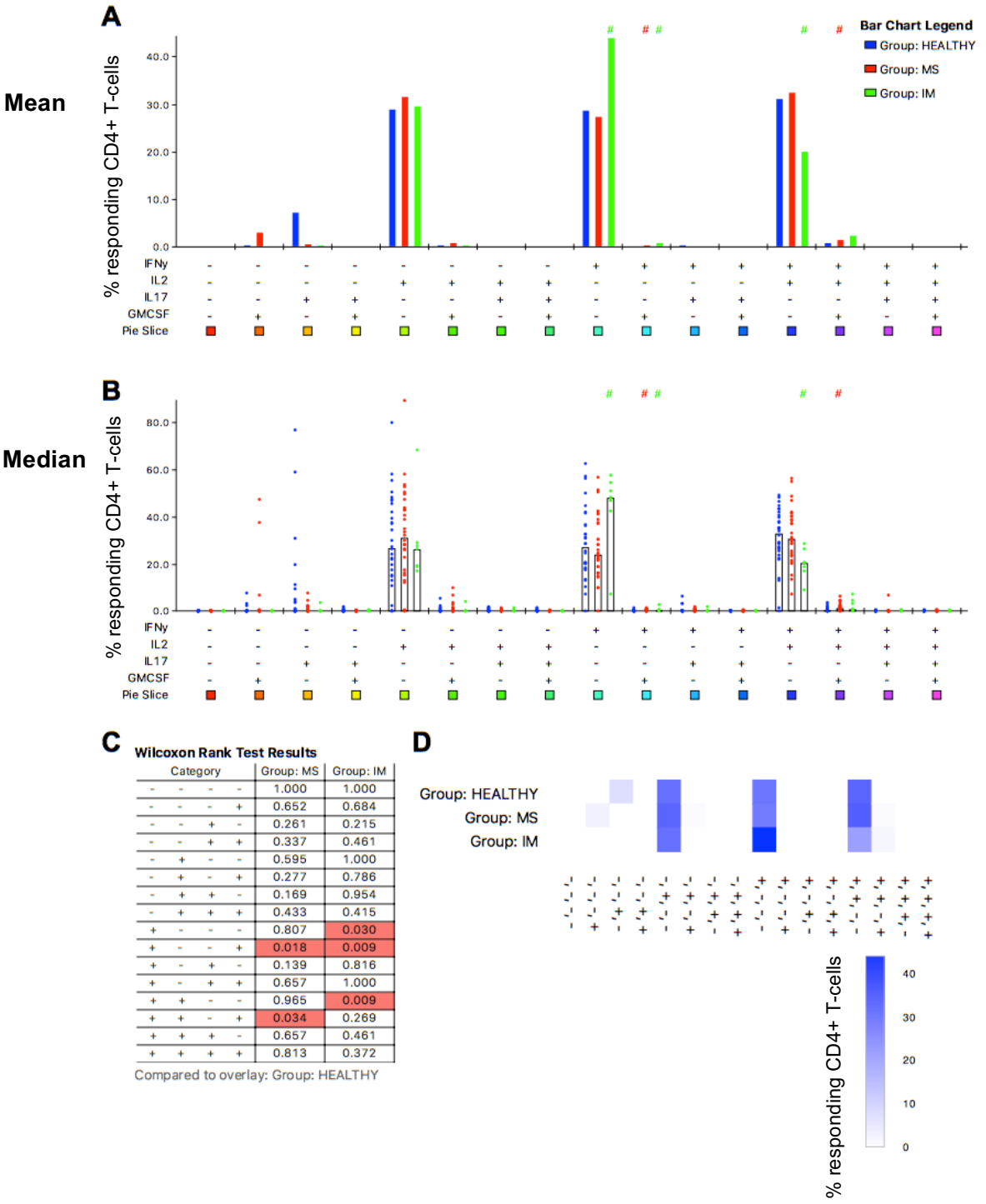

Figure 5.2.4 Cytokine profile of *ex vivo* wild type LCL-specific CD4+ T-cells. Whole PBMC were stimulated *ex vivo* with wild type LCL and ICS was performed (HC n=28, MS n=27, IM n=7). Responding CD4+ T-cells were defined as T-cells positive for any combination of cytokines. **A.** Graphical representation of responding cells in each combination gate with bars representing the mean of data set. Statistics were calculated using the Wilcoxon Signed Rank test. **B.** Scatter plot showing percentage of responding cells for each donor in combination gates. Black bars represent median of data set **C**. Table shows results from Wilcoxon Rank test. **D.** Percentage of responding CD4+ T-cells shown in heatmap form. Combination gate data was processed using Funky Cells software and graphically displayed using the program SPICE.

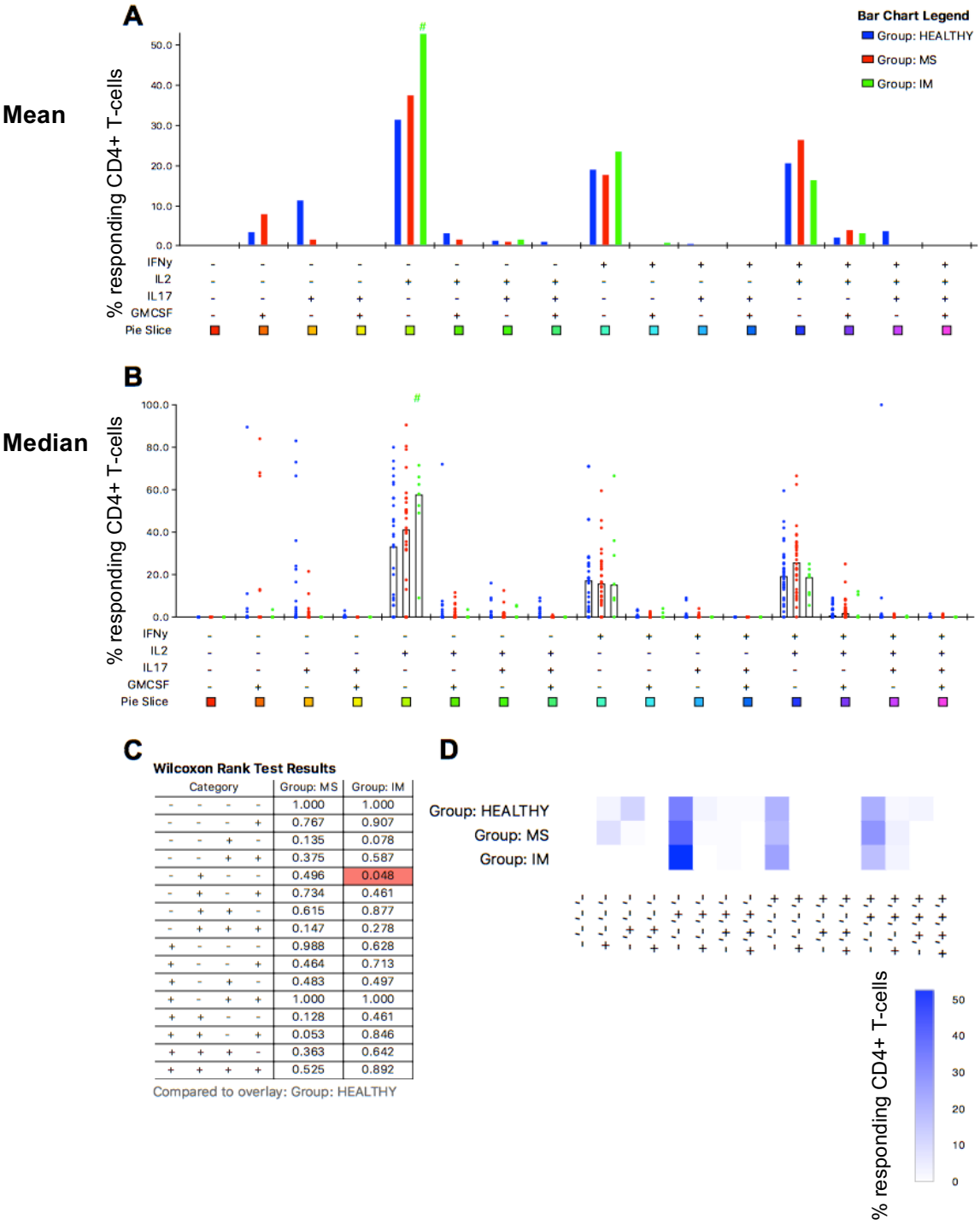

Figure 5.2.5 Cytokine profile of *ex vivo* BZLF1 KO LCL-specific CD4+ T-cells. Whole PBMC were stimulated *ex vivo* with BZLF1 KO LCL and ICS was performed (HC n=28, MS n=27, IM n=7). Responding CD4+ T-cells were defined as T-cells positive for any combination of cytokines. **A.** Graphical representation of responding cells in each combination gate with bars representing the mean of data set. Statistics were calculated using the Wilcoxon Signed Rank test. **B.** Scatter plot showing percentage of responding cells for each donor in combination gates. Black bars represent median of data set **C**. Table shows results from Wilcoxon rank test. **D.** Percentage of responding CD4+ T-cells shown in heatmap form. Combination gate data was processed using Funky Cells software and graphically displayed using the program SPICE.

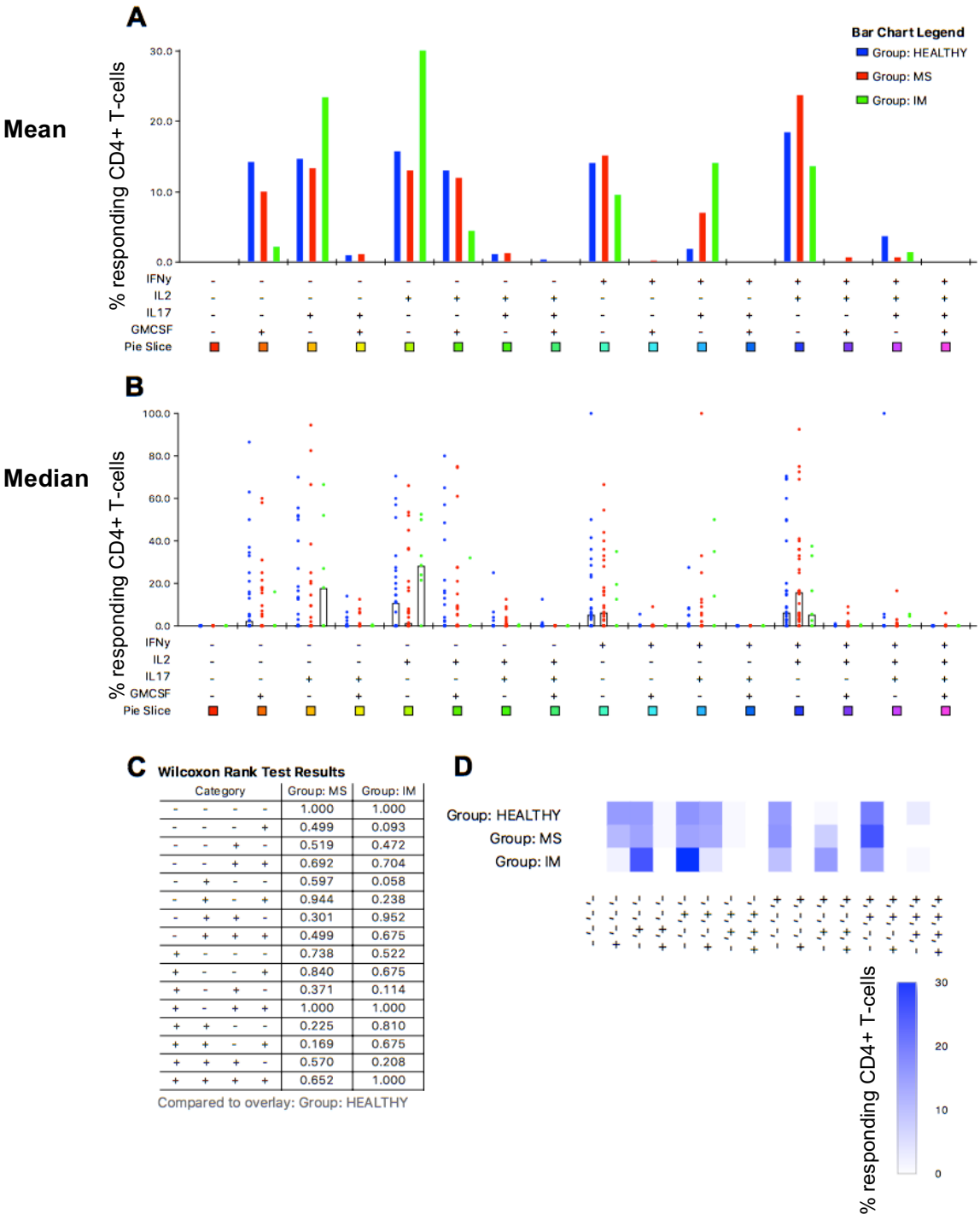

Figure 5.2.6 Cytokine profile of *ex vivo* EBNA1-specific CD4+ T-cells. Whole PBMC were stimulated *ex vivo* with EBNA1 peptide mix and ICS was performed (HC n=28, MS n=27, IM n=7). Responding CD4+ T-cells were defined as T-cells positive for any combination of cytokines. **A.** Graphical representation of responding cells in each combination gate with bars representing the mean of data set. Statistics were calculated using the Wilcoxon Signed Rank test. **B.** Scatter plot showing percentage of responding cells for each donor in combination gates. Black bars represent median of data set. **C**. Table showing results from Wilcoxon rank test. **D.** Percentage of responding CD4+ T-cells shown in heatmap form. Combination gate data was processed using Funky Cells software and graphically displayed using the program SPICE.

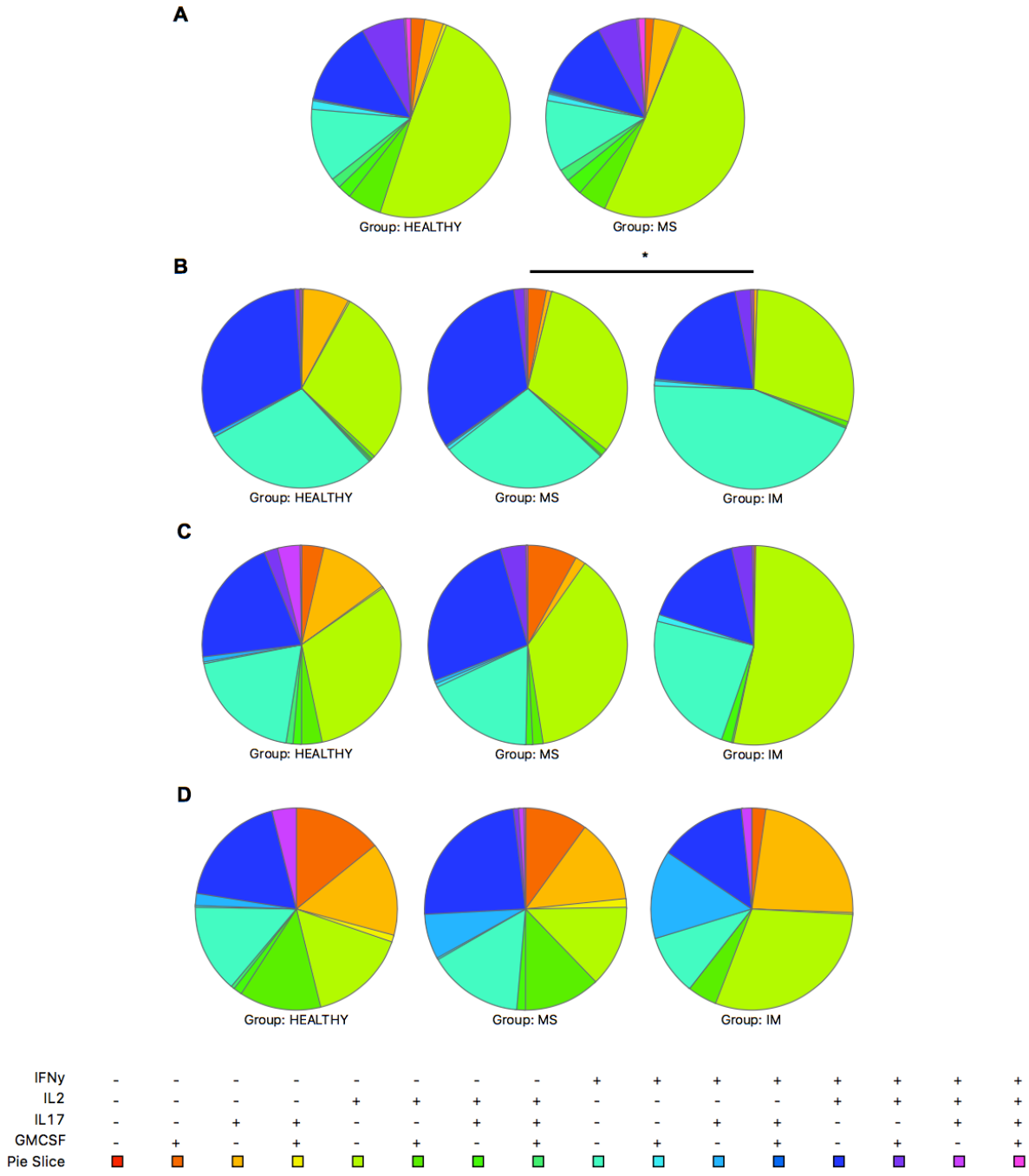

Figure 5.2.7 Cytokine profile of *ex vivo* EBV-specific CD4+ T-cells. Whole PBMC from each donor were stimulated before ICS the following day. CD4+ T-cells were categorised into 16 combination gates for cytokine production. Pie charts show the mean percentage of responding CD4+ T-cells belonging to each gate after stimulation with: **A.** SEB (HC n=21) (MS n=19) **B.** wild type LCL (HC n=28) (MS n=27) (IM n=7) **C.** BZLF1 KO LCL (HC n=28) (MS n=27) (IM n=7) and **D.** EBNA1 (HC n=28) (MS n=27) (IM n=7). Combination gate data was processed using Funky Cells software and graphically displayed using the program SPICE, statistics were calculated using a permutation test (ns $p>0.05$, * $p<0.05$).

5.2.3 EBV-specific CD8+ T-cell responses

Cytokine production in CD8+ T-cells responding to *ex vivo* stimuli showed a different pattern to that of CD4+ T-cells. Example staining for SEB, wild type LCL, BZLF1 KO LCL and EBNA1 protein is shown in Figure 5.1.5. We characterised the cytokine production of *ex vivo* CD8+ T-cells responding to stimuli to elucidate if they are phenotypically different between patient groups or different from those secreted by CD4+ T-cells. This was performed by sorting responding CD8+ T-cells in to Boolean combination gates which allows production of multiple cytokines to be measured and compared between groups.

IFNγ production by responding CD8+ T-cells was found to be significantly higher in HC in response to SEB (HC:MS *p=0.0051*, Mann-Whitney test), with GM-CSF production significantly lower in healthy controls compared to MS patients (*p=0.0259*, Mann-Whitney test) (Figure 5.2.8A). IL-2 production was also higher in MS patient CD8+ T-cells but this did not reach significance (Figure 5.2.8A).

CD8+ T-cells responding to LCLs were similar between groups for IFNγ, IL-17 and GM-CSF, however for both wild type LCL and BZLF1 KO LCL a higher proportion of responding cells from healthy donors produced IL-2 (Figure 5.2.8B and C). The variation in levels of IL-2 production in response to wild type LCL across three groups reached significance (*p=0.0026*, Kruskal-Wallis test), but did not for the BZLF1 KO LCL response (Figure 5.2.8B and C). There were no differences observed in cytokine responses towards EBNA1 peptide mix (Figure 5.2.8D).

HLA-DR15+ donors were analysed for their cytokine production in responding CD8+ T-cells (Figure 5.2.9). The increased IFNγ production of HC in response to SEB remained elevated when only HLA-DR15+ donors were analysed. Elevated GM-CSF no longer reached significance when only HLA-DR15+ donors were analysed (Figure 5.2.9A).

There was no significant difference between the three groups in IL-2 production following wild type LCL stimulation when only HLA-DR15+ donors were analysed, and variation in production of GM-CSF between cohorts was seen when comparing all three groups directly (*p=0.0138*, Kruskal-Wallis test) (Figure 5.2.9B).

GM-CSF production in wild type LCL-specific CD8+ T-cells from HLA-DR15+ MS patients was higher than that of HC (HC:MS *p=0.0318*, Mann-Whitney test) (Figure 5.2.9B), an effect that was not apparent when all donors were analysed. Significant variation was also seen across all three donor groups when the Wilcoxon rank test was applied (HC:MS:post-IM *p=0.0138*). Interestingly, CD8+ T-cells from HLA-DR15+ MS donors had a significantly higher production of IL-2 in response to EBNA1 peptide mix than healthy donors (HC:MS *p=0.0245*, Mann-Whitney test) (Figure 5.2.9D). This increase was seen with all donors were analysed but did not reach significance, suggesting that CD8+ T-cells from HLA-DR15+ MS donors produce more IL-2 in response to EBNA1 than other groups.

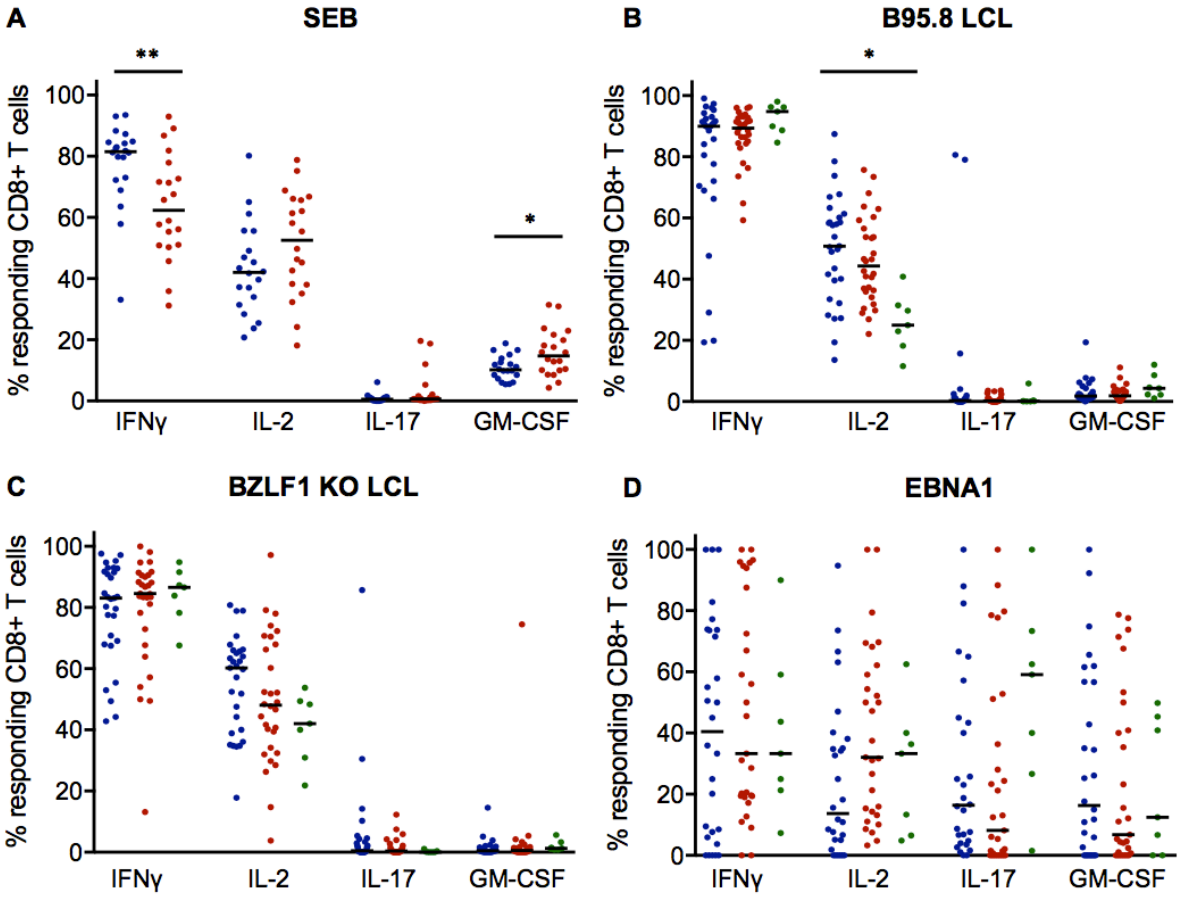

Figure 5.2.8 Cytokine production of EBV-specific CD8+ T-cells. Whole PBMC were stimulated and subjected to ICS. Responding T-cells were defined as producing any combination of four cytokines. Percentage of responding cells positive for each cytokine were analysed between patient groups in response to: **A.** SEB **B.** wild type LCL **C.** BZLF1 KO LCL and **D.** EBNA1 peptide mix. Colour of dots define patient group: blue=healthy control donors, red=RRMS patients and green=IM patients. Horizontal black line represents median of data set (SEB stimulation: HC n=20, MS n=19, all other stimulations: HC n=29, MS n=29, post-IM n=7). The Kruskal-Wallis test was used for direct comparisons of the three groups and the Mann-Whitney test was used to analyse two patient groups at a time (ns $p>0.05$, * $p\leq0.05$, ** $p\leq0.01$).

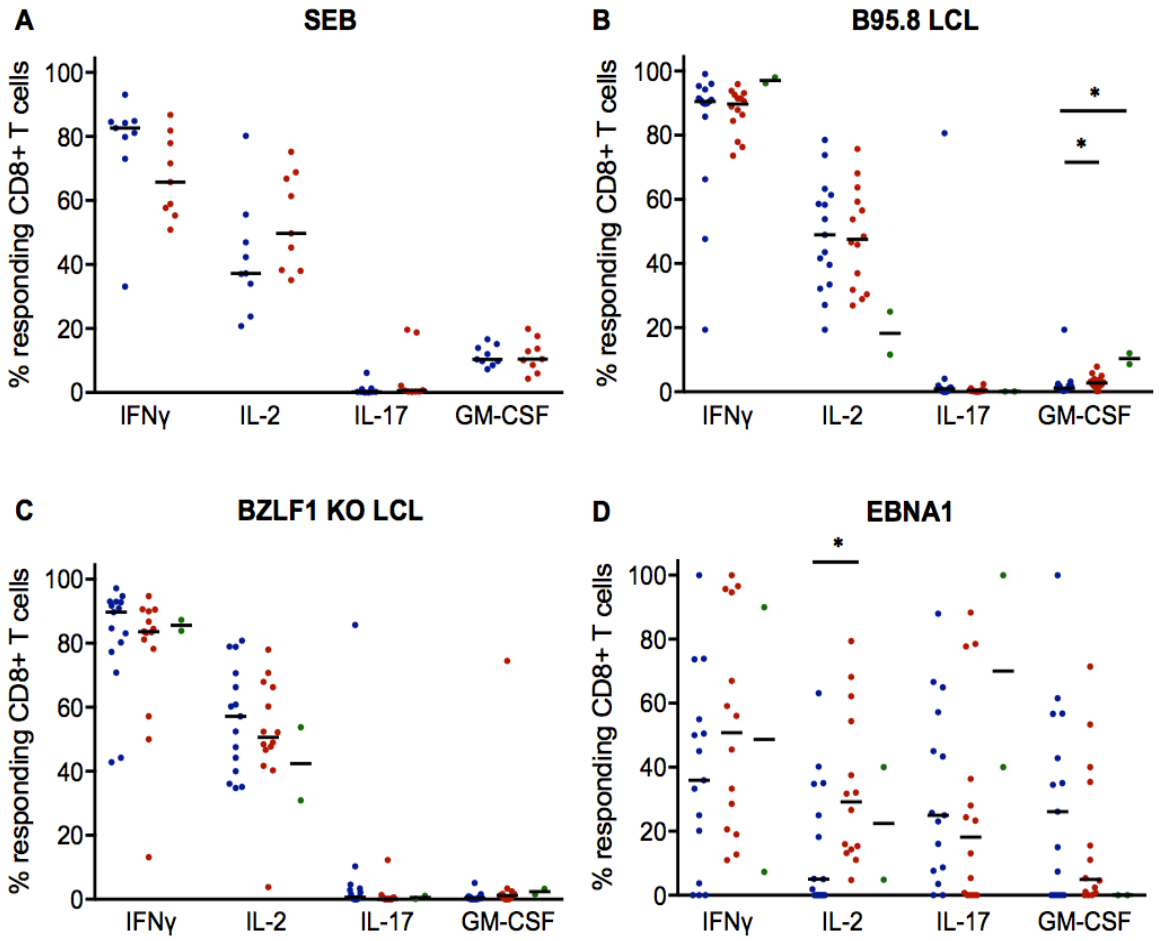

Figure 5.2.9 Cytokine production of EBV-specific CD8+ T-cells from HLA-DR15+ donors. Whole PBMC were stimulated and subjected to ICS. Results from HLA-DR15+ donors only were compared. Responding CD8+ T-cells were defined as T-cells producing any combination of four cytokines in response to four stimuli: **A.** SEB **B.** wild type LCL **C.** BZLF1 KO LCL and **D.** EBNA1 peptide mix. Colour of dots define patient group: blue=healthy control donors, red=RRMS patients and green=IM patients. Horizontal black line represents median of data set (SEB stimulation: HC n=8, MS n=9, all other stimulations: HC n=14. MS n=14, post-IM n=2). The Kruskal-Wallis test was used for direct comparisons of the three groups and the Mann-Whitney test was used to analyse two patient groups at a time (ns $p>0.05$, * $p\leq0.05$).

5.2.4 Boolean gate analysis of EBV-specific CD8+ T-cells

As previously described for *ex vivo* CD4+ T-cell data, SPICE software was used to analyse Boolean combination gate data for responding CD8+ T-cells and allows analysis of cells producing multiple cytokines. The notation for cytokine production shown in Table 5.1 was also applied to CD8+ T-cell Boolean gates.

Cytokine production seen in SEB stimulated CD8+ T-cells reflects that seen in Figure 5.2.8, and an increased proportion of cells from MS patients were IL-2+ and IL-2+GM-CSF+ compared to healthy donors (HC:MS -+-- *p=0.048*, HC:MS -+-+ *p=0.009*) (Figure 5.2.10). Healthy donors showed an increased proportion of responding CD8+ T-cells expressing IFNγ only (HC:MS +--- *p=0.037*) (Figure 5.2.10).

No significant differences were seen in cytokine production between responding CD8+ T-cell from HC and MS patients following wild type LCL stimulation (Figure 5.2.11). However, post-IM donors showed increased proportion of cells belonging to the IFNγ+ and IFNγ+GM-CSF+ subsets (HC:IM +--- *p=0.001I*, HC:IM, +--+ *p=0.005*), with a decreased number of IFNγ+IL-2+ CD8+ T-cells (HC:IM ++-- *p=0.004*) (Figure 5.2.11). These findings might reflect the disruption of the CD8+ T-cell compartment that occurs during IM, indicating that EBV-specific CD8+ cells are still altered in phenotype as well as frequency 4-6 months following symptomatic primary infection.

Cytokine production in response to BZLF1 KO LCL stimulation follows the same pattern as that for wild type LCL stimulation, with post-IM donors showing increased proportion of IFNγ+ and IFNγ+GM-CSF+ subsets with decreased number co-expressing IFNγ and IL-2 (HC:IM +--- *p=0.013*, HC:IM +--+ *p=0.001*, HC:IM ++-- *p=0.032*) (Figure 5.2.12). Cytokine

production following BZLF1 KO LCL stimulation in MS patient CD8+ T-cells was not different from that of healthy donors (Figure 5.2.12).

High variation in CD4+ T-cell responses to EBNA1 were observed across all groups (Figure 5.2.6D) and this was also shown in EBNA1-specific CD8+ T-cells (Figure 5.2.13D). Despite this variability in responses no significant differences were seen in cytokine profile of responding CD8+ cells between donor groups.

As previously shown for responding CD4+ T-cells, permutation tests were performed on cytokine combination gate data from CD8+ T-cells, and the proportion of cells in each gate are displayed in pie chart format in Figure 5.2.14. MS patient and HC CD8+ T-cells responding to SEB stimulation showed significantly different subset usage, with differences mainly with the proportion of donor responses producing IFNγ only and IL-2 only (HC:MS *p=0.0268*) (Figure 5.2.14A).

The phenotype of CD8+ T-cells responding to wild type LCL also differed significantly between groups, with post-IM donors showing the biggest change. The vast majority of responding CD8+ T-cells in post-IM donors produced IFNγ only after wild type LCL stimulation, with this subset making up ~70% of the response (Figure 5.2.14B). However, HC and MS patients showed a decreased proportion of cells producing IFNγ alone compared to post-IM donors. A larger proportion of the wild type LCL response in HC and MS donors co-produced IFNγ and IL-2, indicating a more mature and polyfunctional response in donors who have carried the virus for longer (HC:IM *p=0.0017*, MS:IM *p=0.0016*) (Figure 5.2.14B), and showing responses in HC and MS were similar in phenotype.

CD8+ T-cell responses to the BZLF1 KO LCL again showed similar cytokine production between all three cohort groups, however a difference was observed between HC and post-IM donors, who exhibited a higher proportion of CD8+ T-cells producing IFNγ only following stimulus (HC:IM *p=0.0134*) (Figure 5.2.14C).

More varied production of cytokines was present in CD8+ T-cells responding to EBNA1 peptide mix but responses between patient groups did not show any significant differences between groups (Figure 5.2.14D).

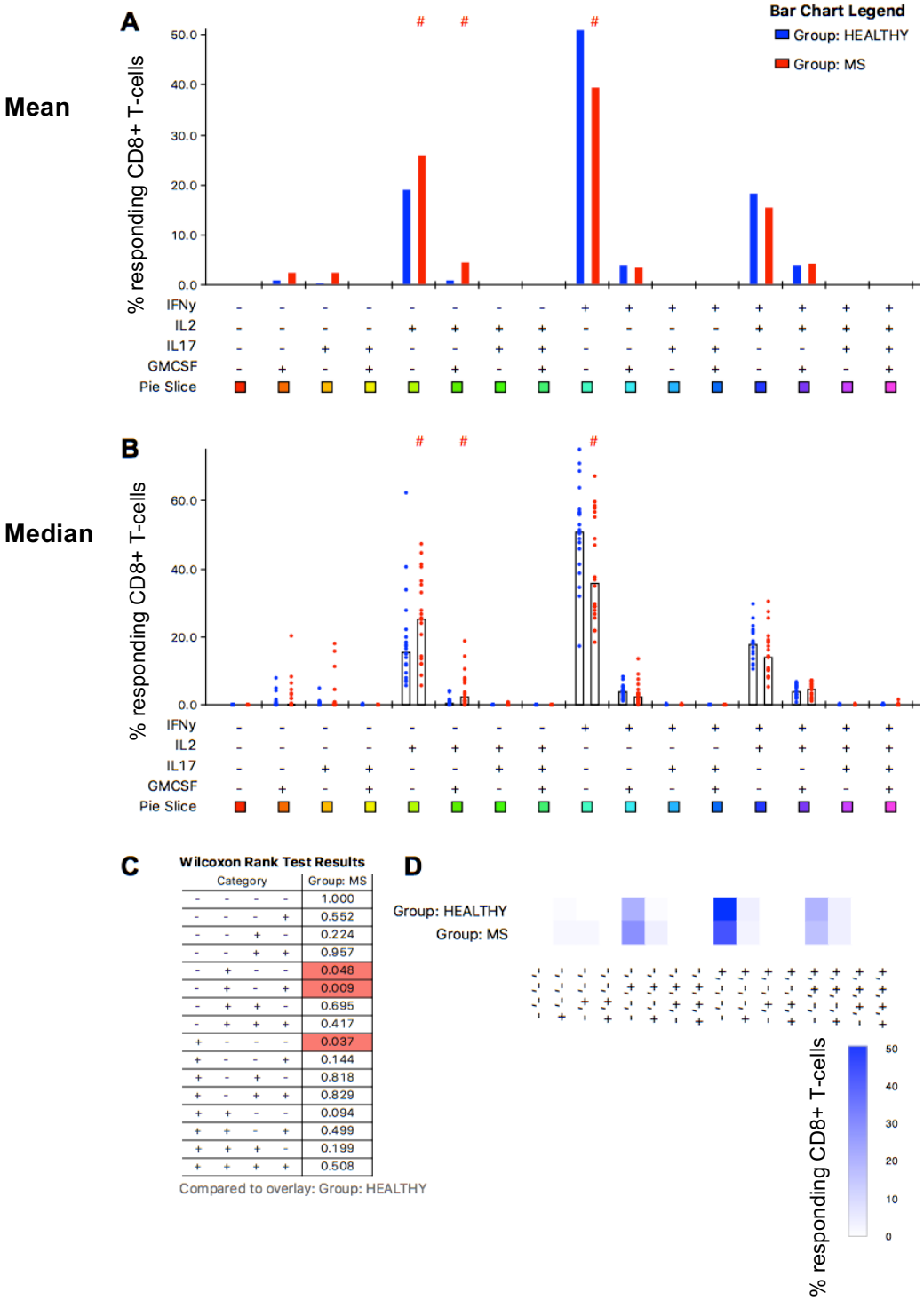

Figure 5.2.10 Cytokine profile of *ex vivo* SEB-specific CD8+ T-cells. Whole PBMC were stimulated *ex vivo* with SEB before ICS was performed. (HC n=21, MS n=19). Responding CD8+ T-cells were defined as T-cells positive for any combination of cytokines. **A.** Graphical representation of responding cells in each combination gate with bars representing the mean of data set. Statistics were calculated using the Wilcoxon Signed Rank test **B.** Scatter plot showing percentage of responding cells for each donor in combination gates. Black bars represent median of data set. **C**. Table showing results from Wilcoxon rank test. **D.** Percentage of responding CD8+ T-cells shown in heatmap form. Combination gate data was processed using Funky Cells software and graphically displayed using the program SPICE (ns $p>0.05$, * $p<0.05$).

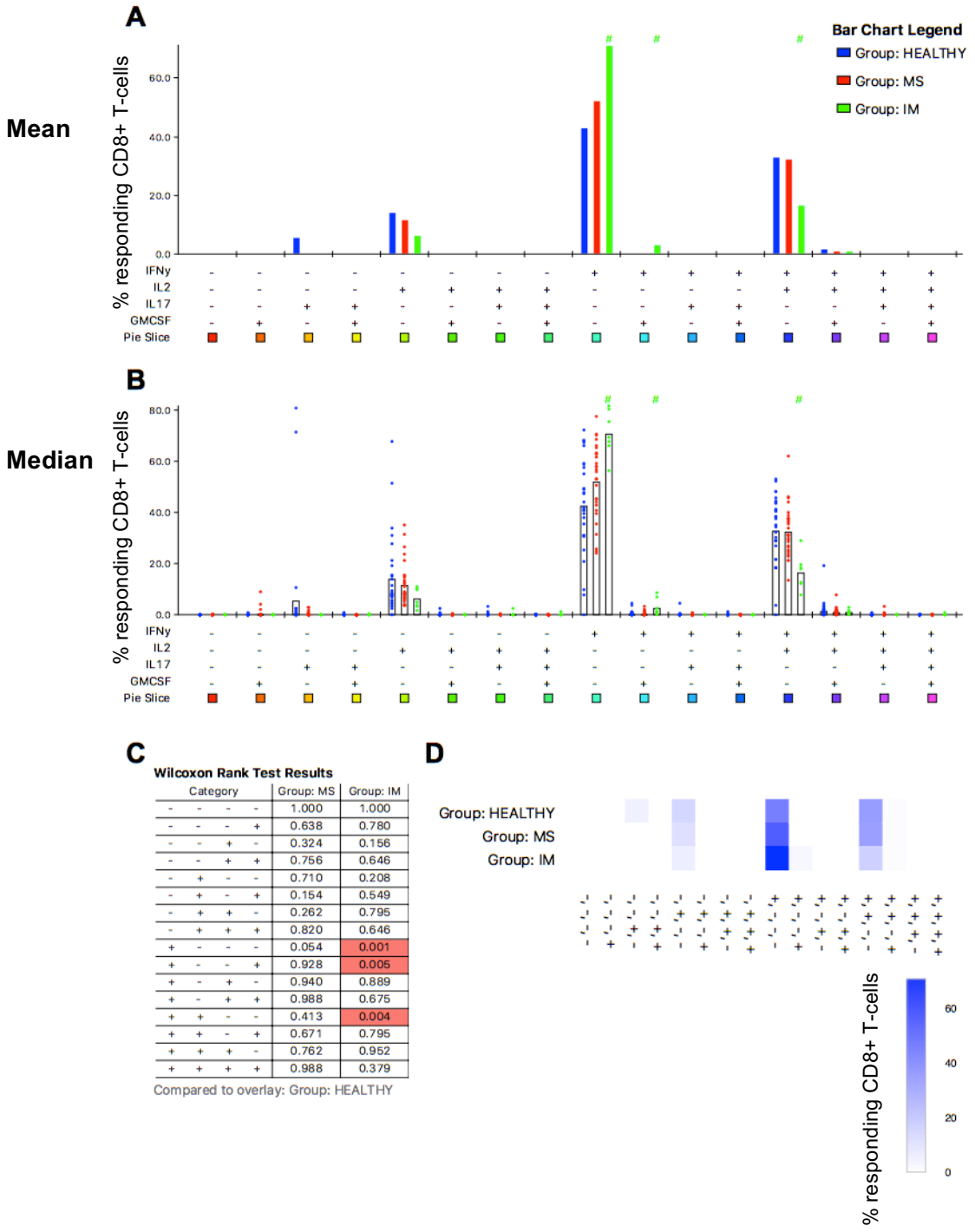

Figure 5.2.11 Cytokine profile of *ex vivo* wild type LCL-specific CD8+ T-cells. Whole PBMC were stimulated *ex vivo* with wild type LCL before ICS was performed (HC n=28, MS n=27, IM n=7). Responding CD8+ T-cells were defined as T-cells positive for any combination of cytokines. **A.** Graphical representation of responding cells in each combination gate with bars representing the mean of data set. Statistics were calculated using the Wilcoxon Signed Rank test. **B.** Scatter plot showing percentage of responding cells for each donor in combination gates. Black bars represent median of data set. **C**. Table of results from Wilcoxon rank test. **D.** Percentage of responding CD8+ T-cells shown in heatmap form. Combination gate data was processed using Funky Cells software and graphically displayed using the program SPICE (ns $p>0.05$, * $p<0.05$).

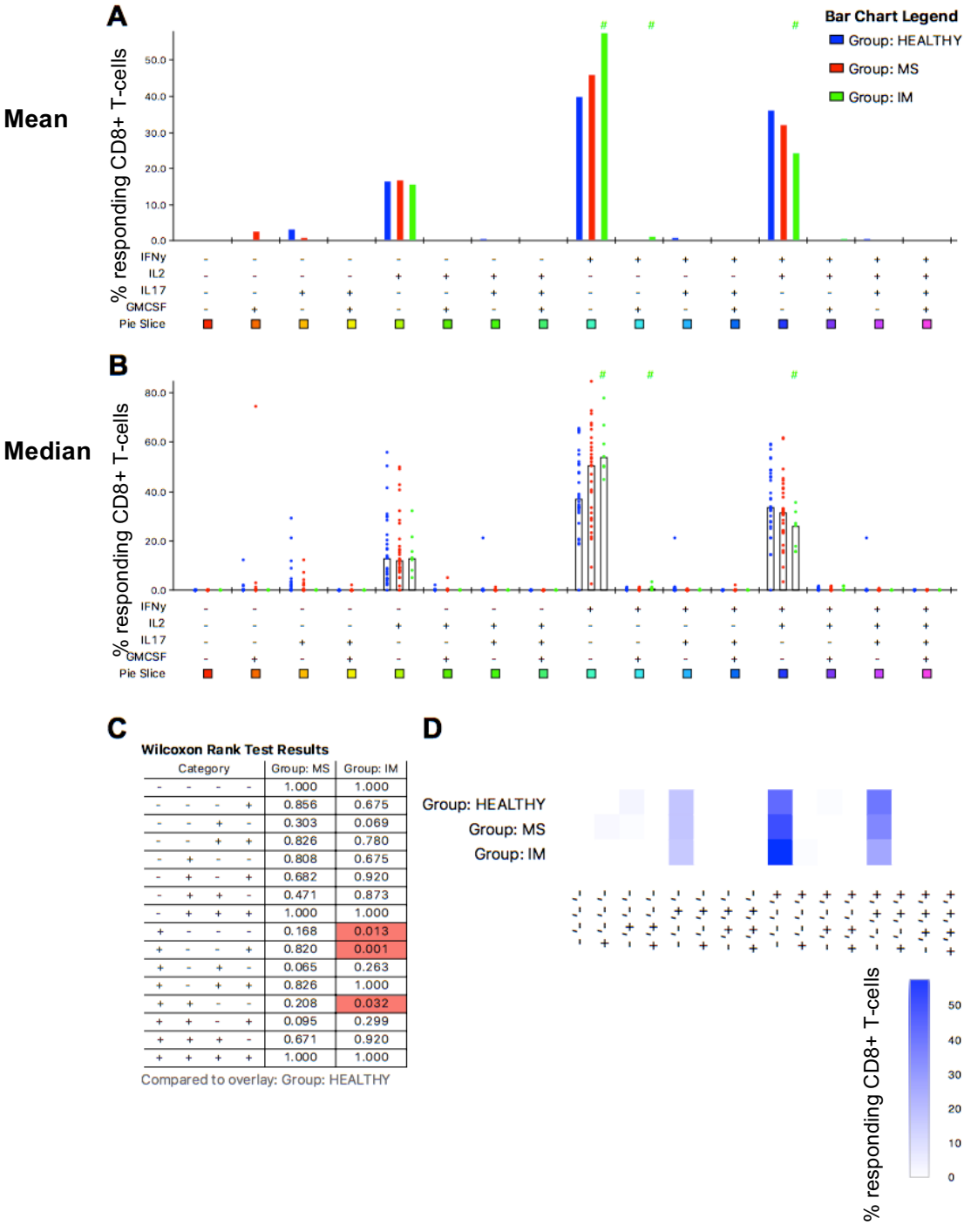

Figure 5.2.12 Cytokine profile of *ex vivo* BZLF1 KO LCL-specific CD8+ T-cells. Whole PBMC were stimulated *ex vivo* with BZLF1 KO LCL subjected to ICS (HC n=28, MS n=27, IM n=7). Responding CD8+ T-cells were defined as T-cells positive for any combination of cytokines. **A.** Graphical representation of responding cells in each combination gate with bars representing the mean of data set. Statistics were calculated using the Wilcoxon Signed Rank. **B.** Scatter plot showing percentage of responding cells for each donor in combination gates. Black bars represent median of data set. **C**. Table shows results of Wilcoxon rank test. **D.** Percentage of responding CD8+ T-cells shown in heatmap form. Combination gate data was processed using Funky Cells software and graphically displayed using the program SPICE (ns $p>0.05$, * $p<0.05$).

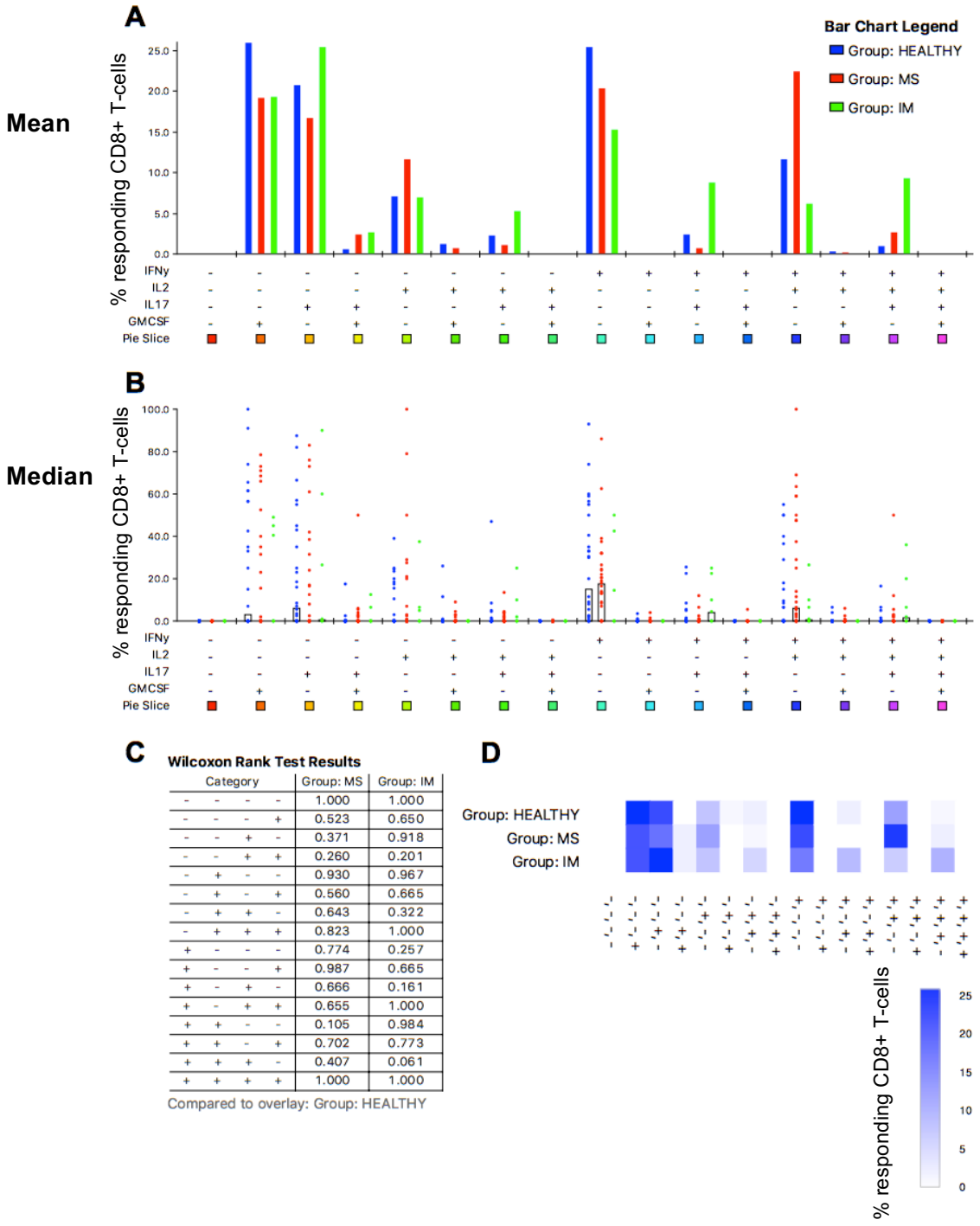

Category	Group: MS	Group: IM
- - - -	1.000	1.000
- - - +	0.523	0.650
- - + -	0.371	0.918
- - + +	0.260	0.201
- + - -	0.930	0.967
- + - +	0.560	0.665
- + + -	0.643	0.322
- + + +	0.823	1.000
+ - - -	0.774	0.257
+ - - +	0.987	0.665
+ - + -	0.666	0.161
+ - + +	0.655	1.000
+ + - -	0.105	0.984
+ + - +	0.702	0.773
+ + + -	0.407	0.061
+ + + +	1.000	1.000

Figure 5.2.13 Cytokine profile of *ex vivo* EBNA1-specific CD8+ T-cells. Whole PBMC were stimulated *ex vivo* with EBNA1 peptide mix subjected to ICS (HC n=28, MS n=27, IM n=7). Responding CD8+ T-cells were defined as T-cells positive for any combination of cytokines. **A.** Graphical representation of responding cells in each combination gate with bars representing the mean of data set. Statistics were calculated using the Wilcoxon Signed Rank test **B.** Scatter plot showing percentage of responding cells for each donor in combination gates. Black bars represent median of data set. **C**. Table showing results from Wilcoxon rank test. **D.** Percentage of responding CD8+ T-cells shown in heatmap form. Combination gate data was processed using Funky Cells software and graphically displayed using the program SPICE (ns $p>0.05$, * $p<0.05$).

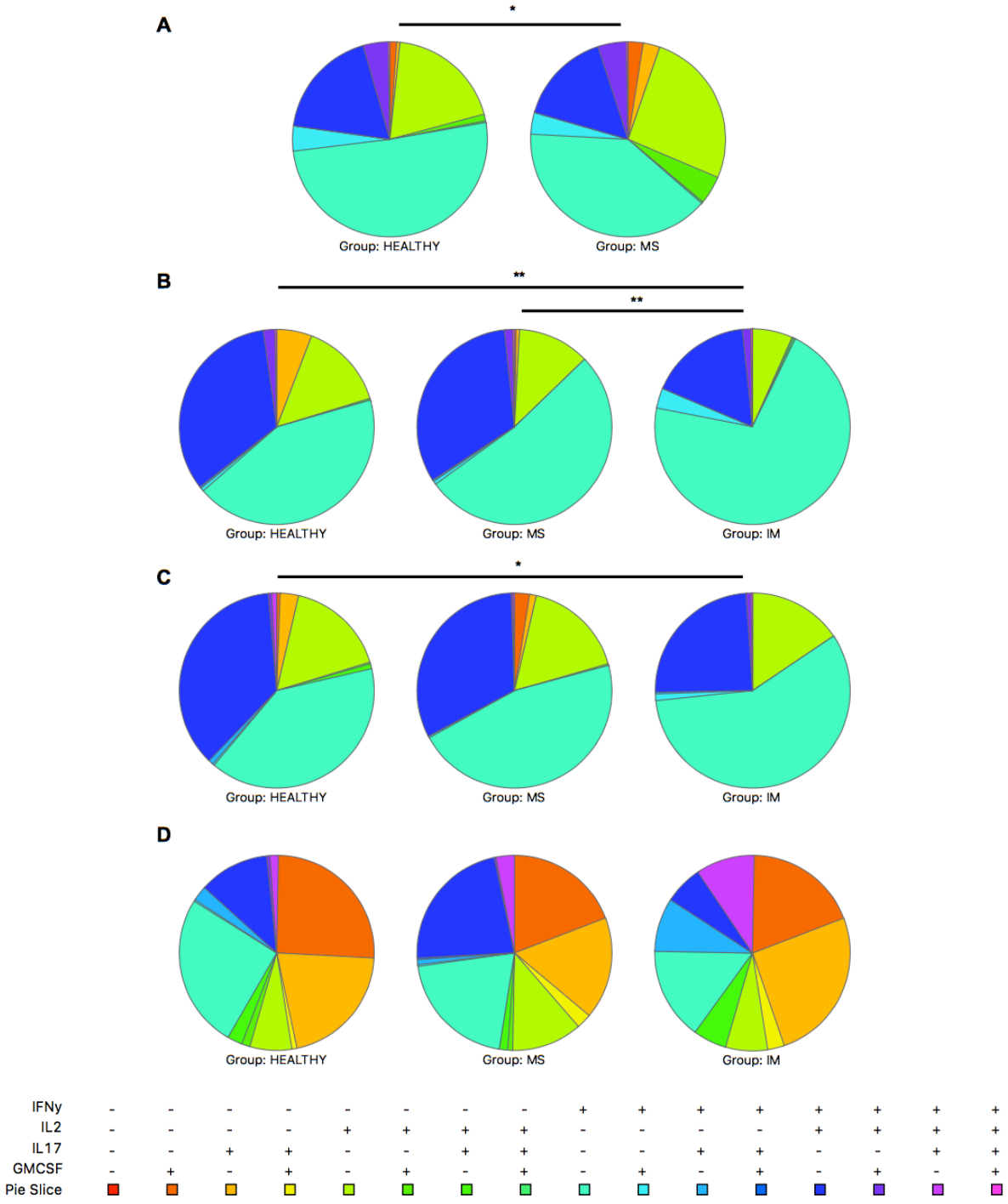

Figure 5.2.14 Cytokine profile of *ex vivo* EBV-specific CD8+ T-cells. Whole PBMC were stimulated overnight and subjected to ICS. Responding CD8+ T-cells were defined as cells producing any combination of cytokines and were categorised into 16 combination gates. Pie charts show the mean percentage of responding CD8+ T-cells belonging to each gate after stimulation with: **A.** SEB (HC n=21, MS n=19) **B.** wild type LCL (HC n=28, MS n=27, IM n=7). **C.** BZLF1 KO LCL (HC n=28, MS n=27, IM n=7) and **D.** EBNA1 peptide mix (HC n=28, MS n=27, IM n=7). Combination gate data was processed using Funky Cells software and graphically displayed using the program SPICE, statistics were calculated using a permutation test (ns $p>0.05$, * $p<0.05$, ** $p<0.005$).

5.3 Polyfunctionality of EBV-specific T-cell responses

Multidimentional analysis of T-cell cytokine production is a growing area of interest which, due to advances in flow cytometry, has significantly changed the way we view T-cells in the past 10 years. Using the Boolean data mining software Funky Cells, we investigated multiple cytokine production by EBV-specific T-cells in our cohorts.

5.3.1 Polyfunctionality Index

Polyfunctionality index (PI) is a value calculated by an algorithm developed and patented as part of the Funky Cells software, and provides a numerical value which takes into account the degree and variation in the data from all the combinatorial cell phenotypes (Larsen et al., 2012b). Using this measure, we were able to compare directly the level of co-secretion of cytokines in response to different stimuli and compare values between patient groups.

No difference was seen in PI of CD4+ T-cells between groups in response to SEB, wild type LCL, BZLF1 KO LCL or EBNA1 peptide mix stimulation, indicating that there is no difference in the co-secretion of cytokines in this T-cell subset and no difference was revealed when only the DR15+ donors were considered (Figures 5.3.1A and C).

CD8+ T-cells showed variation across groups in the polyfunctionality of cells responding to wild type LCL, with HC and MS donors having significantly higher scores than IM donors (*p=0.0069*, Kruskal-Wallis test) (Figure 5.3.1B). No difference was seen between PI values of groups when only DR15+ donors were analysed (Figure 5.3.1D).

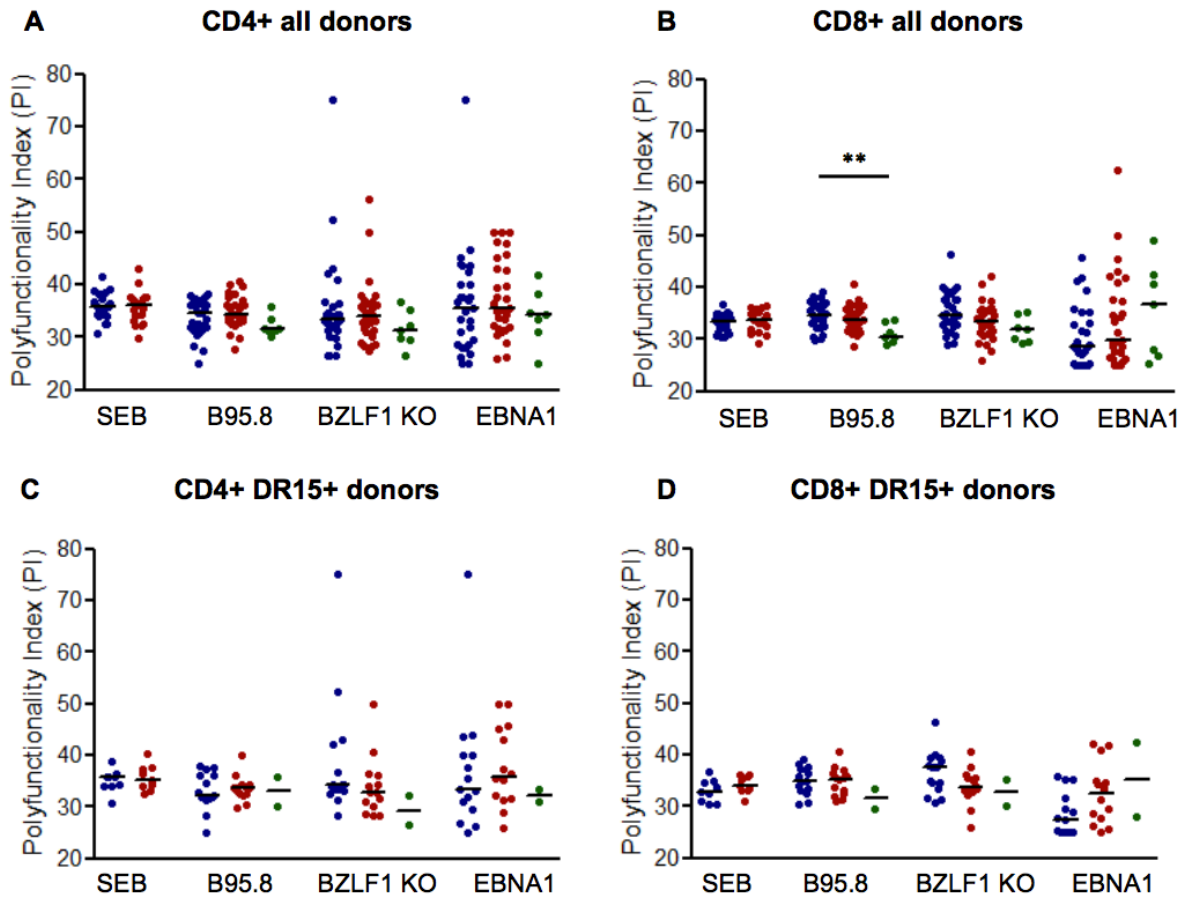

Figure 5.3.1 Polyfunctionality index of EBV-specific T-cells. T-cells were stimulated *ex vivo* and subjected to ICS. Responding T-cells were defined as CD4+ or CD8+ producing any combination of cytokines after stimulations. Polyfunctionality index (PI) was calculated using Funky Cells software for **A.** CD4+ T-cells and **B.** CD8+ T-cells. Responses in HLA-DR15+ donors only are shown in **C.** for CD4+ and **D.** for CD8+ subsets. Colour of dots define patient group: blue=healthy control donors, red=RRMS patients and green=IM patients. Horizontal black line represents median of data set. The Kruskal-Wallis test was used for direct comparisons of the three groups and the Mann-Whitney test was used to analyse two patient groups at a time (ns $p>0.05$, * $p\leq0.05$, ** $p\leq0.01$).

5.3.2 Number of functions

As a different measure of polyfunctionality we compared the percentage of responding cells producing 1, 2, 3 or 4 cytokines after stimulation. This provides a different measure of polyfunctionality and shows the number of functions T-cells responding to EBV stimuli have. A higher number of functions could have both implications for the speed in which pathogens are cleared *in vivo* and for other immune functions such as T-cell subset skewing, innate cell recruitment and promoting inflammation.

Data for CD4+ T cells is presented in Figure 5.3.2 and agrees with polyfunctionality index – no significant differences are seen in the number of cells producing multiple cytokines in response to SEB or EBV antigen stimulus. IM donor CD4+ T-cells appear to produce fewer cytokines in response to wild type LCL compared to the other groups (*p=0.0224*, Kruskal-Wallis test) (Figure 5.3.2).

Number of functions in responding CD8+ T-cells were similarly analysed with variation seen in the proportion of responding cells producing one or two cytokines. IM donors had a lower proportion of CD8+ T-cells with two functions and a higher proportion of cells with a single function compared to HC and MS donors (two functions *p=0.0076*, Kruskal-Wallis test; one function *p=0.0079*, Kruskall-Wallis test) (Figure 5.3.3B). Responses to BZLF1 KO LCL showed a similar pattern for IM donors with data for production of one cytokine not reaching significance (two functions *p=0.0395*, Kruskal-Wallis test; one function *p=0.0508*, Kruskal-Wallis test) (Figure 5.3.3C).

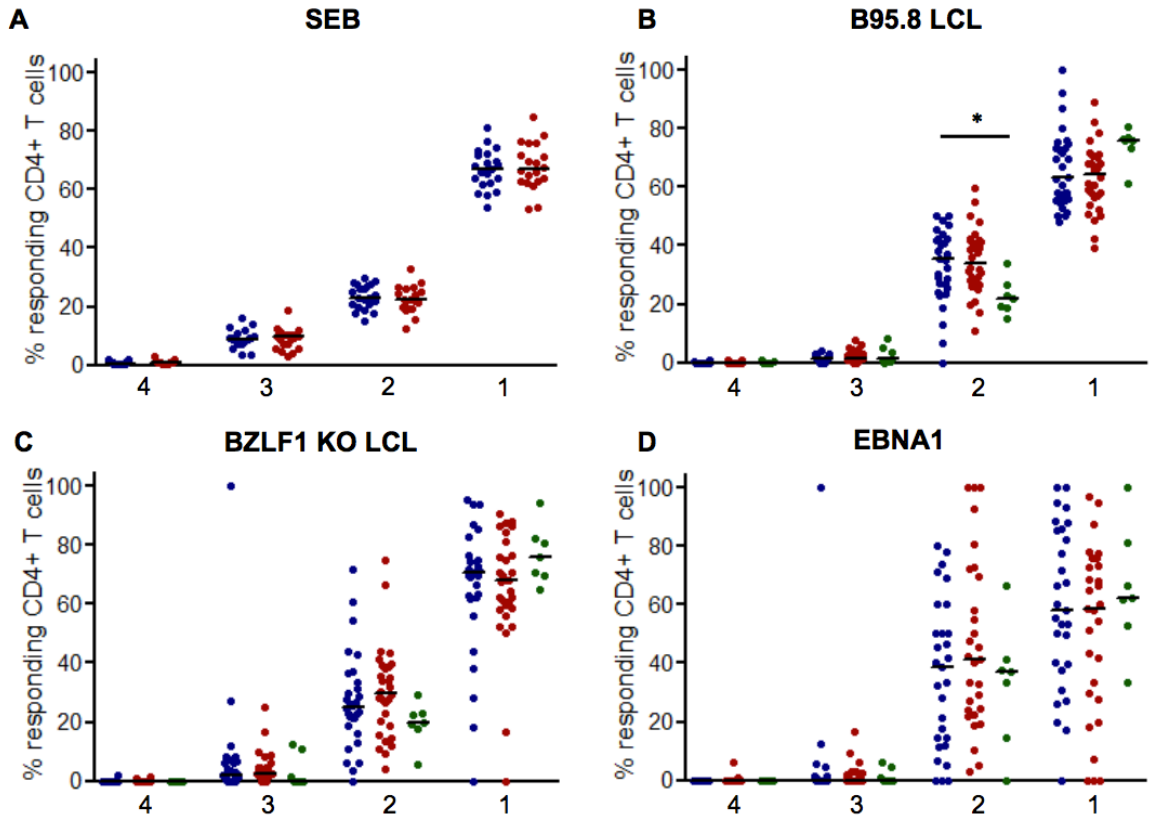

Figure 5.3.2 Number of functions of *ex vivo* EBV-specific CD4+ T-cells. T-cells were stimulated *ex vivo* and subjected to ICS. Number of functions of CD4+ T-cells were compared between patient groups in response to **A.** SEB **B.** wild type LCL **C.** BZLF1 KO LCL and **D.** EBNA1 peptide mix. Horizontal black line represents median of data set. Colour of dots define patient group: blue=healthy control donors, red=RRMS patients and green=IM patients. The Kruskal-Wallis test was used for direct comparisons of three groups and the Mann-Whitney test was used to analyse two patient groups at a time (ns $p>0.05$, * $p\leq0.05$).

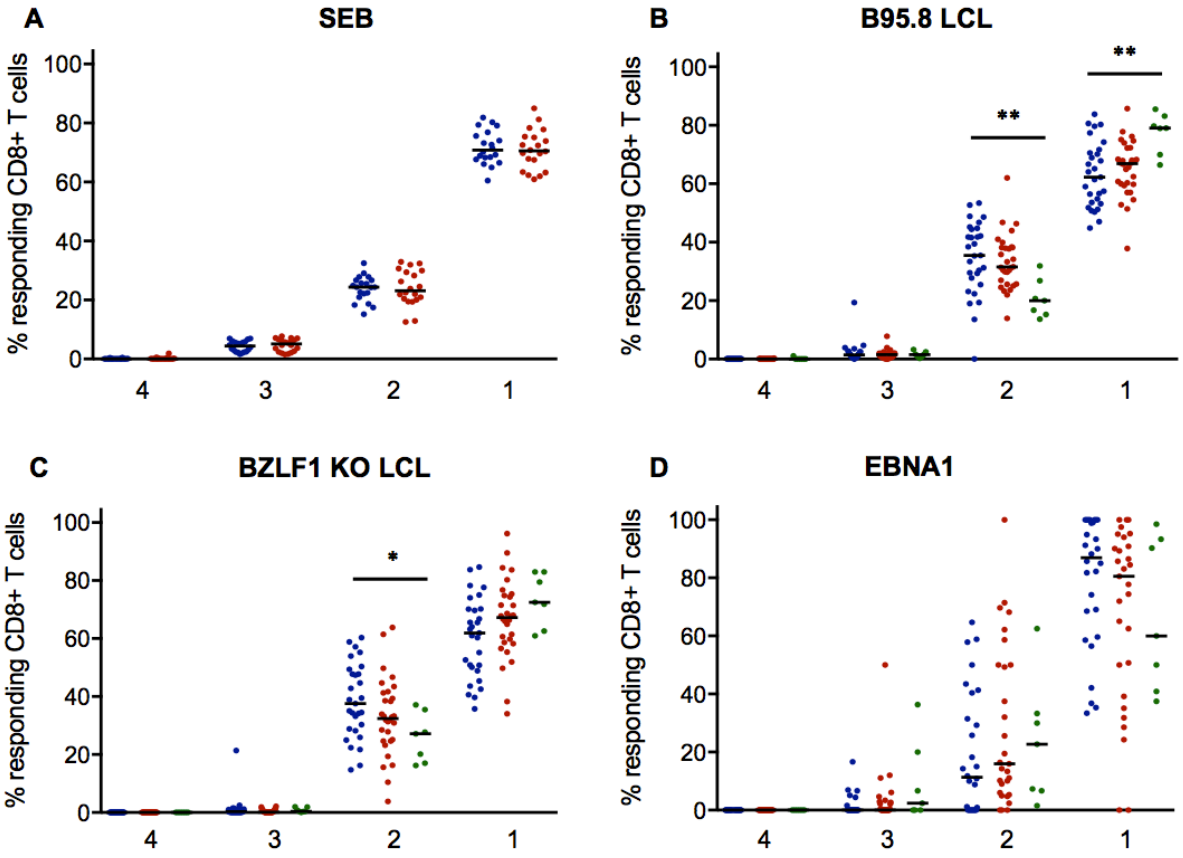

Figure 5.3.3 Number of functions of EBV-specific CD8+ T-cells. T-cells were stimulated *ex vivo* and subjected to ICS. Number of functions of responding CD8+ T-cells were compared between patient groups in response to **A.** SEB **B.** wild type LCL **C.** BZLF1 KO LCL and **D.** EBNA1 peptide mix. Horizontal black line represents median of data set. Colour of dots define patient group: blue=healthy control donors, red=RRMS patients and green=IM patients. The Kruskal-Wallis test was used for direct comparisons of three groups and the Mann-Whitney test was used to analyse two patient groups at a time (ns $p>0.05$, * $p\leq0.05$, ** $p\leq0.01$).

HLA-DR15+ donors, analysed separately for number of functions of their responding CD4+ T-cells, did not show any significant differences between patient groups (Figure 5.3.4). Analysis of HLA-DR15 donors only showed the pattern of increased number of functions in CD8+ T-cells from healthy donors compared to MS patients however these differences did not reach significance (Figure 5.3.5).

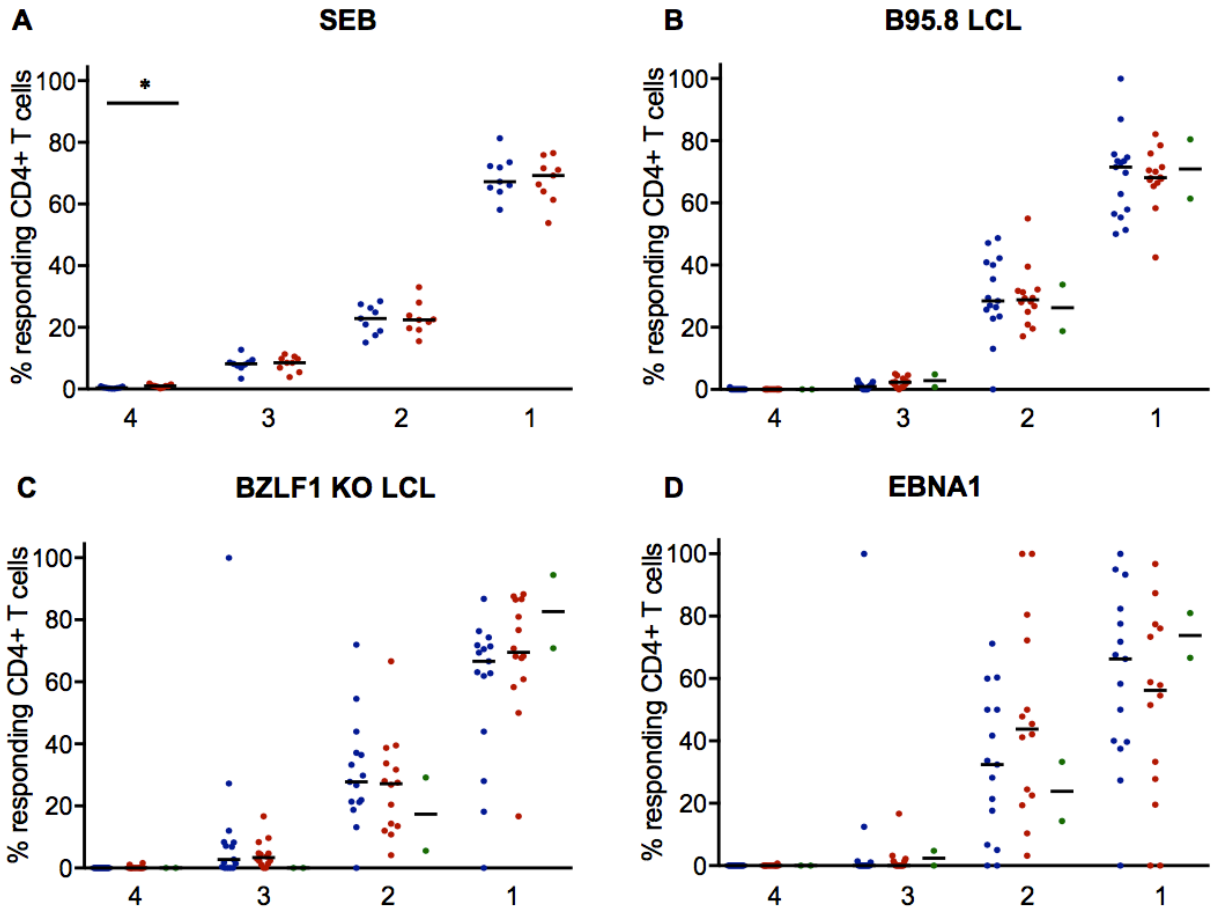

Figure 5.3.4 Number of functions of *ex vivo* EBV-specific CD4+ T-cells from HLA-DR15+ donors. T-cells were stimulated *ex vivo* and subjected to ICS. Number of functions of CD4+ T-cells in HLA-DR15+ donors only were compared in response to different stimuli: **A.** SEB **B.** wild type LCL **C.** BZLF1 KO LCL and **D.** EBNA1 peptide mix. Colour of dots define patient group: blue=healthy control donors, red=RRMS patients and green=IM patients. Horizontal black line represents median of data set (SEB stimulation: HC n=8, MS n=9, all other stimulations: HC n=14, MS n=14, post-IM n=2). The Kruskal-Wallis test was used for direct comparisons of three groups and the Mann-Whitney test was used to analyse two patient groups at a time (ns $p>0.05$, * $p\leq0.05$).

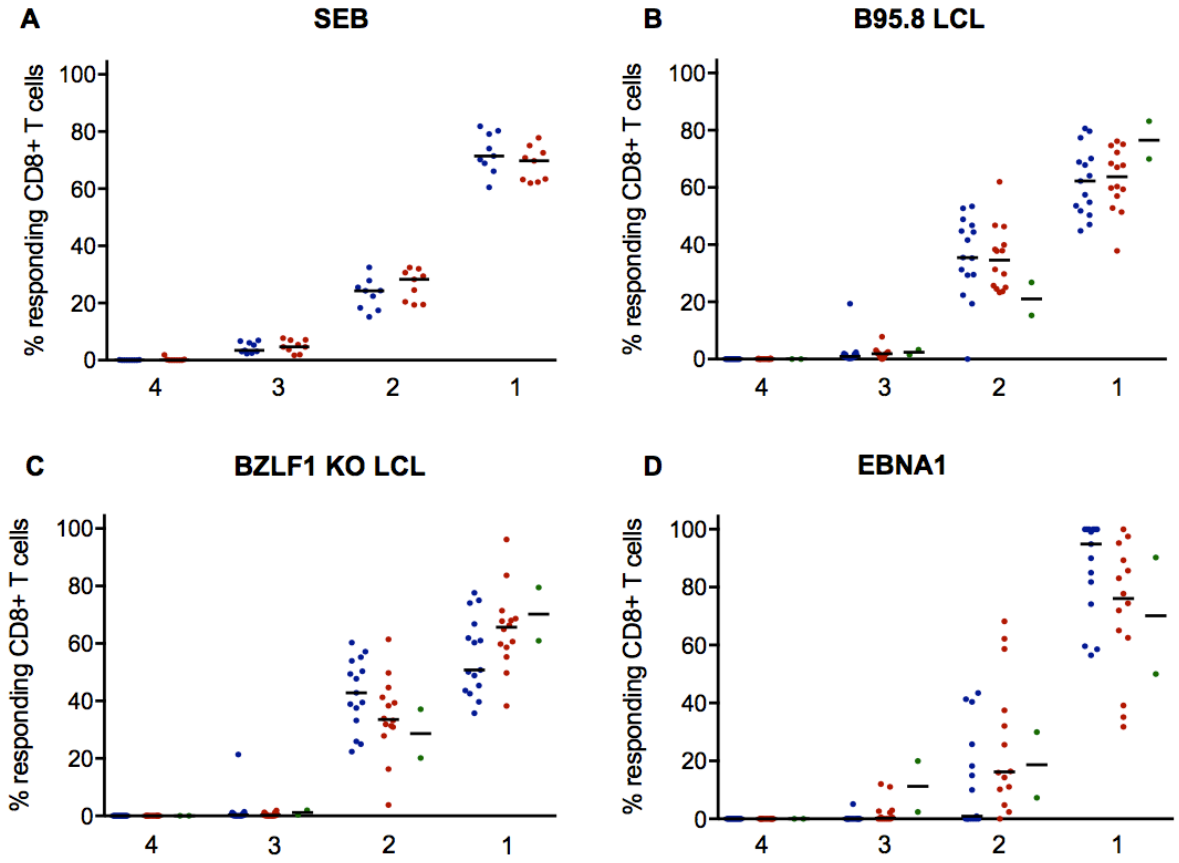

Figure 5.3.5 Number of functions of *ex vivo* EBV-specific CD8+ T-cells from HLA-DR15+ donors. T-cells were stimulated *ex vivo* and subjected to ICS. Number of functions in CD8+ T-cells from HLA-DR15+ donors were compared after stimulation with: **A.** SEB **B.** wild type LCL **C.** BZLF1 KO LCL and **D.** EBNA1 peptide mix. Colour of dots define patient group: blue=healthy control donors, red=RRMS patients and green=IM patients. Horizontal black lines represent median of data set. The Kruskal-Wallis test was used for direct comparisons of three groups and the Mann-Whitney test was used to analyse two patient groups at a time (ns $p>0.05$, * $p\leq0.05$).

5.4 Correlation of EBNA1 T-cell responses with antibody production

It is known that CD4+ T-cells provide immunological help to B-cells, and therefore it may be expected that CD4+ T-cell responses correlate with antibody titres to the same antigen. Despite previous, separate analysis of EBNA1-specific antibody and T-cell responses in MS patients by other research groups there has been no investigation of whether these two aspects of the adaptive immune response to EBV correlate.

We correlated plasma EBNA1 IgG with CD4+ and CD8+ T-cell responses from each donor to examine whether there was a trend from experimental data previously described for EBNA1 antibody responses in Chapter 4.2 and for EBNA1-specific T-cell responses in Chapter 5.1.

CD4+ T-cell responses to EBNA1 peptide mix were measured by production of each cytokine in the ICS panel: IFNγ, IL-2, IL-17 and GM-CSF. CD4+ T-cell cytokine production was correlated with plasma EBNA1 IgG production in each individual donor and the correlation calculated using Spearman's rank correlation coefficient (r). IFNγ production in CD4+ T-cells after EBNA1 stimulation was found to correlate positively with level of EBNA1 IgG when all donors were analysed (r=0.2620, *p=0.0450*), however this effect was not significant when other cohort groups were analysed individually (Figure 5.4.1). Positive correlations were observed for HC and MS donor IFNγ CD4+ T-cell responses with antibody responses to EBNA1 however these did not reach significance, possibly due to the reduced number of data points for individual groups reducing power of statistical analysis (Figure 5.4.1).

IL-2 production by EBNA1-specific CD4+ T-cells did not correlate with antibody titre when all donors were analysed, however a slight positive correlation was observed for HC donors (Figure 5.4.1). No correlation was seen when MS donor IL-2 responses were plotted against EBNA1-specific IgG (Figure 5.4.1).

No correlations were observed between IL-17 or GM-CSF production from EBNA1-specific CD4+ T-cells and EBNA1 IgG in any cohort groups (Figure 5.4.1).

Due to restrictions in cell numbers only 7 post-IM donors were screened for EBNA1 responses in *ex vivo* T-cell stimulations, and therefore fewer data points were available to analysed in this group. Low patient numbers make it difficult to draw conclusions from data regarding a correlation between T-cell and antibody responses, and we found no correlation between numbers of EBNA1-specific CD4+ T-cells and antibody levels in post-IM donors.

CD4+ T-cells provide immunological "help" to CD8+ T-cells as well as B-cells, and as such we sought to investigate a possible correlation between EBNA1-specific antibodies and cytotoxic CD8+ T-cell responses.

As previously described, CD8+ T-cell cytokine production from *ex vivo* EBNA1 stimulations were correlated with plasma EBNA1-specific IgG. IFNγ production by EBNA1-specific CD8+ T-cells was found to have a significant positive correlation with antibody levels when all donors were analysed (r=0.3437, *p=0.0072*) (Figure 5.4.2); positive correlation was maintained when HC and MS cohort groups were analysed separately but were no longer significant (HC donors r=0.3824 *p=0.0538*, MS donors *p=0.0790*) (Figure 5.4.2).

IL-2 production from CD8+ T-cells in response to EBNA1 stimulation also correlated significantly with antibody responses, both when all donors were analysed and when HC donors were analysed on their own (all donors r=0.2901 *p=0.0245*, HC donors r=0.4551 *p=0.0195*) (Figure 5.4.2). No correlation was observed between IL-2 production from CD8+ T-cells and antibody production from MS and post-IM donors when analysed in their groups, indicating that the significant positive correlation seen in IL-2 production from all donors was mostly due to HC donors (Figure 5.4.2).

No correlations were observed between IL-17 or GM-CSF production from EBNA1-specific CD8+ T-cells and antibody production in any donor groups (Figure 5.4.2). As previously

mentioned for CD4+ T-cells, only 7 data points were available for post-IM donors correlating EBNA1-specific CD8+ T-cell responses with IgG in plasma. This again made it difficult to draw any conclusions for adaptive immune responses to EBNA1 in post-IM donors, and this would need to be carried out with more samples to establish if any correlation was present.

Despite correlations showing significance when statistical tests were applied, low positive correlations – such as those for IFNγ producing EBNA1-specific CD4+ T-cells versus anti-EBNA1 IgG – may not be high enough in this context to indicate a positive relationship between T-cell and B-cell responses to the viral antigen. Visual interpretation of the correlation would suggest that there is little relationship between these two aspects of immunity in our cohort, and therefore we should be cautious in assuming that these two aspects of adaptive immunity are highly linked in individual donors from our cohort. A larger cohort with a fully quantitative EBNA1-specific IgG assay would enable these two parameters to be investigated further and reliable conclusions to be drawn.

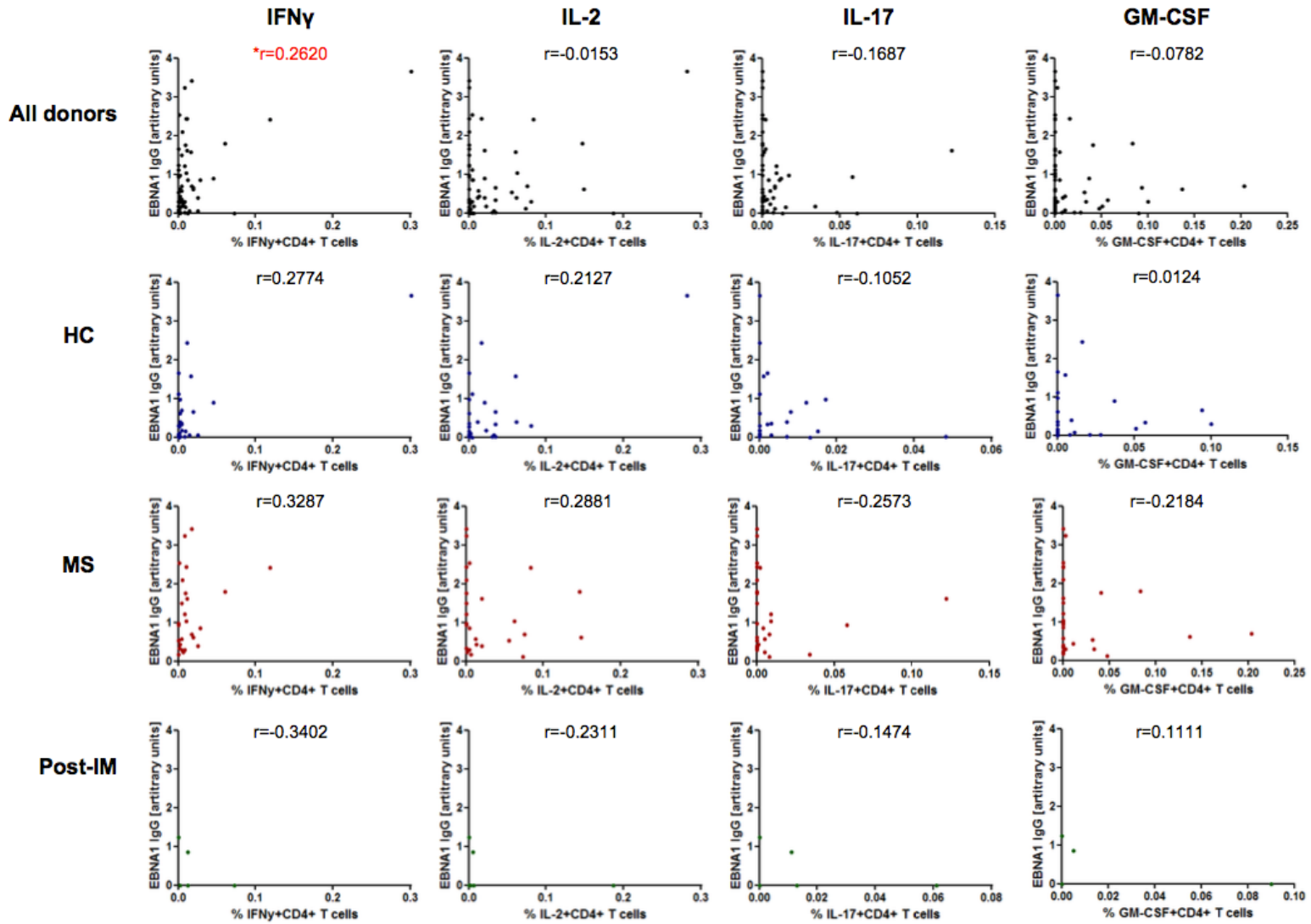

Figure 5.4.1 Correlation of EBNA1 IgG responses with EBNA1-specific CD4+ T-cell responses. Plasma EBNA1 IgG responses from donors were correlated with cytokine production by CD4+ T-cells in response to *ex vivo* EBNA1 peptide mix stimulation. Plasma EBNA1 IgG was analysed by ELISA and values represent the median of at least 3 separate experiments. Cytokine production by *ex vivo* CD4+ T-cells was analysed using ICS. Colour of dots represents cohort group: black = all donors, blue = HC, red = MS, green = post-IM. Spearman's rank correlation coefficient was used to calculate correlation (HC n=26, MS n=27, IM n=7) (ns $p>0.05$, * $p<0.05$).

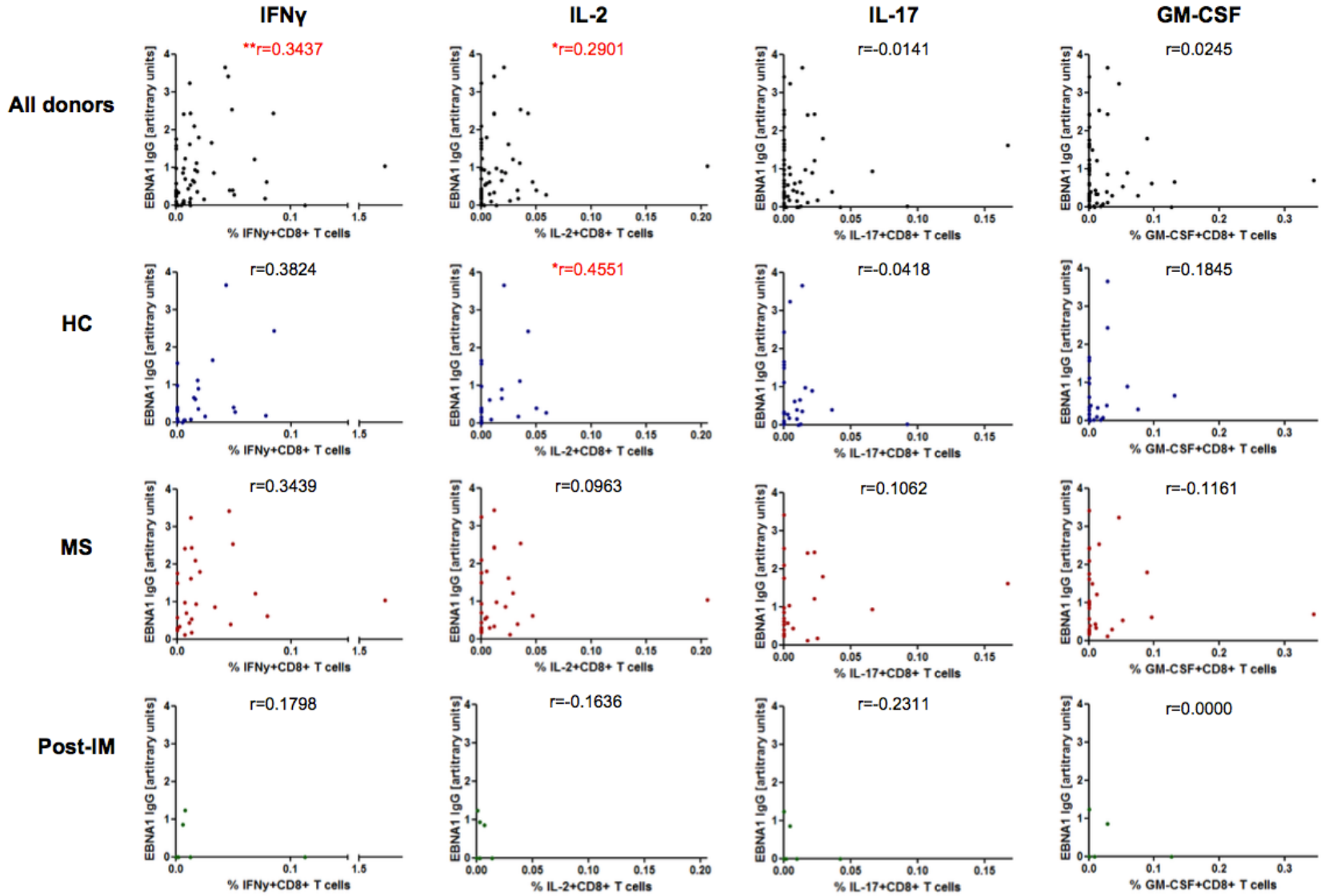

Figure 5.4.2 Correlation of EBNA1 IgG responses with EBNA1-specific CD8+ T-cell responses. Plasma EBNA1 IgG responses from donors were correlated with cytokine production by CD8+ T-cells in response to *ex vivo* EBNA1 peptide mix stimulation. Plasma EBNA1 IgG was analysed by ELISA and values represent the median of at least 3 separate experiments. Cytokine production by *ex vivo* CD8+ T-cells was analysed using ICS. Colour of dots represents cohort group: black = all donors, blue = HC, red = MS, green = post-IM. Spearman's rank correlation coefficient was used to calculate correlation (HC n=26, MS n=27, IM n=7) (ns $p>0.05$, * $p<0.05$, ** $p<0.005$).

5.5 Discussion

Studies of *ex vivo* analysis EBV-specific T-cell responses in MS patients have produced varied results, and such mixed conclusions from published data makes it extremely difficult to decipher exactly what role T-cell responses to the virus are playing in disease development.

We analysed CD4+ and CD8+ T-cell responses *ex vivo* from RRMS patients, HC and patients with a recently history of IM (4-6 months post-infection) to elucidate if there were any clear differences in cytokine production between groups in response to EBV antigens, using SEB as a positive control of T-cell activation and cytokine production.

IFNγ was selected for its key role in cytotoxic responses and is rapidly produced by T_H1 CD4+ and CD8+ T-cells upon exposure to their cognate antigen (Schoenborn and Wilson, 2007). CD4+ T-cells with T_H1 phenotype are part of the cell-mediated immune response and rapidly produce IFNγ in response to viral and other intracellular pathogens (Schoenborn and Wilson, 2007). Other cytokines in our staining panel consisted of IL-2, IL-17 and GM-CSF, all selected for their potential role in immune responses directed against the CNS in MS pathogenesis.

IL-2 is a key cytokine regulating T-cell maturation and tolerance mechanisms, and polymorphisms in the IL-2 receptor α-chain (IL2Rα, also called CD25) have been associated with multiple sclerosis development and relapse rates (International Multiple Sclerosis Genetics et al., 2007, Wang et al., 2011b, Ainiding et al., 2014). Daclizumab, an anti-IL2Rα monoclonal antibody, has been shown in trials to reduce disease activity and slow down progression in patients currently not responding to other treatments (Rose et al., 2004, Wiendl and Gross, 2013), indicating a role for IL-2 signalling in MS disease mechanisms. These findings are interesting given the therapeutic potential for CD25 blockade in the treatment of cancer. In a clinical trial of patients with metastatic breast cancer, daclizumab was administered alongside a cancer vaccine and was shown to selectively downregulate FoxP3 in T_{reg} cells,

deplete these cells long-term and also to mediate reprogramming of T_{reg} cells to an IFNγ-producing phenotype. Results also showed that patient CD4+ and CD8+ T cell responses to vaccine antigens were boosted by daclizumab without autoimmune side effects (Rech et al., 2012). Daclizumab's impact on T_{reg}-cells in this study suggests that its therapeutic potential in MS is not due to effects on this subset, and it is possible that effects on activated T-cells expressing CD25 are responsible for the amelioration of disease exacerbations (Fazekas de St Groth et al., 2004).

IL-17 was selected for our cytokine staining panel as its production has been linked to disease processes in autoimmunity and inflammation, and with relation to MS its role is mainly thought to be involved in early disease (Kostic et al., 2014, Wing et al., 2016). Additional studies of MS and neuromyelitis optica (NMO) – a T-cell-mediated autoimmune disease – have also shown levels of circulating CD4+ T-cells with a T_H17 phenotype to be more frequent in patients compared to controls during disease exacerbation, with serum IL-17 also found to be elevated (Wang et al., 2011a). Extensive research using the EAE mouse models of MS have also shown IL-17 to have a role in disease (Waisman et al., 2015).

GM-CSF pathways have been identified to be antagonistically controlled to those of IL-17, with a role identified for GM-CSF only producing CD4+ T-cells in the inflamed brain in MS (Noster et al., 2014). Expression of GM-CSF has also been found to be increased in T- and B-cells from MS patients and it is linked to inflammatory pathways of pathogenic T-cells (Rasouli et al., 2015, Sheng et al., 2014, Li et al., 2015). Analysis of these cytokines produced by EBV-specific T-cells *ex vivo* enabled us to get a clear picture of any phenotypic differences that may be present in these responses between HC, MS patients and post-IM donors.

Overall, levels of IFNγ-producing CD4+ and CD8+ cells were not changed between MS patients or HC, indicating that there is no altered frequency of these cells in the blood. However, we observed small differences in production of other cytokines in response to both

wild type and BZLF1 KO LCL, indicating that there may be a slight phenotypic difference in cells responding to EBV antigens between groups.

Multiple cytokine production of T-cells responding to EBV antigens has not been analysed in depth in the context of MS, with previous studies mainly investigating IFNγ secretion with some also investigating IL-2 (Pender et al., 2017, Lunemann et al., 2008b, Gronen et al., 2006, Jilek et al., 2008). We sought to characterise expression of multiple cytokines by T-cells responding to EBV for the first time in RRMS patients and healthy controls.

We did not find any significant differences in the overall frequency of IFNγ-secreting wild type or BZLF1 KO LCL-specific CD4+ or CD8+ T-cells in MS patients compared to healthy controls. The wild type LCL-specific CD8+ T-cell response in post-IM donors was a little higher than for other groups and this was probably due to incomplete resolution of expansion of lytic antigen-specific T-cells seen in primary infection (Figures 5.1.6 and 5.1.7).

IL-2 production was mostly unchanged between groups in response to LCL or EBNA1 stimuli, and CD4+ T-cell responses from HLA-DR15+ donors showed a slight trend towards increased IL-2 production in response to wild type LCL but this did not reach significance (Figure 5.1.4).

Also notable was a modest increase in LCL-specific CD4+ and CD8+ T-cells producing IL-17 in healthy donors compared to levels from MS patients, and this was surprising given that increased IL-17 production and signalling is generally associated with autoimmunity and has been shown to have a role in pathogenesis of EAE (Volpe et al., 2015, Reboldi et al., 2009, Kostic et al., 2015). A higher proportion of responding CD4+ T-cells after BZLF1 KO LCL simulation were IL-17+ in HC compared to MS patients, suggesting that healthy donors have increased IL-17 production in response to latent proteins, as this effect was not seen in response to wild type LCL (Figures 5.1.3 and 5.2.1). This difference in IL-17 production was not observed between HC and MS donors following wild type LCL stimulation, suggesting that

either IL-17 production was higher in MS patients in response to lytic cycle proteins not expressed by BZLF1 KO LCL.

It is unclear what this may mean for the involvement of EBV-specific T-cell responses in MS pathogenesis, however these differences in IL-17 production are in very small populations of responding cells and therefore results may be slightly skewed by the low numbers of cells stained positive for IL-17; a larger number of donors would be needed to see if this effect is real.

GM-CSF production in MS patients was significantly increased in CD4+ T-cells responding to wild type LCL, a trend that was also maintained when only looking at HLA-DR15+ donors (Figure 5.1.3 and 5.1.4). GM-CSF is a cytokine promotes proliferation of lymphocytes and differentiation of T_H1 CD4+ and cytotoxic CD8+ T-cell responses (Francisco-Cruz et al., 2014). Increased GM-CSF production by EBV-specific T-cells may indicate a greater capacity to drive immune cell proliferation and local activation of innate cells. Increased GM-CSF production may also be a consequence of increased frequency of IL-2Rα polymorphisms in MS, and mutations in IL-2Rα have been shown to increase production of IL-2 and other cytokines in patient immune cells (Hartmann et al., 2014).

GM-CSF is produced mainly by T_H1 CD4+ T-cells in humans and increased production of GM-CSF by MS patient CD4+ T-cells in response to EBV antigens suggest that these cells might be skewed towards a T_H1 phenotype (Codarri et al., 2011). Findings of an increased proportion of LCL-specific CD4+ T-cells expressing GM-CSF in response to EBV antigens indicates a phenotypic alteration of these responses in MS patients, and this may affect the inflammation and recruitment of other immune cells to the CNS, causing further demyelination and axonal damage.

GM-CSF-positive microglia and macrophages have also been shown to be present in brain lesions of MS patients with the GM-CSF receptor shown to be expressed on neurones,

suggesting a role for this cytokine in lesion pathology (Vogel et al., 2015). GM-CSF is also known to be involved in recruitment of microglia and other immune cells to sites of inflammation (Mayo et al., 2014).

EBV antigen-specific CD4+ T-cells from MS patients produce significantly higher levels of GM-CSF when activated, and if these cells were to gain access to the CNS they may propagate inflammation and lesion formation. Molecular mimicry suggests that CD4+ T-cells with receptors able to recognise both EBV and CNS antigens are responsible for attack on neuronal tissue. Increased cytokine production by EBV-specific CD4+ T-cells may lead to inflammatory events *in vivo* and permeabilisation of the BBB, permitting influx of T-cells and other immune cells into the CNS promoting further tissue damage. Increased GM-CSF production by wild type LCL-specific CD4+ T cells in MS patients from our study suggests a qualitative difference in T-cell responses between groups and may account for why some individuals develop MS and others do not.

Analysis of CD8+ T-cells responding to EBNA1 peptide mix revealed a higher proportion of cells that produce IL-2 in MS patients compared to HC and post-IM donors, an effect which became significant when analysing the HLA-DR15+ donors only (Figure 5.2.8D and 5.2.9D). This finding is interesting given that previous literature describes an increased frequency and broadened specificity of EBNA1-specific CD4+ T-cell responses in MS patients (Lunemann et al., 2006). Our study did not replicate these results as we saw no elevated frequency of EBNA1-specific CD4+ T-cells in MS patient blood. Other publications show EBNA-1 specific T-cell responses to be decreased in MS following administration of clinically effective IFNβ therapy, suggestive of a pathogenic role for these T-cells in disease relapses (Comabella et al., 2012).

Increased IL-2 expression by SEB-stimulated CD8+ T-cells indicates that some predisposition may occur to high IL-2 production in MS patient T-cells (Figure 5.1.6), however this was not

mirrored in responses to wild type or BZLF1 KO LCL. Increased IL-2 production by CD8+ T-cells in response to EBNA1 may be due to some other effect, potentially CD4+ T-cell "help" perpetuating responses or other immune mechanisms not yet known.

In-depth analysis of multiple cytokine production by EBV-specific T-cell responses in MS patients has not been performed before, and our study sought to address this to not only investigate frequency of these cells but also function. Funky cells software enabled the subtraction of background staining and avoided skewing of results by this effect. This analysis, combined with presentation of combination gate data in SPICE software, allowed us to gain an extremely detailed picture of CD4+ and CD8+ T-cell function in response to both LCL stimulations and to EBNA1. Despite this in-depth characterisation, we were not able to detect any major variation in responses between HC and MS patients in polyfunctionality or differential cytokine expression. This suggests that circulating responses to EBV latent and lytic antigens are largely unchanged in MS patients, and there were no clear indications of how immune responses to EBV may be contributing towards MS disease development. However, as our blood samples were from patients who were currently in the remission phase of disease we may have missed some differences that only become apparent during clinical exacerbations, and future work would need to investigate relapse samples before any definitive conclusions can be made.

Rapid cytokine production in response to stimulation *ex vivo* is indicative of T-cells that have a memory phenotype, as naïve T-cells do not produce cytokine in response to pathogens as readily. EBV-specific T-cells producing multiple cytokines after stimulation with autologous LCL by indicates a memory compartment with previous EBV antigenic experience, and a larger proportion of these cells with increased effector function may suggest a larger memory T-cell pool responding to the virus. It may be that, whilst there were no major differences in cytokine production by EBV-specific T-cells between MS and healthy controls, differences in

ratio of naïve and effector memory T-cell compartments may exist. Future investigation of *ex vivo* T-cell responses to EBV antigens in MS patients should include T-cell memory subset markers to investigate this further.

Publications investigating relapses in MS have shown disease activity to be positively correlated with EBV-specific T-cell responses. Angelini *et al.* showed frequency of lytic antigen-specific CD8+ T-cells to be positively correlated with disease activity as measured by MRI (Angelini et al., 2013). However, other groups have failed to find a correlation between T-cell or antibody responses to EBV and MS disease exacerbations, leading some to argue that immune responses to EBV are not stable enough markers to use in diagnosis or prognostic analysis (Ingram et al., 2010).

Obtaining reliable samples of clinical relapses from MS patients is difficult due to the insidious onset of symptoms, causing patients to delay seeking medical attention until their condition gets worse. This, combined with time delays between hospital referrals and sample collections, means that it is often several weeks before blood is collected by which time symptoms may have started to resolve. Analysis of EBV-specific T-cell responses during relapses may reveal a difference in frequency or phenotype that might give crucial insight into disease processes, analysis of CSF responses in addition to the blood will give a more detailed picture of responses during clinical exacerbations. CSF samples are also difficult to gather due to delays in lumber puncture from onset of symptoms and also due to the frequent contamination of CSF with blood during the procedure, rendering the sample useless for immunological investigation in this context. Despite problems faced in gathering CSF samples, some studies have shown intrathecal enrichment of EBV-specific CD8+ T-cell responses during early disease (Jaquiery et al., 2010).

Differences in disease status or lack of clinical data regarding time of sample collection may account for the tremendous amount of variation in reports of EBV-specific T-cell responses

being increased, unchanged or decreased in MS (van Nierop et al., 2016a, Pender et al., 2009, Cepok et al., 2005); careful patient recruitment with detailed and strict criteria for blood and CSF donation are needed in order to perform reliable studies of MS relapse pathogenesis.

Due to no obvious differences between the frequency of EBV-specific CD4+ or CD8+ T-cells in MS patient blood compared to that of HC or post-IM donors in our cohort, we analysed the production of different cytokines by T-cells to see if differences occurred in the phenotype of EBV-specific responses that were not apparent from our initial analysis.

Analysis of production of other cytokines by MS patient T-cells responding to EBV antigens may reveal differences that were not apparent in this study, and additional *ex vivo* analysis of cytokines such as IL-22 and IL-23 might give a broader picture of CD4+ T-cells with a T_H17 phenotype in MS (Wing et al., 2016, Wang et al., 2011a).

Staining of T-cells for homing markers might also give an idea of which cells are capable of migrating to the CNS causing disease: CCR7 is a key protein used in identifying populations of mature T-cells and its function allows T-cells to home to lymphoid tissues (Forster et al., 2008). Studies of leukaemic mouse models have shown CCR7 to be essential in mediating migration of T-cells into the CNS (Buonamici et al., 2009), and investigation of CSF-resident T-cells from MS patients found up to 90% of them to express the chemokine CCR7 (Kivisakk et al., 2004). CCR7+ T_{FH} cells have also been linked with clinical relapses of MS in one cohort (Fan et al., 2015), and it would therefore be a marker of interest when investigating EBV-specific T-cells in MS patients during relapse and their potential to home to the CNS.

Antibody responses and T-cell responses to EBV have been extensively investigated separately for many years, however few studies have attempted to correlate both of these parameters in individuals. Little is known about the kinetics of asymptomatic infection, but EBNA1-specific CD4+ T-cell and antibody responses have been shown to be delayed after IM with responses only appearing 4-6 months post-infection (Long et al., 2013). However, EBNA1 responses

have so far not been correlated in individual donors to show that these antigen responses are directly linked *in vivo*. Research from other systems studying parasites and cancer/testis antigens have shown there to be limited correlation between antibody and T-cell responses to the same antigen (Walker et al., 2015, Gnjatic et al., 2003), and lack of publications describing a link potentially reflects the difficulty or lack of correlation between these two aspects of adaptive immunity.

We correlated EBNA1-specific IgG responses with cytokine production from both CD4+ and CD8+ T-cells following stimulation with EBNA1 peptide mix and found there to be a modest correlation with IFNγ production in both T-cell subsets (Figure 5.4.1 and 5.4.2). The positive correlation of antibody responses with EBNA1-specific IFNγ+ CD4+ T-cells was significant when all donors were analysed, and this effect was maintained but no longer significant when HC and MS patient data were correlated independently (Figure 5.4.1). These findings suggest that IFNγ+CD4+ T-cell responses to EBNA1 in MS patients match elevations seen in EBNA1-specific IgG titres but higher numbers in cohorts are needed to determine if this effect is significant (Lunemann et al., 2010, Lunemann et al., 2008a). However, previous publications have reported an increased frequency of peripheral EBNA1-specific CD4+ T-cells in MS patients (Lunemann et al., 2006) which was not found in our cohort, and this is reflected in the absence of strong positive correlation seen in our cohort between EBNA1-specific antibody and CD4+ T-cell responses in Figure 5.4.1.

EBNA1-specific CD4+ T-cells that produced other cytokines – IL-2, IL-17 or GM-CSF – were not found to be correlated with anti-EBNA1 IgG in plasma in all cohort groups, indicating that it is specifically IFNγ-producing CD4+ T-cells that positively correlate with antibody responses to the antigen in the blood (Figure 5.4.1). Lack of correlation between CD4+ T-cells producing other cytokines and antibody responses suggests that it is mainly the IFNγ-producing subset that is linked to EBNA1 IgG synthesis, and implicates T_H subsets that are able to secrete

IFNγ in generation of antibody responses. CD4+ T_H subsets that are characterised by IFNγ production include T_H1 cells, however it has also been shown that T_{FH} cells are able to produce small amounts of the cytokine (Vinuesa et al., 2005) and that IFNγ production promotes class-switching in B-cells to IgG2 antibody production during antiviral responses (MacLennan et al., 2003). It is therefore perhaps not surprising that EBNA1-specific IFNγ+CD4+ T-cells are shown to be correlated with IgG responses to the same antigen but T-cells producing other cytokines in our study are not.

EBNA1-specific CD8+ T-cell responses producing IFNγ and IL-2 were also found to be positively correlated with anti-EBNA1 IgG production when all donors were analysed (Figure 5.4.2). This finding is interesting, and perhaps to be expected, given that naïve CD8+ T-cells (as well as B-cells) require immunological help from CD4+ T-cells to mature and elicit their full cytotoxic potential (Bevan, 2004). Absence of positive correlation between IL-2-producing EBNA1-specific CD8+ T-cells and IgG in MS donors potentially reflects the elevated antibody titres not reflected by T-cell responses in these patients (Figure 5.4.2). Data from our cohort suggest that elevations of EBNA1-specific IgG occur independently of CD8+ T-cell responses and support evidence for unchanged CD8+ T-cell responses to the antigen in MS patients (van Nierop et al., 2016a), and contradict publications reporting an increase in EBNA1-specific CD8+ T-cells in the blood of MS (Cepok et al., 2005). However, the commercially available kit used for analysis of plasma EBNA1-specific IgG responses in our cohort is only semi-quantitative, and conclusions from our data need to consider this. Further studies should use a fully quantitative method of measuring EBNA1-specific antibody responses to determine if this effect is real.

Currently there is no conclusive mechanism for how EBV infection might contribute towards the development of MS, and analysis of *ex vivo* T-cell responses to the virus in our cohort have not shown any clear difference in frequency of circulating virus-specific CD4+ or CD8+ T-

cells. Subtle changes in the cytokines produced following latent and lytic LCL stimulation between HC and MS patients indicate that there might be differences, but these do not shed any light on why some individuals develop disease. Analysis of T-cell responses in patients with a recent history of IM were analysed due to their increased subsequent risk of developing CNS-directed autoimmunity, however no significant correlations were seen in frequency or function of CD4+ or CD8+ T-cells between the two groups which might shed light on this association. Analysis of EBV-specific T-cell responses in clinical relapse of MS might shed light on the immunology of disease exacerbations and the contribution of the virus-specific immune response during relapse.

Positive correlation of CD4+ and CD8+ T-cell responses to EBNA1 with antibody levels has not previously been investigated in individual donors and data from HC in our cohort suggest that these are intrinsically linked. This is likely to be due to the immunological help provided by CD4+ T-cells to other cells of the adaptive immune response with specificity for the same antigen. Absence of significant positive correlation between these two parameters in MS patients reflects the increased plasma EBNA1 IgG levels without elevated T-cell responses, suggesting that this increase in antibody titres is independent of the T-cell compartment. However, analysis of more donors would provide more statistical weight to this finding and further research in this area is warranted to understand immunological kinetics of EBV immunity in MS.

Small differences observed between *ex vivo* T-cell responses to EBV antigens between MS patients and healthy controls do not shed light on how these responses may drive disease in MS patients, leading us to investigate further characteristics of the EBV-specific T-cell repertoire in donors. The ability of T-cells to become activated relies on specificity of the T-cell receptor, and we investigated whether functional differences existed between donor groups by exploring whether EBV-specific T-cells could also become activated by neuronal antigens.

6 Generation of LCL-specific polyclonal T-cell lines and their reactivity with the CNS

CD4+ T-cells with reactivity to both EBV and CNS antigens in MS patients have been previously reported (Lunemann et al., 2008b, Lang et al., 2002), and the cross-reactive hypothesis remains one of the mechanisms best supported by the currently available data to explain how EBV contributes towards disease pathogenesis (discussed Chapter 1.5.5).

Following on from *ex vivo* analysis of circulating EBV-specific CD4+ and CD8+ T-cells, we sought to investigate whether EBV-reactive T-cells would become activated by CNS proteins. To perform these experiments, we developed a panel of recombinant MVA viruses containing EBV and CNS antigens which enabled the expression of EBV and CNS proteins in autologous, EBV-negative B-cell lines. Optimisation and employment of this system is described in this chapter, and has allowed us to thoroughly examine the cross-reactive potential of EBV-specific T-cells *in vitro*.

6.1 Generation of recombinant MVA viruses expressing CNS antigens

In order to study T-cell responses to CNS antigens, an expression system was developed based on a genetically engineered poxvirus, modified vaccinia Ankara (MVA) virus (Chapter 2.2). Nine potential autoantigenic targets were selected for cloning into MVA viruses and these included CNP, MAG, MOG, PLP, MBP, MBP-V8, MOBP, TAL-H and CRYAB. MVA virus was previously attenuated by serial passage through chicken embryo fibroblasts resulting in genomic deletions and subsequent loss of the ability to replicate in multiple cell types. MVA viruses were selected as vectors for CNS protein expression for our project as they are a safe

vector to work with and can be used to stably overexpress large, recombinant proteins. Despite its diminished replication capacity, MVA virus has retained the ability to infect most cell types and produce recombinant protein, making MVA an efficient vector with which to express desired proteins safely in a wide variety of cell types.

Alongside the CNS proteins, two other recombinant MVAs were made containing EBNA1 and an empty vector negative control (pYWK). EBNA1ΔGA is the truncated EBNA1 protein from EBV with its GA repeat sequence deleted. The GA repeat sequence of EBNA1 acts to inhibit its own translational processing, preventing presentation of epitopes via MHC class I molecules on the cell surface (Levitskaya et al., 1995). By deleting this sequence EBNA1 epitope presentation efficiency is greatly improved and immune responses to the unrepeated region can be properly studied. In addition to this, an empty vector control MVA virus was made to serve as a negative control and contains no recombinant protein insert downstream of the T7 promoter (pYWK). This enabled background immune responses to the recombinant MVAs to be accurately measured in the same system.

A schematic of recombinant proteins expressed in this system under the control of the T7 promoter can be found in Figure 6.1.1. This system was selected for two main reasons; first, to prevent theoretical induction of autoimmunity in the event of accidental human infection with the recombinant CNS protein MVAs. Second, to prevent over-expression of the proteins during amplification of the viruses, as their high hydrophobicity can be cytotoxic to cells. Placing CNS proteins under control of the T7 promoter ensures that the gene locus should only be transcribed and translated when the T7 polymerase is expressed in the same cell. As the enzyme is not expressed in eukaryotic cells, T7 polymerase was supplied in this system by co-infection with a second MVA virus expressing the bacteriophage T7 polymerase *in trans*.

MVA viruses were engineered to express GFP constitutively which allows recombinant virus quantification by fluorescent microscopy, and further modifications were made to aid the

proteins' detection *in vitro*. A FLAG-tag is a short, hydrophilic polypeptide tag which can be added on to proteins without affecting their biological function or cellular processing (Lichty et al., 2005), and its addition to recombinant CNS proteins allowed detection of the recombinant CNS protein expression in Western blots by a FLAG tag-specific monoclonal antibody (Figure 6.1.2). The FLAG tag was also added as a means of purifying protein were this needed for future experiments.

Construction of vaccinia shuttle plasmids containing the CNS genes or T7 polymerase were completed by two previous students; Yolanda van Wijck (van Wijck, Y. (2011) *Construction of recombinant MVAs encoding CNS proteins and testing the MVA-T7 system with EBNA1-specific T-cells.* MSc internship unpublished thesis. Vrije Universiteit, Amsterdam, the Netherlands and the University of Birmingham, UK) and Marye Hogenboom (Hogenboom, M.

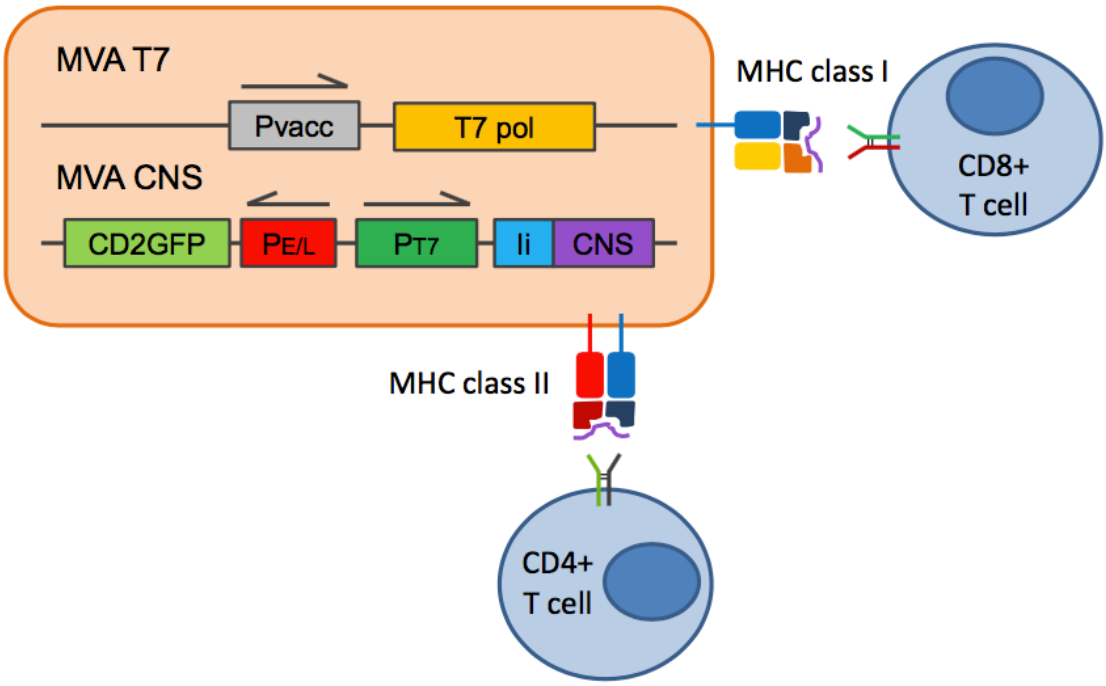

Figure 6.1.1 Schematic of CNS protein expression by recombinant MVA viruses. MVA T7 virus was engineered to express T7 polymerase *in trans* in host ccells and does not express GFP or FLAG protein. MVA CNS viruses were engineered to only express CNS proteins in the presence of bacterial T7 polymerase. MVA CNS viruses were GFP positive, FLAG and invariant chain tagged, ensuring expression of CNS epitopes in both MHC class I and II presentation pathways.

(2012) *Cloning of CNS proteins as cross-reactive targets for EBNA1-specific T-cells of MS patients.* MSc internship unpublished thesis. Vrije Universiteit, Amsterdam, the Netherlands and the University of Birmingham, UK).

Development of a system using recombinant MVA viruses expressing CNS proteins is a key tool in the investigation of autoreactive T-cell responses in MS, and we used this system to screen EBV-specific T-cell responses for cross-reactivity with neuronal antigens *in vitro.*

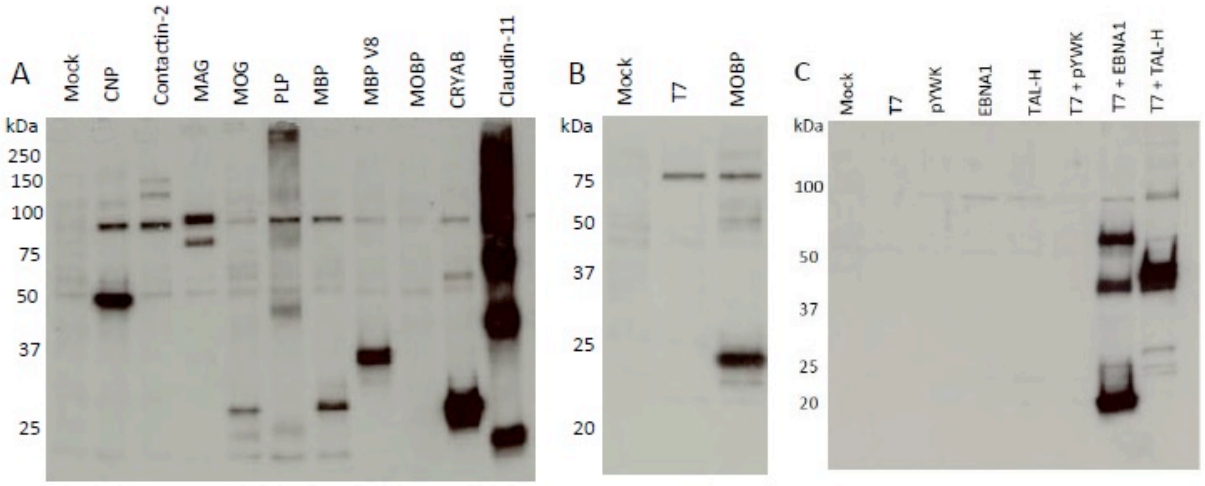

Figure 6.1.2 Confirmation of CNS protein expression in MVA viruses. 293 cells were infected individually with MVA CNS or alongside MVA T7 virus. Membranes were probed with anti-FLAG monoclonal antibody and correct band size was used to confirm presence of CNS protein insert. **A.** Bands of correct sizes were detected in MVAs containing CNP (46kDa), MAG (67kDa), MOG (27kDa), PLP (25kDa), MBP (33kDa), MBP V8 (38kDa), CRYAB (28kDa), Claudin-11 (24kDa). MVA Contactin-2 was subsequently dropped from analysis due to difficulties in protein expression. **B.** MVA MOBP blot contained a band (24kDa) indicating MOBP protein expression. **C.** Bands of correct sizes were detected in MVAs pYWK (no band), EBNA1 (63kDa) and TAL-H (38kDa). Cells without co-infection of MVA T7 did not produce bands.

6.2 Optimisation of MVA T-cell stimulation assay

Optimisation of conditions in which best to screen for reactivity to proteins expressed in MVA-infected cells is crucial in order to reliably investigate T-cell recognition of autoantigenic targets. Therefore, assay sensitivity is key to detecting any low-level cytokine production that may occur. In addition to this requirement, assay optimisation will both preserve target cell (B-cell blast) and MVA stocks, allowing their use for all experiments throughout the project to maintain consistency.

IFNγ ELISA was performed using lab donor-derived CD4+ and CD8+ T-cell clones which recognise different epitopes from EBNA1. Autologous B-cell blasts were infected at differing multiplicity of infection (MOI) to determine the amount of virus needed to get good recognition of target cells by T-cells. Different effector to target ratios were used to determine the optimal number of targets needed to ensure that antigen recognition can occur in both CD4+ and CD8+ T-cells.

As our assay will be used for screening polyclonal T-cell lines containing both CD4+ and CD8+ T-cells, we selected the conditions at which both T-cell subsets were able to recognise targets efficiently. The CD8+ T-cell clone preferentially recognised targets that were infected at a MOI of 1.0, with a target cell:T-cell ratio of 20:1 respectively. The CD4+ T-cell clone also recognised MVA EBNA1-infected B-cell blasts that were infected at a MOI of 1.0, but the most effective target cell:T-cell ratio was 50:1. It was therefore concluded that the optimal MOI for B-cell blast infection was 1.0 and that T-cells should be incubated with target cells at a ratio of 30:1, as this would provide the best conditions for both responding CD4+ and CD8+ T-cells in future assays (Figure 6.2.1).

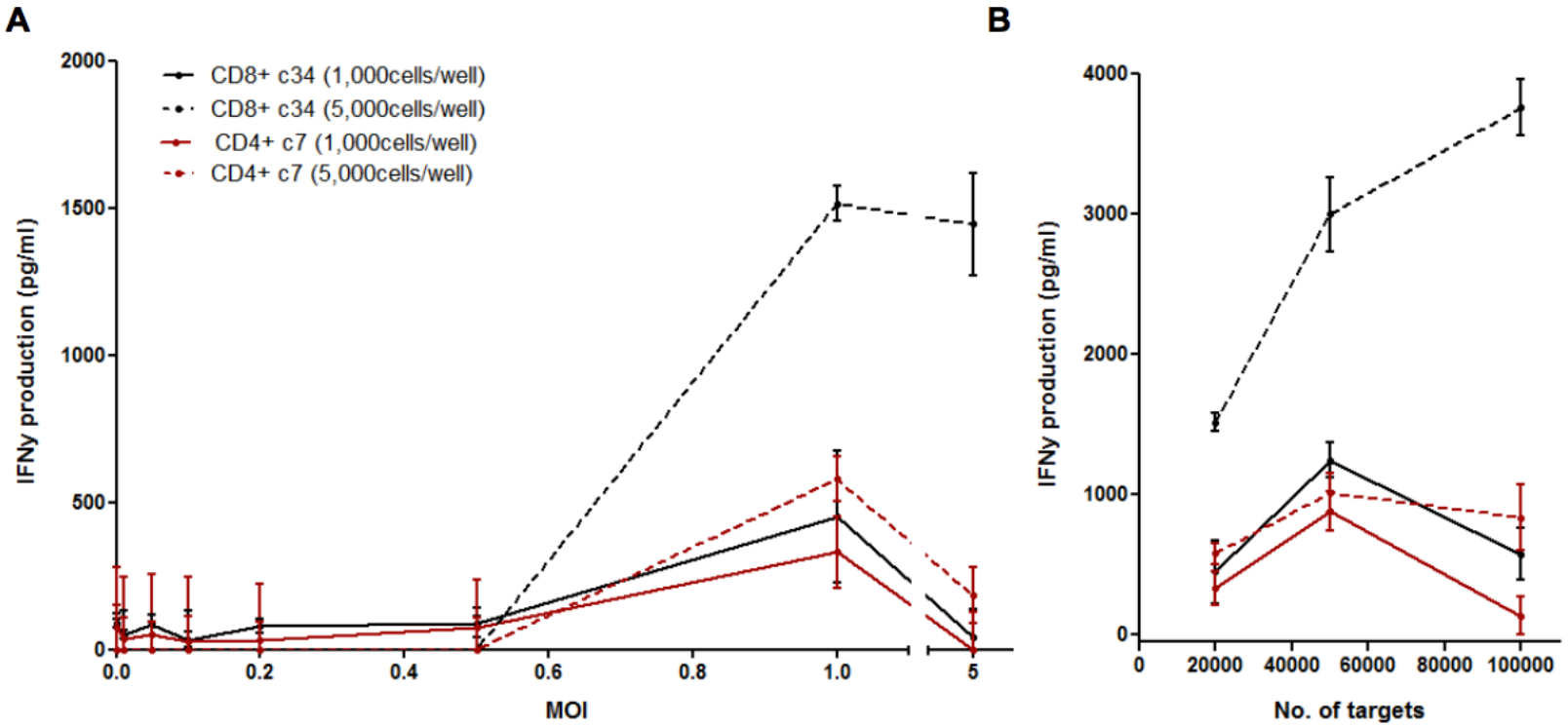

Figure 6.2.1 Optimisation of MOI and effector to target ratio for recognition of recombinant MVA-infected B-cell blasts by T-cells. Two EBNA1-specific T-cell clones isolated from healthy lab donors were used to investigate optimal conditions for T-cell recognition assays using MVA EBNA1-infected B-cell blasts. Clone 34 was CD8+ T-cell clone recognized the HLA-B35-restriced HPV epitope and the CD4+ T-cell clone 7 recognised the HLA-DR51-restricted epitope SNP. T-cell clones were screened by IFNγ ELISA against autologous B-cell blasts infected with MVA EBNA1 at various **A.** MOIs and **B.** effector to target ratios. Points represent mean of data with error bars indicating standard deviation of results from triplicate wells.

6.3 Investigation of CNS antigen reactivity in EBV-stimulated T-cell lines

We investigated whether T-cells specific for EBV antigens are able to cross-react with myelin proteins in our cohort using the MVA CNS system previously described in Chapter 6.1.

EBV-specific polyclonal T-cell lines were generated from HC and MS donors by stimulating with irradiated, autologous LCL on days 0 and 7 and allowing T-cells to expand in culture. After 4 weeks, the polyclonal T-cell lines were screened for both reactivity with EBV antigens and to CNS proteins expressed via our MVA panel. Autologous B-cell blasts served as an EBV-negative B-cell background in which to express CNS proteins and measure responses. B-cell blasts were infected separately with MVAs for 4 hours in low serum media, washed to remove unattached virus and added to polyclonal T-cell lines before incubating overnight. The following day cells were analysed by ICS. Example staining for CD4+ and CD8+ T-cell responses to CNS MVAs and LCL are shown in Figures 6.3.1 and 6.3.2 respectively.

T-cell responses to the majority of proteins expressed in our MVA panel induced IFNγ production, however there was also production of IL-2, IL-17 and GM-CSF in response to certain proteins in the panel, enabling in-depth analysis of the cytokine profile of responding cells.

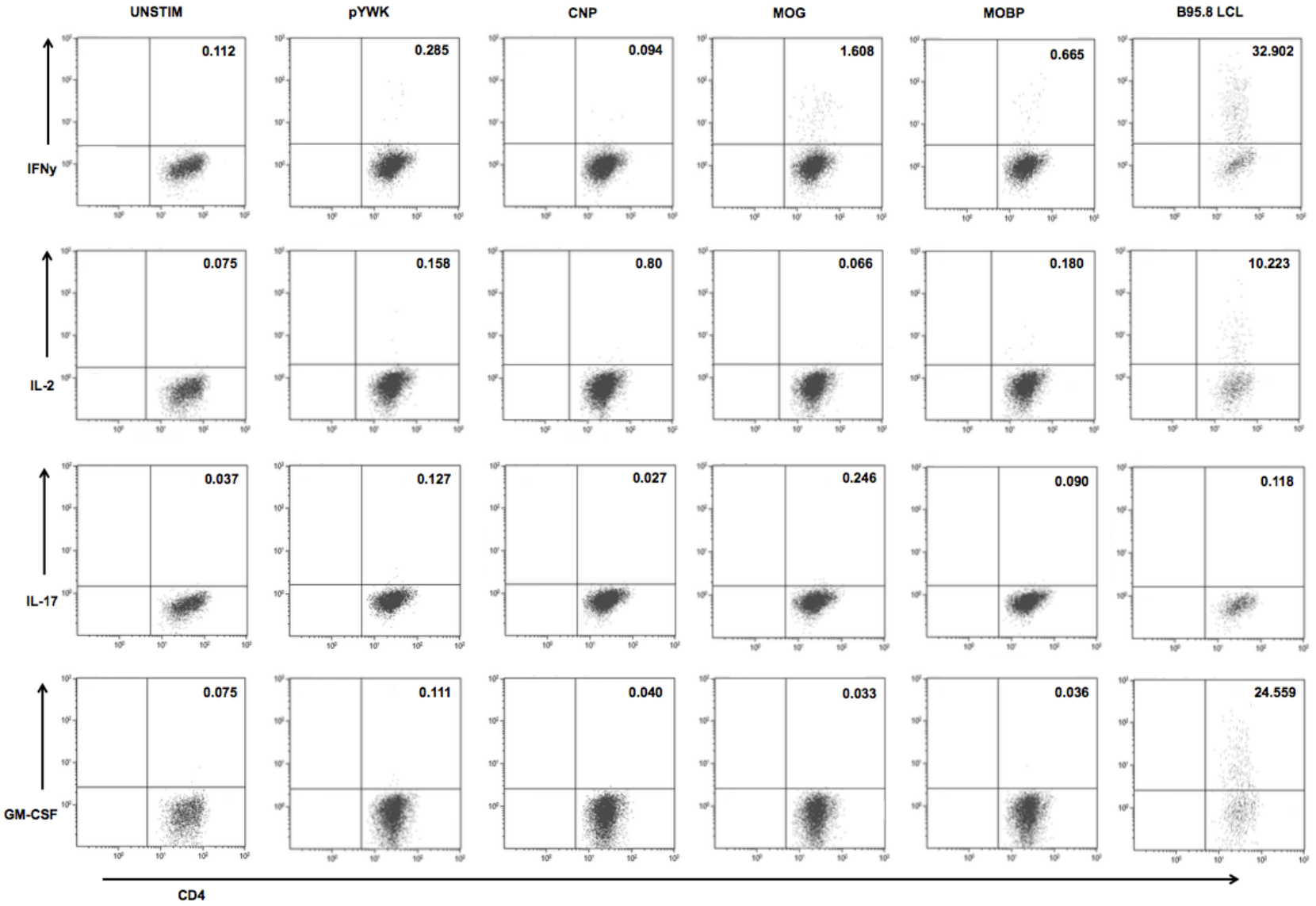

Figure 6.3.1 CD4+ T-cell responses to CNS proteins in polyclonal lines stimulated with wild type LCL. Example CD4+ T-cell staining from MS14 showing cytokine production in response to selected CNS antigens. The empty vector control (pYWK) showed minimal background staining, cytokine production in response to empty vector was subtracted as background from all stimulations using MVAs. Values represent percentage of total CD4+ T-cells producing each cytokine.

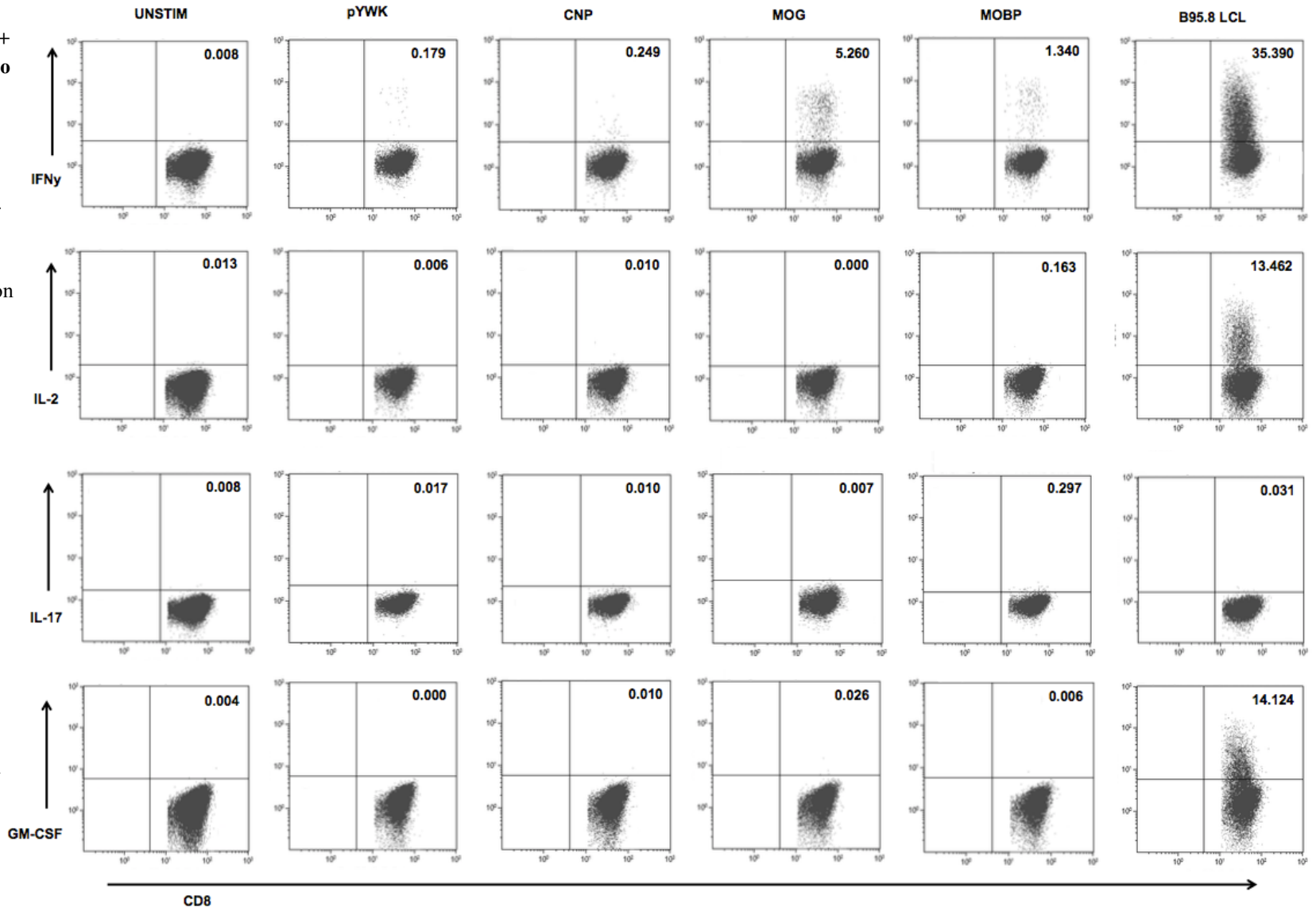

Figure 6.3.2 CD8+ T-cell responses to CNS proteins in polyclonal lines stimulated with wild type LCL. Example CD8+ T-cell staining from MS14 showing cytokine production in response to selected CNS antigens. The empty vector control (pYWK) showed minimal background staining, cytokine production in response to empty vector was subtracted as background from all stimulations using MVAs. Values represent percentage of total CD8+ T-cells producing each cytokine.

6.4 EBV-specific T-cell lines display reactivity with CNS proteins

6.4.1 CD4+ T-cell responses

Stimulation of whole PBMC with wild type LCL induced both CD4+ and CD8+ T-cell responses expanded over several weeks in culture into polyclonal lines that were enriched for specificity to EBV antigens, allowing us to screen lines simultaneously for reactivity in both of these subsets. Overall frequency of CD4+ T-cells compared to CD8+ T-cells in the LCL-stimulated polyclonal lines varied and this is probably a result of natural variation in responses between donors, attributed to factors including HLA type, age, gender and differences between the autologous LCLs established between individuals. Polyclonal T-cell lines expanded after stimulation with autologous wild type LCL were subsequently screened for reactivity to the original stimulus to investigate frequency of EBV-specific cells in cultures.

Responding T-cells were defined as any cells positive for any combination of the four cytokines in our staining panel – IFNγ, IL-2, IL-17 and GM-CSF – and percentages of CD4+ T-cells responding to each target in our stimulation panel are shown in Figure 6.4.1. MS patient CD4+ T-cell responses to CNS and EBV antigens from LCL-stimulated polyclonal lines (with background subtracted by Funky Cells) are shown in Figure 6.4.1B. Variation in size and frequency of responses to CNS antigens was observed in MS patient CD4+T-cells, with a pattern emerging showing particular proteins in the panel as frequent targets. Antigens eliciting the highest responses were MOG, PLP, MBP, TAL-H and MOBP, with ~4% of one MS patient's CD4 T-cells in the EBV-specific polyclonal exhibiting cytokine production in response to MBP (Figure 6.4.1A).

Surprising results were obtained from HC when their EBV-stimulated polyclonal lines were subjected to the same experiment. CD4+ T-cells from healthy donors showed a very similar pattern to that seen in MS patients, with MOG, PLP, MBP, TAL-H and MOBP shown as targets. However less variation between donors was seen between responses of HC than was observed in MS patients, suggesting that there is more heterogeneity in the patient group (Figure 6.4.1B).

In addition to investigating CNS responses, we also screened LCL-stimulated polyclonal T-cell lines for responses to the EBV proteins EBNA1 and EBNA3A. EBNA1 and EBNA3A peptides are naturally processed and presented on MHC molecules in LCLs, and as such responses to the proteins may have been generated in polyclonal lines. T-cell responses to EBNA1 have been described as cross-reactive in MS patients (Lunemann et al., 2008b), and we sought to correlate EBNA1 responses in polyclonal lines with those to CNS proteins expressed by our MVA panel. Reports of increased circulating EBNA1-specific CD4+ T-cells in MS patients also indicate that EBNA1 is a key target in MS patient responses to EBV (Lunemann et al., 2006, Lunemann et al., 2010). EBNA3A was selected due to interesting antibody response data from our project suggesting increased antibody responses towards EBNA3A. EBNA3A is also a common target of CD4+ and CD8+ T-cell responses in healthy people but one that has so far not been studied in the context of MS (Taylor et al., 2015).

From these experiments, it is evident that stimulating whole PBMC with autologous LCL not only allows EBV antigen-specific T-cells to grow out, but also stimulates those with reactivity to CNS antigens. This suggests that EBV epitopes displayed by autologous MHC molecules share some structural homology with peptides processed and presented from CNS proteins, and may shed light on the mechanism by which the risk allele HLA-DR15 contributes towards disease development. Presence of circulating T-cells that are able to target both EBV and CNS antigens has strong implications for EBV's role in the development of MS, however similar

responses in polyclonal lines from healthy donors suggests that presence of cross-reactive cells alone is not enough to cause disease, and these cells must be investigated further in order to understand their contribution towards MS pathogenesis.

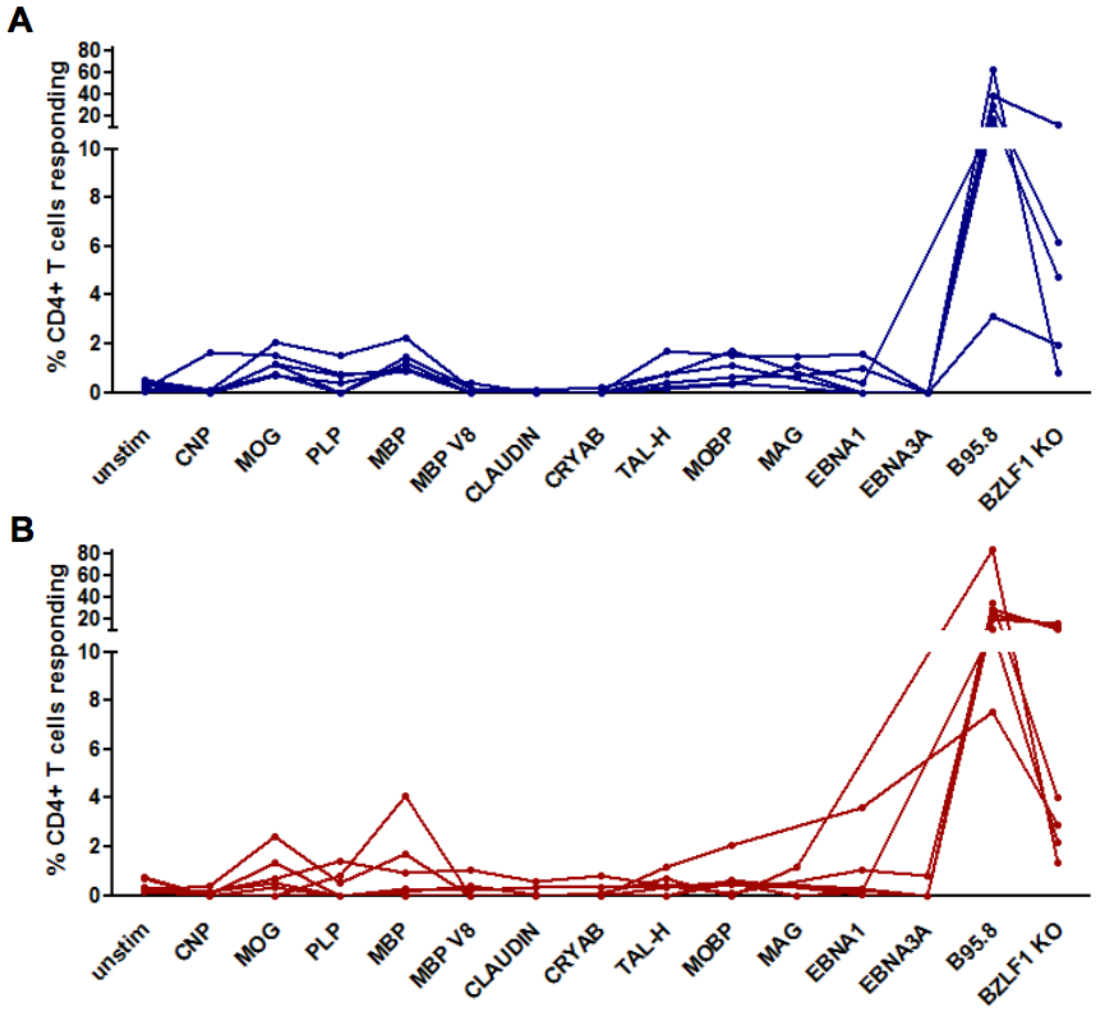

Figure 6.4.1 CD4+ T-cell responses to CNS proteins in wild type LCL-stimulated polyclonal T-cell lines. Whole PBMC from separate donors were stimulated with wild type LCL twice (day 0 and day 7) and responding T-cells were expanded over 4 weeks. Polyclonal lines generated were then stimulated with autologous, MVA-infected B-cell blasts expressing CNS and EBV proteins individually and subjected to ICS. Responding CD4+ T-cells were defined as producing any combination cytokines. Background staining from MVA empty vector stimulations was subtracted from CNS and EBV protein stimulations, background staining in unstimulated T-cell samples was subtracted from LCL stimulations. **A.** HC polyclonal T-cell lines (n=6) **B.** MS patient polyclonal T-cell lines (n=7).

6.4.2 CD8+ T-cell responses

From the same polyclonal T-cell lines generated by stimulating with autologous wild type LCL, we were also able to investigate frequency and cytokine production of CD8+ T-cells in response to CNS and EBV proteins with results shown in Figure 6.4.2.

CD8+ T-cell responses to CNS proteins from wild type LCL-stimulated polyclonal T-cell lines showed a similar pattern to those of CD4+ T-cells. After subtraction of background responses, MS patient CD8+ T-cell responses to CNS proteins were overall higher than those observed in CD4+ T-cells, with the same antigens as major targets of responses: MOG, PLP, MBP, TAL-H and MOBP (Figure 6.4.2). Some of the highest responses observed were to MOBP, with ~8% of one MS donor's CD8+ T-cells in the polyclonal T-cell line showing reactivity to MOBP.

A similar picture was seen again in the CD8+ T-cells from healthy donors, and responses to CNS antigens were at comparable levels with those from MS patients (Figure 6.4.2). CD8+ T-cell responses to CNS proteins in both HC and MS patients were proportionally higher than those observed to CD4+ T-cells, and this pattern of responses was consistent between the groups (Figure 6.4.1 and 6.4.2). These data suggest that LCL stimulation not only activates CD4+ T-cell responses but also CD8+ T-cells to potentially higher levels, indicating that there may also be cross-reactivity in the CD8+ T-cell compartment between EBV and CNS antigens. This comparison between groups was carried out looking at total responding cells, taking into account all cells producing any one of the four cytokines in our flow cytometry staining panel: IFNγ, IL-2, IL-17 and GM-CSF. It is clear from these graphs that there is no overall difference in frequency of "cross-reactive" T-cells between HC and MS patients, and we therefore sought to investigate function and phenotype of responses, investigating if there is a difference in cytokine profile of responding CD4+ and CD8+ T-cells between groups.

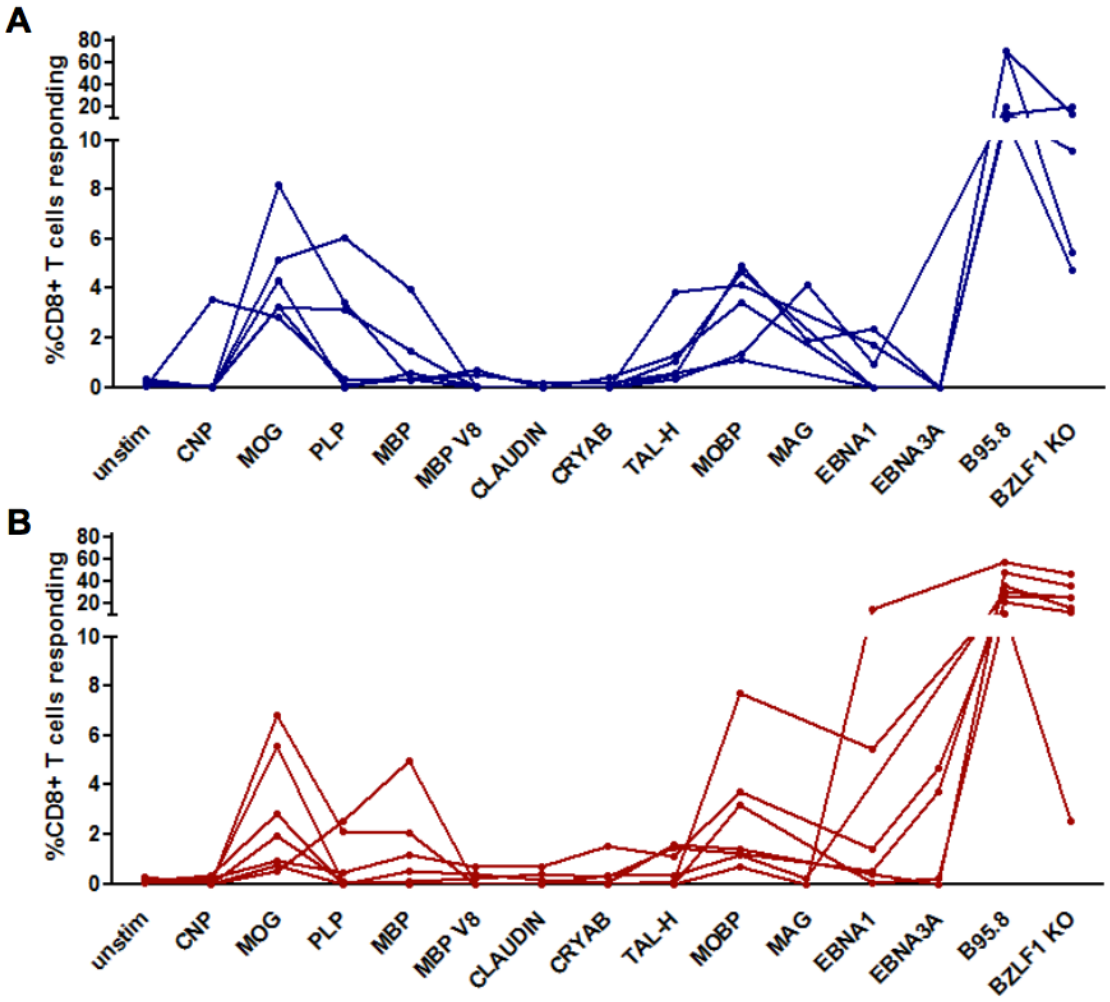

Figure 6.4.2 CD8+ T-cell responses to CNS proteins in wild type LCL-stimulated polyclonal T-cell lines. Whole PBMC from separate donors were stimulated with wild type LCL twice (day 0 and day 7) and responding T-cells were expanded over 4 weeks. Polyclonal lines generated were then stimulated with autologous, MVA-infected B-cell blasts expressing CNS and EBV proteins individually and subjected to ICS. Responding CD8+ T-cells were defined as producing any combination cytokines. Background staining from MVA empty vector stimulations was subtracted from CNS and EBV protein stimulations, background staining in unstimulated T-cell samples was subtracted from LCL stimulations. **A.** HC polyclonal T-cell lines (n=6) **B.** MS patient polyclonal T-cell lines (n=7).

6.5 Polyfunctionality and cytokine profile of cross-reactive cells

6.5.1 Polyfunctionality index

Similar frequencies of CNS protein responses in wild type LCL-stimulated polyclonal T-cell lines from HC and MS patients led us to further investigate function of responding CD4+ and CD8+ T-cells. This was achieved using Boolean combination gating as previously described in Chapter 5 for analysis of *ex vivo* T-cell responses.

As previously described in Chapter 5.3.1, polyfunctionality can be measured in Funky Cells software to give an arbitrary score calculated by an algorithm, termed polyfunctionality index (PI). Comparing these values enables direct comparison of the number of functions responding cells have to different targets, and these can also be used to compare CD4+ and CD8+ T-cells to each other.

Figure 6.5.1A shows the PI of CD4+ T-cells in wild type LCL-stimulated polyclonal T-cell lines after stimulation with autologous B-cell blasts infected with the MVA CNS panel. The majority of CNS protein CD4+ T-cell responses were similar in polyfunctionality between HC and MS patients, with much variation in degree of function between CNS targets (Figure 6.5.1A). CD4+ responses from healthy donor T-cell lines to claudin had significantly higher PI values than those of MS patients (HC:MS $p=0.0082$, Mann-Whitney test), an interesting finding as claudin was not a major CNS target for CD4+ T-cell responses described in Figure 6.4.1, indicating a qualitative difference in cells responding to this antigen.

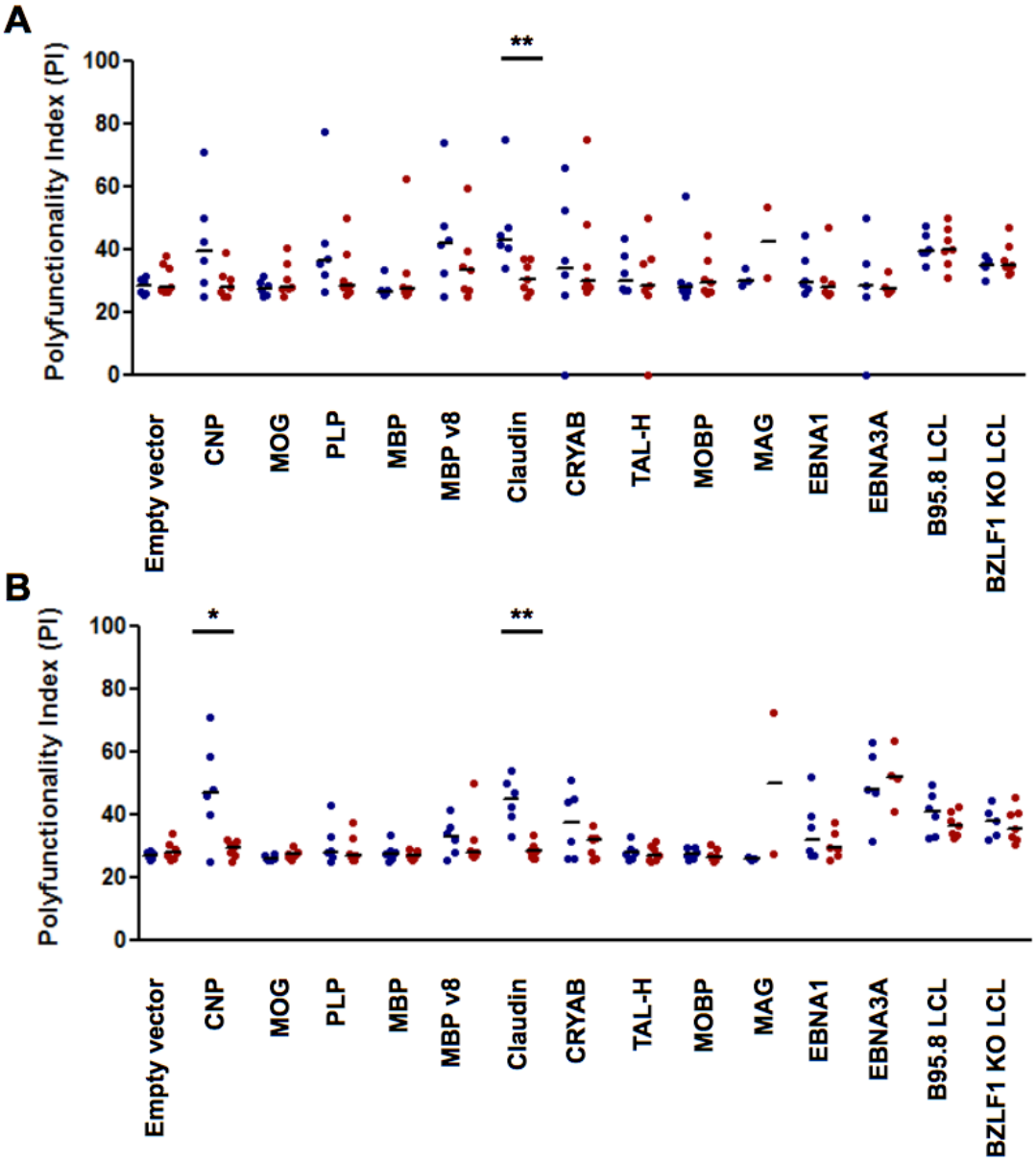

Figure 6.5.1 Polyfunctionality of CD4+ and CD8+ T-cells responding to CNS antigens from wild type LCL-stimulated polyclonal T-cell lines. CNS responses observed in wild type LCL-stimulated polyclonal T-cell lines were analysed for multiple cytokine production (IFNγ, IL-2, IL-17 and GM-CSF) using Funky Cells software which was used to calculate polyfunctionality index (PI) of responding CD4+ (**A.**) and CD8+ (**B.**) T-cells. Black lines represent median of data set. Colour of dots represent cohort group: blue=HC, red=MS. Statistics analysis performed using the Mann-Whitney test (ns *p>0.05*, * *p>0.05*, ** p>*0.005*).

CD8+ T-cell responses from wild type LCL-stimulated polyclonal lines showed a similar pattern of limited variation between groups, however PI value for CD8+ responses to claudin were also significantly higher in HC than MS patients (HC:MS *p=0.0023*, Mann-Whitney test) (Figure 6.5.1B). PI values of CD8+ T-cells responding to CNP were also significantly higher than in MS patients (HC:MS *p=0.0452*, Mann-Whitney test) (Figure 6.5.1B), a trend that was also seen in healthy control CNP-specific CD4+ T-cell responses but did not reach significance (Figure 6.5.1A).

The target MAG showed great variation between donors, however due to difficulties with virus production only 5 donors were tested (two MS and three HC), meaning that the Mann-Whitney test could not be applied as a minimum of three data points per group are needed to apply this particular statistical test. Further studies of responses to this target may reveal significant differences between groups but this was not possible for our project.

6.5.2 Cytokine profile of cross-reactive CD4+ T-cells

ICS of wild type LCL-stimulated polyclonal T-cell lines allowed in-depth analysis of the cytokine profile of cells responding to CNS antigens, and their exact combination of IFNγ, IL-2, IL-17 and GM-CSF production was analysed as previously described in Chapter 5.3 using both Funky Cells and SPICE analysis software.

MVA empty vector control stimulations were used for each donor to remove background staining from MVA CNS stimulations, giving a clear picture of effector molecules produced by CD4+ and CD8+ T-cells in response to each CNS protein without background staining. Levels of staining from unstimulated T-cell controls were applied in the same way to wild type and BZLF1 KO LCL stimulations to remove background.

Patterns of cytokine production for responding CD4+ T-cells in each of sixteen combination gates are shown for all targets in our stimulation panel in Figures 6.5.2 to 6.5.17, with all figures showing the same format: the mean values of combination gates are shown in A, with individual data points and median values shown by black bars in B. The non-parametric Wilcoxon Signed Rank Test was applied to statistically analyse cytokine production between groups with statistics shown in table format in C. A heat map of responses in each combination gate is shown in D of figures. Cytokine notation from table 5.1 is used to denote production of IFNγ, IL-2, IL-17 and GM-CSF (ie. ++-- would mean IFNγ+ IL-2+ IL-17- GM-CSF-).

Figure 6.5.2 shows the cytokines produced by polyclonal CD4+ T-cells after overnight stimulation with the same autologous wild type LCL used initially when setting up the lines. Cytokine production between responding cells from HC and MS patients was similar and did not show any significant differences between groups (Figure 6.5.2). Polyclonal line stimulation with autologous BZLF1 KO LCL showed an increased proportion of cells in healthy donors

producing IFNγ, but levels did not reach significance after applying the Wilcoxon Signed Rank Test (Figure 6.5.3).

LCL-stimulated polyclonal T-cell lines were also screened for reactivity to EBNA1 and EBNA3A to investigate whether any qualitative differences in cytokine production could be seen in responding cells between groups. MVA EBNA1 and EBNA3A-infected autologous B-cell blasts were used to stimulate wild type LCL-specific polyclonal T-cell lines separately and cytokine profile of responding cells analysed. CD4+ T-cell responses to EBNA1 were similar between groups but a higher proportion of responding cells from MS patients produced either GM-CSF only or IFNγ only. Responding cells from HC showed an increase in the subset producing IL-17 only, and this mirrors findings from *ex vivo* T-cell responses in Chapter 5.3 showing an increased production of IL-17 in response to EBV antigens (Figure 6.5.4). However, these differences did not reach significance and more data points may be needed to see if this effect is real.

CD4+ T-cell responses to EBNA3A were distinct between groups, with MS patients showing a high proportion of cells producing IFNγ only in response to the antigen compared with none observed in those from HC, an effect that did not quite reach significance (HC:MS +---*p=0.066*) (Figure 6.5.5). Also notable was the increased proportion of cells from HC producing GM-CSF only in response to the antigen, but this also did not reach significance.

Figure 6.5.6 shows cytokine profile of CD4+ T-cells responding to stimulation with MVA empty vector-infected autologous B-cell blasts with no significant differences observed between groups.

Overall response data did not show CNP to be an important, cross-reactive CD4+ target in our experiments, with only a few donors showing a small response to the protein after stimulation with wild type LCL (Figure 6.4.1). However, upon looking at the mean percentage of CD4+ T-cell responses to CNP in each combination gate, we found them to be significantly different

between groups. Healthy controls showed a response that was predominantly producing IL-17 only, with other responding cells co-expressing IFNγ, IL-2 and GM-CSF in various combinations (Figure 6.5.7). In contrast MS patients showed a CD4+ T-cell response that was mostly producing one cytokine only, with most cells singularly expressing IL-2, IFNγ or GM-CSF (Figure 6.5.7). Using the median percentage of responding CD4+ T-cells in each cytokine group skews data less and removes this effect, and more donors need to be analysed to determine if this effect is true; results did not reach significance between groups after statistical analysis using the Wilcoxon Signed Rank test (Figure 6.5.7C).

Cytokine production of responding CD4+ T-cells between groups in response to MOG was very similar, with the majority of cells fitting into the IFNγ only category (Figure 6.5.8). MOG was one of the antigens which induced the highest overall responses after wild type LCL stimulation, and interestingly the quality of response was very similar in level and function between HC and MS.

PLP is an antigen that induced modest responses from LCL-stimulated polyclonal T-cell lines with quite a lot of variation (7.2.3). The cytokine production between groups did vary, with more CD4+ T-cells producing IFNγ only in MS patients compared to HC, a level that did not reach significance (Figure 7.3.9). Healthy donors showed an increase in a subset of responding CD4+ T-cells co-producing IL-2, IL-17 and GM-CSF, an increase that reached statistical significance (Figure 7.3.9C).

MBP CD4+ T-cell responses been investigated extensively in the context of MS, and this protein was a frequent response in our cultured LCL-specific polyclonal T-cell lines (Figure 6.5.3). Cytokine production in responding cells showed a marked decrease in variation compared to other CNS responses, with the majority of MBP-reactive CD4+ T-cells from HC and MS patients producing IFNγ only (Figure 6.5.10).

MBP's splice variant MBP V8 is a shorter molecule and CD4+ T-cell responses were overall lower to this protein than to MBP, with analysis of cytokine production also showing a different pattern. MS patients showed an increase in CD4+ T-cells producing IFNγ only after stimulation with MBP V8 compared to HC, but this effect did not quite reach significance when analysed using the Wilcoxon Signed Rank test (HC:MS +--- *p=0.086*) (Figure 6.5.11C). HC showed a significant increase in cells producing IL-17 only in response to MBP V8 compared to MS patients (HC:MS --+- *p=0.045*) (Figure 6.5.11C).

CD4+ T-cell responses from polyclonal lines showed a great variation in cytokine production in response to claudin, a result reflected in analysis of polyfunctionality index between groups (Figure 6.5.1A). Most notable is the increase in proportion of CD4+ T-cells from MS patients producing IFNγ only, with no cells in this gate from healthy controls (HC:MS +--- *p=0.032*) (Figure 6.5.12).

CRYAB induced CD4+ T-cell responses with great variation in quality of response, with subsets producing IL-2 or GM-CSF only showing an increase in MS patients compared to healthy controls. (Figure 6.5.13). MS donors also showed an increase in proportion of responding cells co-producing IL-2 and GM-CSF, but this did not reach significance (HC:MS -+-+ *p=0.074*) (Figure 6.5.13).

TAL-H CD4+ T-cell responses in polyclonal T-cell lines were again a modest target for overall responses in healthy and MS donors, however less variation was seen in cytokine production by CD4+ T-cell responses to the protein than to other proteins. An increase in cells singularly producing IFNγ amongst HC did not reach significance (HC:MS +--- *p=0.116*) (Figure 6.5.14).

CD4+ T-cells from polyclonal lines responding to the major CNS target in our study MOBP showed similar cytokine production patterns between groups, with the majority producing IFNγ only in response to the antigen (Figure 6.5.15).

Fewer wild type LCL-stimulated polyclonal T-cell lines were screened against MVA MAG due to difficulties halfway through the project in virus stock production, meaning that only three healthy controls and two MS donors were screened against the protein. An increased proportion of cells producing IFNγ only in response to MAG was observed in HC, but this did not reach significance (HC:MS +--- $p=0.083$) (Figure 6.5.16). MS patient responding cells showed a broader range of cytokines produced in response to MAG proteins, but reduced number of data points makes drawing conclusions from data difficult, and more donors need to be screened to determine if this effect is real (Figure 6.5.16).

Pie charts showing the proportion of CD4+ T-cells in each combination gate can be viewed for all targets in Figure 6.5.17, allowing visual comparison of the contribution of each cellular phenotype to responses between groups. Using this visual analysis allows CNS and EBV antigens to be divided into roughly two groups: those which induce a response that predominantly produces IFNγ only (turquoise segments) and another that induces a response which is much more polymorphic (Figure 6.5.17). This observation is interesting as the targets which make up the first group – MOG, MBP, MOBP and TAL-H – are the antigens that were able to stimulate the highest proportion of cells from wild type LCL-stimulated polyclonal cell lines.

A permutation test is used to determine the amount of variation between groups by random sampling and this analysis was applied to our data set using SPICE software, allowing us to determine if there were significant differences between HC and MS donor groups in distribution of cytokine responses. No differences were seen in CD4+ T-cell responses to wild type and BZLF1 KO LCLs between groups, and in addition to this EBNA1 responses were not significantly different between groups in their cytokine expression (Figure 6.5.17).

EBNA3A was added to our screening panel after early observations from our cohort indicated that MS donors more frequently had an antibody response to the protein than HC (Figure 4.2.3).

Analysis of EBNA3A-specific CD4+ T-cell responses in wild type LCL-stimulated polyclonal lines indicate that cytokine production between healthy controls and MS patients is very different. In HC ~50% of the EBNA3A-specific cells are in the subset producing GM-CSF only, however MS patient responses are predominantly made up from cells producing IFNγ, with permutation tests indicating that the two groups' responses are significantly different (HC:MS *p=0.0296*) (Figure 6.5.17).

CD4+ T-cell cytokine responses to CNS proteins in our panel varied greatly between targets, with the majority not showing any significant differences between HC and MS patients (Figure 6.5.17). However, several antigens induced a CD4+ T-cell response that was markedly different between groups, one of these being MBP V8. Responses to MBP V8 were highly polymorphic in their production of cytokines with MS patients producing a response that was mainly IFNγ positive, in contrast with HC CD4+ T-cells which mainly generated an IL-17 response; this difference did not reach statistical significance (HC:MS *p=0.0587*) (Figure 6.5.17).

Differences in the production of cytokines between HC and MS groups were statistically significant for the CNS protein CNP, with MS patients displaying a CD4+ T-cell repertoire skewed towards single cytokine production of IFNγ, IL-2 and GM-CSF; HC donor responses were more polymorphic and predominantly produced IL-17 alongside other cytokines (HC:MS *p=0.474*) (Figure 6.5.17).

From these experiments, cytokine production by "cross-reactive" CD4+ T-cells in response to EBV and CNS antigens has been found to be very different from that of antigens which did not elicit a high response in LCL-stimulated polyclonal lines. Cytokines produced by CD4+ T-cells reflect the effector function which has implications for their pathogenic potential *in vivo*.

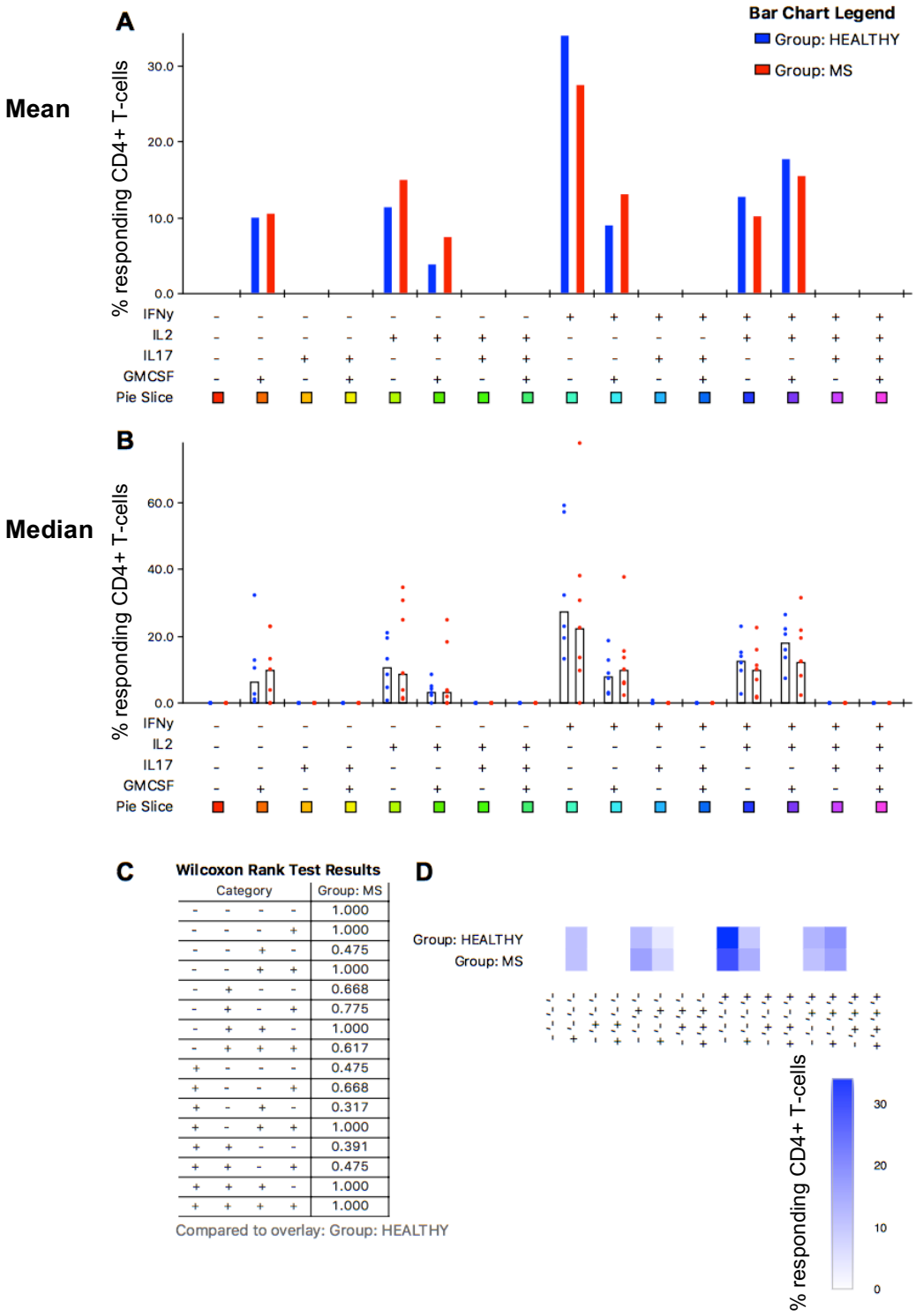

Figure 6.5.2 Cytokine profile of CD4+ T-cells responding to wild type LCL from wild type LCL-specific polyclonal lines. Wild type LCL-stimulated polyclonal T-cell lines were stimulated with autologous wild type LCL and subjected to ICS (HC n=6, MS n=7). Responding CD4+ T-cells were defined as positive for any combination of four cytokines in our panel: IFNγ, IL-2, IL-17 and GM-CSF. **A.** Graphical representation of responding cells in each combination gate with bars representing the mean of data set. Statistics were calculated using the Wilcoxon Signed Rank. **B.** Scatter plot showing percentage of responding cells for each donor in combination gates. Black bars represent median of data set. **C**. Table shows results of Wilcoxon rank test. **D.** Percentage of responding CD4+ T-cells shown in heatmap form. Combination gate data was processed using Funky Cells software and graphically displayed using the program SPICE (ns $p>0.05$, * $p<0.05$).

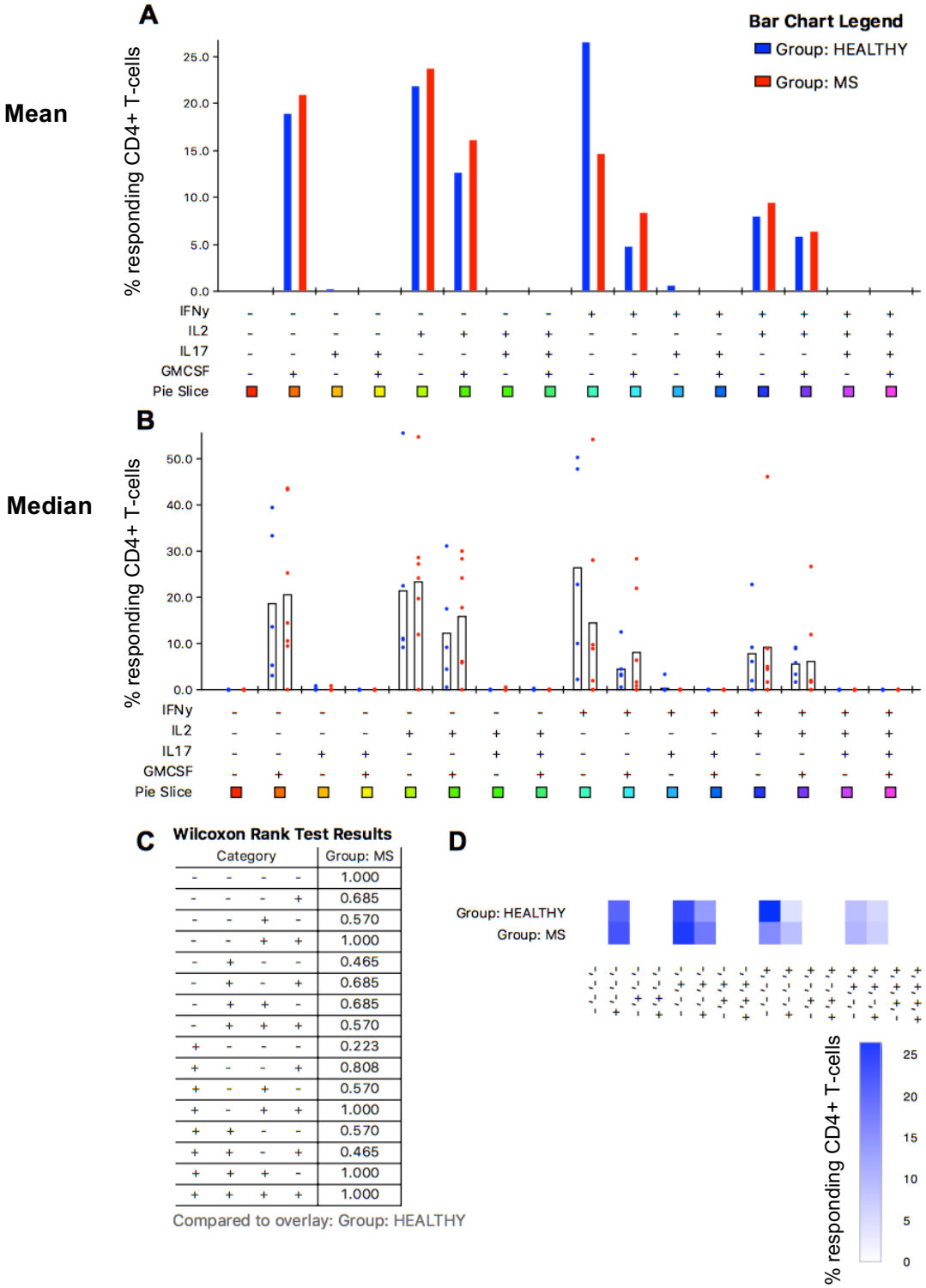

Figure 6.5.3 Cytokine profile of CD4+ T-cells responding to BZLF1 KO LCL from wild type LCL-specific polyclonal lines. Wild type LCL-stimulated polyclonal T-cell lines were stimulated with autologous BZLF1 KO LCL and subjected to ICS (HC n=6, MS n=7). Responding CD4+ T-cells were defined as positive for any combination of four cytokines in our panel: IFNγ, IL-2, IL-17 and GM-CSF. **A.** Graphical representation of responding cells in each combination gate with bars representing the mean of data set. Statistics were calculated using the Wilcoxon Signed Rank. **B.** Scatter plot showing percentage of responding cells for each donor in combination gates. Black bars represent median of data set. **C**. Table shows results of Wilcoxon rank test. **D.** Percentage of responding CD4+ T-cells shown in heatmap form. Combination gate data was processed using Funky Cells software and graphically displayed using the program SPICE (ns $p>0.05$, * $p<0.05$).

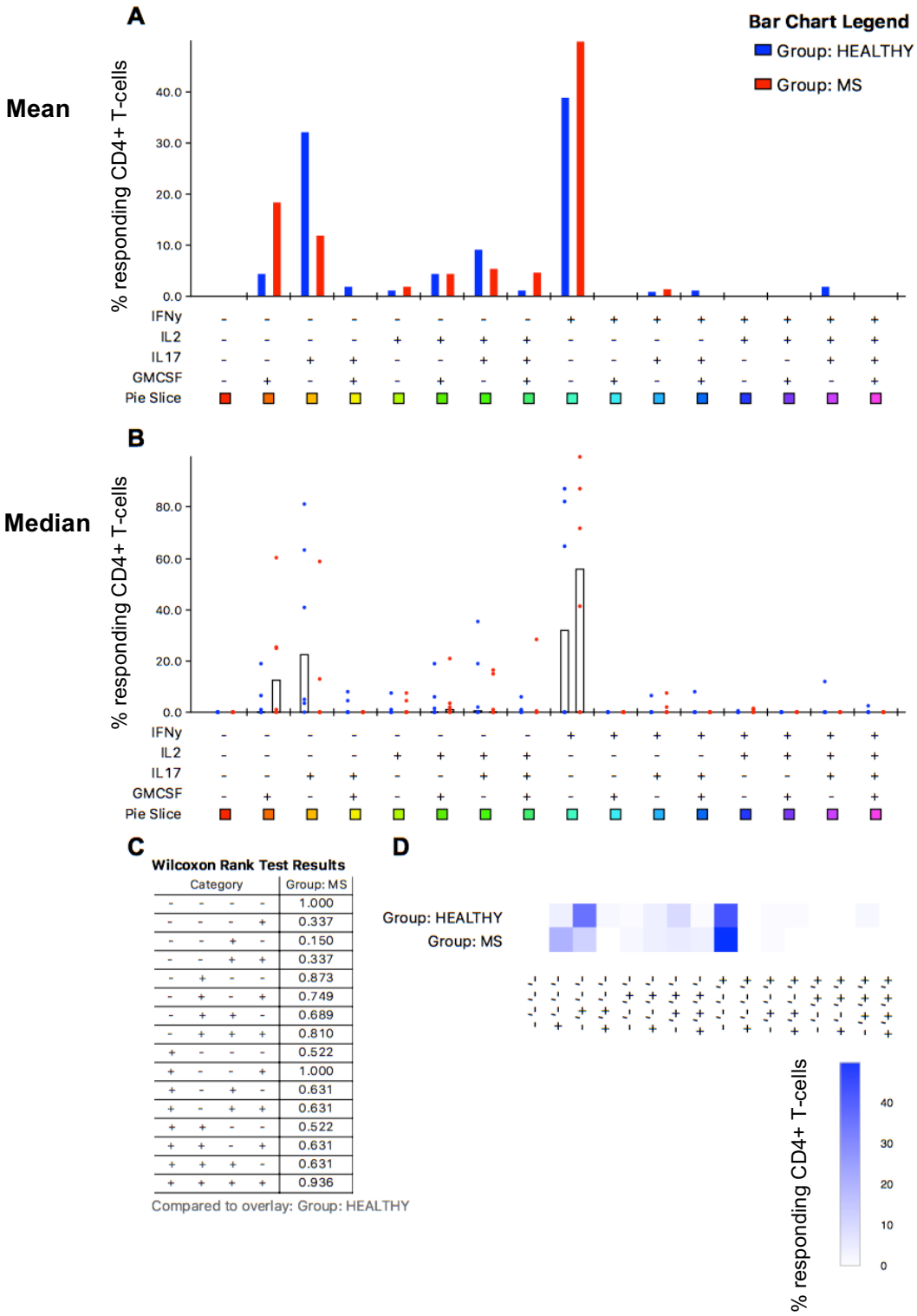

Figure 6.5.4 Cytokine profile of CD4+ T-cells responding to EBNA1 from wild type LCL-specific polyclonal lines. Wild type LCL-stimulated polyclonal T-cell lines were stimulated with MVA EBNA1-infected B cell blasts and subjected to ICS (HC n=6, MS n=7). Responding CD4+ T-cells were defined as positive for any combination of four cytokines in our panel: IFNγ, IL-2, IL-17 and GM-CSF. **A.** Graphical representation of responding cells in each combination gate with bars representing the mean of data set. Statistics were calculated using the Wilcoxon Signed Rank. **B.** Scatter plot showing percentage of responding cells for each donor in combination gates. Black bars represent median of data set. **C**. Table shows results of Wilcoxon rank test. **D.** Percentage of responding CD4+ T-cells shown in heatmap form. Combination gate data was processed using Funky Cells software and graphically displayed using the program SPICE (ns $p>0.05$, * $p<0.05$).

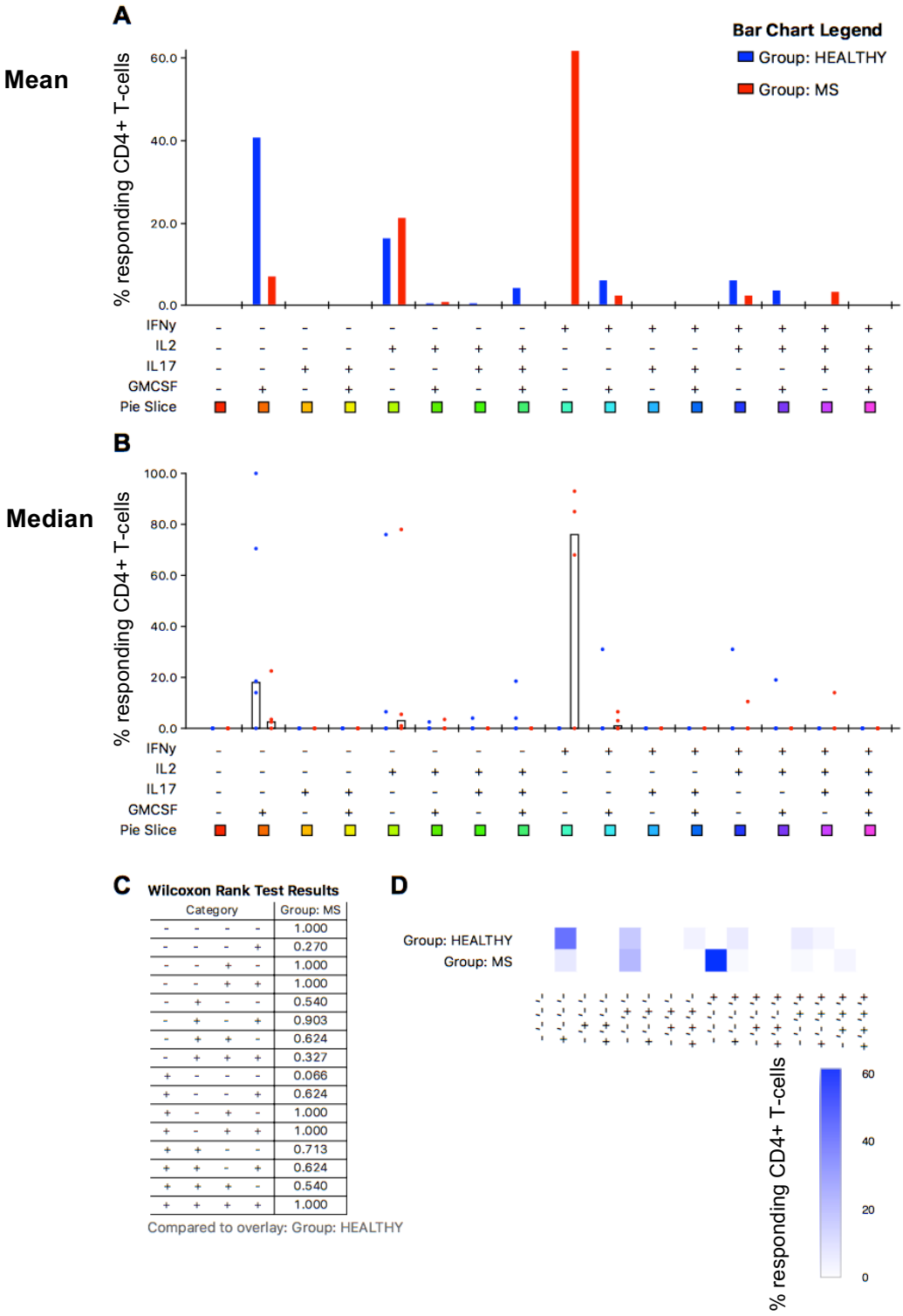

Figure 6.5.5 Cytokine profile of CD4+ T-cells responding to EBNA3A from wild type LCL-specific polyclonal lines. Wild type LCL-stimulated polyclonal T-cell lines were stimulated with MVA EBNA3A-infected B cell blasts and subjected to ICS (HC n=5, MS n=4). Responding CD4+ T-cells were defined as positive for any combination of four cytokines in our panel: IFNγ, IL-2, IL-17 and GM-CSF. **A.** Graphical representation of responding cells in each combination gate with bars representing the mean of data set. Statistics were calculated using the Wilcoxon Signed Rank. **B.** Scatter plot showing percentage of responding cells for each donor in combination gates. Black bars represent median of data set. **C**. Table shows results of Wilcoxon rank test. **D.** Percentage of responding CD4+ T-cells shown in heatmap form. Combination gate data was processed using Funky Cells software and graphically displayed using the program SPICE (ns $p>0.05$, * $p<0.05$).

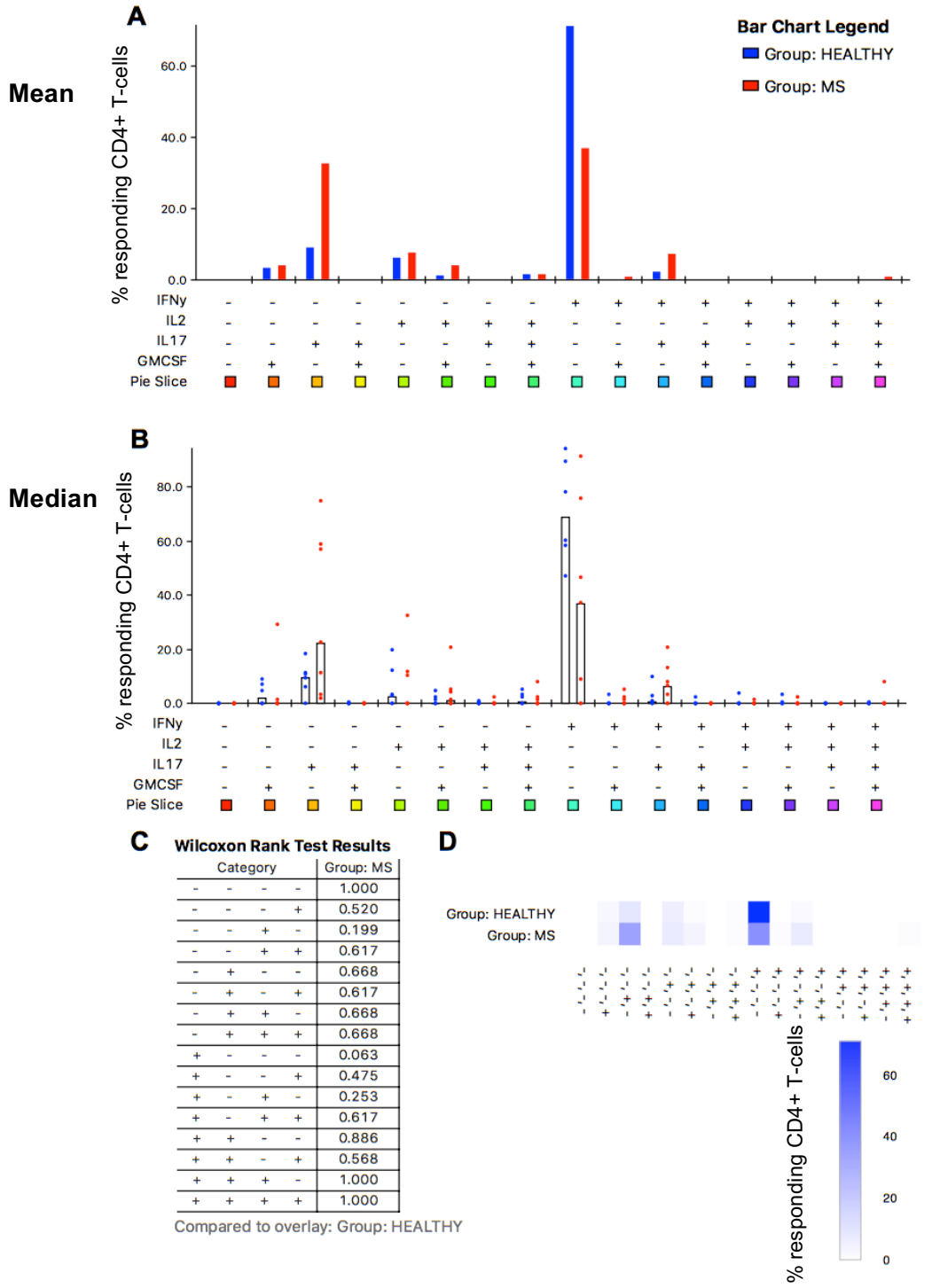

Figure 6.5.6 Cytokine profile of CD4+ T-cells responding to empty vector from wild type LCL-specific polyclonal lines. Wild type LCL-stimulated polyclonal T-cell lines were stimulated with MVA empty vector-infected B cell blasts and subjected to ICS (HC n=6, MS n=7). Responding CD4+ T-cells were defined as positive for any combination of four cytokines in our panel: IFNγ, IL-2, IL-17 and GM-CSF. **A.** Graphical representation of responding cells in each combination gate with bars representing the mean of data set. Statistics were calculated using the Wilcoxon Signed Rank. **B.** Scatter plot showing percentage of responding cells for each donor in combination gates. Black bars represent median of data set. **C**. Table shows results of Wilcoxon rank test. **D.** Percentage of responding CD4+ T-cells shown in heatmap form. Combination gate data was processed using Funky Cells software and graphically displayed using the program SPICE (ns $p>0.05$, * $p<0.05$).

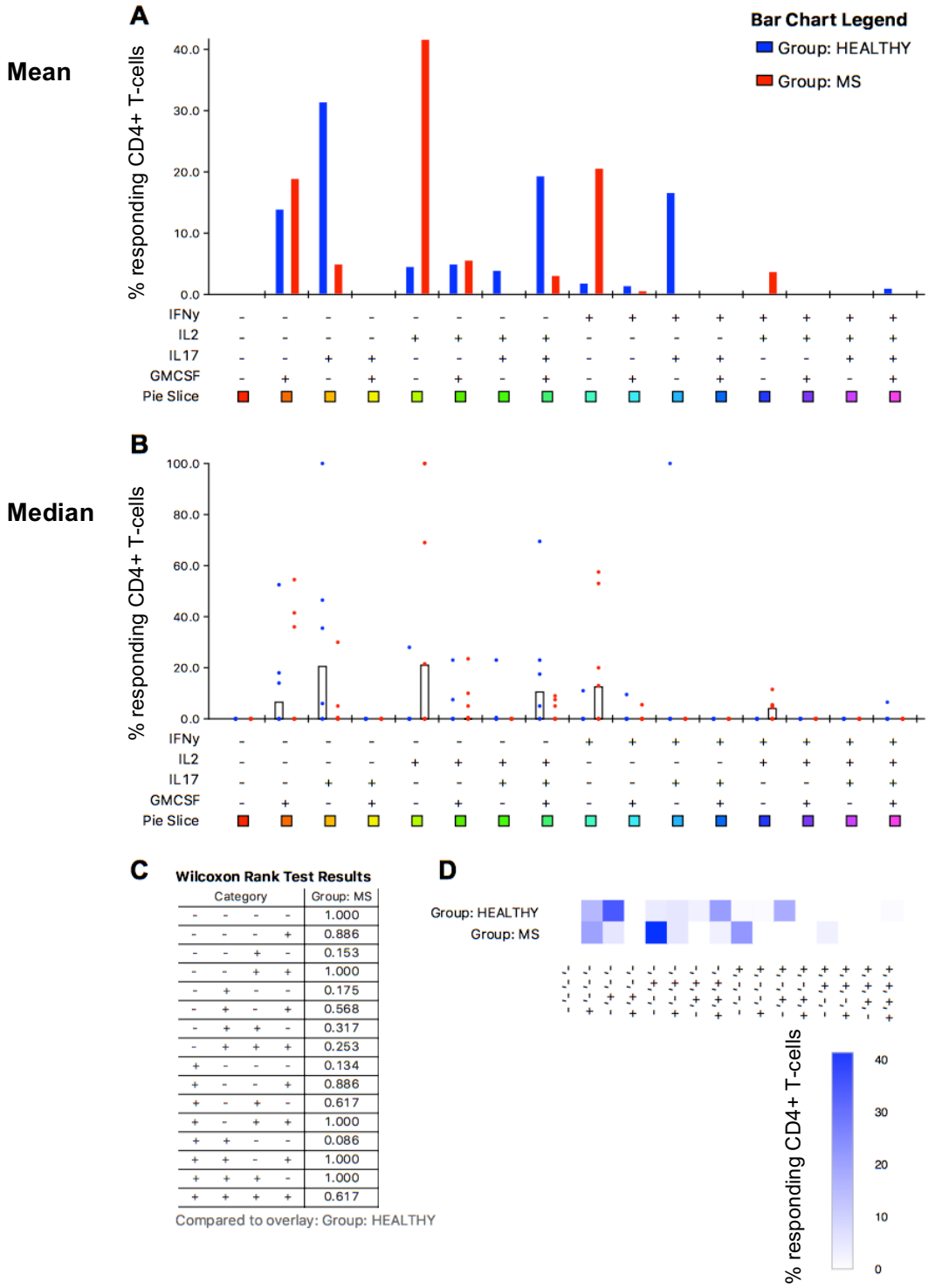

Figure 6.5.7 Cytokine profile of CD4+ T-cells responding to CNP from wild type LCL-specific polyclonal lines. Wild type LCL-stimulated polyclonal T-cell lines were stimulated with MVA CNP-infected B cell blasts and subjected to ICS (HC n=6, MS n=7). Responding CD4+ T-cells were defined as positive for any combination of four cytokines in our panel: IFNγ, IL-2, IL-17 and GM-CSF. **A.** Graphical representation of responding cells in each combination gate with bars representing the mean of data set. Statistics were calculated using the Wilcoxon Signed Rank. **B.** Scatter plot showing percentage of responding cells for each donor in combination gates. Black bars represent median of data set. **C**. Table shows results of Wilcoxon rank test. **D.** Percentage of responding CD4+ T-cells shown in heatmap form. Combination gate data was processed using Funky Cells software and graphically displayed using the program SPICE (ns $p>0.05$, * $p<0.05$).

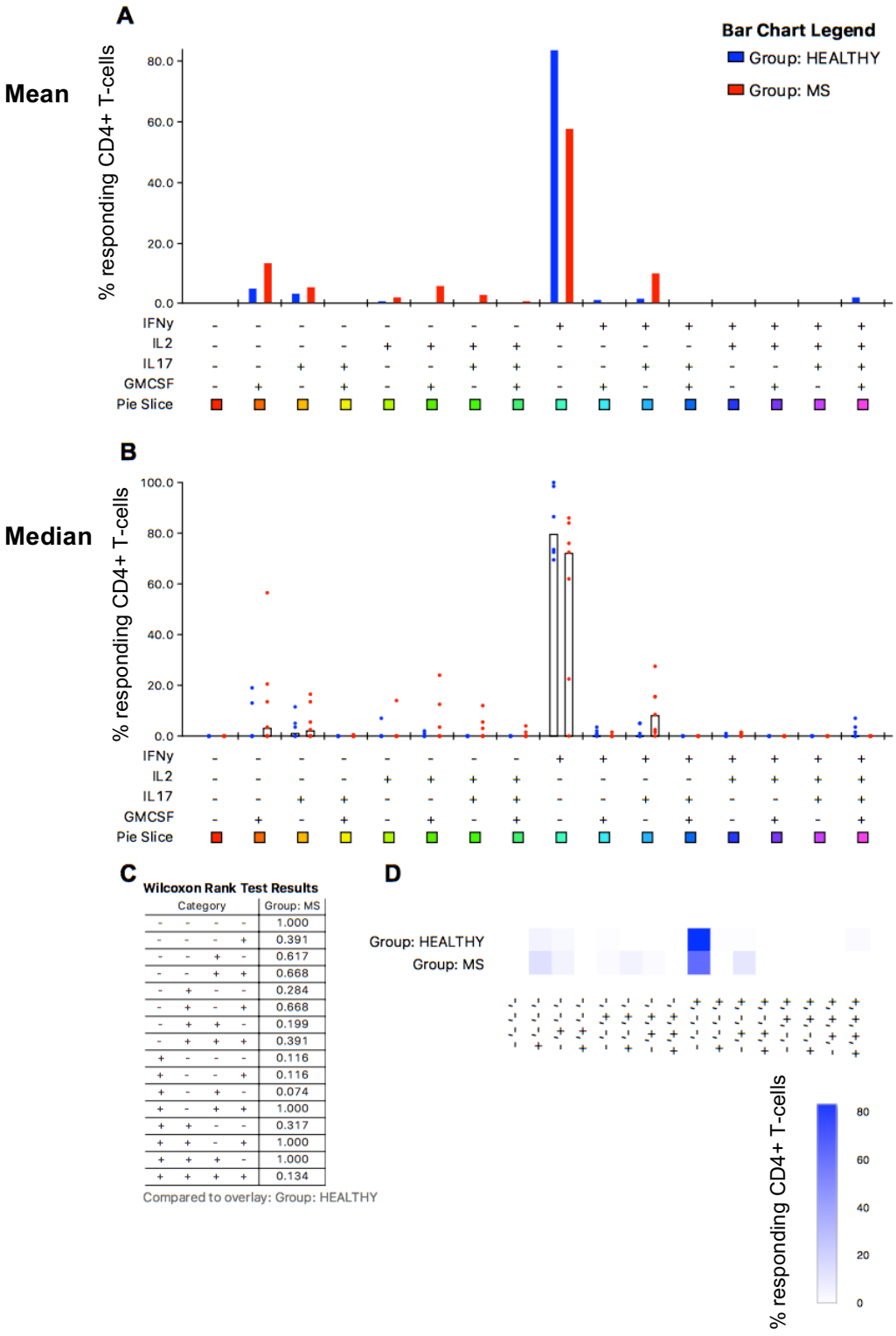

Figure 6.5.8 Cytokine profile of CD4+ T-cells responding to MOG from wild type LCL-specific polyclonal lines. Wild type LCL-stimulated polyclonal T-cell lines were stimulated with MVA MOG-infected B cell blasts and subjected to ICS (HC n=6, MS n=7). Responding CD4+ T-cells were defined as positive for any combination of four cytokines in our panel: IFNγ, IL-2, IL-17 and GM-CSF. **A.** Graphical representation of responding cells in each combination gate with bars representing the mean of data set. Statistics were calculated using the Wilcoxon Signed Rank. **B.** Scatter plot showing percentage of responding cells for each donor in combination gates. Black bars represent median of data set. **C**. Table shows results of Wilcoxon rank test. **D.** Percentage of responding CD4+ T-cells shown in heatmap form. Combination gate data was processed using Funky Cells software and graphically displayed using the program SPICE (ns $p>0.05$, * $p<0.05$).

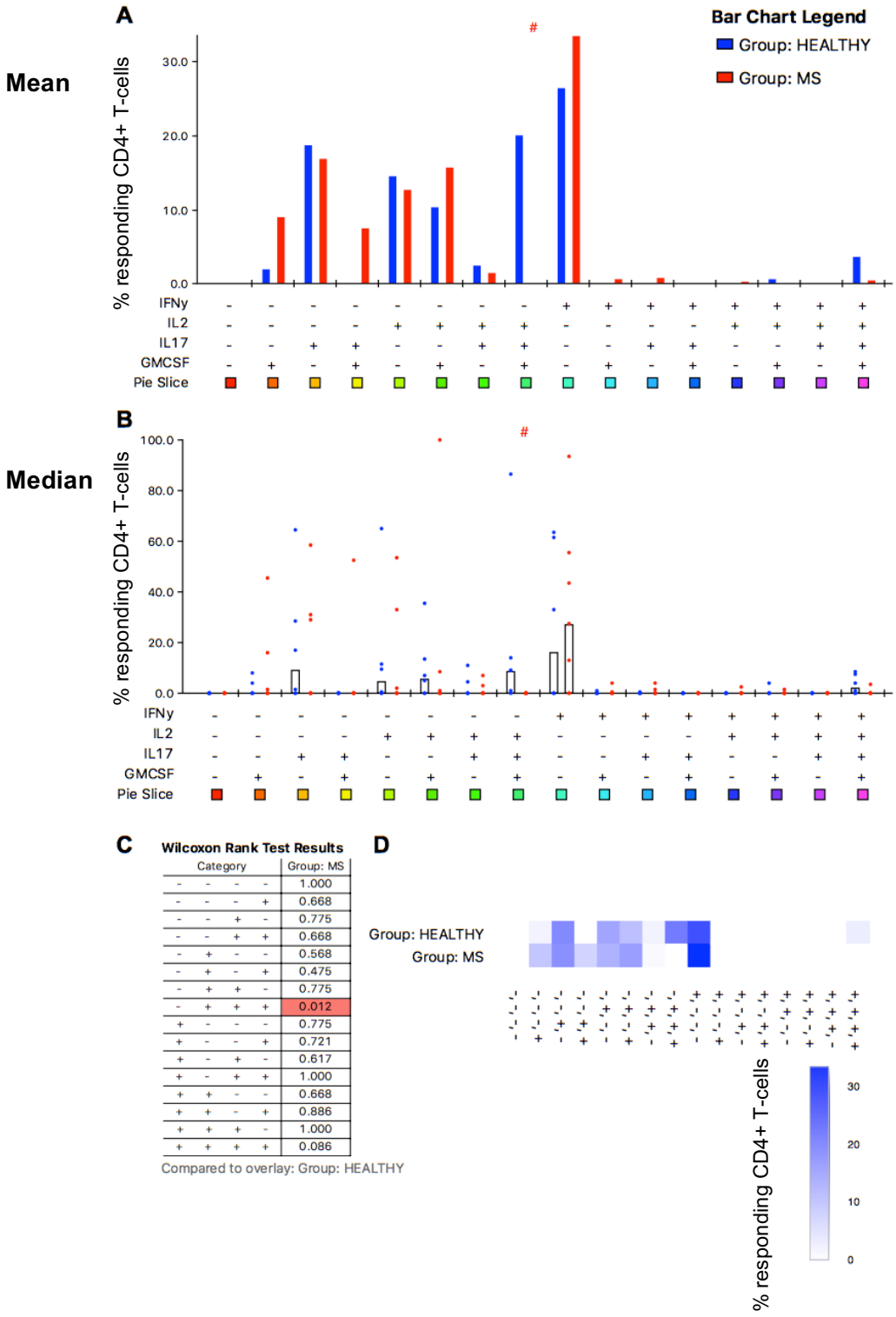

Figure 6.5.9 Cytokine profile of CD4+ T-cells responding to PLP from wild type LCL-specific polyclonal lines. Wild type LCL-stimulated polyclonal T-cell lines were stimulated with MVA PLP-infected B cell blasts and subjected to ICS (HC n=6, MS n=7). Responding CD4+ T-cells were defined as positive for any combination of four cytokines in our panel: IFNγ, IL-2, IL-17 and GM-CSF. **A.** Graphical representation of responding cells in each combination gate with bars representing the mean of data set. Statistics were calculated using the Wilcoxon Signed Rank. **B.** Scatter plot showing percentage of responding cells for each donor in combination gates. Black bars represent median of data set. **C**. Table shows results of Wilcoxon rank test. **D.** Percentage of responding CD4+ T-cells shown in heatmap form. Combination gate data was processed using Funky Cells software and graphically displayed using the program SPICE (ns $p>0.05$, * $p<0.05$).

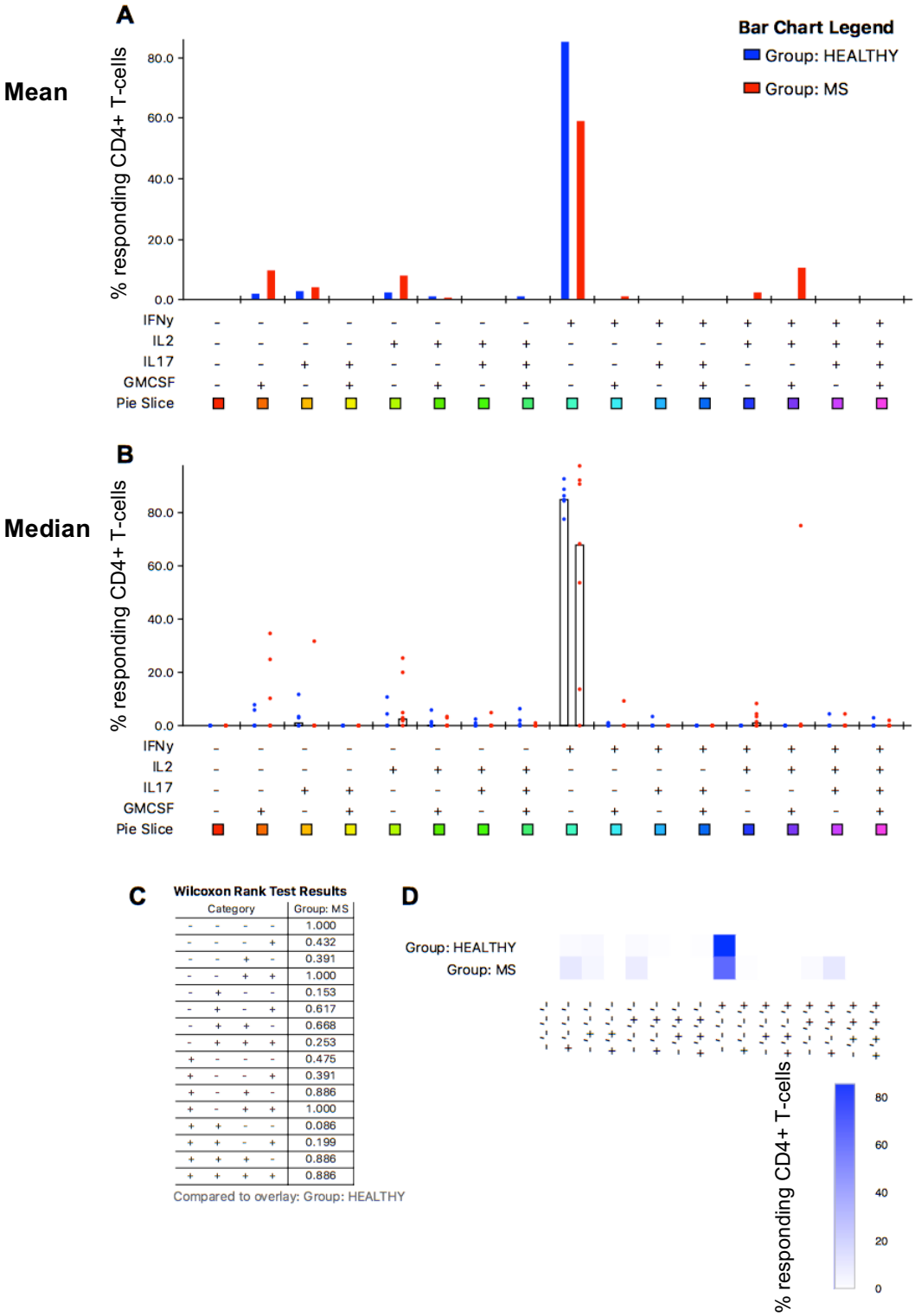

Figure 6.5.10 Cytokine profile of CD4+ T-cells responding to MBP from wild type LCL-specific polyclonal lines. Wild type LCL-stimulated polyclonal T-cell lines were stimulated with MVA MBP-infected B cell blasts and subjected to ICS (HC n=6, MS n=7). Responding CD4+ T-cells were defined as positive for any combination of four cytokines in our panel: IFNγ, IL-2, IL-17 and GM-CSF. **A.** Graphical representation of responding cells in each combination gate with bars representing the mean of data set. Statistics were calculated using the Wilcoxon Signed Rank. **B.** Scatter plot showing percentage of responding cells for each donor in combination gates. Black bars represent median of data set. **C**. Table shows results of Wilcoxon rank test. **D.** Percentage of responding CD4+ T-cells shown in heatmap form. Combination gate data was processed using Funky Cells software and graphically displayed using the program SPICE (ns $p>0.05$, * $p<0.05$).

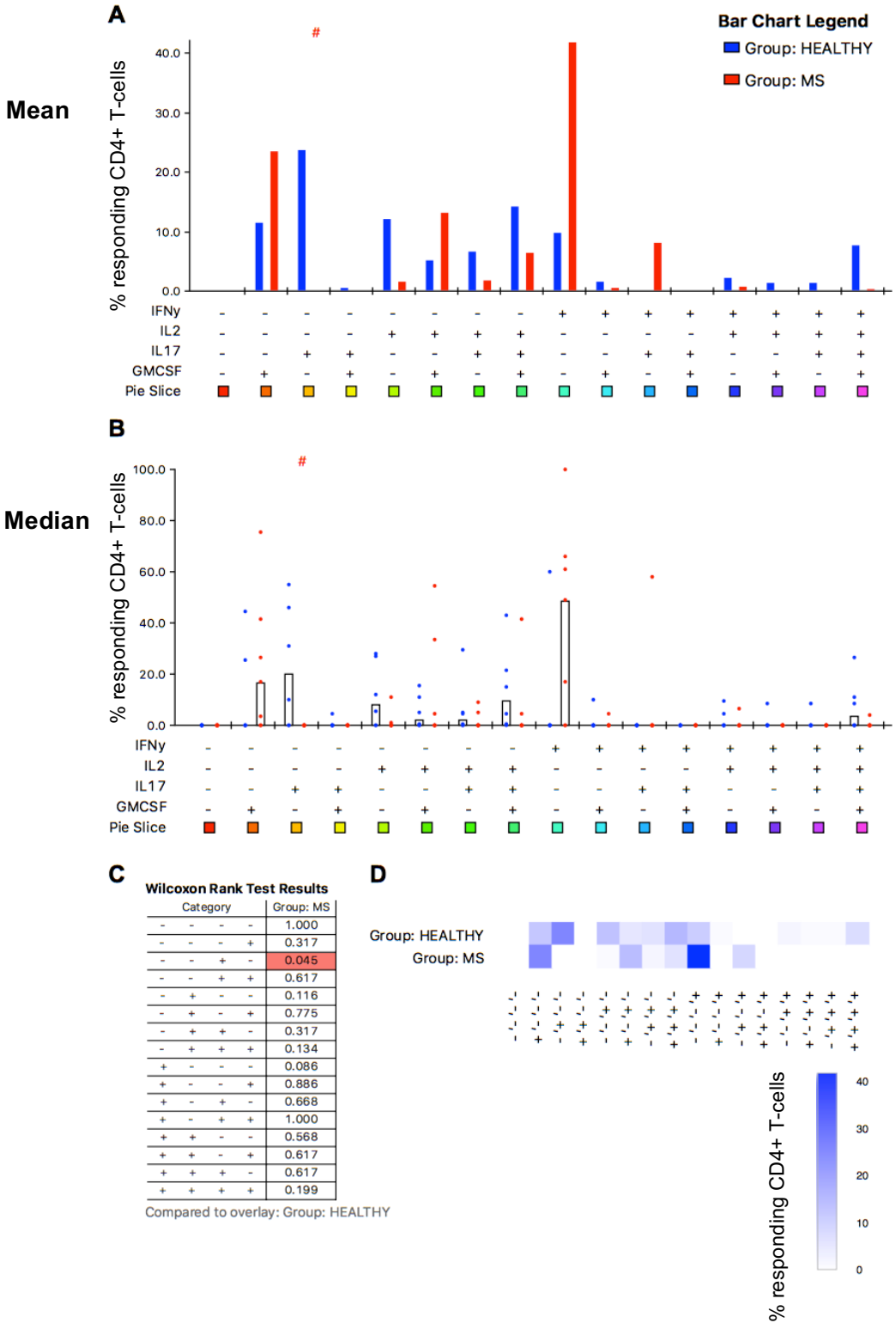

Figure 6.5.11 Cytokine profile of CD4+ T-cells responding to MBP V8 from wild type LCL-specific polyclonal lines. Wild type LCL-stimulated polyclonal T-cell lines were stimulated with MVA MBP V8-infected B cell blasts and subjected to ICS (HC n=6, MS n=7). Responding CD4+ T-cells were defined as positive for any combination of four cytokines in our panel: IFNγ, IL-2, IL-17 and GM-CSF. **A.** Graphical representation of responding cells in each combination gate with bars representing the mean of data set. Statistics were calculated using the Wilcoxon Signed Rank. **B.** Scatter plot showing percentage of responding cells for each donor in combination gates. Black bars represent median of data set. **C**. Table shows results of Wilcoxon rank test. **D.** Percentage of responding CD4+ T-cells shown in heatmap form. Combination gate data was processed using Funky Cells software and graphically displayed using the program SPICE (ns $p>0.05$, * $p<0.05$).

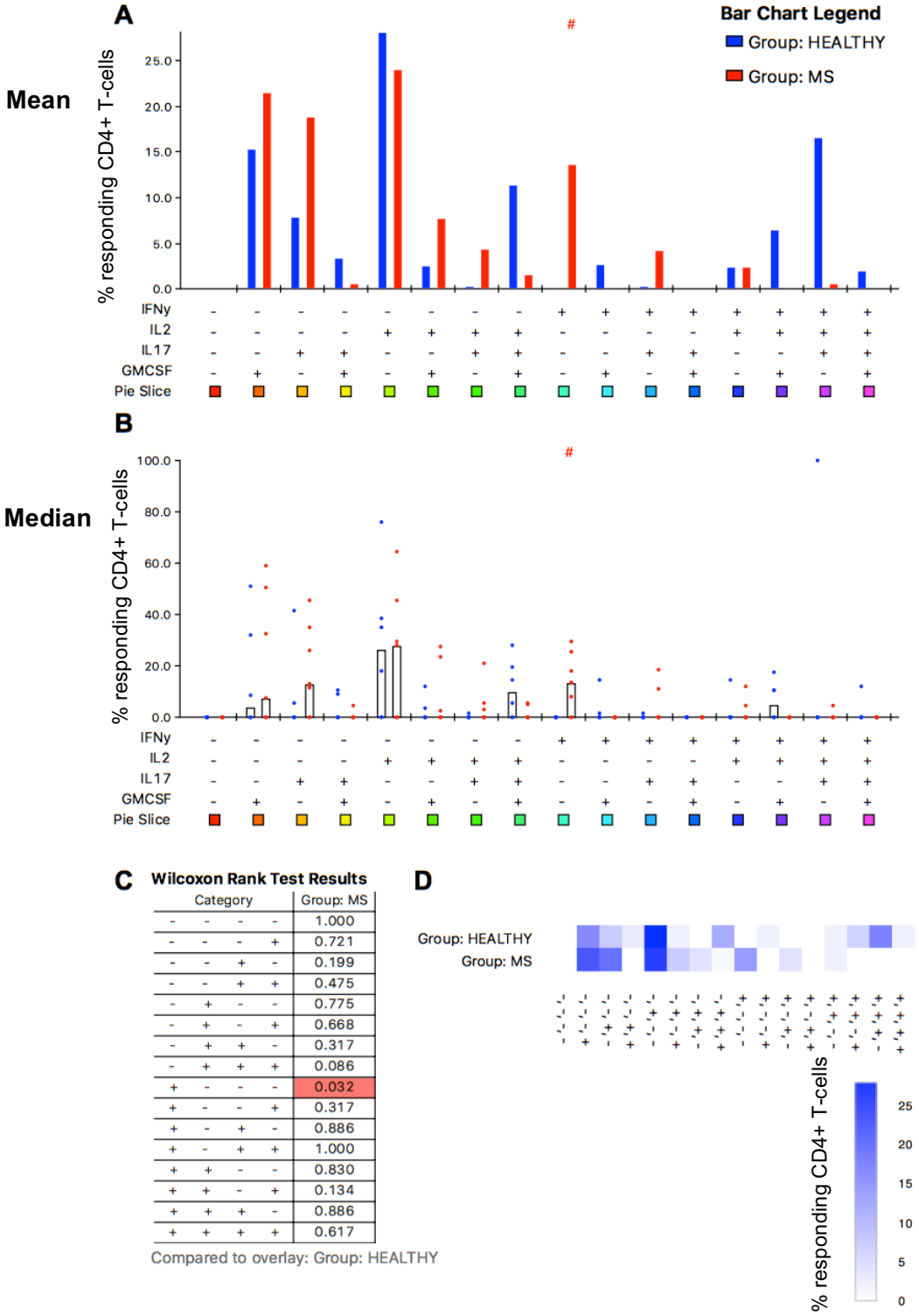

Figure 6.5.12 Cytokine profile of CD4+ T-cells responding to claudin from wild type LCL-specific polyclonal lines. Wild type LCL-stimulated polyclonal T-cell lines were stimulated with MVA claudin-infected B cell blasts and subjected to ICS (HC n=6, MS n=7). Responding CD4+ T-cells were defined as positive for any combination of four cytokines in our panel: IFNγ, IL-2, IL-17 and GM-CSF. **A.** Graphical representation of responding cells in each combination gate with bars representing the mean of data set. Statistics were calculated using the Wilcoxon Signed Rank. **B.** Scatter plot showing percentage of responding cells for each donor in combination gates. Black bars represent median of data set. **C**. Table shows results of Wilcoxon rank test. **D.** Percentage of responding CD4+ T-cells shown in heatmap form. Combination gate data was processed using Funky Cells software and graphically displayed using the program SPICE (ns $p>0.05$, * $p<0.05$).

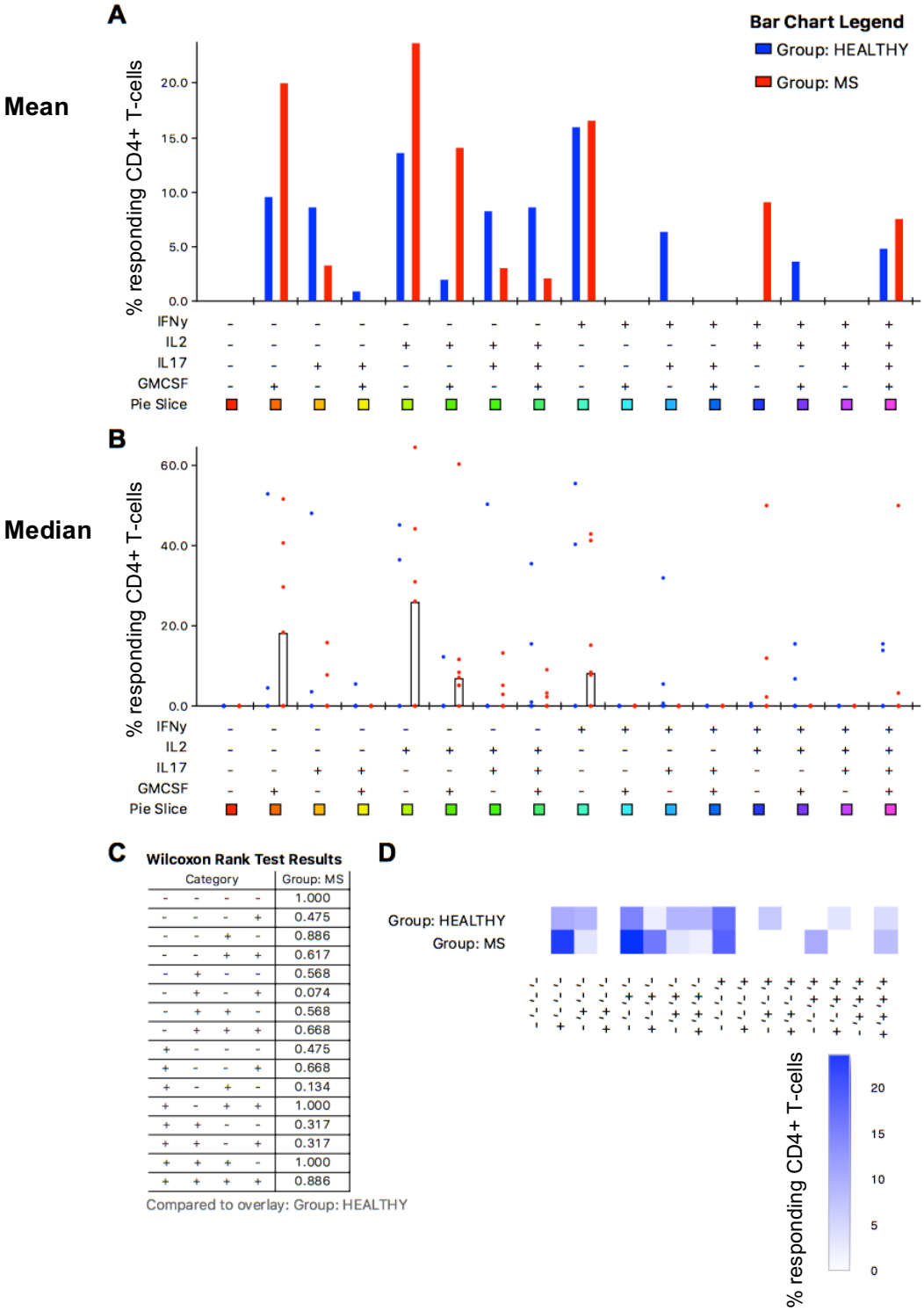

Figure 6.5.13 Cytokine profile of CD4+ T-cells responding to CRYAB from wild type LCL-specific polyclonal lines. Wild type LCL-stimulated polyclonal T-cell lines were stimulated with MVA CRYAB-infected B cell blasts and subjected to ICS (HC n=6, MS n=7). Responding CD4+ T-cells were defined as positive for any combination of four cytokines in our panel: IFNγ, IL-2, IL-17 and GM-CSF. **A.** Graphical representation of responding cells in each combination gate with bars representing the mean of data set. Statistics were calculated using the Wilcoxon Signed Rank. **B.** Scatter plot showing percentage of responding cells for each donor in combination gates. Black bars represent median of data set. **C**. Table shows results of Wilcoxon rank test. **D.** Percentage of responding CD4+ T-cells shown in heatmap form. Combination gate data was processed using Funky Cells software and graphically displayed using the program SPICE (ns $p>0.05$, * $p<0.05$).

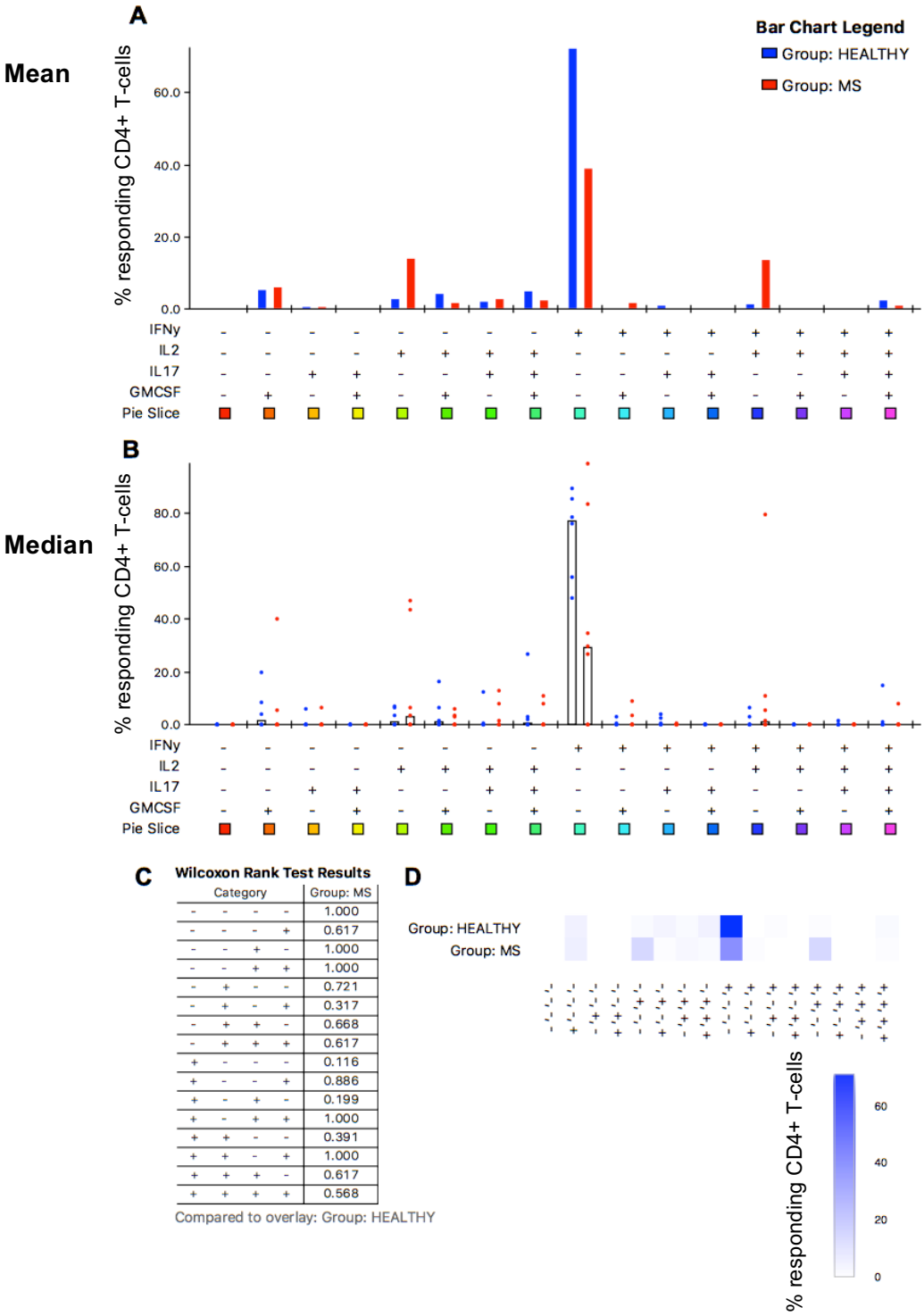

Figure 6.5.14 Cytokine profile of CD4+ T-cells responding to TAL-H from wild type LCL-specific polyclonal lines. Wild type LCL-stimulated polyclonal T-cell lines were stimulated with MVA TAL-H-infected B cell blasts and subjected to ICS (HC n=6, MS n=7). Responding CD4+ T-cells were defined as positive for any combination of four cytokines in our panel: IFNγ, IL-2, IL-17 and GM-CSF. **A.** Graphical representation of responding cells in each combination gate with bars representing the mean of data set. Statistics were calculated using the Wilcoxon Signed Rank. **B.** Scatter plot showing percentage of responding cells for each donor in combination gates. Black bars represent median of data set. **C**. Table shows results of Wilcoxon rank test. **D.** Percentage of responding CD4+ T-cells shown in heatmap form. Combination gate data was processed using Funky Cells software and graphically displayed using the program SPICE (ns $p>0.05$, * $p<0.05$).

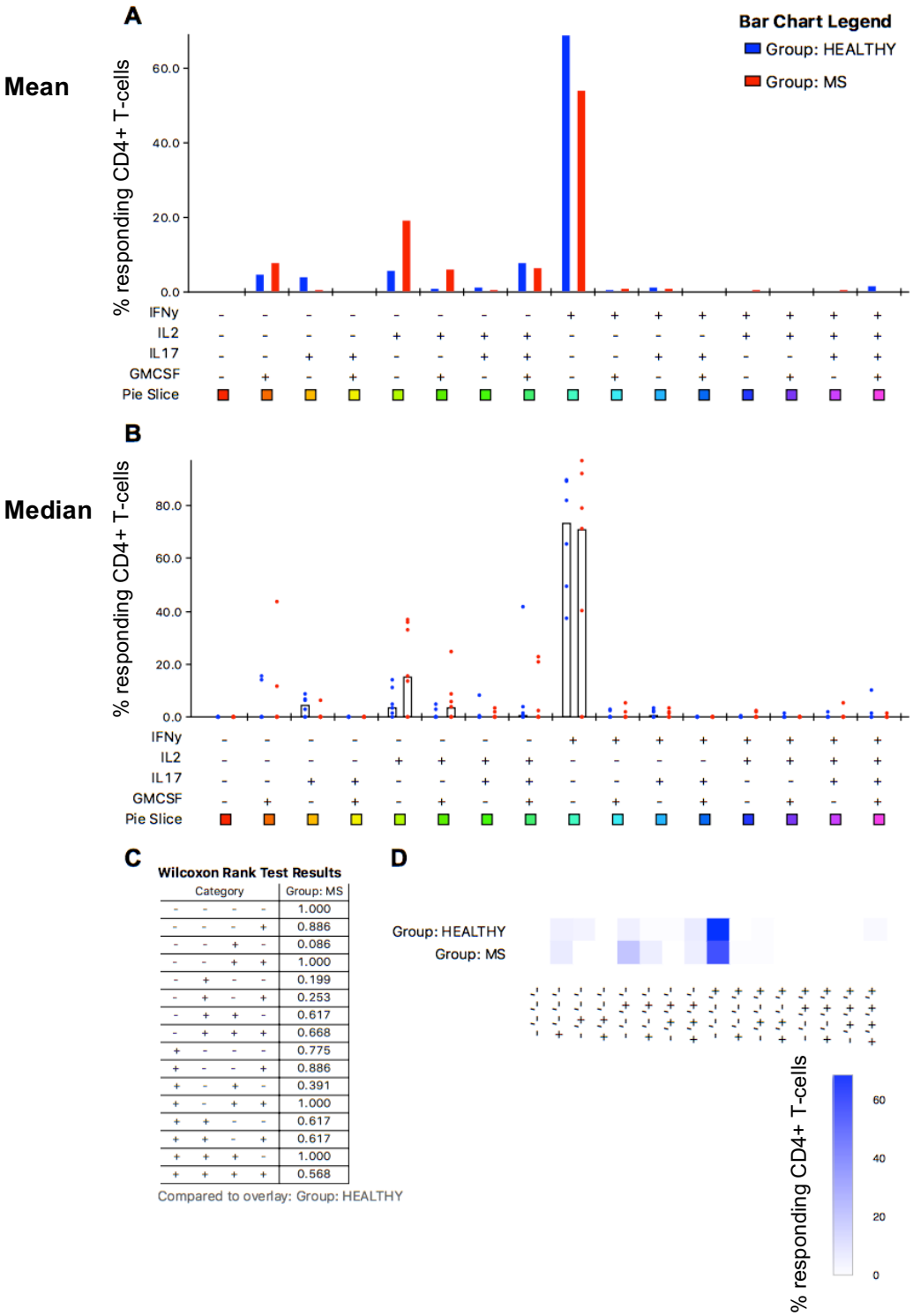

Figure 6.5.15 Cytokine profile of CD4+ T-cells responding to MOBP from wild type LCL-specific polyclonal lines. Wild type LCL-stimulated polyclonal T-cell lines were stimulated with MVA MOBP-infected B cell blasts and subjected to ICS (HC n=6, MS n=7). Responding CD4+ T-cells were defined as positive for any combination of four cytokines in our panel: IFNγ, IL-2, IL-17 and GM-CSF. **A.** Graphical representation of responding cells in each combination gate with bars representing the mean of data set. Statistics were calculated using the Wilcoxon Signed Rank. **B.** Scatter plot showing percentage of responding cells for each donor in combination gates. Black bars represent median of data set. **C**. Table shows results of Wilcoxon rank test. **D.** Percentage of responding CD4+ T-cells shown in heatmap form. Combination gate data was processed using Funky Cells software and graphically displayed using the program SPICE (ns $p>0.05$, * $p<0.05$).

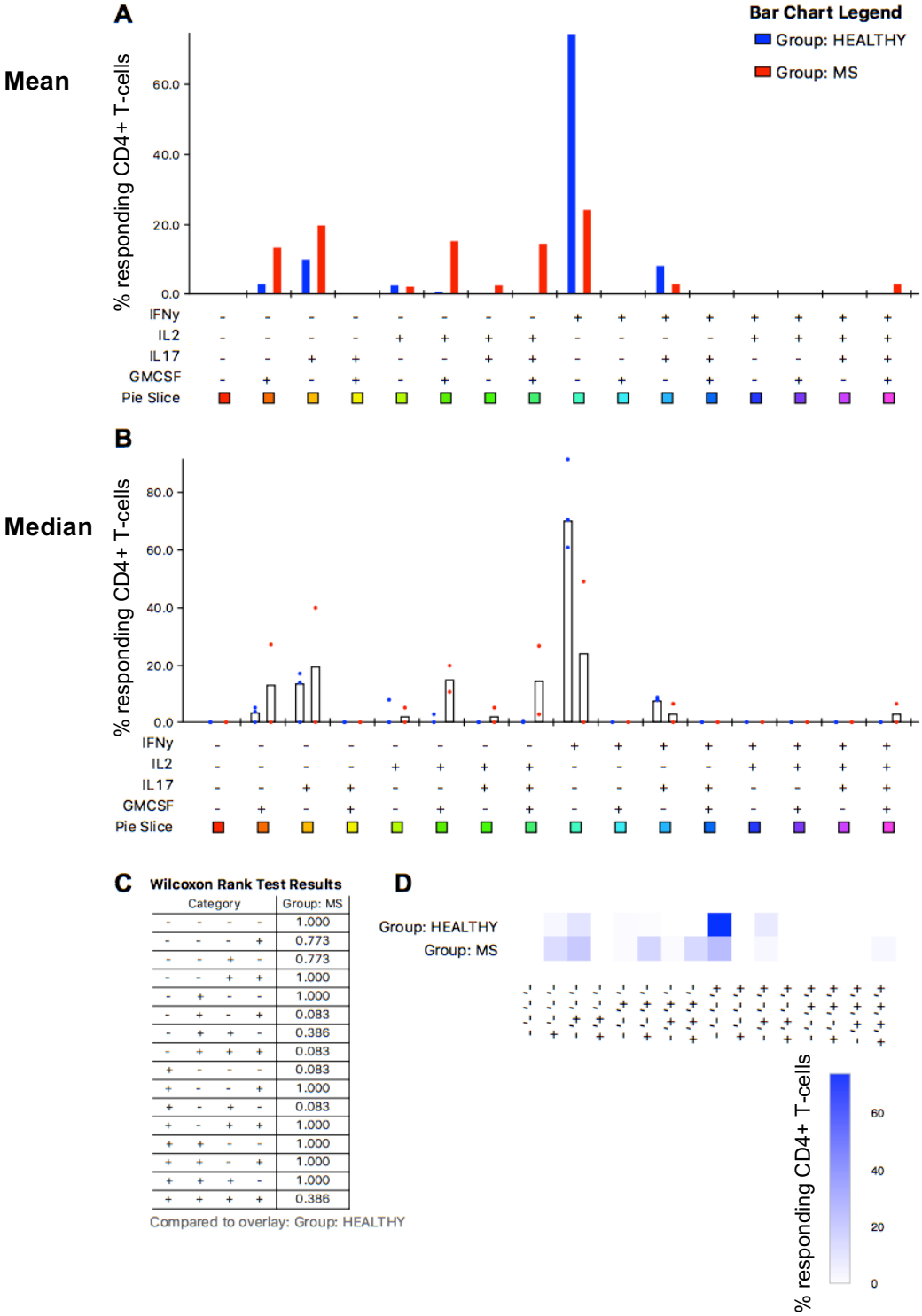

Figure 6.5.16 Cytokine profile of CD4+ T-cells responding to MAG from wild type LCL-specific polyclonal lines. Wild type LCL-stimulated polyclonal T-cell lines were stimulated with MVA MAG-infected B cell blasts and subjected to ICS (HC n=3, MS n=2). Responding CD4+ T-cells were defined as positive for any combination of four cytokines in our panel: IFNγ, IL-2, IL-17 and GM-CSF. **A.** Graphical representation of responding cells in each combination gate with bars representing the mean of data set. Statistics were calculated using the Wilcoxon Signed Rank. **B.** Scatter plot showing percentage of responding cells for each donor in combination gates. Black bars represent median of data set. **C**. Table shows results of Wilcoxon rank test. **D.** Percentage of responding CD4+ T-cells shown in heatmap form. Combination gate data was processed using Funky Cells software and graphically displayed using the program SPICE (ns $p>0.05$, * $p<0.05$).

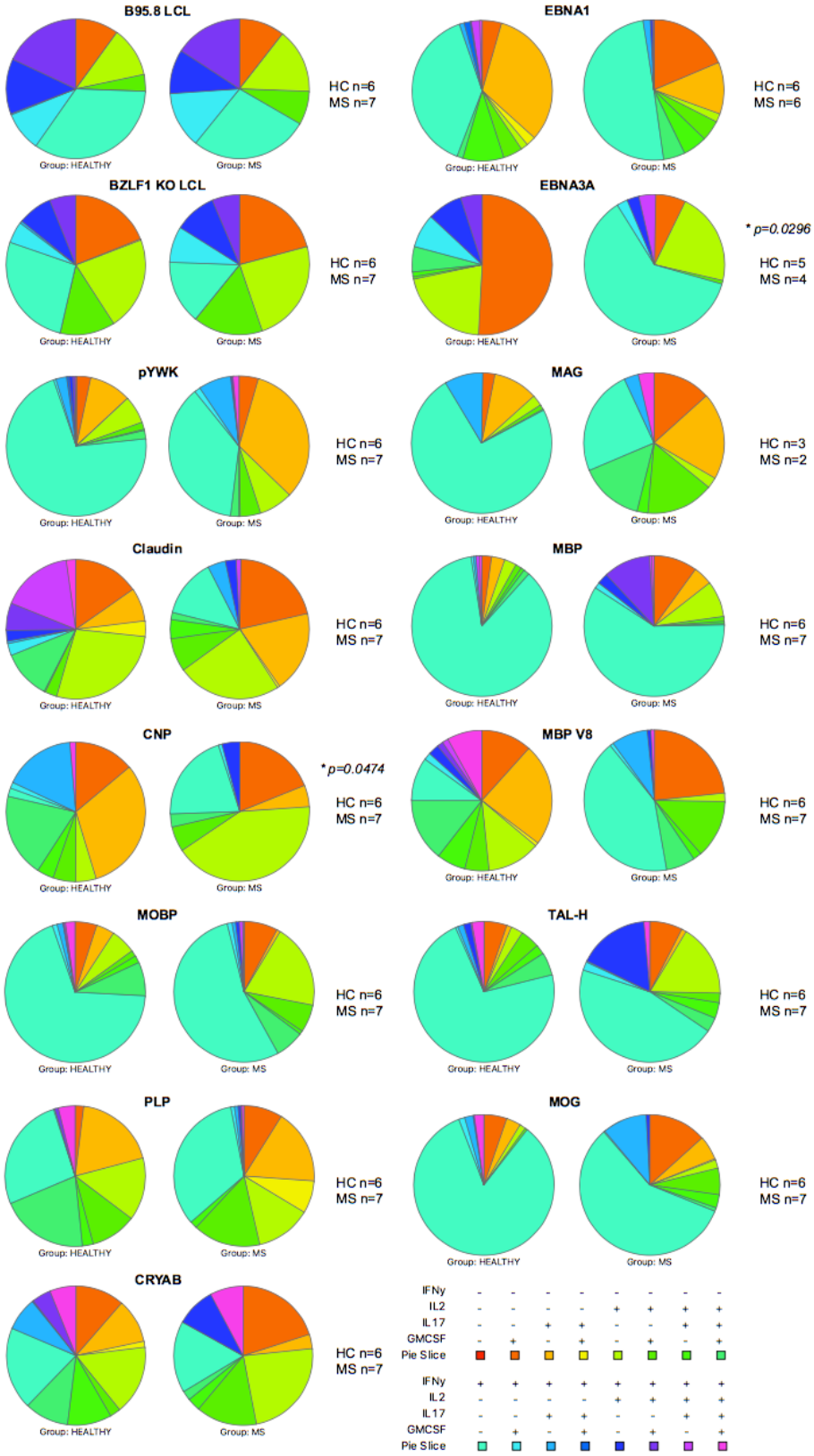

Figure 6.5.17 Different cytokine profiles of CNS-stimulated CD4+ T cells from wild type LCL-specific polyclonal T cell lines. Wild type LCL-specific polyclonal T-cell lines were stimulated with autologous B-cell blasts infected with MVA viruses containing the CNS and EBV proteins individually. Responding CD4+ T-cells were defined as positive for any combination of cytokines in our panel: IFNγ, IL-2, IL-17 and GM-CSF. Pie charts show median values of all donors in each group. Groups were compared using the permutation test (ns $p>0.05$, * $p<0.05$).

6.5.3 Cytokine profile of cross-reactive CD8+ T-cells

CD8+ T-cell responses to EBV and CNS antigens in wild type LCL-stimulated polyclonal T-cell lines were also investigated alongside those of CD4+ T-cells to determine if any there was any difference in cytokine production between groups. As for CD4+ T-cell analysis, Funky Cells and SPICE software was used to remove background and perform statistical analysis of CD8+ T-cells respectively, and results are shown in Figures 6.5.18-6.5.32.

Wild type LCL-stimulated polyclonal T-cell lines were first analysed for their cytokine production in response to the original stimulus – wild type LCL – and BZLF1 KO LCL. Both cell lines induced responses that predominantly produced IFNγ only, and no differences were seen in the CD8+ T-cell cytokine production in response to wild type or BZLF1 KO LCL between donor groups (Figures 6.5.18 and 6.5.19). No differences in cytokine production from CD8+ T-cells to the empty vector control were observed between groups (Figure 6.5.22).

CD8+ T-cell responses to EBNA1 from wild type LCL-stimulated polyclonal lines showed similar cytokine production between HC and MS donors with a slightly higher proportion of MS donor cells producing IL-2 only, however this did not reach significance using the Wilcoxon Signed Rank Test (HC:MS -+-- *p=0.109*) (Figure 6.5.20).

EBNA3A, as previously mentioned, was introduced to the screening panel after interesting preliminary data from our project suggested that EBNA3A-specific antibody responses were more frequent in MS patients than healthy controls (Figure 4.2.3). Analysis of CD4+ T-cell responses from wild type LCL-stimulated polyclonal T-cell lines showed that cytokine production was very different between HC and MS patients (Figure 6.5.5), and investigation of CD8+ responses to the protein were also different between groups. EBNA3A induced a heterogeneous CD8+ T-cell response in MS patients characterised by IFNγ production

alongside IL-2 and GM-CSF, a contrast to HC who showed a broader and marginally less polyfunctional CD8+ T-cell response (Figure 6.5.21).

CD8+ T-cell responses to CNP in LCL-stimulated polyclonal T-cell lines showed variation between MS patients and HC, with MS patient responses being dominated by cells which singularly produced IFNγ, IL-2 or GM-CSF (Figure 6.5.23). HC generated a response to CNP which was characterised by IL-17 production with a significantly higher proportion of cells co-expressing IL-2 and IL-17 making up the responding repertoire in HC compared to MS subjects (HC:MS -++- *p=0.045*) (Figure 6.5.23). However as previously mentioned CNP responses were very small and therefore fewer events may have skewed cytokine production in each group.

MOG induces CD8+ T-cell responses in healthy and MS donors with comparatively little variation in cytokine production, with the majority of cells from both groups producing IFNγ (Figure 6.5.24). A small proportion of CD8+ T-cells from MS donors also express IL-17 in response to MOG antigen but this did not reach significance (Figure 6.5.24).

Cytokine production in PLP-specific CD8+ T-cells showed little variation between groups, with most cells singularly expressing IFNγ after stimulation (Figure 6.5.25). Responses to MBP were also similar between groups with CD8+ T-cells mostly producing IFNγ in response to the antigen (Figure 6.5.26).

The isoform MBP-V8 showed a different cytokine profile in responding CD8+ T-cells than MBP, with a broader range of cytokine combinations produced. HC showed a higher proportion of cells that produced IL-17 only in response to MBP-V8 but did not quite reach significance (HC:MS --+- *p=0.074*) (Figure 6.5.27). HC also had higher proportions of MBP-V8-specific CD8+ T-cells co-expressing IFNγ and IL-17 (HC:MS +-+- *p=0.012*) (Figure 6.5.27).

CD8+ T-cell responses to claudin from LCL-stimulated polyclonal T-cell lines were heterogeneous between donor groups, MS patients showing a higher proportion of responding

cells producing IFNγ only, and healthy donors showing higher proportions of cells co-producing IFNγ and IL-2 in response to the antigen (Figure 7.3.28). Despite these differences the results did not reach statistical significance and more donors would need to be screened to determine if the effect is true.

CD8+ T-cell responses to CRYAB protein did not overall show significant differences in cytokine production after stimulation with this target, however a broad range of phenotypes is displayed by responding cells, with MS patients having higher proportions overall of cells singularly producing IL-2 and GM-CSF (Figure 7.3.29).

TAL-H, as previously described, was one of the proteins which induced the highest overall response in LCL-stimulated polyclonal T-cell lines, and further analysis of cytokine production shows that CD8+ T-cell responses to the antigen from HC mainly produce IFNγ. However, for MS patients TAL-H specific cells fit into two main groups of those producing IFNγ only or IL-2 only (Figure 7.3.30), but these differences in cytokine secretion did not reach significance.

MOBP was also one of the antigens with the highest overall response in polyclonal T-cell lines, with up to ~5% of certain polyclonal T-cell lines responding to the antigen. As with TAL-H, the majority of responding CD8+ T-cells from both patient groups produced IFNγ. However, a small subset of IFNγ+IL-17+ cells were significantly higher in HC than MS patients who had no responding cells that fit into this subset (HC:MS +-+- $p=0.022$) (Figure 7.3.31).

Due to previously mentioned problems with the MVA MAG virus stock, only a few donors were screened against the protein allowing very few conclusions to be drawn from the data. Over 80% MAG-specific CD8+ T-cells from HC produced IFNγ only. MS patient responses were much more spread, with CD8+ T-cells mostly producing a mix of IFNγ and IL-2 following MAG stimulation (Figure 7.3.32).

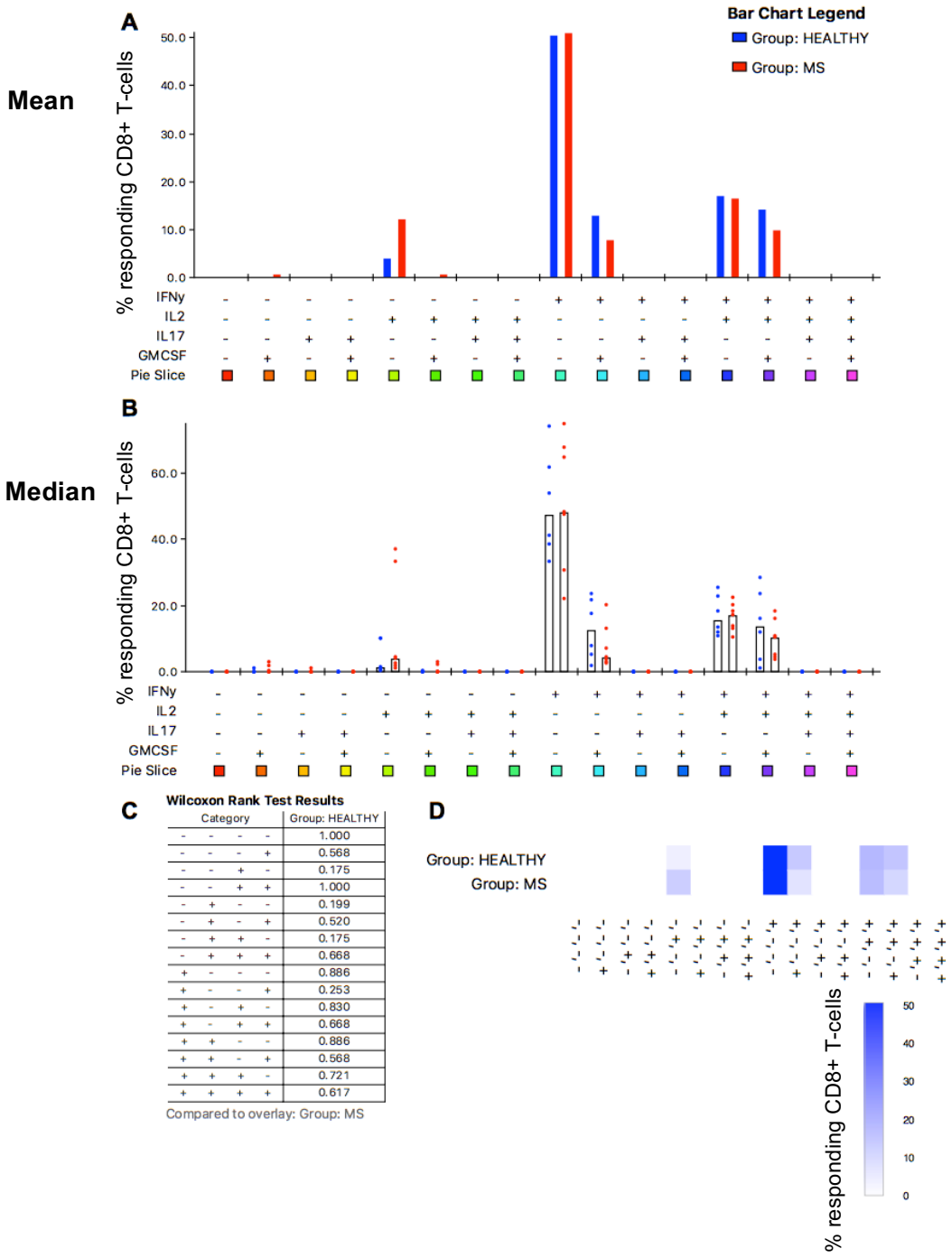

Figure 6.5.18 Cytokine profile of CD8+ T-cells responding to wild type LCL from wild type LCL-specific polyclonal lines. Wild type LCL-stimulated polyclonal T-cell lines were stimulated with autologous wild type LCL and subjected to ICS (HC n=6, MS n=7). Responding CD8+ T-cells were defined as positive for any combination of four cytokines in our panel: IFNγ, IL-2, IL-17 and GM-CSF. **A.** Graphical representation of responding cells in each combination gate with bars representing the mean of data set. Statistics were calculated using the Wilcoxon Signed Rank. **B.** Scatter plot showing percentage of responding cells for each donor in combination gates. Black bars represent median of data set. **C**. Table shows results of Wilcoxon rank test. **D.** Percentage of responding CD8+ T-cells shown in heatmap form. Combination gate data was processed using Funky Cells software and graphically displayed using the program SPICE (ns $p>0.05$, * $p<0.05$).

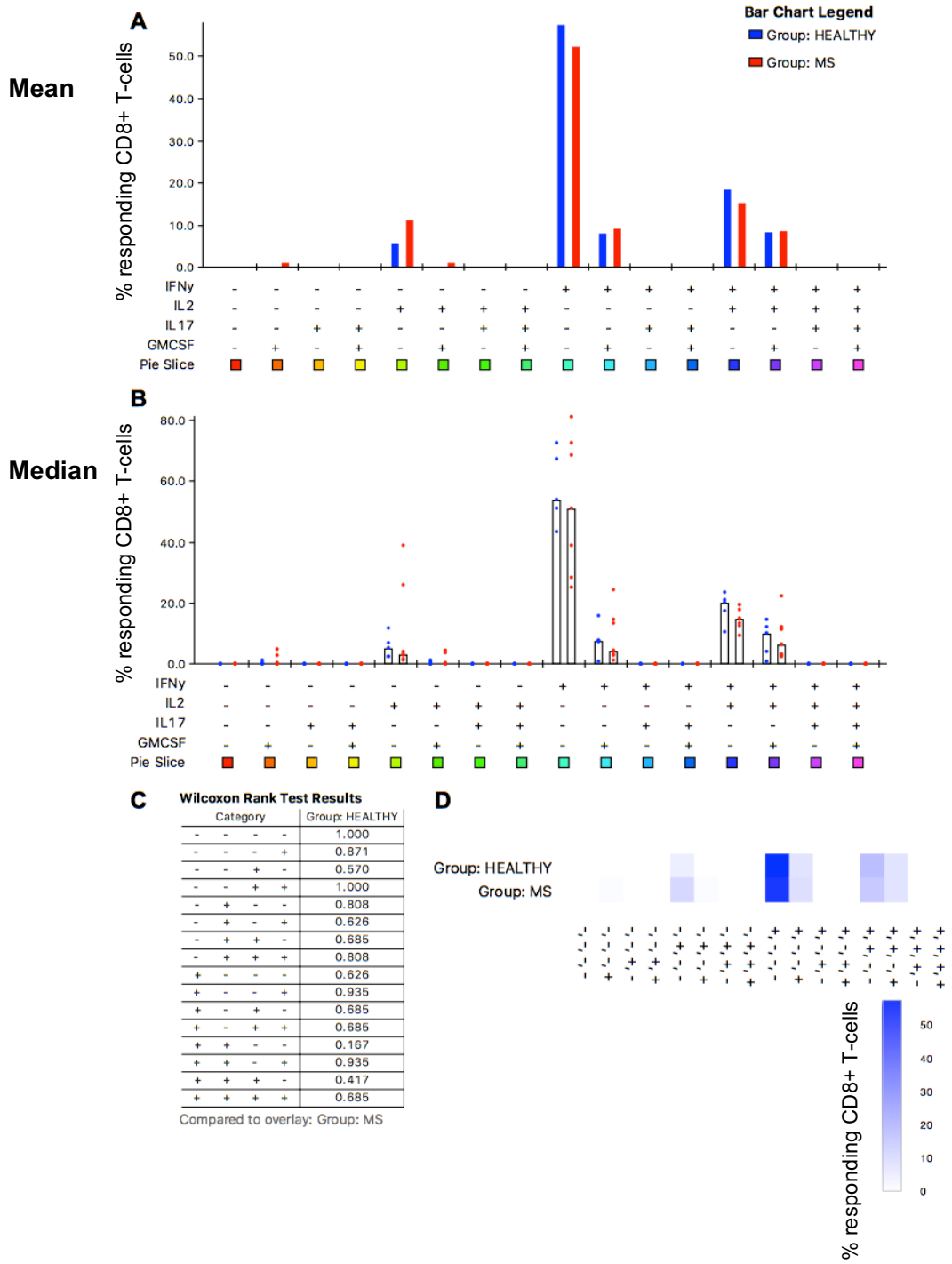

Figure 6.5.19 Cytokine profile of CD8+ T-cells responding to BZLF1 KO LCL from wild type LCL-specific polyclonal lines. Wild type LCL-stimulated polyclonal T-cell lines were stimulated with autologous BZLF1 KO LCL and subjected to ICS (HC n=6, MS n=7). Responding CD8+ T-cells were defined as positive for any combination of four cytokines in our panel: IFNγ, IL-2, IL-17 and GM-CSF. **A.** Graphical representation of responding cells in each combination gate with bars representing the mean of data set. Statistics were calculated using the Wilcoxon Signed Rank. **B.** Scatter plot showing percentage of responding cells for each donor in combination gates. Black bars represent median of data set. **C**. Table shows results of Wilcoxon rank test. **D.** Percentage of responding CD8+ T-cells shown in heatmap form. Combination gate data was processed using Funky Cells software and graphically displayed using the program SPICE (ns $p>0.05$, * $p<0.05$).

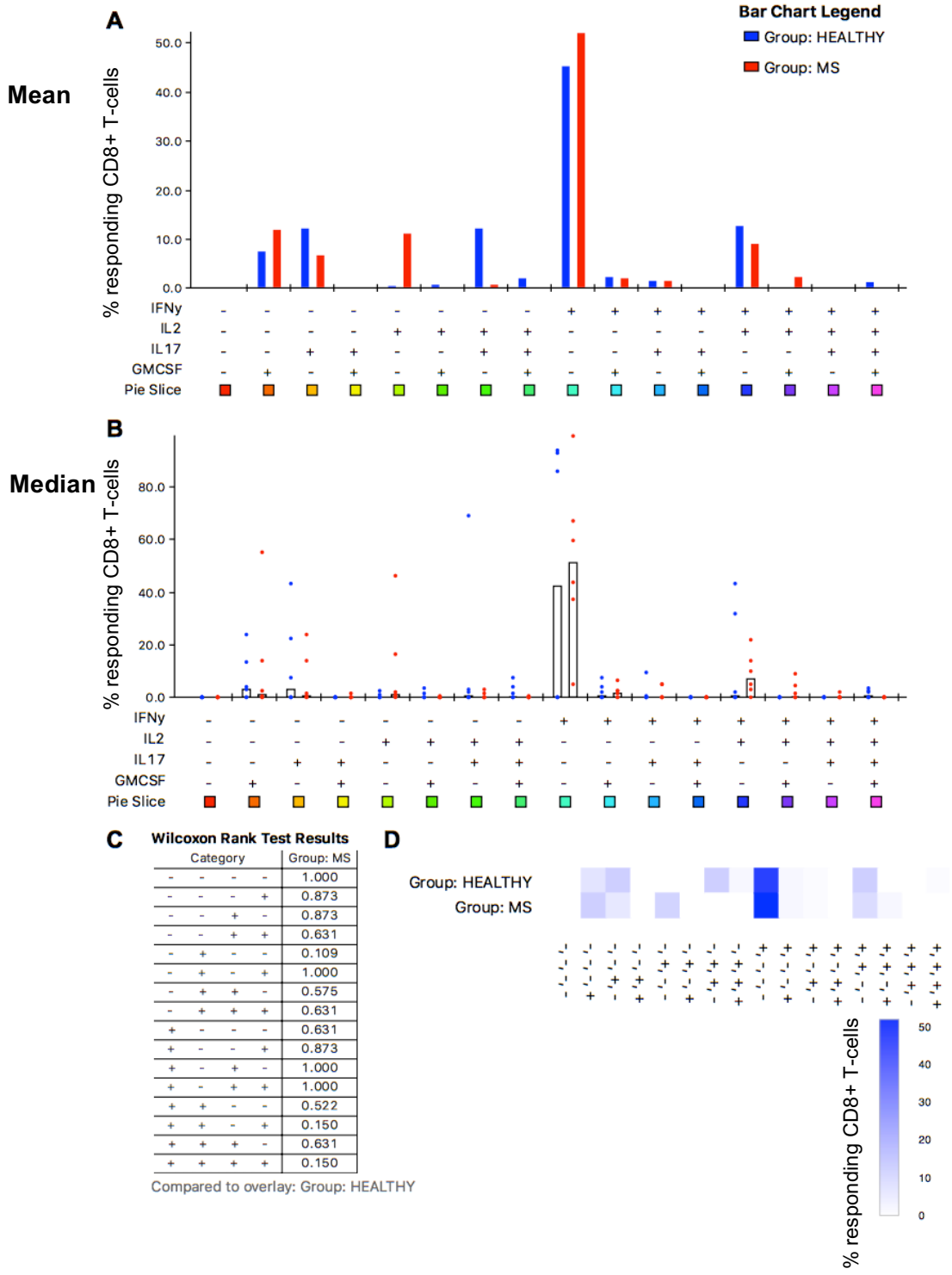

Figure 6.5.20 Cytokine profile of CD8+ T-cells responding to EBNA1 from wild type LCL-specific polyclonal lines. Wild type LCL-stimulated polyclonal T-cell lines were stimulated with MVA EBNA1-infected B cell blasts and subjected to ICS (HC n=6, MS n=7). Responding CD8+ T-cells were defined as positive for any combination of four cytokines in our panel: IFNγ, IL-2, IL-17 and GM-CSF. **A.** Graphical representation of responding cells in each combination gate with bars representing the mean of data set. Statistics were calculated using the Wilcoxon Signed Rank. **B.** Scatter plot showing percentage of responding cells for each donor in combination gates. Black bars represent median of data set. **C**. Table shows results of Wilcoxon rank test. **D.** Percentage of responding CD8+ T-cells shown in heatmap form. Combination gate data was processed using Funky Cells software and graphically displayed using the program SPICE (ns $p>0.05$, * $p<0.05$).

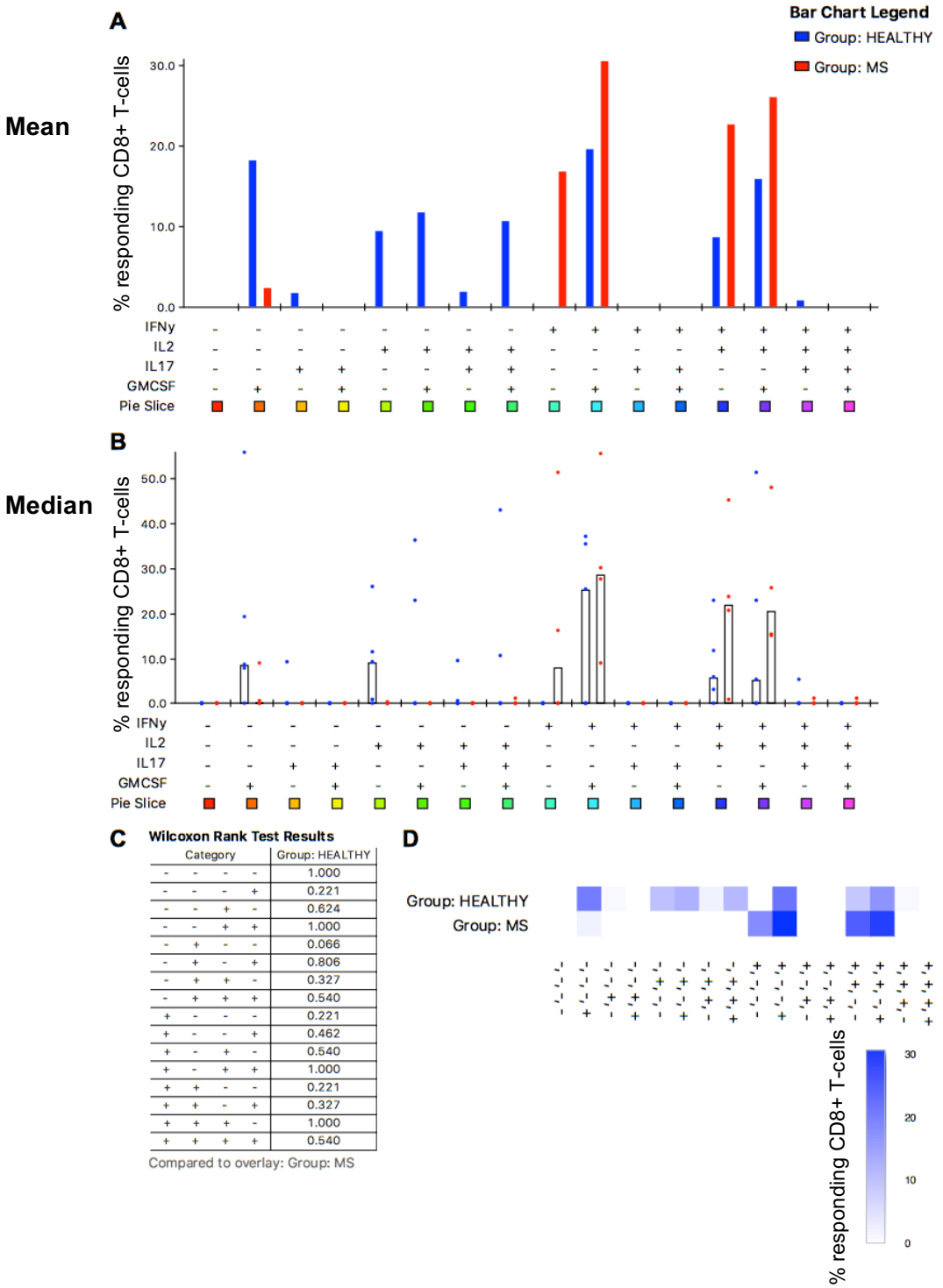

Figure 6.5.21 Cytokine profile of CD8+ T-cells responding to EBNA3A from wild type LCL-specific polyclonal lines. Wild type LCL-stimulated polyclonal T-cell lines were stimulated with MVA EBNA3A-infected B cell blasts and subjected to ICS (HC n=5, MS n=4). Responding CD8+ T-cells were defined as positive for any combination of four cytokines in our panel: IFNγ, IL-2, IL-17 and GM-CSF. **A.** Graphical representation of responding cells in each combination gate with bars representing the mean of data set. Statistics were calculated using the Wilcoxon Signed Rank. **B.** Scatter plot showing percentage of responding cells for each donor in combination gates. Black bars represent median of data set. **C**. Table shows results of Wilcoxon rank test. **D.** Percentage of responding CD8+ T-cells shown in heatmap form. Combination gate data was processed using Funky Cells software and graphically displayed using the program SPICE (ns $p>0.05$, * $p<0.05$).

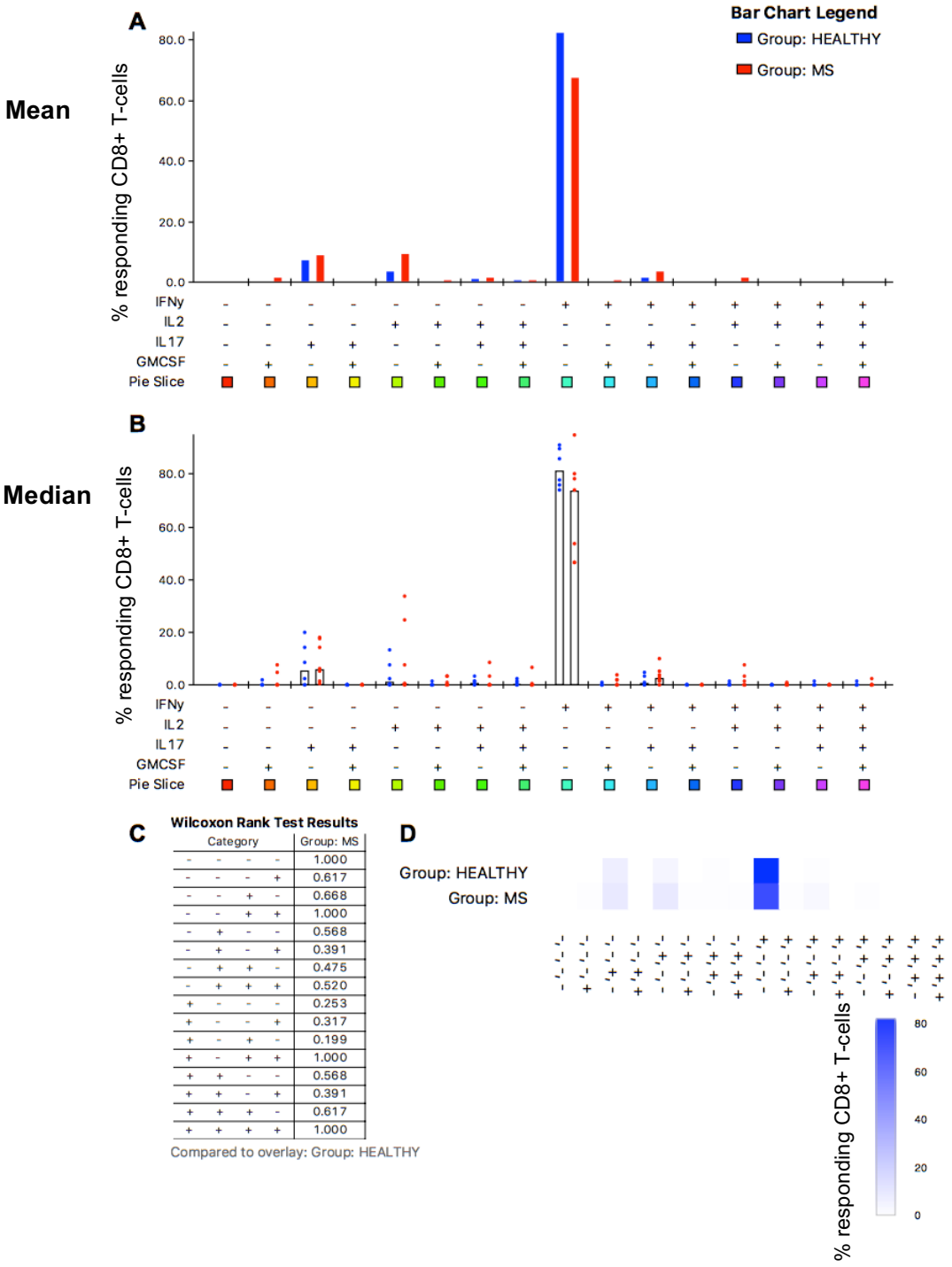

Figure 6.5.22 Cytokine profile of CD8+ T-cells responding to empty vector from wild type LCL-specific polyclonal lines. Wild type LCL-stimulated polyclonal T-cell lines were stimulated with MVA empty vector-infected B cell blasts and subjected to ICS (HC n=6, MS n=7). Responding CD8+ T-cells were defined as positive for any combination of four cytokines in our panel: IFNγ, IL-2, IL-17 and GM-CSF. **A.** Graphical representation of responding cells in each combination gate with bars representing the mean of data set. Statistics were calculated using the Wilcoxon Signed Rank. **B.** Scatter plot showing percentage of responding cells for each donor in combination gates. Black bars represent median of data set. **C**. Table shows results of Wilcoxon rank test. **D.** Percentage of responding CD8+ T-cells shown in heatmap form. Combination gate data was processed using Funky Cells software and graphically displayed using the program SPICE (ns $p>0.05$, * $p<0.05$).

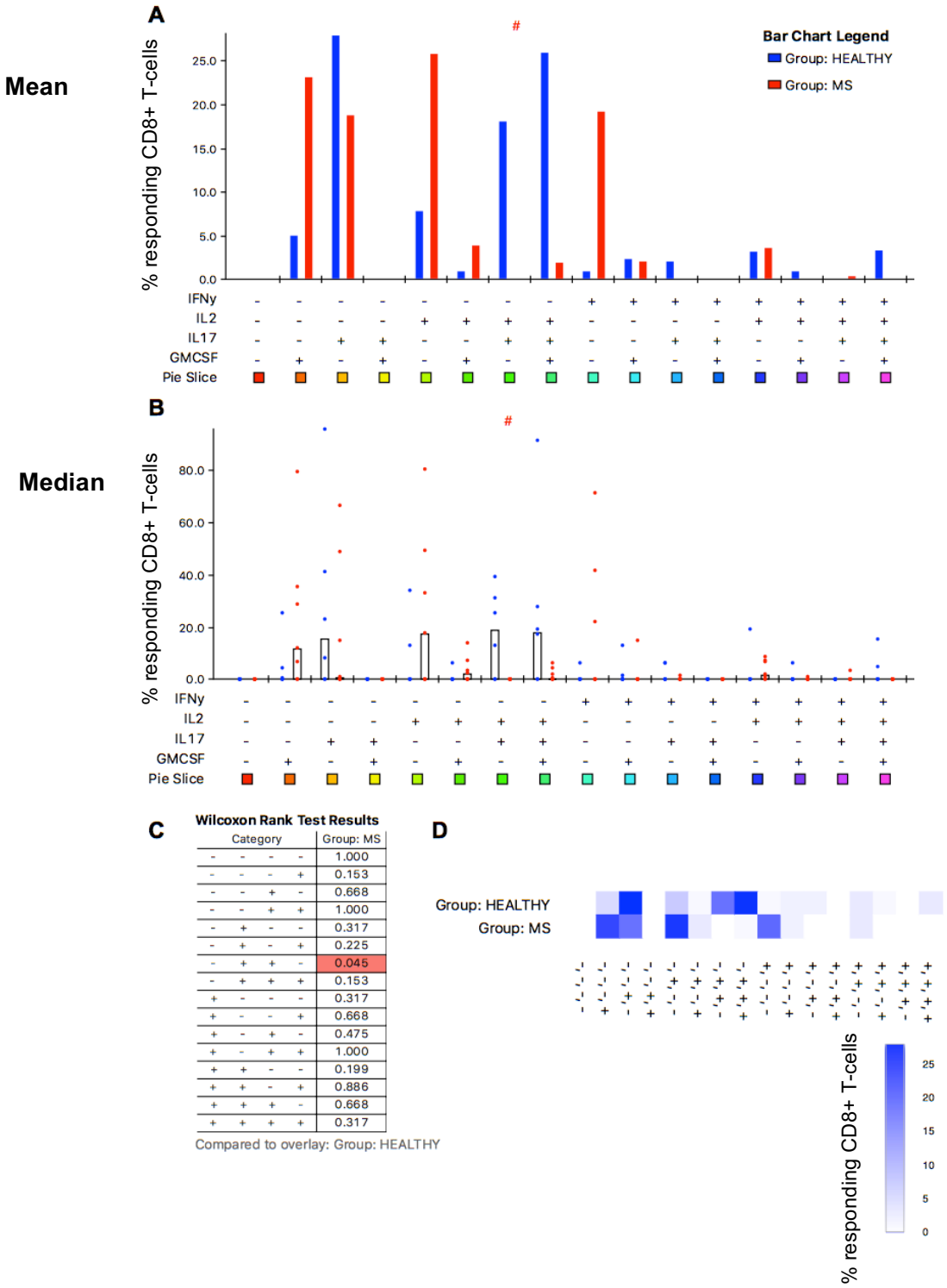

Figure 6.5.23 Cytokine profile of CD8+ T-cells responding to CNP from wild type LCL-specific polyclonal lines. Wild type LCL-stimulated polyclonal T-cell lines were stimulated with MVA CNP-infected B cell blasts and subjected to ICS (HC n=6, MS n=7). Responding CD8+ T-cells were defined as positive for any combination of four cytokines in our panel: IFNγ, IL-2, IL-17 and GM-CSF. **A.** Graphical representation of responding cells in each combination gate with bars representing the mean of data set. Statistics were calculated using the Wilcoxon Signed Rank. **B.** Scatter plot showing percentage of responding cells for each donor in combination gates. Black bars represent median of data set. **C**. Table shows results of Wilcoxon rank test. **D.** Percentage of responding CD8+ T-cells shown in heatmap form. Combination gate data was processed using Funky Cells software and graphically displayed using the program SPICE (ns $p>0.05$, * $p<0.05$).

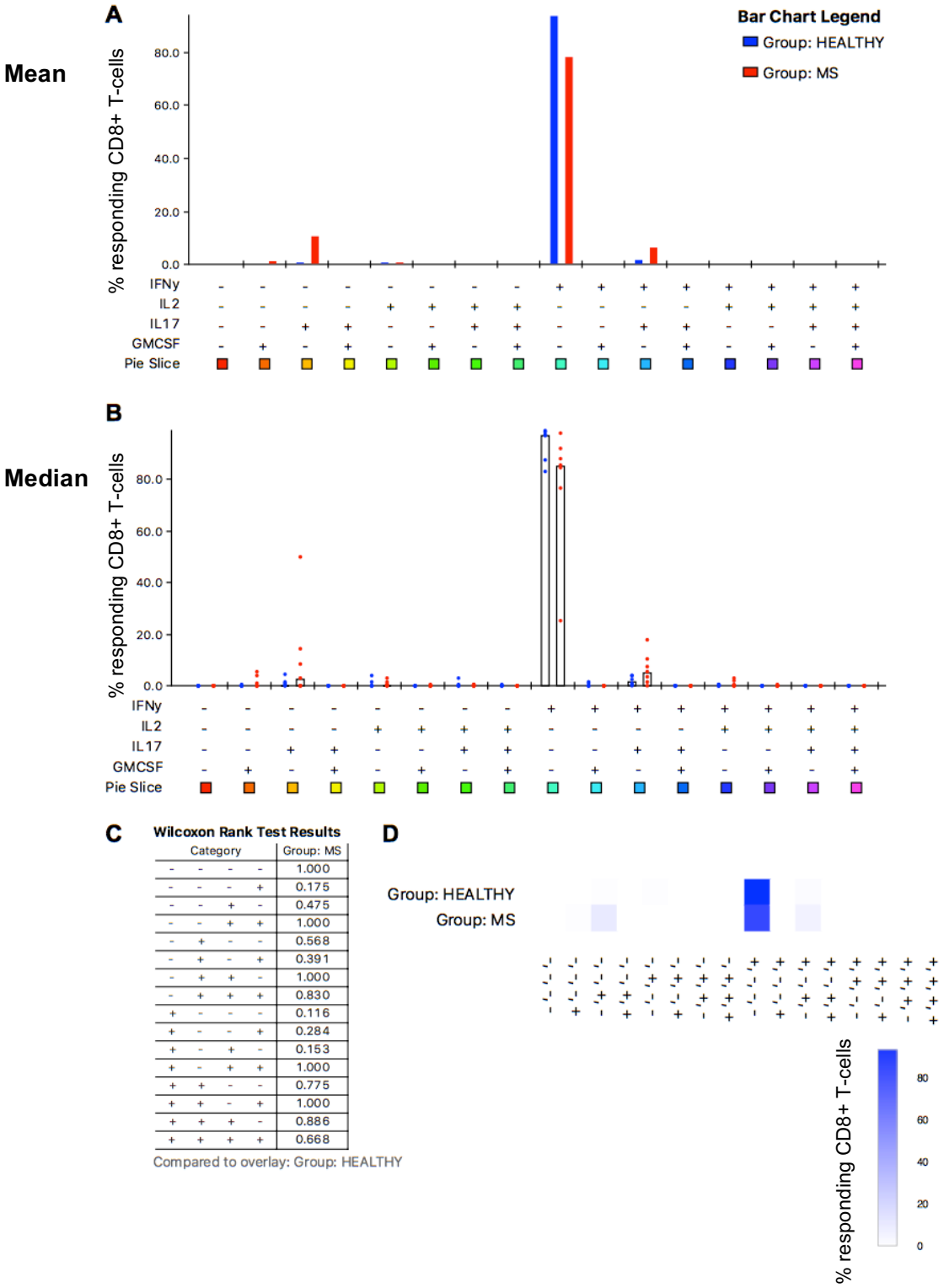

Figure 6.5.24 Cytokine profile of CD8+ T-cells responding to MOG from wild type LCL-specific polyclonal lines. Wild type LCL-stimulated polyclonal T-cell lines were stimulated with MVA MOG-infected B cell blasts and subjected to ICS (HC n=6, MS n=7). Responding CD8+ T-cells were defined as positive for any combination of four cytokines in our panel: IFNγ, IL-2, IL-17 and GM-CSF. **A.** Graphical representation of responding cells in each combination gate with bars representing the mean of data set. Statistics were calculated using the Wilcoxon Signed Rank. **B.** Scatter plot showing percentage of responding cells for each donor in combination gates. Black bars represent median of data set. **C**. Table shows results of Wilcoxon rank test. **D.** Percentage of responding CD8+ T-cells shown in heatmap form. Combination gate data was processed using Funky Cells software and graphically displayed using the program SPICE (ns $p>0.05$, * $p<0.05$).

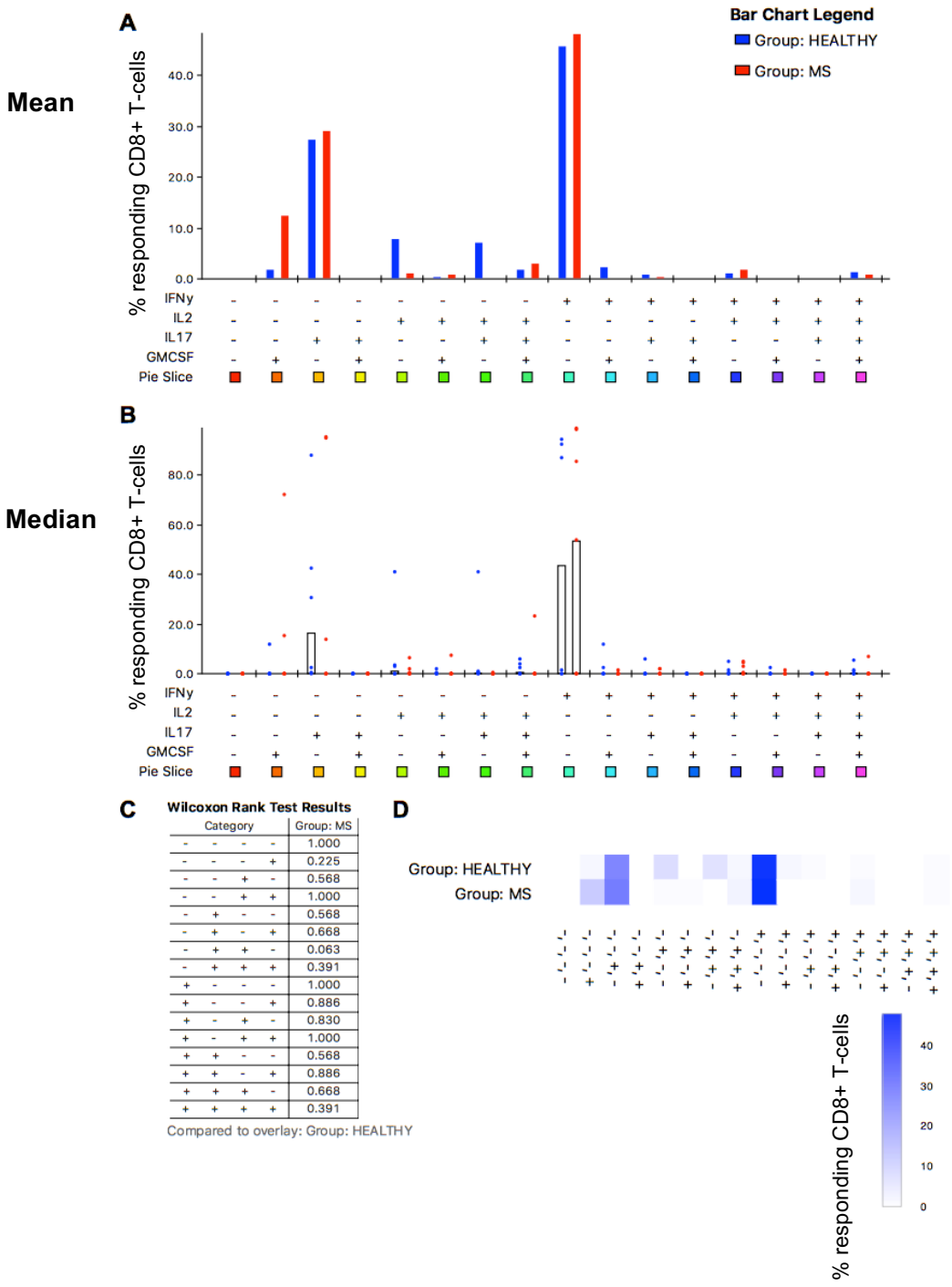

Figure 6.5.25 Cytokine profile of CD8+ T-cells responding to PLP from wild type LCL-specific polyclonal lines. Wild type LCL-stimulated polyclonal T-cell lines were stimulated with MVA PLP-infected B cell blasts and subjected to ICS (HC n=6, MS n=7). Responding CD8+ T-cells were defined as positive for any combination of four cytokines in our panel: IFNγ, IL-2, IL-17 and GM-CSF. **A.** Graphical representation of responding cells in each combination gate with bars representing the mean of data set. Statistics were calculated using the Wilcoxon Signed Rank. **B.** Scatter plot showing percentage of responding cells for each donor in combination gates. Black bars represent median of data set. **C**. Table shows results of Wilcoxon rank test. **D.** Percentage of responding CD8+ T-cells shown in heatmap form. Combination gate data was processed using Funky Cells software and graphically displayed using the program SPICE (ns $p>0.05$, * $p<0.05$).

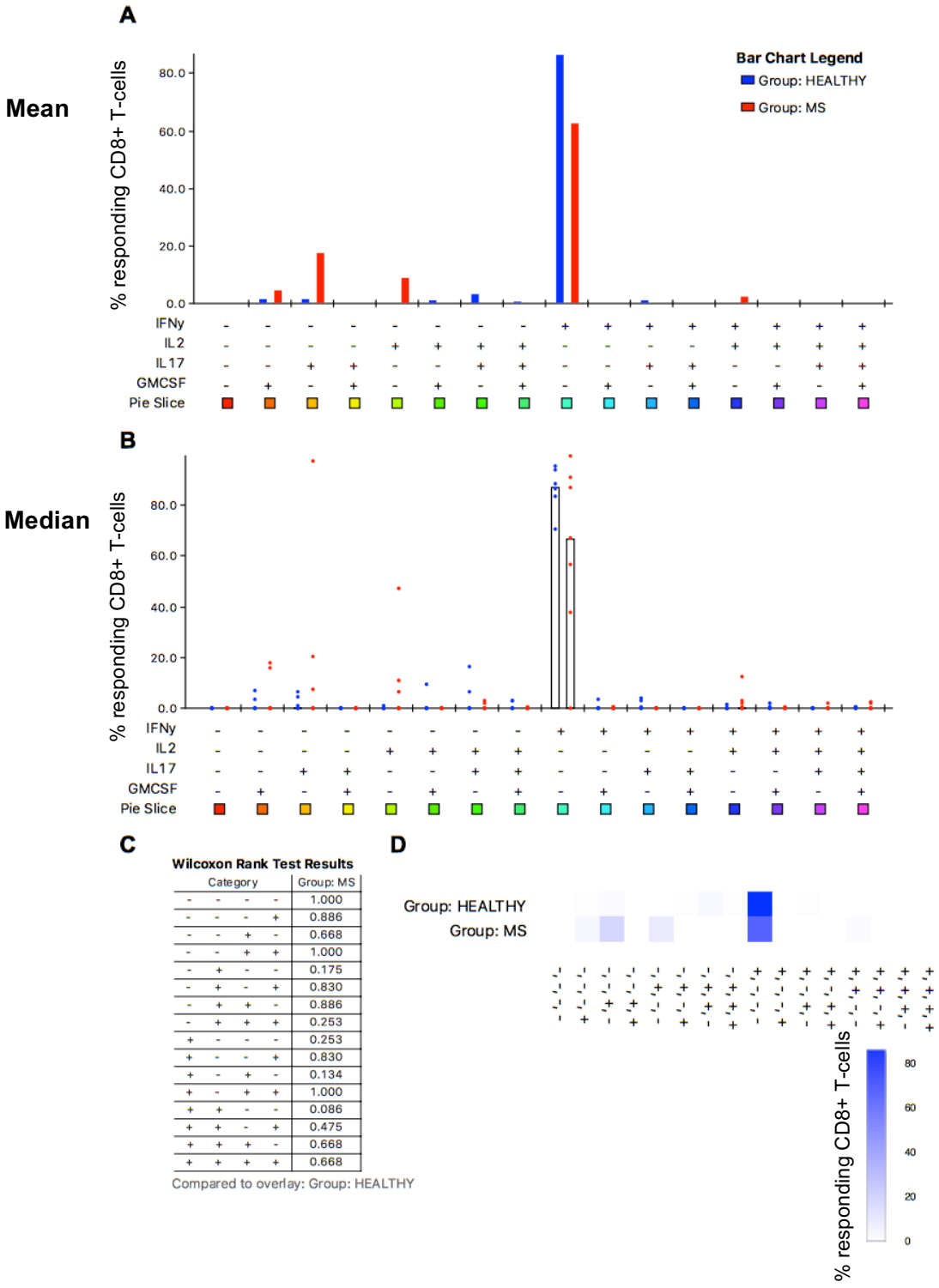

Figure 6.5.26 Cytokine profile of CD8+ T-cells responding to MBP from wild type LCL-specific polyclonal lines. Wild type LCL-stimulated polyclonal T-cell lines were stimulated with MVA MBP-infected B cell blasts and subjected to ICS (HC n=6, MS n=7). Responding CD8+ T-cells were defined as positive for any combination of four cytokines in our panel: IFNγ, IL-2, IL-17 and GM-CSF. **A.** Graphical representation of responding cells in each combination gate with bars representing the mean of data set. Statistics were calculated using the Wilcoxon Signed Rank. **B.** Scatter plot showing percentage of responding cells for each donor in combination gates. Black bars represent median of data set. **C**. Table shows results of Wilcoxon rank test. **D.** Percentage of responding CD8+ T-cells shown in heatmap form. Combination gate data was processed using Funky Cells software and graphically displayed using the program SPICE (ns $p>0.05$, * $p<0.05$).

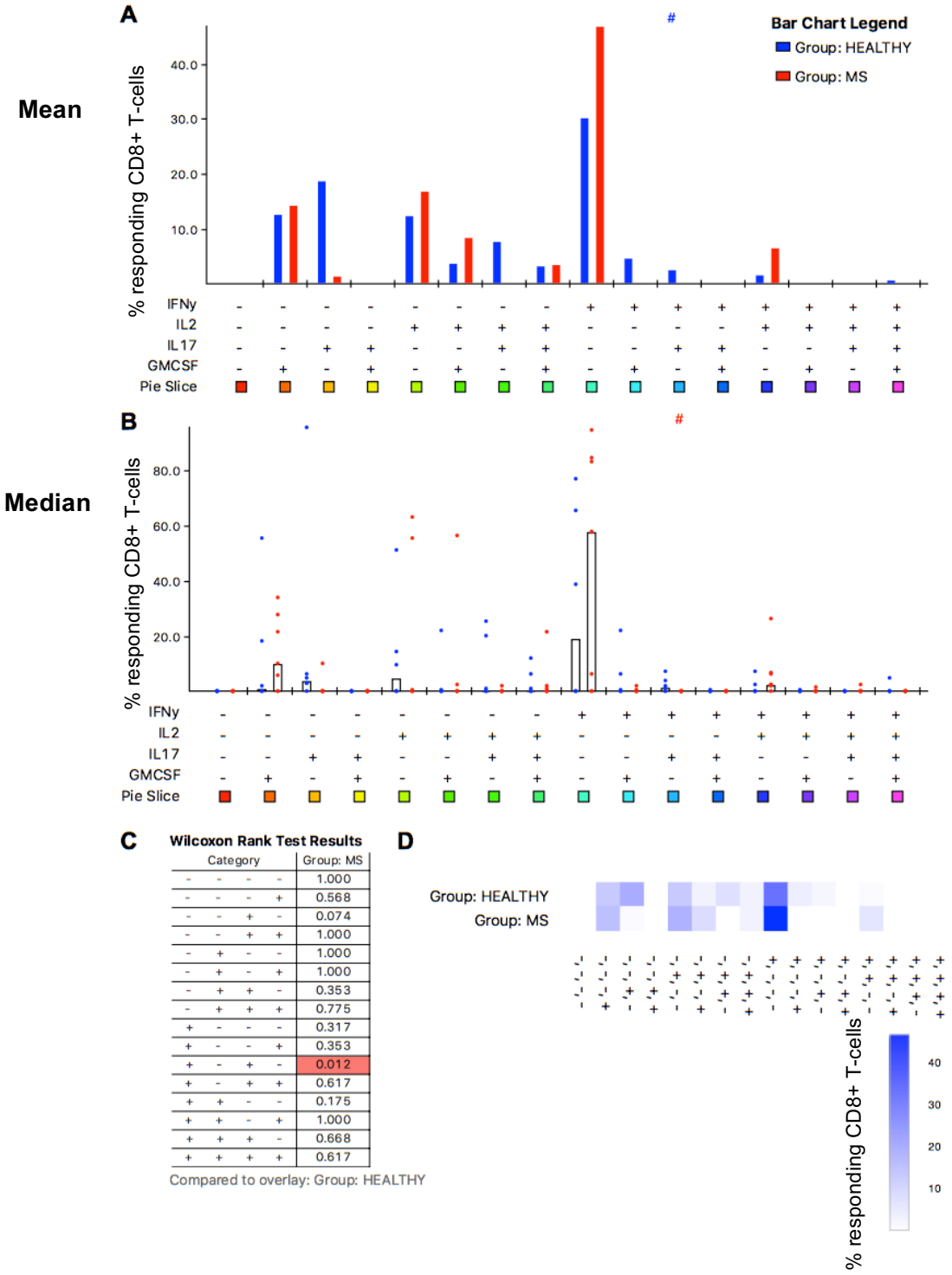

Figure 6.5.27 Cytokine profile of CD8+ T-cells responding to MBP V8 from wild type LCL-specific polyclonal lines. Wild type LCL-stimulated polyclonal T-cell lines were stimulated with MVA MBP V8-infected B cell blasts and subjected to ICS (HC n=6, MS n=7). Responding CD8+ T-cells were defined as positive for any combination of four cytokines in our panel: IFNγ, IL-2, IL-17 and GM-CSF. **A.** Graphical representation of responding cells in each combination gate with bars representing the mean of data set. Statistics were calculated using the Wilcoxon Signed Rank. **B.** Scatter plot showing percentage of responding cells for each donor in combination gates. Black bars represent median of data set. **C**. Table shows results of Wilcoxon rank test. **D.** Percentage of responding CD8+ T-cells shown in heatmap form. Combination gate data was processed using Funky Cells software and graphically displayed using the program SPICE (ns $p>0.05$, * $p<0.05$).

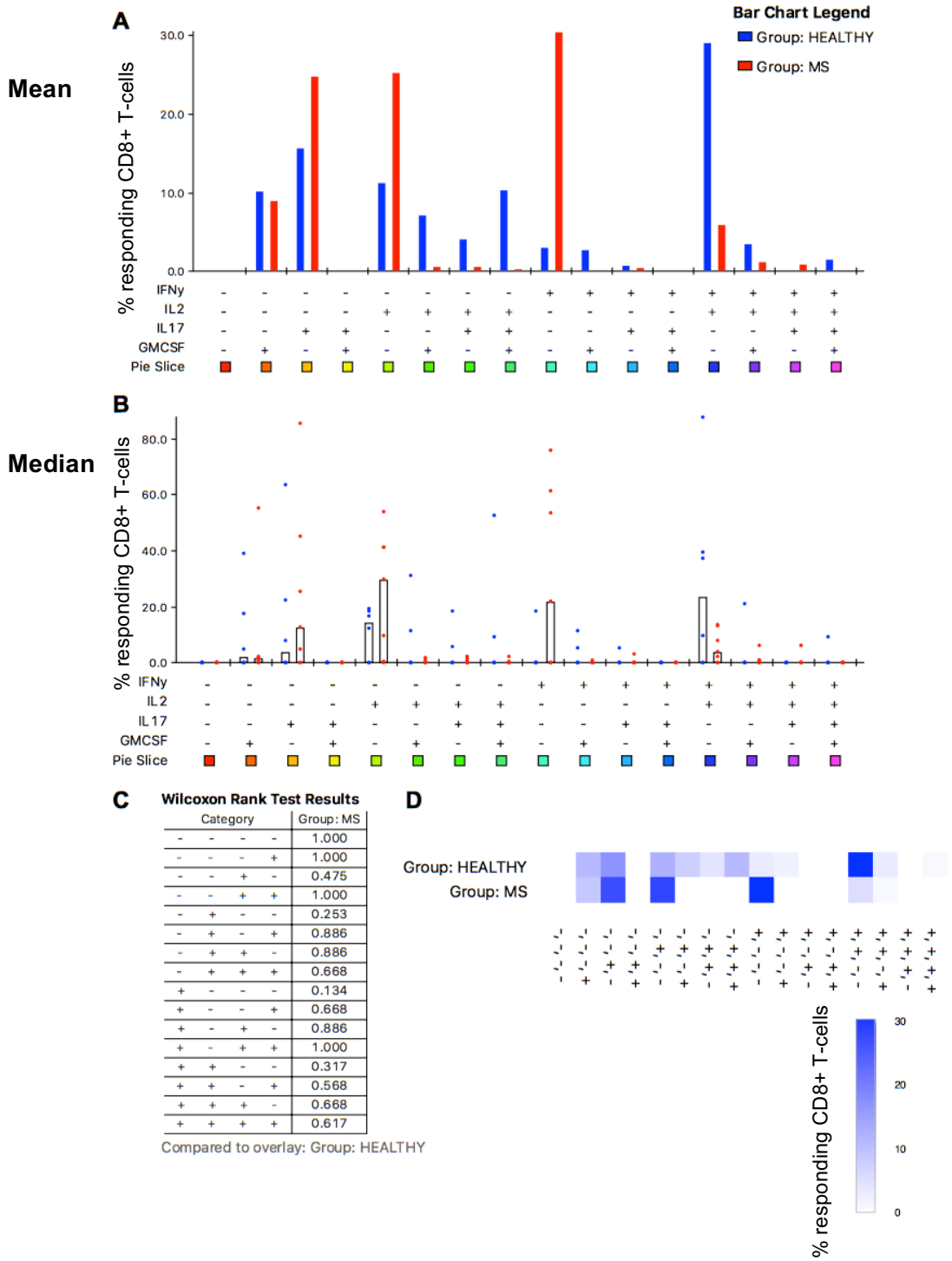

Figure 6.5.28 Cytokine profile of CD8+ T-cells responding to claudin from wild type LCL-specific polyclonal lines. Wild type LCL-stimulated polyclonal T-cell lines were stimulated with MVA claudin-infected B cell blasts and subjected to ICS (HC n=6, MS n=7). Responding CD8+ T-cells were defined as positive for any combination of four cytokines in our panel: IFNγ, IL-2, IL-17 and GM-CSF. **A.** Graphical representation of responding cells in each combination gate with bars representing the mean of data set. Statistics were calculated using the Wilcoxon Signed Rank. **B.** Scatter plot showing percentage of responding cells for each donor in combination gates. Black bars represent median of data set. **C**. Table shows results of Wilcoxon rank test. **D.** Percentage of responding CD8+ T-cells shown in heatmap form. Combination gate data was processed using Funky Cells software and graphically displayed using the program SPICE (ns $p>0.05$, * $p<0.05$).

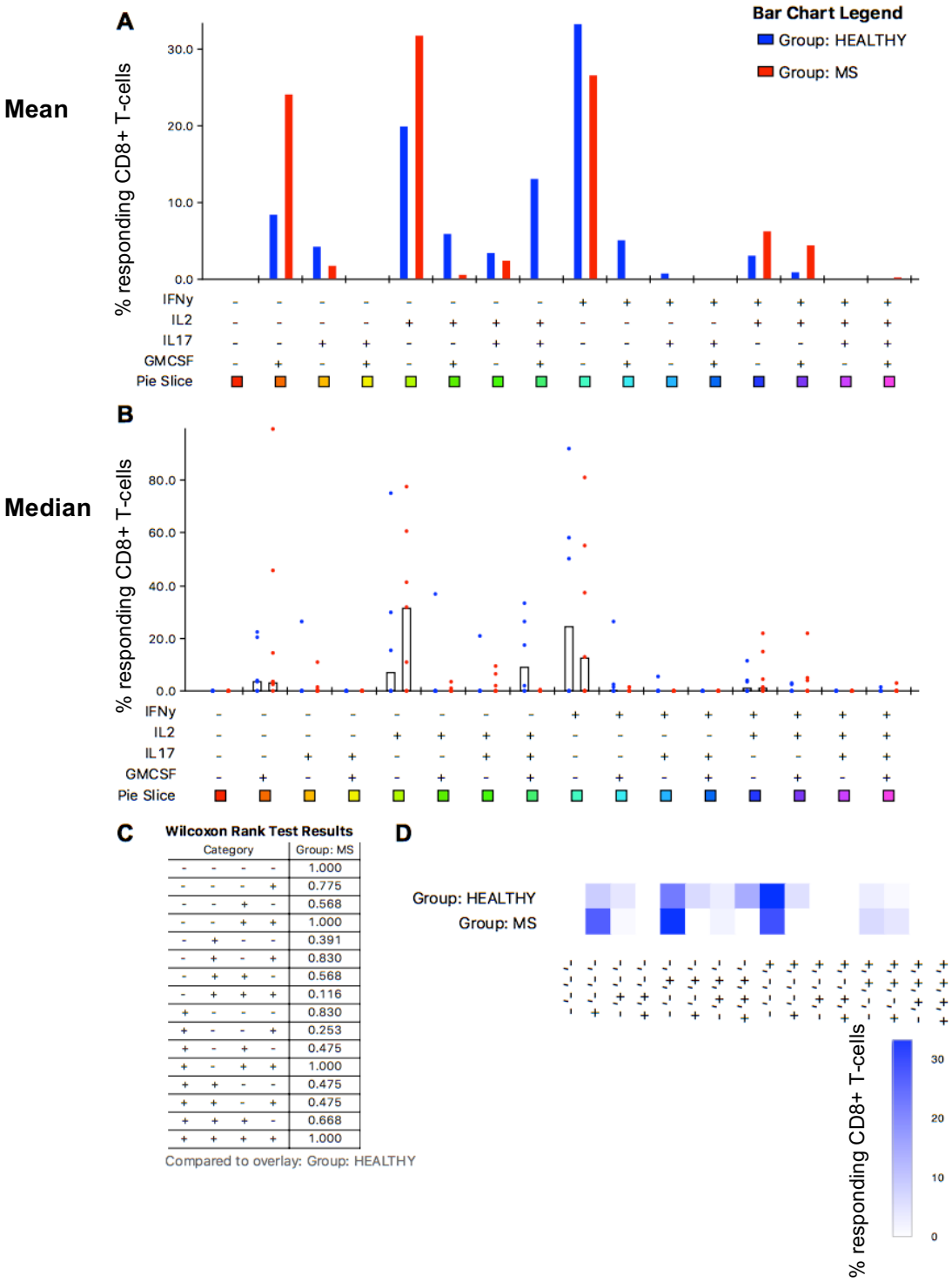

Figure 6.5.29 Cytokine profile of CD8+ T-cells responding to CRYAB from wild type LCL-specific polyclonal lines. Wild type LCL-stimulated polyclonal T-cell lines were stimulated with MVA CRYAB-infected B cell blasts and subjected to ICS (HC n=6, MS n=7). Responding CD8+ T-cells were defined as positive for any combination of four cytokines in our panel: IFNγ, IL-2, IL-17 and GM-CSF. **A.** Graphical representation of responding cells in each combination gate with bars representing the mean of data set. Statistics were calculated using the Wilcoxon Signed Rank. **B.** Scatter plot showing percentage of responding cells for each donor in combination gates. Black bars represent median of data set. **C**. Table shows results of Wilcoxon rank test. **D.** Percentage of responding CD8+ T-cells shown in heatmap form. Combination gate data was processed using Funky Cells software and graphically displayed using the program SPICE (ns $p>0.05$, * $p<0.05$).

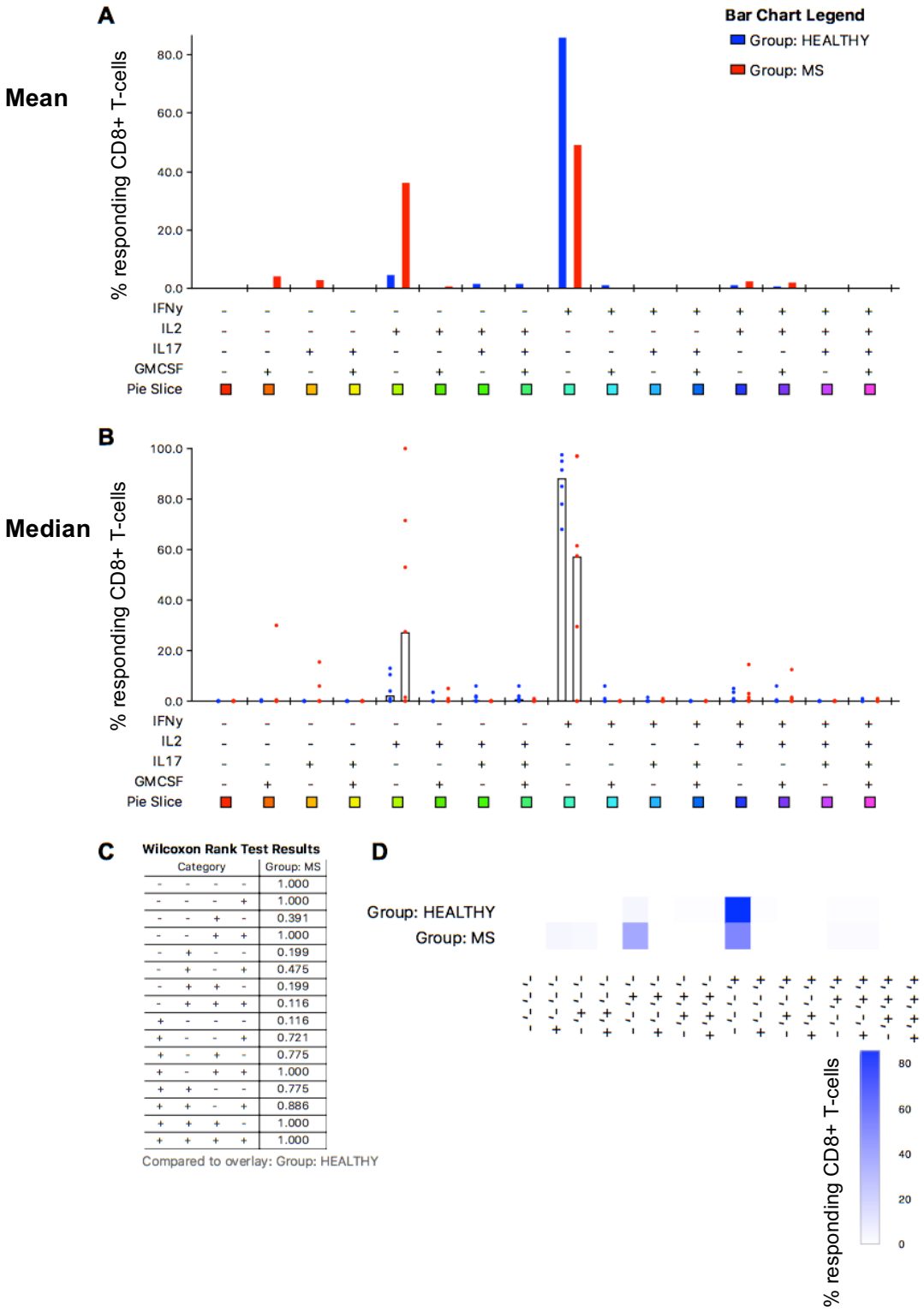

Figure 6.5.30 Cytokine profile of CD8+ T-cells responding to TAL-H from wild type LCL-specific polyclonal lines. Wild type LCL-stimulated polyclonal T-cell lines were stimulated with MVA TAL-H-infected B cell blasts and subjected to ICS (HC n=6, MS n=7). Responding CD8+ T-cells were defined as positive for any combination of four cytokines in our panel: IFNγ, IL-2, IL-17 and GM-CSF. **A.** Graphical representation of responding cells in each combination gate with bars representing the mean of data set. Statistics were calculated using the Wilcoxon Signed Rank. **B.** Scatter plot showing percentage of responding cells for each donor in combination gates. Black bars represent median of data set. **C**. Table shows results of Wilcoxon rank test. **D.** Percentage of responding CD8+ T-cells shown in heatmap form. Combination gate data was processed using Funky Cells software and graphically displayed using the program SPICE (ns $p>0.05$, * $p<0.05$).

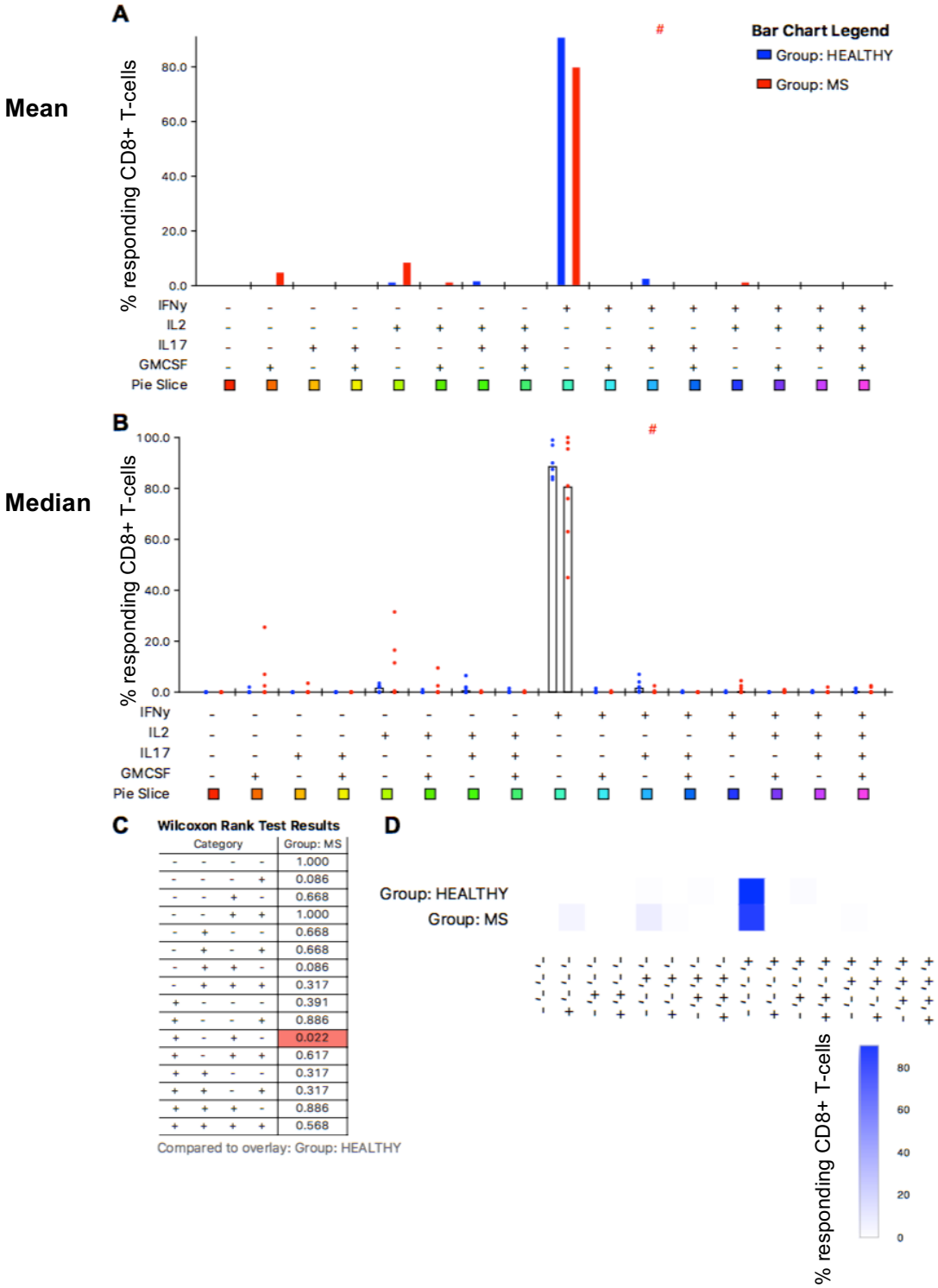

Figure 6.5.31 Cytokine profile of CD8+ T-cells responding to MOBP from wild type LCL-specific polyclonal lines. Wild type LCL-stimulated polyclonal T-cell lines were stimulated with MVA MOBP-infected B cell blasts and subjected to ICS (HC n=6, MS n=7). Responding CD8+ T-cells were defined as positive for any combination of four cytokines in our panel: IFNγ, IL-2, IL-17 and GM-CSF. **A.** Graphical representation of responding cells in each combination gate with bars representing the mean of data set. Statistics were calculated using the Wilcoxon Signed Rank. **B.** Scatter plot showing percentage of responding cells for each donor in combination gates. Black bars represent median of data set. **C**. Table shows results of Wilcoxon rank test. **D.** Percentage of responding CD8+ T-cells shown in heatmap form. Combination gate data was processed using Funky Cells software and graphically displayed using the program SPICE (ns $p>0.05$, * $p<0.05$).

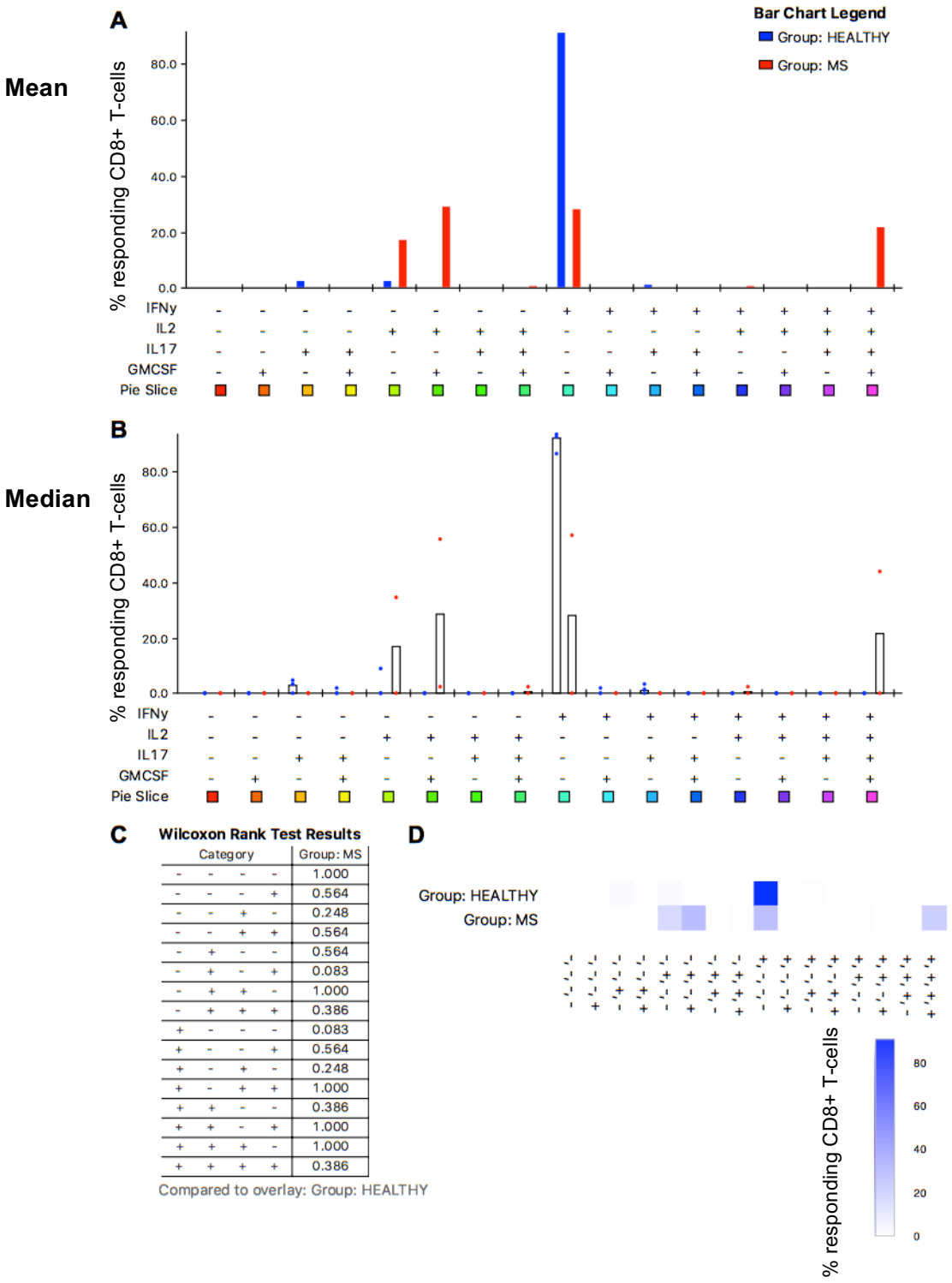

Figure 6.5.32 Cytokine profile of CD8+ T-cells responding to MAG from wild type LCL-specific polyclonal lines. Wild type LCL-stimulated polyclonal T-cell lines were stimulated with MVA MAG-infected B cell blasts and subjected to ICS (HC n=3, MS n=2). Responding CD8+ T-cells were defined as positive for any combination of four cytokines in our panel: IFNγ, IL-2, IL-17 and GM-CSF. **A.** Graphical representation of responding cells in each combination gate with bars representing the mean of data set. Statistics were calculated using the Wilcoxon Signed Rank. **B.** Scatter plot showing percentage of responding cells for each donor in combination gates. Black bars represent median of data set. **C**. Table shows results of Wilcoxon rank test. **D.** Percentage of responding CD8+ T-cells shown in heatmap form. Combination gate data was processed using Funky Cells software and graphically displayed using the program SPICE (ns $p>0.05$, * $p<0.05$).

As previously described for CD4+ T-cell response analysis, pie charts were used to visualise the contribution of each cytokine production combination gate to overall CD8+ T-cell responses to antigens. Pie charts for all CD8+ targets are shown in Figure 6.5.33. Permutation tests were performed to analyse differences between distribution of cytokine production between groups, an advantage of this is that it allows analysis of whole cytokine profile of responding cells between groups and not just individual subsets.

Cytokine production in response to stimulation with wild type LCL and BZLF1 KO LCL was similar between HC and MS patient groups, with no significant differences apparent after permutation tests were performed (Figure 6.5.33).

EBNA1 CD8+ T-cell responses from LCL-stimulated polyclonal T-cell lines were similar between groups with no major differences in cytokine production after permutation tests were applied, however EBNA3A responses were very different in subset usage with most of the responding cells from both groups producing multiple cytokines (Figure 6.5.33).

CNS antigens that induced the highest responses in wild type LCL-stimulated polyclonal T-cell lines (Figure 6.4.2) tended to produce a predominantly IFNγ positive response: MBP, MOBP and MOG, with TAL-H mainly inducing an IFNγ-mediated response in HC but a broader response in MS patients (Figure 6.5.33). A larger proportion of TAL-H CD8+ responses in MS patients produced IL-2 only but permutation tests showed overall cytokine profiles to not be significantly different to those of HC (HC:MS $p=0.0742$) (Figure 6.5.33).

MAG antigen in HC also produced a mainly IFNγ-driven response, and MS patients produced a more polymorphic response with almost 25% of the response positive for all four cytokines (Figure 6.5.33). However, as previously mentioned, no conclusions can be drawn from this observation due to the low patient numbers studied in this response; more donors would need to be tested to see if this effect is real.

CNS antigens that produce more diverse cytokine responses were MBP V8, CRYAB, PLP, claudin and CNP and are generally small responses, however no significant variations were seen in the overall cytokine profile of responding CD8+ T-cells between patient groups. CD8+ T-cell responses to CNP differed the most between HC and MS patients with a trend towards higher polyfunctionality in those from HC, however difference in combination gate usage did not reach significance between groups (HC:MS *p=0.0666*) (Figure 6.5.33).

No permutation tests performed on pie charts representing CD8+ T-cell responses from wild type LCL-stimulated polyclonal lines revealed significant differences between healthy and MS donors, unlike for CD4+ T-cell responses which exhibited a few key differences in the repertoire of cytokine production following CNS and EBV antigen stimulation (Figure 6.5.18 and 6.5.33). No differences were observed in cytokine profile of unstimulated T-cells between groups prior to analysis in Funky Cells (data not shown).

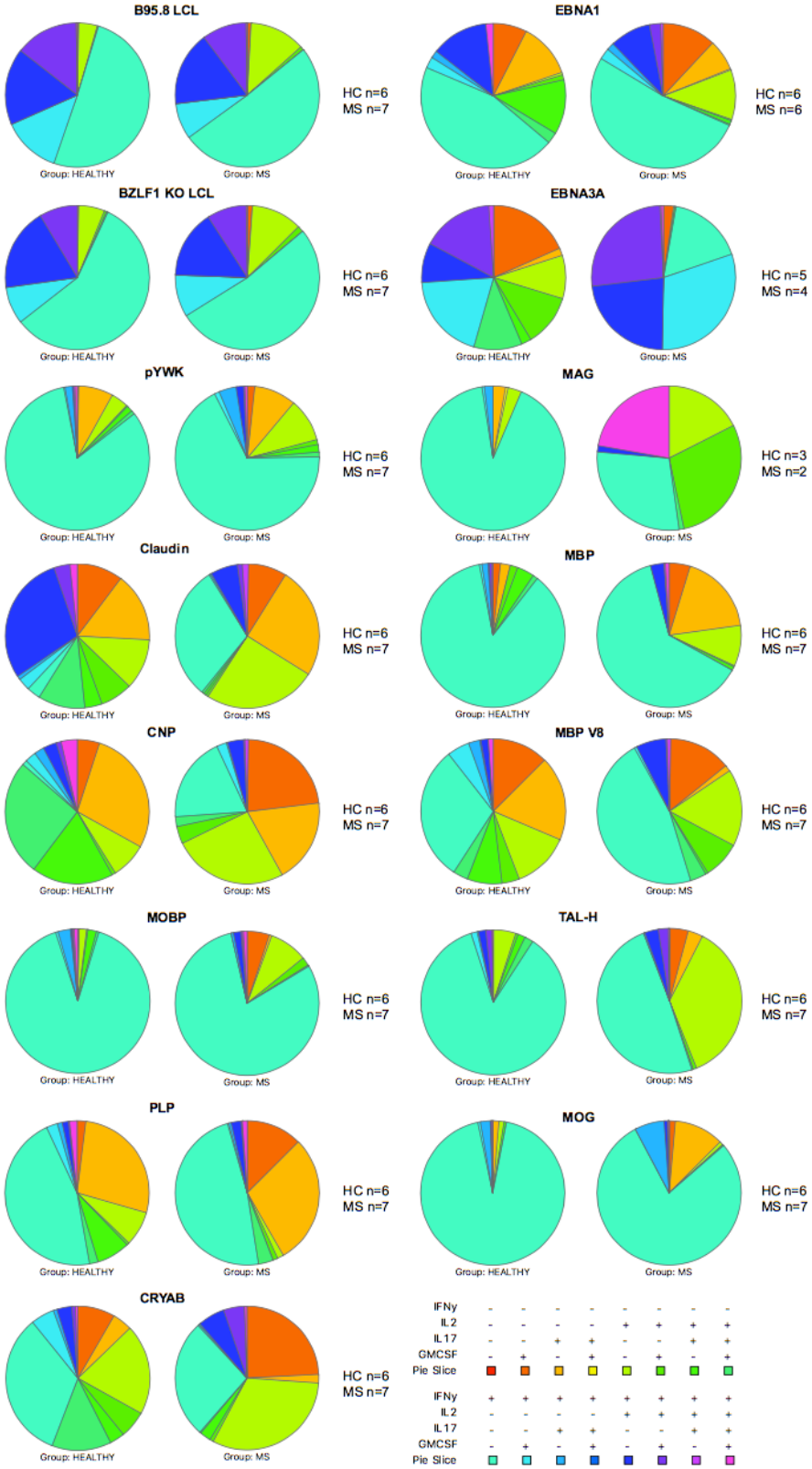

Figure 6.5.33 Different cytokine profiles of CNS-stimulated CD8+ T-cells from wild type LCL-specific polyclonal T cell lines. Wild type LCL-specific polyclonal T-cell lines were stimulated with autologous B-cell blasts infected with MVA viruses containing the CNS and EBV proteins individually. Responding CD8+ T-cells were defined as positive for any combination of cytokines in our panel: IFNγ, IL-2, IL-17 and GM-CSF. Pie charts show median values of all donors in each group. Groups were compared using the permutation test (ns $p>0.05$, * $p<0.05$).

6.6 Single cell isolation of cross-reactive T-cells

High levels of CNS-reactive T-cells in EBV-stimulated polyclonal lines suggests that there is structural mimicry between neuronal and viral antigens, however to formally show this we sought to isolate single cells with dual specificity.

To isolate single T-cells with specificity for both EBV and CNS antigens we explored several methods, the first of which was limiting dilution. T-cells which had been expanded in culture for 2 weeks following autologous wild type LCL stimulation were stimulated again on the day of T-cell cloning with LCL and then diluted in T-cell medium with feeder cells before being seeded out. Plates were incubated for two weeks to enable expansion of activated clones, which were subsequently screened for specificity using IFNγ ELISA against LCL, or individual EBV and CNS antigens. The aim was to isolate many T-cell clones with specificity for EBV antigens and which could then be screened against CNS antigens using our MVA panel, and this experiment was performed five times using different donors.

We found that, whilst many of the LCL-stimulated clones reacted to EBV antigens, none of the T-cell clones screened exhibited reactivity to neuronal proteins in our MVA panel. An overview of limiting dilution cloning experiments is summarised in Table 6.1. Due to the large number of non-specific and only EBV-specific T-cell clones this method produced, we subsequently used a different approach, utilising CNS antigen stimulation on the day of cloning to selectively stimulate T-cell clones with dual reactivity.

We selectively expanded T-cells with reactivity to neuronal proteins and enriched populations using IFNγ capture. We selected four proteins in our CNS panel with the highest frequency of responding cells in our previous stimulation assays as a focus of efforts to isolate cross-reactive T-cells: MOG, PLP, MBP and MOBP.

IFNγ capture uses magnetic beads to isolate cells producing the cytokine, and was used to selectively enrich responding cells following CNS antigen stimulation and increase the yield of clones that show specificity for EBV and CNS antigens. However, this method requires several steps in which cells are subjected to low temperatures and removal of culture medium over a period of six hours, meaning that many of them die during the process or shortly afterwards. Two experiments were performed using this technique and the results are shown in table 6.1. Despite the large number of microcultures that were established, very few clones expanded after incubation. This result led us to employ a third technique that did not expose T-cells to harsh conditions for such long periods of time.

In this third approach, we employed an assay which prevented cleavage of an activation marker from the cell surface using an inhibitor. The TNFα processing inhibitor-0 (TAPI-0) acts on a

Table 6.1 Table of yields from T-cell cloning using different methods. Three methods were used for cloning of cross-reactive T-cells from polyclonal T-cell lines: limiting dilution, IFNγ capture and TNFα capture. Number of expanded clones varied between donors and cloning method used to isolate cells. EBV reactivity was defined as cytokine production in response to any EBV antigen, but most responded either to the wild type or to the BZLF1 KO LCL. Stimulus with wild type LCL refers to the autologous LCL made from each individual donor. CNS antigen stimulation was performed using autologous B-cell blasts from each donor infected with the respective recombinant MVA viruses.

Method of T cell isolation	Donor	Initial stimulus	Stimulus before cloning	Number of expanded clones	Number of clones with EBV reactivity	Number of clones with CNS reactivity
Limiting dilution	MS19	Wild type LCL	Wild type LCL	91	44	0
	MS20	Wild type LCL	Wild type LCL	176	53	0
	MS20	Wild type LCL	MOG/MBP/PLP/MOBP	43	14	0
	MS34	Wild type LCL	Wild type LCL	53	6	0
	MS35	Wild type LCL	Wild type LCL	120	47	0
	MS35	Wild type LCL	Wild type LCL	312	23	0
IFNγ capture	MS34	Wild type LCL	MOG/MBP/PLP/MOBP	8	3	0
	MS34	Wild type LCL	MOG/MBP/PLP/MOBP	10	1	0
TNFα capture	HC29	Wild type LCL	MOG	114	54	0
	MS1	Wild type LCL	MOG	36	11	0
	MS1	Wild type LCL	MOG/MBP/PLP/MOBP	36	7	0
	MS1	Wild type LCL	MOG/MBP/PLP/MOBP	15	9	0
	MS1	Wild type LCL	MOG/MBP/PLP/MOBP	37	11	0
	MS6	Wild type LCL	MOG	16	3	0
	MS6	Wild type LCL	MOG	14	2	0
	MS13	Wild type LCL	MOG/MBP/PLP/MOBP	4	2	0
	MS13	Wild type LCL	MOG/MBP/PLP/MOBP	5	2	0
	MS34	Wild type LCL	MOG	8	3	4
	MS1	MOG/PLP	MOG/PLP	2	0	0
	MS13	MOG/PLP	MOG/PLP	0	0	0
	MS20	MOG/MBP/PLP/MOBP	MOG/MBP/PLP/MOBP	0	0	0
	MS34	MOG/MBP/PLP/MOBP	MOG/MBP/PLP/MOBP	0	0	0

metalloproteinase on the surface of T-cells called TNFα converting enzyme (TACE, also called ADAM17) thereby preventing extracellular release of TNFα from the outer surface of T-cells. This removes the need to fix and permeabilise T-cells for TNFα staining and detection, and viable antigen-specific T-cells can therefore be easily detected and isolated by FACS.

Several experimental approaches using the TNFα capture technique were used to investigate cross-reactive T-cells from MS donors and HC. A schematic of the cloning strategies is show in Figure 6.6.1. The first method was similar to previously described strategies (limiting dilution and IFNγ capture) and aimed to isolate single T-cell clones with dual specificity for EBV and CNS antigens from MS patients to map their restrictions and epitope specificity on the single cell level (Figure 6.6.1A). Four proteins were selected from the CNS panel that had the highest frequency of responding cells in previous stimulation assays: MOG, PLP, MBP and MOBP. All polyclonal lines generated for sorting were screened for LCL specificity prior to single cell sorting by TNFα capture and staining to ensure that experiments would yield positive T-cell clones.

As previously described, polyclonal T-cell lines from each donor were expanded by stimulating with autologous wild type LCL for three weeks. Cells were then stimulated with autologous B-cell blasts infected with selected CNS MVAs on the day of sorting and T-cells were surface stained in the presence of TAPI-0 and single, LiveCD19-CD3+TNFα+ sorted clones were incubated in 96-well plates in the presence of feeder cells and anti-CD3 antibody (OKT3). A schematic of experimental strategy is shown in Figure 6.6.1A, with gating strategy and example staining from two MS donors shown in Figure 6.6.2. After incubation for two weeks, all expanded clones were screened by IFNγ ELISA against autologous wild type and BZLF1 KO LCL and CNS antigens and a summary of the results of these assays are shown in Table 6.1.

T-cell cloning was carried out after stimulating wild type LCL-specific T-cell lines with CNS antigens on the day of sorting; approximately a third of sorted T-cells expanded after sorting

into 96-well plates. Further functional studies performed on growing clones revealed a proportion of them to have reactivity against autologous LCL, but almost none with reactivity to CNS antigens in our panel, and this method yielded only T-cell clones with reactivity to EBV antigens (summary of experiments and results using these stimulations is shown in Table 6.1).

However, T-cell cloning from one donor – MS34 – did produce four T-cell clones which exhibited reactivity to both EBNA1 and MOG antigens, and their cytokine production in response to stimuli is shown in Figure 6.6.3. All four clones, despite producing different amounts of IFNγ in response to antigen, displayed good recognition of MVA EBNA1-infected B-cell blasts and lower recognition MVA MOG-infected cells. Due to these similarities between the four T-cell clones from patient MS34 is possible that they are descended the same T-cell clone. After initial analysis for function, all four clones appeared to lose specificity (or to have become anergic) *in vitro* as they no longer responded to stimulation with the cognate antigen. This unfortunately prevented further characterisation of HLA and epitope restriction of T-cell clones and further investigation of these cells could not continue.

However, evidence of a cross-reactive T-cell receptor recognising EBNA1 and MOG at a lower level is consistent with observations from polyclonal T-cell lines in the patient and previous studies findings of cross-reactivity in MS donors' EBNA1-specific T-cell pool (Lunemann et al., 2008b, Lang et al., 2002, Holmoy et al., 2004). Further characterisation is needed to confirm these observations, and mapping epitope and HLA restriction is of prime importance when considering potential contribution of these cross-reactive T-cell clones to MS pathogenesis.

It is possible that single, cross-reactive T-cells do not expand *in vitro* post-single cell sorting, or that these cells do not maintain functionality or specificity. Failure to grow or characterise

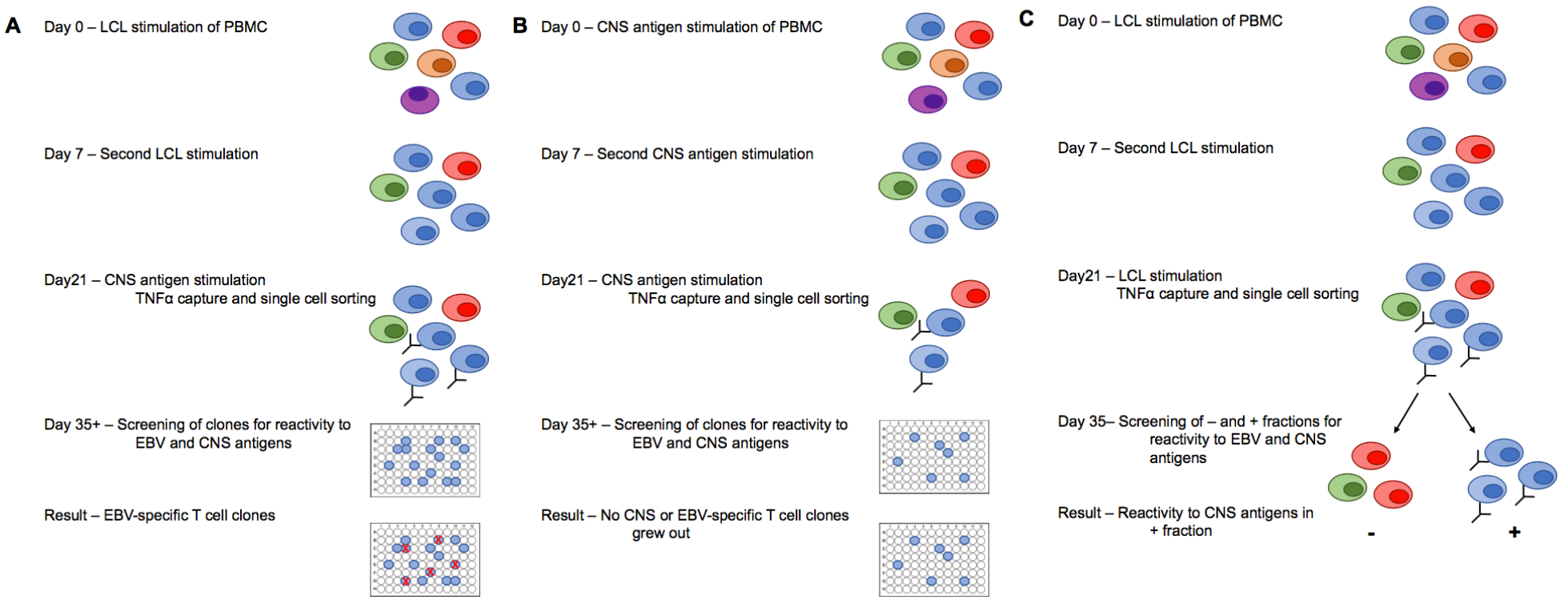

Figure 6.6.1 Schematic of experimental approach using TNFα capture to isolate cross-reactive T-cells. A. Whole PBMC from donors were stimulated with autologous wild type LCL and cultured for 7 days, after which a second LCL stimulus was given to cells. On day 21 polyclonal T-cell lines had grown out and cells were stimulated with CNS antigens in the presence of TAPI-0. Polyclonal lines were surface stained and the LiveCD19-CD3+TNFα+ sorted into 96-well plates. 2 weeks later expanded T-cell clones were screened by IFNγ ELISA for reactivity to EBV and CNS antigens. This approach yielded many EBV-reactive clones with varying specificity; four clones with reactivity to both EBV and CNS antigen were isolated from one MS donor using this method. **B.** B-cell blasts infected with CNS MVAs were used to stimulate whole PBMC from donors on day 0, and 7 days later PBMCs were stimulated a second time. The resulting polyclonal lines that grew out did not expand very efficiently and cell numbers dropped dramatically. 3 weeks after initial stimulation the expanded polyclonal T-cell culture was stimulated with CNS antigens in the presence of TAPI-0 before surface staining and single cell sorting of LiveCD19-CD3+TNFα+ T-cells. Plates were incubated for 2 weeks and expanded clones were screened for reactivity to CNS an EBV antigens by ELISA: no clones were found to be specific. **C.** Whole PBMC from donors were stimulated with autologous wild type LCL on day 0 and day 7 and cultures for 3 weeks. Expanded LCL-specific T-cell lines were then stimulated with LCL a third time in the presence of TAPI-0 and surface stained to identify the responding population. The positive (LiveCD19-CD3+TNFα+) and negative (LiveCD19-CD3+TNFα-) fractions were bulk sorted separately and both lines cultured for two weeks to expand populations. Positive and negative fractions were then screened for reactivity against CNS and EBV antigens: reactivity to CNS proteins was identified in the positive, LCL-specific T-cell population.

in detail single, cross-reactive T-cell clones in culture prompted a change in experimental direction, analysing bulk populations of cells which survive and are better maintained *in vitro.* The reverse approach using initial stimulation with CNS antigens to expand a population of T-cells with neuronal specificity yielded similar results. We stimulated whole PBMC with autologous B-cell blasts infected with selected CNS MVAs in our panel (MOG, PLP, MBP, MOBP) on day 0 and day 7, allowing responding cells to grow out over 3 weeks before single cell sorting of CNS-specific T-cells using TNFα capture (Figure 6.6.1B). CNS-specific T-cell lines expanded in this way showed different growth kinetics to those stimulated with viral antigens, and expanded more slowly with end cell numbers being lower than those of initial PBMCs in the starting population (data not shown). Despite these low cell numbers, we stimulated with MVA CNS-infected autologous B-cell blasts on the day of sorting, performing TNFα capture and single cell sorting into 96-well plates containing feeder cells and anti-CD3 antibody as previously described. The TNFα+ population from CNS-stimulated T-cell lines was small and fewer single cells were sorted than previously for EBV-stimulated lines. A summary of T-cell clone yield using this stimulation technique can be found in Table 6.6.1.

The aim was to screen by ELISA sorted clones from CNS-stimulated polyclonal T-cell lines against EBV antigens, as the CNS antigens have fewer epitopes than in LCLs carrying all EBV latency proteins and we hypothesised that this would enable us to narrow down the pool of responses and thus increase the chances of isolating T-cell clones with dual specificity. However, few T-cell clones sorted following CNS antigen stimulation grew in culture, and we observed only 2 expanded microcultures in plates from these experiments (Table 6.6.1).

These findings supported previous experimental outcomes that suggested an inability to grow autoreactive T-cells *in vitro*, and it is possible that these cells require different conditions to live in culture or that they do not receive such strong signals upon exposure to their cognate antigen due to lower avidity of their TCR for peptide:MHC complexes. It is also possible that

autoreactive T-cells do not grow well in single cell suspension or not as part of a heterogeneous population. T-cells in a state of replicative senescence are able to produce high levels of cytokine in response to stimulus but are not able to proliferate, and T-cells which belong to effector memory subsets often have limited replicative capacity. Multiple rounds of stimulation during cloning experiments may have sorted T-cells that were subsequently unable to expand in culture, limiting our ability to study these cells in further experiments.

We therefore explored bulk sorting of wild type LCL-specific polyclonal T-cell lines as a means of investigating whether CNS reactivity could still be found in expansions that only contained cells with EBV-specificity.

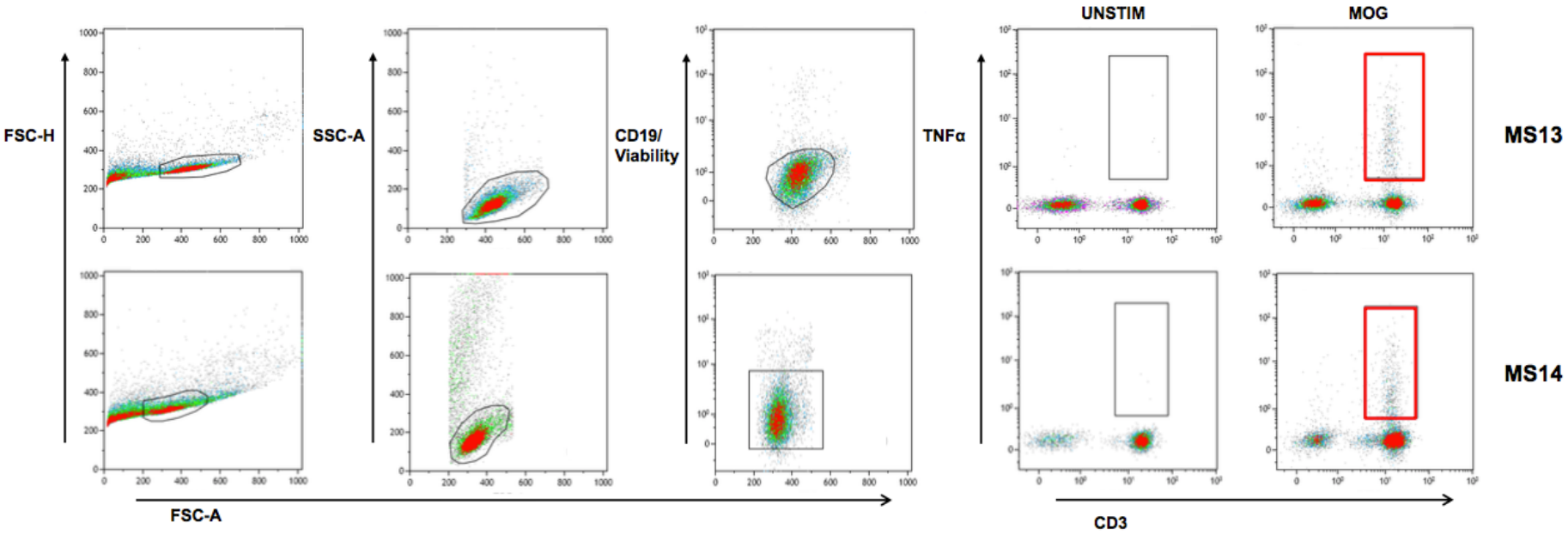

Figure 6.6.2 Gating strategy for single cell sorting of T-cells with potential dual-specificity for EBV and CNS antigens using TNFα capture. Whole PBMC were stimulated with autologous wild type LCL for 3 weeks, and on the day of sorting expanded, LCL-specific T-cell lines were stimulated with autologous B-cell blasts infected with selected MVAs containing CNS antigens in the presence of TAPI-0. Following stimulation T-cells were surface stained and single, LiveCD19-CD3+TNFα+ cells sorted into 96-well plates. Gating strategy is shown for two representative donors (MS13 and MS14); sorted populations from MOG-stimulated wild type LCL-specific polyclonal T-cell lines are shown by the red boxes.

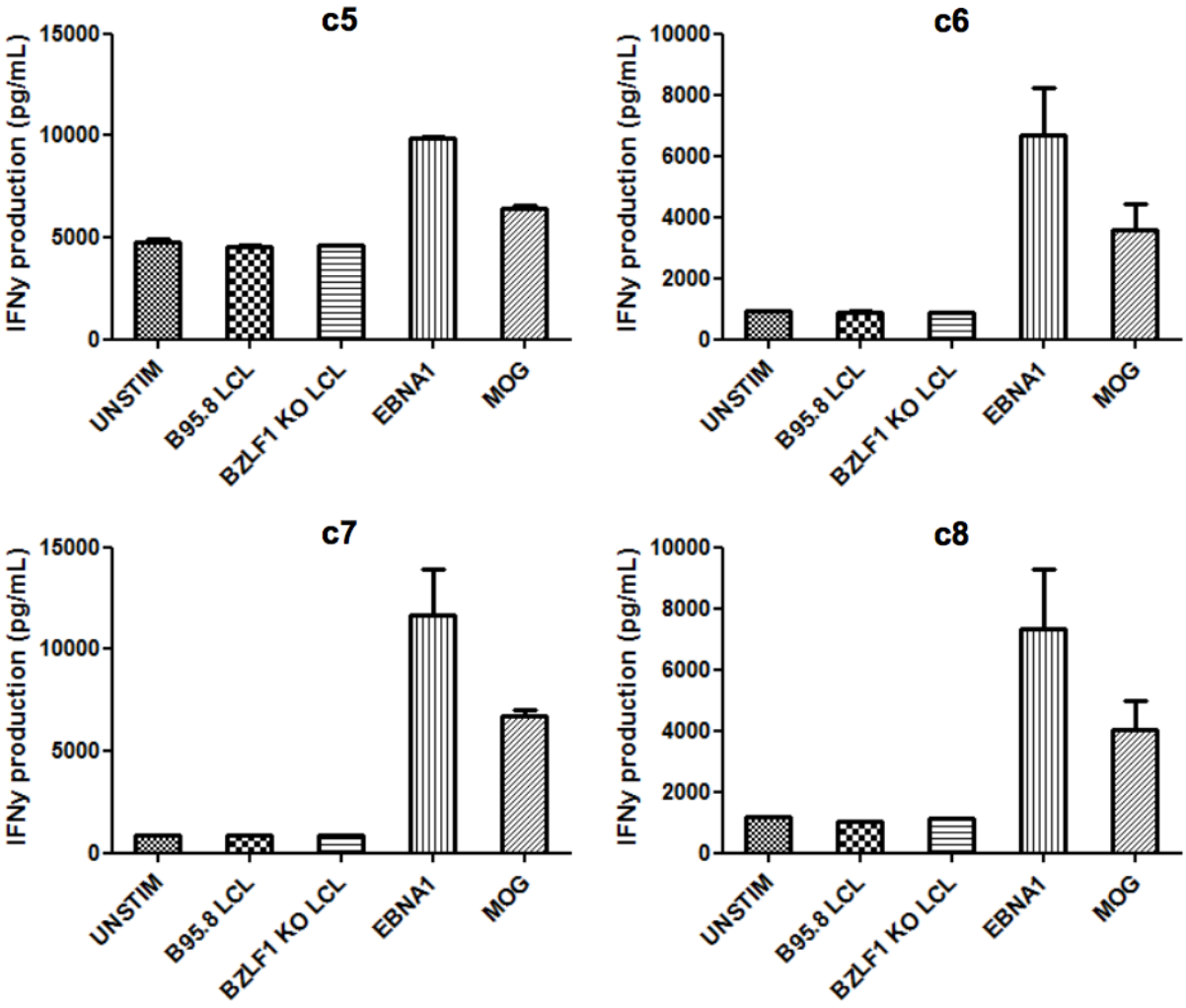

Figure 6.6.3 T-cell clones isolated from MS patient exhibit cross-reactive recognition of EBNA1 and MOG. Single T-cells were expanded for two weeks in culture following TNFα capture and single cell sorting. Expanded clones were screened for reactivity to autologous wild type and BZLF1 KO LCLs, EBNA1 and MOG by IFNγ ELISA. Four clones exhibited reactivity to both EBNA1 and MOG stimulation. Bars represent mean IFNγ concentration from three triplicate data points with error bars displaying the standard error of the mean (SEM).

6.7 Analysis of bulk sorted wild type LCL-specific polyclonal T-cell lines

Despite high levels of CNS antigen reactivity in wild type LCL-stimulated polyclonal T-cell lines it could not be confirmed that the cells responding to EBV – or cellular antigens up-regulated by EBV – are the same cell that respond to neuronal antigens. Our inability to expand autoreactive T-cells in culture long term also prevented functional studies, epitope mapping and HLA-restriction being performed on the T-cell clones which appeared to have reactivity with EBNA1 and MOG. We therefore sought to address these questions by bulk sorting wild type LCL-specific T-cells to produce a population of T-cells with 100% specificity, and in turn screen this against the MVA CNS panel to determine if CNS antigen reactivity is retained in the positively sorted population.

TNFα capture was again used to sort wild type LCL-specific T-cells (LiveCD19-CD3+TNFα+ cells) but this time as one bulk population. Following bulk-sorting, T-cells were added to 24-well plates with feeder cells (without anti-CD3 antibody). T-cell lines sorted into positive and negative fractions were cultured for two weeks post-sorting, enabling cell numbers to increase for subsequent experiments and to allow cytokine production to recover to normal levels ahead of screening against CNS antigens. T-cells from the non-specific (LiveCD19-CD3+TNFα- cells) population were bulk sorted as a negative control and screened against the recombinant MVA panel to investigate if CNS antigen specificity also existed in this fraction (experimental approach described in Figure 6.6.1C).

Representative staining from one donor's positive and negative sorted LCL-specific T-cell lines is shown for CD4+ T-cells in Figure 6.7.1 and for CD8+ T-cells in Figure 6.7.2. CD4+ T-cells in the positive fractions sorted following autologous wild type LCL stimulation showed ~82% specificity for the LCL after screening as measured by TNFα production (top line Figure 6.7.1). The negative fraction sorted from T-cells that were not responding to wild type LCL on

the day of sorting also showed some reactivity to LCL when screened two weeks later, with ~41% of CD4+ T-cells responding with TNFα production (bottom line Figure 6.7.1). This might be due to the fact that sorted cells were rested in culture for two weeks following antigenic stimulation and sorting, which might mean that any wild type LCL-specific T-cells that did not produce TNFα on the day of the sorting experiment will have been included in the negative fraction and subsequently expanded *in vitro*.

Background TNFα staining was observed in both positive and negative fractions of CD4+ T-cells from sorted wild type LCL-stimulated polyclonal lines, with more in the negatively sorted population (Figure 6.7.1). TNFα production in response to autologous B-cell blasts infected with MVAs expressing CNS antigens was not much above background levels in the negatively sorted fraction. However, CNS antigen reactivity was higher in CD4+ T-cells from the positively sorted population, indicating that the reactivity to neuronal proteins might occur in CD4+ cells that also respond to autologous wild type LCL. This experiment was performed for a further 3 MS donors with very similar results, suggesting that CNS reactivity lies with the wild type LCL-specific CD4+ T-cells in polyclonal lines. Sorted fractions were screened against all other neuronal antigens in the CNS MVA panel but TNFα production was shown to be not above background levels, showing no specific recognition of these antigens (data not shown).

CD8+ T-cells from the same experiment, sorting T-cells based on their TNFα production in response to autologous wild type LCL, also showed high levels of background cytokine staining in the negative fraction, and staining is shown from one representative MS donor's CD8+ T-cells in Figure 6.7.2. Similar to CD4+ T-cells, CD8+ responses from the negative sorted fraction showed similar proportions of cells that were specific for wild type LCL after culturing for two weeks; ~52% CD8+ T-cells were shown to be wild type LCL-specific in the negative fraction and ~82% were specific in the positive fraction (Figure 6.7.2).

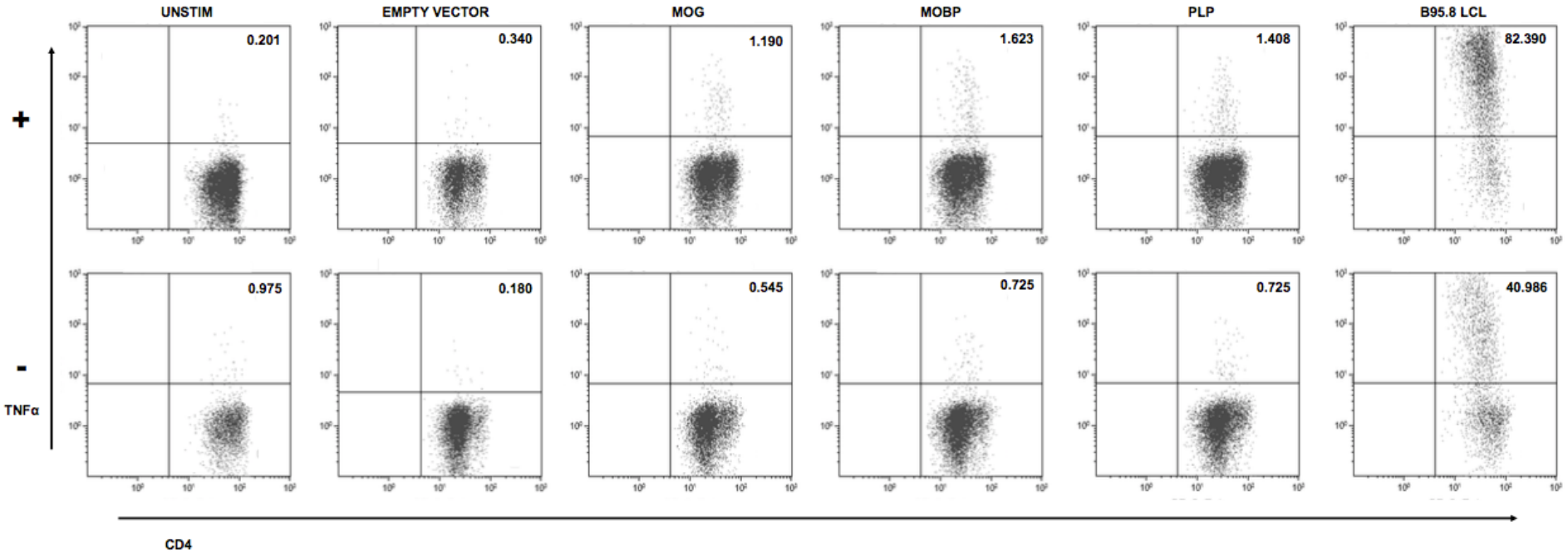

Figure 6.7.1 CNS reactivity of CD4+ T-cells from MS patient sorted, wild type LCL-stimulated polyclonal T-cell lines. Whole PBMC from one representative MS donor (MS14) were stimulated with autologous wild type LCL on day 0 and day 7, and cultured for a further two weeks. On day 21 expanded T-cell lines were stimulated again with wild type LCL in the presence of TAPI-0, surface stained and populations of LiveCD19-CD3+TNFα+ and LiveCD19-CD3+TNFα- were bulk sorted separately. These TNFα+ and – populations were cultured separately for 2 weeks to increase cell number, before screening against MVA CNS panel-infected autologous B-cell blasts, using TNFα capture and surface staining for the CD4+ T-cell subpopulation. This method was repeated for a further 3 MS donors with similar results. Value in the top, right corner of plots shows the percentage of CD4+ T-cells producing TNFα in response to each stimulus; top plots show LiveCD19-CD3+TNFα+ sorted CD4+ T-cells responding to LCL and bottom plots show LiveCD19-CD3+TNFα- cells which did not respond to the LCL at the time of sorting.

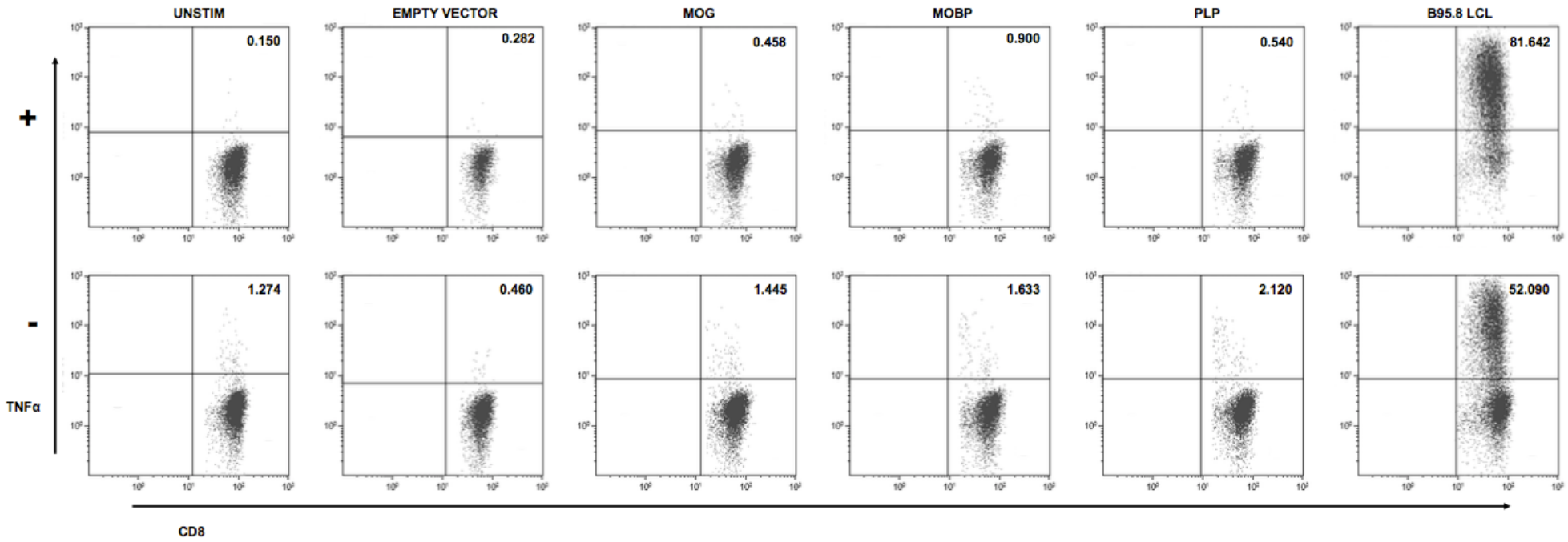

Figure 6.7.2 CNS reactivity of CD8+ T-cells from MS patient sorted, wild type LCL-stimulated polyclonal T-cell lines. Whole PBMC from one representative MS donor (MS14) were stimulated with autologous wild type LCL on day 0 and day 7, and cultured for a further two weeks. On day 21 expanded T-cell lines were stimulated again with wild type LCL in the presence of TAPI-0, surface stained and populations of LiveCD19-CD3+TNFα+ and LiveCD19-CD3+TNFα- were bulk sorted separately. These TNFα+ and – populations were cultured separately for 2 weeks to increase cell number, before screening against MVA CNS panel-infected autologous B-cell blasts, using TNFα capture and surface staining for the CD8+ T-cell subpopulation. This method was repeated for a further 3 MS donors with similar results. Value in the top, right corner of plots shows the percentage of CD8+ T-cells producing TNFα in response to each stimulus; top plots show LiveCD19-CD3+TNFα+ sorted CD8+ T-cells responding to LCL and bottom plots show LiveCD19-CD3+TNFα- cells which did not respond to the LCL at the time of sorting.

This is probably due to the LCL-specific T-cells outgrowing the non-specific cells in the period following sorting (Figure 6.7.2).

Unlike CD4+ T-cells, reactivity to neuronal proteins in CD8+ T-cells from sorted wild-type LCL-specific polyclonal lines was higher than background for CD8+ T-cells in the negative fraction. Low levels of cytokine production following neuronal antigen stimulation in the positive fraction suggests that the CD8+ T-cells sorted for their response to wild type LCL do not highly recognise CNS epitopes in the MVA panel.

EBNA1 has been shown previously to contain several cross-reactive epitopes (Lang et al., 2002, Holmoy et al., 2004, Lunemann et al., 2008b) and, due to difficulties in cloning single T-cells with dual specificity for EBV and neuronal antigens, we used the same bulk sorting approach as for wild type LCL stimulated polyclonal lines to investigate this further.

MVA EBNA1-infected B-cell blasts were used to stimulate whole PBMC from three MS donors on day 0 and day 7. On day 21 the expanded T-cell lines were stimulated again with EBNA1 in the presence of TAPI-0 and stained to identify the T-cell population producing TNFα; LiveCD19-CD3+TNFα+ and LiveCD19-CD3+TNFα- fractions were bulk sorted separately.

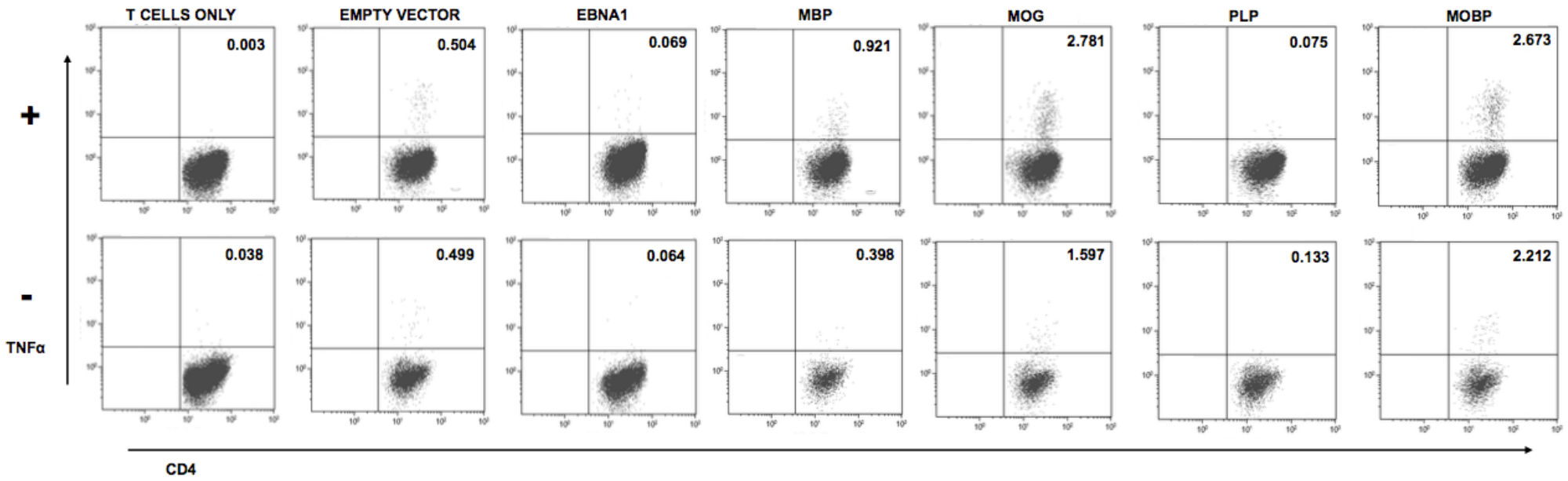

Figure 6.7.3 CNS-specific CD4+ T-cell responses in sorted EBNA1-stimulated polyclonal T-cell line. Whole PBMC were stimulated with autologous B-cell blasts infected with MVA EBNA1 on day 0 and day 7. On day 21 the expanded T-cell cultures were stimulated with MVA EBNA1-infected B-cell blasts in the presence of TAPI-0, surface stained and subpopulations of LiveCD19-CD3+TNFα+ (top row) and LiveCD19-CD3+TNFα- (bottom row) cells bulk sorted. Sorted cells were then expanded in culture for 2 weeks to increase cell numbers and screened against MVA CNS-infected autologous B-cell blasts. Reactivity was measured by TNFα production. Top right corner values represent the percentage of CD4+ T-cells producing TNFα in response to individual antigens.

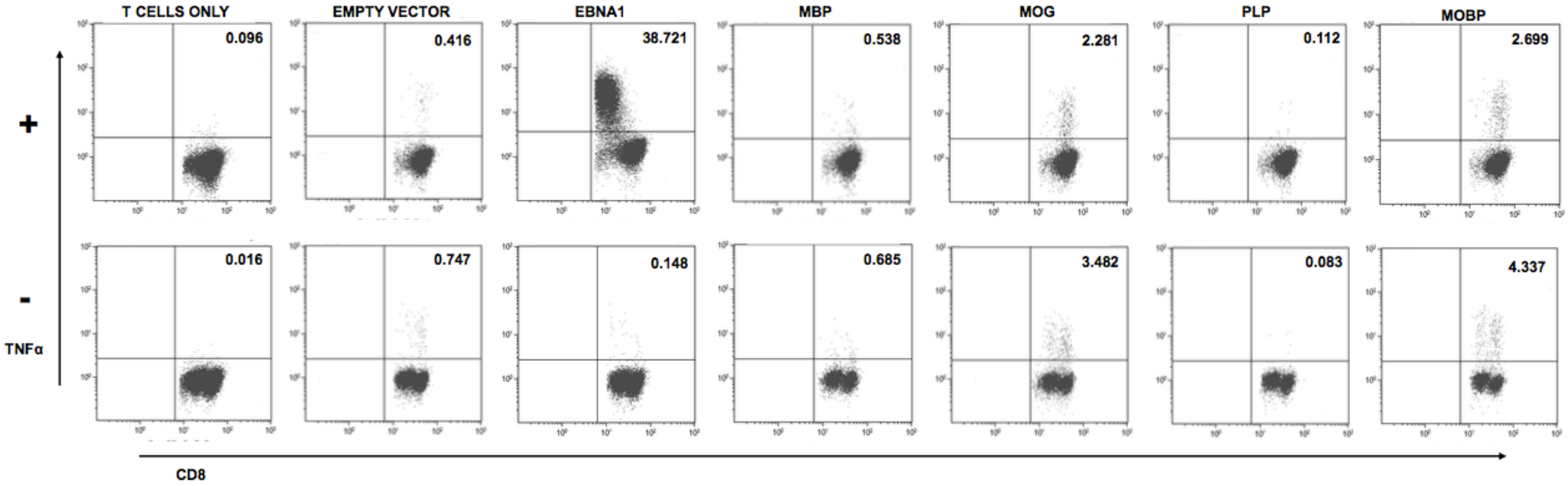

Figure 6.7.4 CNS-specific CD8+ T-cell responses in sorted EBNA1-stimulated polyclonal T-cell line. Whole PBMC were stimulated with autologous B-cell blasts infected with MVA EBNA1 on day 0 and day 7. On day 21 the expanded T-cell cultures were stimulated with MVA EBNA1-infected B-cell blasts in the presence of TAPI-0, surface stained and subpopulations of LiveCD19-CD3+TNFα+ (top row) and LiveCD19-CD3+TNFα- (bottom row) cells bulk sorted. Sorted cells were expanded in culture for 2 weeks to increase cell numbers and screened against MVA CNS-infected autologous B-cell blasts. Reactivity was measured by TNFα production. Top right corner values represent the percentage of CD8+ T-cells producing TNFα in response to individual antigens.

This experiment was performed in three MS donors with sizeable CD4+ and CD8+ responses as shown by *ex vivo* analysis of T-cell responses in Chapter 5.

CD4+ T-cell responses to CNS antigens in the EBNA1-responding positive fraction are presented from one donor in Figure 6.7.3, and show this donor to have no TNFα production above background in response to the initial stimulus EBNA1. This is surprising given that cells were sorted based on their reactivity to the protein two weeks previously, and that pre-sorting screening of EBNA1-expanded lines two days prior to sorting showed ~2% CD4+ T-cells producing TNFα in response to the antigen. It is possible that these responding CD4+ T-cells have lost specificity in culture in the period between sorting and screening versus CNS antigens, but more analysis would be needed on this population to determine whether this is the case.

Interestingly, despite this population showing no specificity for EBNA1, CD4+ T-cells in the positively sorted fraction showed higher TNFα production in response to MOG, MBP and MOBP than that of CD4+ T-cells in the negatively sorted fraction, indicating that sorting for EBNA1 specificity may also enrich for CD4+ T-cells that respond to neuronal proteins. CD4+ T-cell responses in the positive fraction of two other MS patient EBNA1 sorted polyclonal lines showed reactivity to the CNS, but these experiments would need to be repeated in several more donors or polyclonal lines to corroborate results.

In contrast, CD8+ T-cells from the positively sorted fraction of EBNA1 specific T-cell expansions showed a high reactivity to the protein, with example staining from one donor showing ~39% of CD8+ T-cells producing TNFα following EBNA1 stimulation (Figure 6.7.4). CD8+ reactivity to CNS antigens in TNFα positive and negative sorted EBNA1-specific T-cell expansions was seen at similar levels, with an increase in cytokine production seen in the negative fraction for MOG and MOBP (Figure 6.7.4). This is similar to what was observed for CD8+ T-cells in sorted wild type LCL polyclonal lines, and again indicates that selecting CD8+

T-cells for their ability to produce TNFα in response to EBNA1 does not enrich cells for neuronal antigen specificity. Two further FACS sorted EBNA1-specific polyclonal lines established from MS patients were screened for CNS responses in their positive and negative fractions with very similar results, suggesting that neuronal antigen reactivity is enriched by sorting in the CD4+ T-cell subset but not CD8+ (data not shown).

These experiments show that using the TNFα capture and staining system it is possible to enrich T-cell populations reacting to a specific stimulus. High percentage wild type LCL specificity in T-cell lines sorted for reactivity to this same stimulation shows that the bulk sorting of CD4+ T-cells did work and enrich populations successfully. However, the presence of T-cells in the negatively sorted fractions with reactivity to wild type LCL makes it difficult to interpret results with confidence. Discounting results from the negatively sorted fraction, the presence of CD4+ T-cells that are able to react with CNS antigens in a population that is 80-90% specific for wild type LCL is consistent with presence of molecular mimicry between EBV and neuronal peptides displayed by self-MHC molecules. However, reactivity to CNS antigens could also be attributed to the ~10% of CD4+ T-cells that do not react with the wild type LCL after sorting with this stimulus.

Despite low reactivity for EBNA1 in subsequent screening, CD4+ T-cells from the positive fraction of EBNA1-sorted polyclonal lines showed a percentage of cells producing cytokine in response to particular neuronal antigens in our MVA panel. This supports the idea that by stimulating with EBNA1, CD4+ T-cells with affinity for MOG and MOBP are expanded *in vitro*.

6.8 Discussion

Cross-reactivity between viral and CNS epitopes has been previously reported in MS literature (Holmoy et al., 2004, Lunemann et al., 2008b, Lang et al., 2002) and these dual-specific T-cell responses are thought to have a key role in disease development. However, the exact contribution of these cells remains to be determined and there is currently no consensus reached regarding a mechanism of how EBV-specific T-cells might influence early pathological processes in MS.

Experiments performed in our study show that stimulation of *ex vivo* T-cells with wild type LCL – cells which express both EBV latent and lytic cycle antigens – also expands populations of T-cells able to react with certain CNS antigens to high frequency. This observation suggests that a degree of structural mimicry is likely to exist between viral and neuronal epitopes. This theory is consistent with other epidemiological observations previously discussed, such as the increased prevalence of MS in individuals who have had IM (Thacker et al., 2006). These data imply a role for the EBV-specific T-cell repertoire in MS disease development, however their presence in people unaffected by MS suggests their contribution is more complex than a simple causal association.

Previous papers have detected autoreactive T-cells specific for neuronal antigens in healthy donors (Mazzanti et al., 2000), and T-cells with specificity for self-antigens in other autoimmune diseases have also been studied in unaffected individuals (Zou et al., 2008, Danke et al., 2004, Cao et al., 2015). The presence of myelin antigen-reactive T-cells in the blood of healthy donors as well as patients raises many questions as to why some individuals develop disease and others do not, and several studies have investigated the function and phenotype of autoreactive T-cells in MS to try to explain their relevance in disease mechanisms. One study by Cao *et al.* found myelin epitope-specific T-cells from MS patients to have different

transcriptional profiles to those of healthy donors (Cao et al., 2015). T-cells in this study were also found to produce higher levels of IFNγ, IL-17 and GM-CSF which might indicate a more pathogenic phenotype of these cells in patients, contributing to local inflammation and further immune cell recruitment to the CNS.

Due to the nature of T-cell degeneracy it is possible that stimulation with other pathogens would also create responses with a degree of reactivity to neuronal proteins, as is demonstrated in our experiments after stimulation with EBV antigens. Due to limitations in patient cell numbers creating parallel stimulations with alternative pathogens were not possible in our study, however future investigations should include a control pathogen-stimulated polyclonal T-cell line or an extra MVA encoding an alternative self-antigen not derived from the CNS. Investigation of reactivity to a non-myelin-derived self-antigen in EBV-specific T-cell populations would determine if cross-reactivity was specifically targeting neuronal proteins.

Using ICS, we analysed CNS antigen-specific CD4+ and CD8+ T-cells from wild type LCL-stimulated polyclonal T-cell lines, defining responding cells as those which produce one or more of the cytokines in our panel: IFNγ, IL-2, IL-17 and GM-CSF. Our aim was to elucidate whether there was a difference in cytokine production from myelin antigen-specific CD4+ or CD8+ T-cells expanded *ex vivo* from wild type LCL-stimulated PBMC. We found there to be no significant difference in cytokine production between cells responding to most CNS targets between groups, however there were phenotypic distinctions between MS patients and HC in their CD4+ T-cells responding to EBNA3A and CNP. CD4+ T-cell responses to CNP were very low in most individuals but one HC displayed a high percentage of responding cells in LCL-stimulated polyclonal lines which may have skewed the mean value of T-cell cytokine production.

More interesting is the difference in phenotype of EBNA3A responding cells in HC and MS patients. Findings of differential cytokine expression between EBNA3A-specific CD4+ T-cells

showed MS donor responses to predominantly produce IFNγ only, with responses from HC showing a large proportion of cells to produce GM-CSF only (Figures 6.5.5 and 6.5.17). Phenotypic differences in cells responding to this particular antigen between HC and MS patients might indicate a pathogenic role for these cells in MS *in vivo*, and further analysis of EBNA3A-specific CD4+ T-cells in MS is warranted following our study. Analysis of CD8+ T-cell responses to EBNA3A revealed there to be no significant difference in cytokine production between healthy and MS donors (Figures 6.5.21 and 6.5.33), suggesting that this difference between groups is specific to CD4+ T-cells.

No differences were seen in cytokine production or polyfunctionality of CD8+ T-cells to CNS or EBV antigens in wild type LCL-stimulated polyclonal T-cell lines, and this is in contrast with findings by Pender *et al.* who observed a decreased cytokine polyfunctionality in latent antigen-specific CD8+ T-cell responses which they attributed to cellular exhaustion (Pender et al., 2017). However, differences between these results may be due to experimental approach: our screening was performed on T-cell expansions which had been cultured *in vitro* for several weeks, with Pender *et al.* analysing cytokine production in small number of CD8+ epitope responses detected by tetramer analysis of T-cells *ex vivo*.

Cytokine production from CNS reactive T-cells has direct implications for their *in vivo* function as this can control how responses are maintained and affect surrounding tissues, influencing the inflammatory environment and perpetuating further immune cell infiltration of the CNS. Our findings of little difference between HC and MS patients in cytokine phenotype of neuronal antigen-specific T-cells is interesting, but might reflect the long-term culture conditions of cells or that T-cell lines were derived from PBMCs collected from MS patients during disease remission. Investigation of *ex vivo* CNS-specific T-cells from patients currently undergoing relapse might give further insight into the contribution these cells make to MS pathogenesis and would be a logical progressive step in our project.

Our attempts to isolate single, cross-reactive T-cells with specificity for viral and CNS antigens were extensive and employed several different approaches. The difficulty we experienced in growing these cells in culture could be reflected by a number of factors: low frequency of T-cells with dual specificity reducing likelihood of isolation, or by unsuitable growth conditions for autoreactive T-cells. Specificity or function of four T-cell clones isolated from one MS patient with reactivity to both EBNA1 and MOG was lost in culture shortly after the first screening assays for IFNγ production, preventing further characterisation studies of HLA restriction and epitope mapping. This could be attributed to T-cell exhaustion after multiple rounds of antigen stimulation or induction of anergy, and it is possible that stimulation during the TNFα capture protocol did not provide adequate stimulus for subsequent maintenance and growth of cross-reactive T-cells in culture. Our inability to generate clones despite extensive efforts supports this theory and suggests that alternative methods downstream of isolation in analysing functionality of T-cells should not use long-term culture.

Experiments exploring sorted polyclonal T-cell lines specific for wild type LCL and EBNA1 provided an alternative method of verifying reactivity to the CNS in populations of cells that were specific for EBV antigens. T-cells responding to EBV stimulation were sorted and analysed for their reactivity to neuronal proteins, and the same screening against CNS antigens was also carried out for cells that did not react to EBV antigens. Experiments with sorted wild type LCL-specific T-cell lines showed over 80% of the cells in the positive fraction to have direct specificity for LCL and the sorting to have worked. Therefore, maintenance of CNS responses in this fraction post-sorting supports a role for molecular mimicry between neuronal and EBV antigens. However, this cannot be assumed as a proportion of the population still did not react to LCL after sorting, and further investigation is needed to confirm these findings.

CD4+ and CD8+ T-cells in the negative fraction of sorted wild type LCL-stimulated polyclonal T-cell lines were also found to produce cytokine upon subsequent screening against the LCL

after two weeks. It is not clear why such high percentages of LCL-specific T-cell contaminants were left in the negative fraction as the sorting process has been shown to be very stringent, and this is further supported by the high percentage of LCL reactive T-cells found in the positive fraction in our experiments. For this reason, it is unlikely that the sorting process itself was the reason for this contamination and these cells may either have had a different phenotype at the time of sorting (producing other cytokines) before switching to become TNFα producers in culture, or they may have delayed response to LCL longer than the 4-hour incubation allowed for stimulation before sorting.

Despite this reactivity in the negative fraction of LCL and EBNA1-stimulated polyclonal lines, the maintained reactivity to CNS antigens in the T-cells sorted positively for their EBV specificity supports the view that EBV peptides may have structural homology that T-cell responses are able to cross-recognise.

Structural homology between viral and CNS epitopes has previously been described, with detailed analysis of structural interaction of a MBP (85-99) epitope presented by HLA-DR15 and a BALF5 (627-641) epitope presented by HLA-DR51 (Lang et al., 2002), alleles which are inherited together in linkage disequilibrium in the MHC locus. Other reports have identified CD4+ T-cells as having dual specificity for EBV and CNS antigens, adding to literature surrounding this phenomenon and highlighting the role these cells may play in MS disease initiation and progression (Lunemann et al., 2008b, Holmoy et al., 2004). Despite these promising findings few studies have been published since this prior research, and as such the exact contribution of molecular mimicry in MS remains to be elucidated.

Our work supports previous groups' findings of cross-reactive EBV-specific T-cells in MS patient blood. However, our study has gone further to show the extent of molecular mimicry in virus-specific T-cell responses of HC, showing LCL-stimulated polyclonal lines from both MS patients and healthy donors to have high reactivity to certain CNS proteins expressed in our

MVA virus panel. Presence of cross-reactive responses in disease-free individuals suggests that other genetic or environmental circumstances might cause some people to develop disease, and analysis of molecular mimicry in patients alongside detailed aetiological data might provide an insight into this process.

7 Final discussion

As mentioned throughout this thesis, there is increasing evidence of a role for EBV in the both development and progression of MS but no accepted theories on how the virus influences these processes.

The present study had two aims seeking to understand the connection between EBV and MS. First, to analyse the broad immune responses to EBV antigens in RRMS patients, healthy seropositive controls and those with a recent history of symptomatic primary infection. Second, to investigate T-cell responses to EBV antigens and to EBV-transformed B-cells for their ability to recognise neuronal epitopes presented by self-MHC molecules in an *in vitro* system.

7.1 Findings

EBV viral load and antibody responses were assessed in our cohort and the results compared to previous findings in the literature. Viral load was found to be unchanged in MS patients compared to healthy controls. Antibody responses to EBNA1 and VCA were found to be elevated in MS patient blood and were consistent with other MS studies with larger donor cohorts, supporting a role for these markers in calculating risk of disease. In addition to these parameters, antibody responses to EBNA3 proteins were investigated semi-quantitavely with increased frequency found to EBNA3A and EBNA3B antigens observed amongst patients compared to HC.

CD4+ and CD8+ T-cell responses to autologous wild type and BZLF1 KO LCL and EBNA1 were analysed *ex* vivo for both frequency and phenotype of responses, and ICS of T-cells allowed expression of four cytokines to be assessed: IFNγ, IL-2, IL-17 and GM-CSF. A trend

towards increased IL-17 production amongst LCL-specific T-cells from HC was observed, and in contrast MS patient cells showed elevated GM-CSF secretion after stimulation with autologous LCL. In depth analysis of *ex vivo* EBV-specific T-cell responses revealed no overall differences to exist in polyfunctionality or cytokine usage between MS patients and HC.

EBNA1-specific antibody and T-cell responses were correlated in individual donors, revealing a modest correlation between these two arms of the adaptive immune response. To our knowledge this has not previously been carried out for EBV antigens, and provides an insight into the close interplay of CD4+ T-cells with those of CD8+ T-cells and B-cells in directing immune responses to the same cognate antigen.

A panel of MVA viruses expressing neuronal antigens were used in an *in vitro* system to analyse T-cell responses to the CNS. EBV-specific T-cell responses were screened using ICS for their ability to recognise CNS antigens, and it was observed that stimulation of whole PBMC with wild type LCL caused the expansion of CD4+ and CD8+ T-cells with reactivity to certain neuronal antigens. This phenomenon was shown in both MS patients and HC, and in-depth analysis of cytokine production in response to these proteins was carried out, revealing a phenotypic difference in CD4+ T-cells between HC and MS patients responding to CNP and EBNA3A.

Final experiments using multiple protocols sought to address whether cross-reactivity could be shown in EBV-specific T-cells on a single cell level, and employment of a method to stain for TNFα on viable T-cells enabled single cell isolation of T-cells with dual specificity for EBNA1 and MOG antigens by FACS. However, these cells did not grow in culture preventing further characterisation. A separate method was subsequently used to bulk sort T-cells for TNFα production in response to autologous LCL, and it was found that reactivity to selected CNS proteins was maintained at low levels in sorted, wild type LCL-specific T-cell lines. These findings support the presence for molecular mimicry between EBV and CNS antigens, however

more research is needed in this area to fully understand this phenomenon and also to determine the immunological contribution of cross-reactive T-cells in MS.

7.2 Conclusions and future work

A number of important conclusions can be drawn from different sections in this body of work. Unchanged viral load in MS patients is indicative of a stable infection with EBV with no evidence of viral reactivation driving disease or gross loss of EBV control. This is an important clinical observation given that clinical trials are using adoptively-transferred EBV-specific CD8+ T-cells to treat MS patients (Pender et al., 2014b).

Elevated antibody responses to EBNA1 and VCA have previously been reported, but our findings of increased frequency of anti-EBNA3 IgG responses are novel and indicate that more research is needed to investigate responses to these viral antigens in MS. Further characterisation of EBNA3 antibody responses and their correlation with *ex vivo* EBNA3-specific T-cells would provide an insight into their contribution towards MS development.

This is the first in-depth analysis of cytokines produced in MS patients with age, gender and HLA-matched healthy donors, also examining differences in donors with the HLA-DR15 subtype. Extensive analysis of *ex vivo* CD4+ and CD8+ T-cell cytokine responses to autologous LCL and EBNA1 show there to be no overall differences between healthy seropositive controls and MS patients in frequency of these cells in the blood, however small differences in production of IL-17 and GM-CSF were observed in responding populations between groups. This analysis is the first time that polyfunctionality of EBV-specific T-cell responses has been analysed in depth in MS patients and healthy controls, and shows that there is no obvious functional difference between groups. However, analysis of alternative cytokines to those investigated in our study might yet identify differences in phenotype of EBV-specific T-cell

responses between HC and MS patients, and this should be a focus of further research. Investigation of EBV-specific T-cell responses from MS patient blood and CSF during relapse of disease is of prime importance, as this would provide a better insight into immunological mechanisms driving disease exacerbations.

Further analysis of the cross-reactive potential of the EBV-specific T-cell repertoire is warranted to determine the contribution of these cells to MS disease pathology, and of most interest would be differences in the T-cell frequency, phenotype and antigen specificity between periods of relapse and remission.

Inability to maintain T-cells displaying cross-reactivity *in vitro* prevented further characterisation of these cells' function in our study. Future work on these responses should include methods which do not require culture of these cells long-term. Tracking of T-cell responses by sequencing of their receptors would allow detailed analysis of T-cell repertoires through disease, and enable identification of conserved sequences between donors and disease stages. Further information regarding TCR gene usage and dynamics of T-cell populations over time during remission and relapse would provide crucial insight into how these cells contribute to disease initiation and progression.

Identification of cross-reactive epitopes between neuronal and viral proteins would allow these responses to be investigated by tetramer staining over time between relapse and remission of disease. Additional analysis of tissue homing marker expression and cytotoxic markers would allow pathogenicity of these cells to be characterised in detail. Longitudinal analysis of transcriptomes of EBV-specific T-cells from MS patients and healthy controls would also allow simultaneous investigation of many more phenotypic markers than permitted by ICS, and may reveal differences in gene expression between groups. Further sequencing of RNA transcripts from single, sorted cross-reactive cells could provide information on how these cells might be differentially regulated or their gene expression affecting development,

differentiation and function *in vivo*. Furthermore, in-depth investigation of EBV-specific T-cells in MS will allow us to construct a model of how these cells contribute towards disease. Investigation of IM is also crucial in understanding how the immune response to EBV becomes dysregulated after symptomatic primary infection. Analysis of EBV-specific CD4+ T-cell and cross-reactive responses in acute disease and through convalescence may provide a crucial insight into disease processes that pre-dispose people who have had IM to develop MS.

This work has contributed towards understanding of EBV-specific antibody and T-cell responses in MS, an area that is of crucial importance in determining what drives autoimmune attack on the CNS in patients. In the past 10 years, many more immunomodulatory therapies have become available to control inflammation in MS and associated relapses, but none of these are able to prevent progression. Better understanding of early disease is essential in the development of new drugs to target pathogenic processes and, with incidence of MS in Western countries increasing, there is a significant clinical demand for improved knowledge of the underlying autoimmune mechanisms driving CNS tissue destruction.

References

ABBOTT, R. J., QUINN, L. L., LEESE, A. M., SCHOLES, H. M., PACHNIO, A. & RICKINSON, A. B. 2013. CD8+ T cell responses to lytic EBV infection: late antigen specificities as subdominant components of the total response. *J Immunol,* 191**,** 5398-409.

ABRAHAMSSON, S. V., ANGELINI, D. F., DUBINSKY, A. N., MOREL, E., OH, U., JONES, J. L., CARASSITI, D., REYNOLDS, R., SALVETTI, M., CALABRESI, P. A., COLES, A. J., BATTISTINI, L., MARTIN, R., BURT, R. K. & MURARO, P. A. 2013. Non-myeloablative autologous haematopoietic stem cell transplantation expands regulatory cells and depletes IL-17 producing mucosal-associated invariant T cells in multiple sclerosis. *Brain,* 136**,** 2888-903.

AINIDING, G., KAWANO, Y., SATO, S., ISOBE, N., MATSUSHITA, T., YOSHIMURA, S., YONEKAWA, T., YAMASAKI, R., MURAI, H., KIRA, J. & SOUTH JAPAN MULTIPLE SCLEROSIS GENETICS, C. 2014. Interleukin 2 receptor alpha chain gene polymorphisms and risks of multiple sclerosis and neuromyelitis optica in southern Japanese. *J Neurol Sci,* 337**,** 147-50.

ALONSO, A., JICK, S. S., OLEK, M. J. & HERNAN, M. A. 2007. Incidence of multiple sclerosis in the United Kingdom : findings from a population-based cohort. *J Neurol,* 254**,** 1736-41.

ALOTAIBI, S., KENNEDY, J., TELLIER, R., STEPHENS, D. & BANWELL, B. 2004. Epstein-Barr virus in pediatric multiple sclerosis. *JAMA,* 291**,** 1875-9.

ALVAREZ-LAFUENTE, R., DE LAS HERAS, V., BARTOLOME, M., GARCIA-MONTOJO, M. & ARROYO, R. 2006. Human herpesvirus 6 and multiple sclerosis: a one-year follow-up study. *Brain Pathol,* 16**,** 20-7.

ALVAREZ-LAFUENTE, R., MARTIN-ESTEFANIA, C., DE LAS HERAS, V., CASTRILLO, C., PICAZO, J. J., VARELA DE SEIJAS, E. & GONZALEZ, R. A. 2002. Active human herpesvirus 6 infection in patients with multiple sclerosis. *Arch Neurol,* 59**,** 929-33.

ANGELINI, D. F., SERAFINI, B., PIRAS, E., SEVERA, M., COCCIA, E. M., ROSICARELLI, B., RUGGIERI, S., GASPERINI, C., BUTTARI, F., CENTONZE, D., MECHELLI, R., SALVETTI, M., BORSELLINO, G., ALOISI, F. & BATTISTINI, L. 2013. Increased CD8+ T cell response to Epstein-Barr virus lytic antigens in the active phase of multiple sclerosis. *PLoS Pathog,* 9**,** e1003220.

APCHER, S., DASKALOGIANNI, C., MANOURY, B. & FAHRAEUS, R. 2010. Epstein Barr virus-encoded EBNA1 interference with MHC class I antigen presentation reveals a close correlation between mRNA translation initiation and antigen presentation. *PLoS Pathog,* 6**,** e1001151.

APCHER, S., KOMAROVA, A., DASKALOGIANNI, C., YIN, Y., MALBERT-COLAS, L. & FAHRAEUS, R. 2009. mRNA translation regulation by the Gly-Ala repeat of Epstein-Barr virus nuclear antigen 1. *J Virol,* 83**,** 1289-98.

ASCHERIO, A. & MUNGER, K. L. 2010. 99th Dahlem conference on infection, inflammation and chronic inflammatory disorders: Epstein-Barr virus and multiple sclerosis: epidemiological evidence. *Clin Exp Immunol,* 160**,** 120-4.

ASCHERIO, A., MUNGER, K. L., LENNETTE, E. T., SPIEGELMAN, D., HERNAN, M. A., OLEK, M. J., HANKINSON, S. E. & HUNTER, D. J. 2001. Epstein-Barr virus antibodies and risk of multiple sclerosis: a prospective study. *JAMA,* 286**,** 3083-8.

AZZI, T., LUNEMANN, A., MURER, A., UEDA, S., BEZIAT, V., MALMBERG, K. J., STAUBLI, G., GYSIN, C., BERGER, C., MUNZ, C., CHIJIOKE, O. & NADAL, D. 2014. Role for early-differentiated natural killer cells in infectious mononucleosis. *Blood,* 124**,** 2533-43.

BAER, R., BANKIER, A. T., BIGGIN, M. D., DEININGER, P. L., FARRELL, P. J., GIBSON, T. J., HATFULL, G., HUDSON, G. S., SATCHWELL, S. C., SEGUIN, C. & ET AL. 1984. DNA sequence and expression of the B95-8 Epstein-Barr virus genome. *Nature,* 310**,** 207-11.

BAJRAMOVIC, J. J., LASSMANN, H. & VAN NOORT, J. M. 1997. Expression of alphaB-crystallin in glia cells during lesional development in multiple sclerosis. *J Neuroimmunol,* 78**,** 143-51.

BALFOUR, H. H., JR., ODUMADE, O. A., SCHMELING, D. O., MULLAN, B. D., ED, J. A., KNIGHT, J. A., VEZINA, H. E., THOMAS, W. & HOGQUIST, K. A. 2013. Behavioral, virologic, and immunologic factors associated with acquisition and severity of primary Epstein-Barr virus infection in university students. *J Infect Dis,* 207**,** 80-8.

BANWELL, B., KRUPP, L., KENNEDY, J., TELLIER, R., TENEMBAUM, S., NESS, J., BELMAN, A., BOIKO, A., BYKOVA, O., WAUBANT, E., MAH, J. K., STOIAN, C., KREMENCHUTZKY, M., BARDINI, M. R., RUGGIERI, M., RENSEL, M., HAHN, J., WEINSTOCK-GUTTMAN, B., YEH, E. A., FARRELL, K., FREEDMAN, M., IIVANAINEN, M., SEVON, M., BHAN, V., DILENGE, M. E., STEPHENS, D. & BAR-OR, A. 2007. Clinical features and viral serologies in children with multiple sclerosis: a multinational observational study. *Lancet Neurol,* 6**,** 773-81.

BARANZINI, S. E., MUDGE, J., VAN VELKINBURGH, J. C., KHANKHANIAN, P., KHREBTUKOVA, I., MILLER, N. A., ZHANG, L., FARMER, A. D., BELL, C. J., KIM, R. W., MAY, G. D., WOODWARD, J. E., CAILLIER, S. J., MCELROY, J. P., GOMEZ, R., PANDO, M. J., CLENDENEN, L. E., GANUSOVA, E. E., SCHILKEY, F. D., RAMARAJ, T., KHAN, O. A., HUNTLEY, J. J., LUO, S., KWOK, P. Y., WU, T. D., SCHROTH, G. P., OKSENBERG, J. R., HAUSER, S. L. & KINGSMORE, S. F. 2010. Genome, epigenome and RNA sequences of monozygotic twins discordant for multiple sclerosis. *Nature,* 464**,** 1351-6.

BARNETT, M. H., WILLIAMS, D. B., DAY, S., MACASKILL, P. & MCLEOD, J. G. 2003. Progressive increase in incidence and prevalence of multiple sclerosis in Newcastle, Australia: a 35-year study. *Journal of the Neurological Sciences,* 213**,** 1-6.

BARR, T. A., SHEN, P., BROWN, S., LAMPROPOULOU, V., ROCH, T., LAWRIE, S., FAN, B., O'CONNOR, R. A., ANDERTON, S. M., BAR-OR, A., FILLATREAU, S. & GRAY, D. 2012. B cell depletion therapy ameliorates autoimmune disease through ablation of IL-6-producing B cells. *J Exp Med,* 209**,** 1001-10.

BENNETT, C. L., CHRISTIE, J., RAMSDELL, F., BRUNKOW, M. E., FERGUSON, P. J., WHITESELL, L., KELLY, T. E., SAULSBURY, F. T., CHANCE, P. F. & OCHS, H. D. 2001. The immune dysregulation, polyendocrinopathy, enteropathy, X-linked syndrome (IPEX) is caused by mutations of FOXP3. *Nat Genet,* 27**,** 20-1.

BEVAN, M. J. 2004. Helping the CD8(+) T-cell response. *Nat Rev Immunol,* 4**,** 595-602.

BHELA, S., KEMPSELL, C., MANOHAR, M., DOMINGUEZ-VILLAR, M., GRIFFIN, R., BHATT, P., KIVISAKK-WEBB, P., FUHLBRIGGE, R., KUPPER, T., WEINER, H. & BAECHER-ALLAN, C. 2015. Nonapoptotic and extracellular activity of granzyme B mediates resistance to regulatory T cell (Treg) suppression by HLA-DR-

CD25hiCD127lo Tregs in multiple sclerosis and in response to IL-6. *J Immunol,* 194**,** 2180-9.

BIELEKOVA, B., SUNG, M. H., KADOM, N., SIMON, R., MCFARLAND, H. & MARTIN, R. 2004. Expansion and functional relevance of high-avidity myelin-specific CD4+ T cells in multiple sclerosis. *J Immunol,* 172**,** 3893-904.

BLAKE, N., HAIGH, T., SHAKA'A, G., CROOM-CARTER, D. & RICKINSON, A. 2000. The importance of exogenous antigen in priming the human CD8+ T cell response: lessons from the EBV nuclear antigen EBNA1. *J Immunol,* 165**,** 7078-87.

BRAY, P. F., LUKA, J., BRAY, P. F., CULP, K. W. & SCHLIGHT, J. P. 1992. Antibodies against Epstein-Barr nuclear antigen (EBNA) in multiple sclerosis CSF, and two pentapeptide sequence identities between EBNA and myelin basic protein. *Neurology,* 42**,** 1798-804.

BRENNAN, R. M., BURROWS, J. M., BELL, M. J., BROMHAM, L., CSURHES, P. A., LENARCZYK, A., SVERNDAL, J., KLINTENSTEDT, J., PENDER, M. P. & BURROWS, S. R. 2010. Strains of Epstein-Barr virus infecting multiple sclerosis patients. *Mult Scler,* 16**,** 643-51.

BRENNER, M. B., MCLEAN, J., DIALYNAS, D. P., STROMINGER, J. L., SMITH, J. A., OWEN, F. L., SEIDMAN, J. G., IP, S., ROSEN, F. & KRANGEL, M. S. 1986. Identification of a putative second T-cell receptor. *Nature,* 322**,** 145-9.

BREX, P. A., CICCARELLI, O., O'RIORDAN, J. I., SAILER, M., THOMPSON, A. J. & MILLER, D. H. 2002. A longitudinal study of abnormalities on MRI and disability from multiple sclerosis. *New England Journal of Medicine,* 346**,** 158-164.

BROOM, A., DOXEY, A. C., LOBSANOV, Y. D., BERTHIN, L. G., ROSE, D. R., HOWELL, P. L., MCCONKEY, B. J. & MEIERING, E. M. 2012. Modular evolution and the origins of symmetry: reconstruction of a three-fold symmetric globular protein. *Structure,* 20**,** 161-71.

BROWN, J. C. & NEWCOMB, W. W. 2011. Herpesvirus capsid assembly: insights from structural analysis. *Curr Opin Virol,* 1**,** 142-9.

BULJEVAC, D., FLACH, H. Z., HOP, W. C., HIJDRA, D., LAMAN, J. D., SAVELKOUL, H. F., VAN DER MECHE, F. G., VAN DOORN, P. A. & HINTZEN, R. Q. 2002. Prospective study on the relationship between infections and multiple sclerosis exacerbations. *Brain,* 125**,** 952-60.

BULJEVAC, D., VAN DOORNUM, G. J., FLACH, H. Z., GROEN, J., OSTERHAUS, A. D., HOP, W., VAN DOORN, P. A., VAN DER MECHE, F. G. & HINTZEN, R. Q. 2005. Epstein-Barr virus and disease activity in multiple sclerosis. *J Neurol Neurosurg Psychiatry,* 76**,** 1377-81.

BUONAMICI, S., TRIMARCHI, T., RUOCCO, M. G., REAVIE, L., CATHELIN, S., MAR, B. G., KLINAKIS, A., LUKYANOV, Y., TSENG, J. C., SEN, F., GEHRIE, E., LI, M., NEWCOMB, E., ZAVADIL, J., MERUELO, D., LIPP, M., IBRAHIM, S., EFSTRATIADIS, A., ZAGZAG, D., BROMBERG, J. S., DUSTIN, M. L. & AIFANTIS, I. 2009. CCR7 signalling as an essential regulator of CNS infiltration in T-cell leukaemia. *Nature,* 459**,** 1000-4.

CAMINERO, A., COMABELLA, M. & MONTALBAN, X. 2011. Role of tumour necrosis factor (TNF)-alpha and TNFRSF1A R92Q mutation in the pathogenesis of TNF receptor-associated periodic syndrome and multiple sclerosis. *Clin Exp Immunol,* 166**,** 338-45.

CAO, Y., GOODS, B. A., RADDASSI, K., NEPOM, G. T., KWOK, W. W., LOVE, J. C. & HAFLER, D. A. 2015. Functional inflammatory profiles distinguish myelin-reactive T cells from patients with multiple sclerosis. *Sci Transl Med,* 7**,** 287ra74.

CASTELLAZZI, M., CONTINI, C., TAMBORINO, C., FASOLO, F., ROVERSI, G., SERACENI, S., RIZZO, R., BALDI, E., TOLA, M. R., BELLINI, T., GRANIERI, E. & FAINARDI, E. 2014. Epstein-Barr virus-specific intrathecal oligoclonal IgG production in relapsing-remitting multiple sclerosis is limited to a subset of patients and is composed of low-affinity antibodies. *J Neuroinflammation,* 11**,** 188.

CASTELLAZZI, M., TAMBORINO, C., CANI, A., NEGRI, E., BALDI, E., SERACENI, S., TOLA, M. R., GRANIERI, E., CONTINI, C. & FAINARDI, E. 2010. Epstein-Barr virus-specific antibody response in cerebrospinal fluid and serum of patients with multiple sclerosis. *Mult Scler,* 16**,** 883-7.

CAVANILLAS, M. L., ALCINA, A., NUNEZ, C., DE LAS HERAS, V., FERNANDEZ-ARQUERO, M., BARTOLOME, M., DE LA CONCHA, E. G., FERNANDEZ, O., ARROYO, R., MATESANZ, F. & URCELAY, E. 2010. Polymorphisms in the IL2, IL2RA and IL2RB genes in multiple sclerosis risk. *Eur J Hum Genet,* 18**,** 794-9.

CEPOK, S., ZHOU, D., SRIVASTAVA, R., NESSLER, S., STEI, S., BUSSOW, K., SOMMER, N. & HEMMER, B. 2005. Identification of Epstein-Barr virus proteins as putative targets of the immune response in multiple sclerosis. *J Clin Invest,* 115**,** 1352-60.

CERMELLI, C. & JACOBSON, S. 2000. Viruses and multiple sclerosis. *Viral Immunol,* 13**,** 255-67.

CHAN, K. C. 2014. Plasma Epstein-Barr virus DNA as a biomarker for nasopharyngeal carcinoma. *Chin J Cancer,* 33**,** 598-603.

CHAO, M. J., HERRERA, B. M., RAMAGOPALAN, S. V., DELUCA, G., HANDUNETTHI, L., ORTON, S. M., LINCOLN, M. R., SADOVNICK, A. D. & EBERS, G. C. 2010. Parent-of-origin effects at the major histocompatibility complex in multiple sclerosis. *Hum Mol Genet,* 19**,** 3679-89.

CHEN, J. L., WEI, L., BERECZKI, D., HANS, F. J., OTSUKA, T., ACUFF, V., GHERSI-EGEA, J. F., PATLAK, C. & FENSTERMACHER, J. D. 1995. Nicotine raises the influx of permeable solutes across the rat blood-brain barrier with little or no capillary recruitment. *J Cereb Blood Flow Metab,* 15**,** 687-98.

CHIJIOKE, O., MULLER, A., FEEDERLE, R., BARROS, M. H., KRIEG, C., EMMEL, V., MARCENARO, E., LEUNG, C. S., ANTSIFEROVA, O., LANDTWING, V., BOSSART, W., MORETTA, A., HASSAN, R., BOYMAN, O., NIEDOBITEK, G., DELECLUSE, H. J., CAPAUL, R. & MUNZ, C. 2013. Human natural killer cells prevent infectious mononucleosis features by targeting lytic Epstein-Barr virus infection. *Cell Rep,* 5**,** 1489-98.

CHOU, Y. K., BURROWS, G. G., LATOCHA, D., WANG, C., SUBRAMANIAN, S., BOURDETTE, D. N. & VANDENBARK, A. A. 2004. CD4 T-cell epitopes of human alpha B-crystallin. *J Neurosci Res,* 75**,** 516-23.

CITI, S. & CORDENONSI, M. 1998. Tight junction proteins. *Biochim Biophys Acta,* 1448**,** 1-11.

COCUZZA, C. E., PIAZZA, F., MUSUMECI, R., OGGIONI, D., ANDREONI, S., GARDINETTI, M., FUSCO, L., FRIGO, M., BANFI, P., ROTTOLI, M. R., CONFALONIERI, P., REZZONICO, M., FERRO, M. T., CAVALETTI, G. & GROUP, E.-M. I. S. 2014. Quantitative detection of epstein-barr virus DNA in cerebrospinal fluid and blood samples of patients with relapsing-remitting multiple sclerosis. *PLoS One,* 9**,** e94497.

CODARRI, L., GYULVESZI, G., TOSEVSKI, V., HESSKE, L., FONTANA, A., MAGNENAT, L., SUTER, T. & BECHER, B. 2011. RORgammat drives production of the cytokine GM-CSF in helper T cells, which is essential for the effector phase of autoimmune neuroinflammation. *Nat Immunol,* 12**,** 560-7.

COLLABORATION, N. C. D. R. F. 2016. Trends in adult body-mass index in 200 countries from 1975 to 2014: a pooled analysis of 1698 population-based measurement studies with 19.2 million participants. *Lancet,* 387**,** 1377-96.

COMABELLA, M., KAKALACHEVA, K., RIO, J., MUNZ, C., MONTALBAN, X. & LUNEMANN, J. D. 2012. EBV-specific immune responses in patients with multiple sclerosis responding to IFNbeta therapy. *Mult Scler,* 18**,** 605-9.

COMOLI, P., LABIRIO, M., BASSO, S., BALDANTI, F., GROSSI, P., FURIONE, M., VIGANO, M., FIOCCHI, R., ROSSI, G., GINEVRI, F., GRIDELLI, B., MORETTA, A., MONTAGNA, D., LOCATELLI, F., GERNA, G. & MACCARIO, R. 2002. Infusion of autologous Epstein-Barr virus (EBV)-specific cytotoxic T cells for prevention of EBV-related lymphoproliferative disorder in solid organ transplant recipients with evidence of active virus replication. *Blood,* 99**,** 2592-8.

COMPSTON, D. A., BATCHELOR, J. R. & MCDONALD, W. I. 1976. B-lymphocyte alloantigens associated with multiple sclerosis. *Lancet,* 2**,** 1261-5.

COOPER, M. D., PETERSON, R. D. & GOOD, R. A. 1965. Delineation of the Thymic and Bursal Lymphoid Systems in the Chicken. *Nature,* 205**,** 143-6.

COWLAND, J. B. & BORREGAARD, N. 2016. Granulopoiesis and granules of human neutrophils. *Immunol Rev,* 273**,** 11-28.

CRAIG, J. C., HAIRE, M. & MERRETT, J. D. 1988. T-cell-mediated suppression of Epstein-Barr virus-induced B lymphocyte activation in multiple sclerosis. *Clin Immunol Immunopathol,* 48**,** 253-60.

CRAIG, J. C., HAIRE, M., MILLAR, J. H., FRASER, K. B. & MERRETT, J. D. 1983. Immunological control of Epstein-Barr virus-transformed lymphocytes in multiple sclerosis. *Clin Immunol Immunopathol,* 29**,** 86-93.

CULLEN, S. P. & MARTIN, S. J. 2008. Mechanisms of granule-dependent killing. *Cell Death Differ,* 15**,** 251-62.

DANKE, N. A., KOELLE, D. M., YEE, C., BEHERAY, S. & KWOK, W. W. 2004. Autoreactive T cells in healthy individuals. *J Immunol,* 172**,** 5967-72.

DANN, S. M. & ECKMANN, L. 2007. Innate immune defenses in the intestinal tract. *Curr Opin Gastroenterol,* 23**,** 115-20.

DE JAGER, P. L., SIMON, K. C., MUNGER, K. L., RIOUX, J. D., HAFLER, D. A. & ASCHERIO, A. 2008. Integrating risk factors: HLA-DRB1*1501 and Epstein-Barr virus in multiple sclerosis. *Neurology,* 70**,** 1113-8.

DEBBABI, H., GHOSH, S., KAMATH, A. B., ALT, J., DEMELLO, D. E., DUNSMORE, S. & BEHAR, S. M. 2005. Primary type II alveolar epithelial cells present microbial antigens to antigen-specific CD4+ T cells. *Am J Physiol Lung Cell Mol Physiol,* 289**,** L274-9.

DELORENZE, G. N., MUNGER, K. L., LENNETTE, E. T., ORENTREICH, N., VOGELMAN, J. H. & ASCHERIO, A. 2006. Epstein-Barr virus and multiple sclerosis: evidence of association from a prospective study with long-term follow-up. *Arch Neurol,* 63**,** 839-44.

DENDROU, C. A., FUGGER, L. & FRIESE, M. A. 2015. Immunopathology of multiple sclerosis. *Nat Rev Immunol,* 15**,** 545-58.

DHIB-JALBUT, S. & MARKS, S. 2010. Interferon-beta mechanisms of action in multiple sclerosis. *Neurology,* 74 Suppl 1**,** S17-24.

DJELILOVIC-VRANIC, J. & ALAJBEGOVIC, A. 2012. Role of early viral infections in development of multiple sclerosis. *Med Arch,* 66**,** 37-40.

DOOLEY, M. M., DE GANNES, S. L., FU, K. A. & LINDSEY, J. W. 2016. The increased antibody response to Epstein-Barr virus in multiple sclerosis is restricted to selected virus proteins. *J Neuroimmunol,* 299**,** 147-151.

DU, C., LIU, C., KANG, J., ZHAO, G., YE, Z., HUANG, S., LI, Z., WU, Z. & PEI, G. 2009. MicroRNA miR-326 regulates TH-17 differentiation and is associated with the pathogenesis of multiple sclerosis. *Nat Immunol,* 10**,** 1252-9.

DUAN, S., LV, Z., FAN, X., WANG, L., HAN, F., WANG, H. & BI, S. 2014. Vitamin D status and the risk of multiple sclerosis: a systematic review and meta-analysis. *Neurosci Lett,* 570**,** 108-13.

DYMENT, D. A., YEE, I. M., EBERS, G. C., SADOVNICK, A. D. & CANADIAN COLLABORATIVE STUDY, G. 2006. Multiple sclerosis in stepsiblings: recurrence risk and ascertainment. *J Neurol Neurosurg Psychiatry,* 77**,** 258-9.

EBERS, G. C., SADOVNICK, A. D. & RISCH, N. J. 1995. A genetic basis for familial aggregation in multiple sclerosis. Canadian Collaborative Study Group. *Nature,* 377**,** 150-1.

EISEN, H. N. 2014. Affinity enhancement of antibodies: how low-affinity antibodies produced early in immune responses are followed by high-affinity antibodies later and in memory B-cell responses. *Cancer Immunol Res,* 2**,** 381-92.

EPSTEIN, A. 2015. Why and How Epstein-Barr Virus Was Discovered 50 Years Ago. *Curr Top Microbiol Immunol,* 390**,** 3-15.

FAGARASAN, S. & HONJO, T. 2000. T-Independent immune response: new aspects of B cell biology. *Science,* 290**,** 89-92.

FAN, X., JIN, T., ZHAO, S., LIU, C., HAN, J., JIANG, X. & JIANG, Y. 2015. Circulating CCR7+ICOS+ Memory T Follicular Helper Cells in Patients with Multiple Sclerosis. *PLoS One,* 10**,** e0134523.

FARRELL, P. J. 2015. Epstein-Barr Virus Strain Variation. *Curr Top Microbiol Immunol,* 390**,** 45-69.

FARRELL, R. A., ANTONY, D., WALL, G. R., CLARK, D. A., FISNIKU, L., SWANTON, J., KHALEELI, Z., SCHMIERER, K., MILLER, D. H. & GIOVANNONI, G. 2009. Humoral immune response to EBV in multiple sclerosis is associated with disease activity on MRI. *Neurology,* 73**,** 32-8.

FAZEKAS DE ST GROTH, B., SMITH, A. L. & HIGGINS, C. A. 2004. T cell activation: in vivo veritas. *Immunol Cell Biol,* 82**,** 260-8.

FEEDERLE, R., KOST, M., BAUMANN, M., JANZ, A., DROUET, E., HAMMERSCHMIDT, W. & DELECLUSE, H. J. 2000. The Epstein-Barr virus lytic program is controlled by the co-operative functions of two transactivators. *EMBO J,* 19**,** 3080-9.

FEGER, U., LUTHER, C., POESCHEL, S., MELMS, A., TOLOSA, E. & WIENDL, H. 2007. Increased frequency of CD4+ CD25+ regulatory T cells in the cerebrospinal fluid but not in the blood of multiple sclerosis patients. *Clin Exp Immunol,* 147**,** 412-8.

FILIPPI, M., ROCCA, M. A., CICCARELLI, O., DE STEFANO, N., EVANGELOU, N., KAPPOS, L., ROVIRA, A., SASTRE-GARRIGA, J., TINTORE, M., FREDERIKSEN, J. L., GASPERINI, C., PALACE, J., REICH, D. S., BANWELL, B., MONTALBAN, X., BARKHOF, F. & GROUP, M. S. 2016. MRI criteria for the diagnosis of multiple sclerosis: MAGNIMS consensus guidelines. *Lancet Neurol,* 15**,** 292-303.

FLETCHER, J. M., LONERGAN, R., COSTELLOE, L., KINSELLA, K., MORAN, B., O'FARRELLY, C., TUBRIDY, N. & MILLS, K. H. 2009. CD39+Foxp3+ regulatory T Cells suppress pathogenic Th17 cells and are impaired in multiple sclerosis. *J Immunol,* 183**,** 7602-10.

FORSTER, R., DAVALOS-MISSLITZ, A. C. & ROT, A. 2008. CCR7 and its ligands: balancing immunity and tolerance. *Nat Rev Immunol,* 8**,** 362-71.

FORTHAL, D. N. 2014. Functions of Antibodies. *Microbiol Spectr,* 2**,** 1-17.

FRANCISCO-CRUZ, A., AGUILAR-SANTELISES, M., RAMOS-ESPINOSA, O., MATA-ESPINOSA, D., MARQUINA-CASTILLO, B., BARRIOS-PAYAN, J. & HERNANDEZ-PANDO, R. 2014. Granulocyte-macrophage colony-stimulating factor: not just another haematopoietic growth factor. *Med Oncol,* 31**,** 774.

FRASER, K. B., HAIRE, M., MILLAR, J. H. & MCCREA, S. 1979. Increased tendency to spontaneous in-vitro lymphocyte transformation in clinically active multiple sclerosis. *Lancet,* 2**,** 175-6.

FRIEDMAN, H. M. 2006. Keratin, a dual role in herpes simplex virus pathogenesis. *J Clin Virol,* 35**,** 103-5.

FRISCHER, J. M., BRAMOW, S., DAL-BIANCO, A., LUCCHINETTI, C. F., RAUSCHKA, H., SCHMIDBAUER, M., LAURSEN, H., SORENSEN, P. S. & LASSMANN, H. 2009. The relation between inflammation and neurodegeneration in multiple sclerosis brains. *Brain,* 132**,** 1175-89.

FRISULLO, G., NOCITI, V., IORIO, R., PATANELLA, A. K., MARTI, A., CAGGIULA, M., MIRABELLA, M., TONALI, P. A. & BATOCCHI, A. P. 2008. IL17 and IFNgamma production by peripheral blood mononuclear cells from clinically isolated syndrome to secondary progressive multiple sclerosis. *Cytokine,* 44**,** 22-5.

GALE, C. R. & MARTYN, C. N. 1995. Migrant studies in multiple sclerosis. *Prog Neurobiol,* 47**,** 425-48.

GARRETT, T. P., SAPER, M. A., BJORKMAN, P. J., STROMINGER, J. L. & WILEY, D. C. 1989. Specificity pockets for the side chains of peptide antigens in HLA-Aw68. *Nature,* 342**,** 692-6.

GARTNER, B. C., SCHAFER, H., MARGGRAFF, K., EISELE, G., SCHAFER, M., DILLOO, D., ROEMER, K., LAWS, H. J., SESTER, M., SESTER, U., EINSELE, H. & MUELLER-LANTZSCH, N. 2002. Evaluation of use of Epstein-Barr viral load in patients after allogeneic stem cell transplantation to diagnose and monitor posttransplant lymphoproliferative disease. *J Clin Microbiol,* 40**,** 351-8.

GEGINAT, J., PARONI, M., MAGLIE, S., ALFEN, J. S., KASTIRR, I., GRUARIN, P., DE SIMONE, M., PAGANI, M. & ABRIGNANI, S. 2014. Plasticity of human CD4 T cell subsets. *Front Immunol,* 5**,** 630.

GELLERT, M. 2002. V(D)J recombination: RAG proteins, repair factors, and regulation. *Annu Rev Biochem,* 71**,** 101-32.

GITLIN, A. D. & NUSSENZWEIG, M. C. 2015. Immunology: Fifty years of B lymphocytes. *Nature,* 517**,** 139-41.

GNJATIC, S., ATANACKOVIC, D., JAGER, E., MATSUO, M., SELVAKUMAR, A., ALTORKI, N. K., MAKI, R. G., DUPONT, B., RITTER, G., CHEN, Y. T., KNUTH, A. & OLD, L. J. 2003. Survey of naturally occurring CD4+ T cell responses against NY-ESO-1 in cancer patients: correlation with antibody responses. *Proc Natl Acad Sci U S A,* 100**,** 8862-7.

GOLDBERG, S. H., ALBRIGHT, A. V., LISAK, R. P. & GONZALEZ-SCARANO, F. 1999. Polymerase chain reaction analysis of human herpesvirus-6 sequences in the sera and cerebrospinal fluid of patients with multiple sclerosis. *J Neurovirol,* 5**,** 134-9.

GOULDEN, R., IBRAHIM, T. & WOLFSON, C. 2015. Is high socioeconomic status a risk factor for multiple sclerosis? A systematic review. *Eur J Neurol,* 22**,** 899-911.

GRANGEOT-KEROS, L. & COINTE, D. 2001. Diagnosis and prognostic markers of HCMV infection. *J Clin Virol,* 21**,** 213-21.

GREGORY, S. G., SCHMIDT, S., SETH, P., OKSENBERG, J. R., HART, J., PROKOP, A., CAILLIER, S. J., BAN, M., GORIS, A., BARCELLOS, L. F., LINCOLN, R., MCCAULEY, J. L., SAWCER, S. J., COMPSTON, D. A., DUBOIS, B., HAUSER, S. L., GARCIA-BLANCO, M. A., PERICAK-VANCE, M. A., HAINES, J. L. &

MULTIPLE SCLEROSIS GENETICS, G. 2007. Interleukin 7 receptor alpha chain (IL7R) shows allelic and functional association with multiple sclerosis. *Nat Genet,* 39**,** 1083-91.

GRONEN, F., RUPRECHT, K., WEISSBRICH, B., KLINKER, E., KRONER, A., HOFSTETTER, H. H. & RIECKMANN, P. 2006. Frequency analysis of HLA-B7-restricted Epstein-Barr virus-specific cytotoxic T lymphocytes in patients with multiple sclerosis and healthy controls. *J Neuroimmunol,* 180**,** 185-92.

GRYTTEN, N., TORKILDSEN, O. & MYHR, K. M. 2015. Time trends in the incidence and prevalence of multiple sclerosis in Norway during eight decades. *Acta Neurol Scand,* 132**,** 29-36.

HACKETT, J., JR., SWANSON, P., LEAHY, D., ANDERSON, E. L., SATO, S., ROOS, R. P., DECKER, R. & DEVARE, S. G. 1996. Search for retrovirus in patients with multiple sclerosis. *Ann Neurol,* 40**,** 805-9.

HANDEL, A. E., WILLIAMSON, A. J., DISANTO, G., DOBSON, R., GIOVANNONI, G. & RAMAGOPALAN, S. V. 2011. Smoking and multiple sclerosis: an updated meta-analysis. *PLoS One,* 6**,** e16149.

HAQUE, T., WILKIE, G. M., TAYLOR, C., AMLOT, P. L., MURAD, P., ILEY, A., DOMBAGODA, D., BRITTON, K. M., SWERDLOW, A. J. & CRAWFORD, D. H. 2002. Treatment of Epstein-Barr-virus-positive post-transplantation lymphoproliferative disease with partly HLA-matched allogeneic cytotoxic T cells. *Lancet,* 360**,** 436-42.

HARTMANN, F. J., KHADEMI, M., ARAM, J., AMMANN, S., KOCKUM, I., CONSTANTINESCU, C., GRAN, B., PIEHL, F., OLSSON, T., CODARRI, L. & BECHER, B. 2014. Multiple sclerosis-associated IL2RA polymorphism controls GM-CSF production in human TH cells. *Nat Commun,* 5**,** 5056.

HAUSER, S. L., WAUBANT, E., ARNOLD, D. L., VOLLMER, T., ANTEL, J., FOX, R. J., BAR-OR, A., PANZARA, M., SARKAR, N., AGARWAL, S., LANGER-GOULD, A., SMITH, C. H. & GROUP, H. T. 2008. B-cell depletion with rituximab in relapsing-remitting multiple sclerosis. *N Engl J Med,* 358**,** 676-88.

HEDSTROM, A. K., OLSSON, T. & ALFREDSSON, L. 2012. High body mass index before age 20 is associated with increased risk for multiple sclerosis in both men and women. *Mult Scler,* 18**,** 1334-6.

HEDSTROM, A. K., SUNDQVIST, E., BAARNHIELM, M., NORDIN, N., HILLERT, J., KOCKUM, I., OLSSON, T. & ALFREDSSON, L. 2011. Smoking and two human leukocyte antigen genes interact to increase the risk for multiple sclerosis. *Brain,* 134**,** 653-64.

HELLINGS, N., BAREE, M., VERHOEVEN, C., D'HOOGHE M, B., MEDAER, R., BERNARD, C. C., RAUS, J. & STINISSEN, P. 2001. T-cell reactivity to multiple myelin antigens in multiple sclerosis patients and healthy controls. *J Neurosci Res,* 63**,** 290-302.

HENEKA, M. T., KUMMER, M. P. & LATZ, E. 2014. Innate immune activation in neurodegenerative disease. *Nat Rev Immunol,* 14**,** 463-77.

HIRANO, M., DAS, S., GUO, P. & COOPER, M. D. 2011. The evolution of adaptive immunity in vertebrates. *Adv Immunol,* 109**,** 125-57.

HISLOP, A. D., KUO, M., DRAKE-LEE, A. B., AKBAR, A. N., BERGLER, W., HAMMERSCHMITT, N., KHAN, N., PALENDIRA, U., LEESE, A. M., TIMMS, J. M., BELL, A. I., BUCKLEY, C. D. & RICKINSON, A. B. 2005. Tonsillar homing of Epstein-Barr virus-specific CD8+ T cells and the virus-host balance. *J Clin Invest,* 115**,** 2546-55.

HOLLSBERG, P., HANSEN, H. J. & HAAHR, S. 2003. Altered CD8+ T cell responses to selected Epstein-Barr virus immunodominant epitopes in patients with multiple sclerosis. *Clin Exp Immunol,* 132**,** 137-43.

HOLMOY, T., KVALE, E. O. & VARTDAL, F. 2004. Cerebrospinal fluid CD4+ T cells from a multiple sclerosis patient cross-recognize Epstein-Barr virus and myelin basic protein. *J Neurovirol,* 10**,** 278-83.

HORAKOVA, D., ZIVADINOV, R., WEINSTOCK-GUTTMAN, B., HAVRDOVA, E., QU, J., TAMANO-BLANCO, M., BADGETT, D., TYBLOVA, M., BERGSLAND, N., HUSSEIN, S., WILLIS, L., KRASENSKY, J., VANECKOVA, M., SEIDL, Z., LELKOVA, P., DWYER, M. G., ZHANG, M., YU, H., DUAN, X., KALINCIK, T. & RAMANATHAN, M. 2013. Environmental factors associated with disease progression after the first demyelinating event: results from the multi-center SET study. *PLoS One,* 8**,** e53996.

HOUZEN, H., NIINO, M., KIKUCHI, S., FUKAZAWA, T., NOGOSHI, S., MATSUMOTO, H. & TASHIRO, K. 2003. The prevalence and clinical characteristics of MS in northern Japan. *Journal of the Neurological Sciences,* 211**,** 49-53.

HOWELL, O. W., REEVES, C. A., NICHOLAS, R., CARASSITI, D., RADOTRA, B., GENTLEMAN, S. M., SERAFINI, B., ALOISI, F., RONCAROLI, F., MAGLIOZZI, R. & REYNOLDS, R. 2011. Meningeal inflammation is widespread and linked to cortical pathology in multiple sclerosis. *Brain,* 134**,** 2755-71.

HUANG, X. L., FAN, Z., COLLETON, B. A., BUCHLI, R., LI, H., HILDEBRAND, W. H. & RINALDO, C. R., JR. 2005. Processing and presentation of exogenous HLA class I peptides by dendritic cells from human immunodeficiency virus type 1-infected persons. *J Virol,* 79**,** 3052-62.

INGRAM, G., BUGERT, J. J., LOVELESS, S. & ROBERTSON, N. P. 2010. Anti-EBNA-1 IgG is not a reliable marker of multiple sclerosis clinical disease activity. *Eur J Neurol,* 17**,** 1386-9.

INTERNATIONAL MULTIPLE SCLEROSIS GENETICS, C., HAFLER, D. A., COMPSTON, A., SAWCER, S., LANDER, E. S., DALY, M. J., DE JAGER, P. L., DE BAKKER, P. I., GABRIEL, S. B., MIREL, D. B., IVINSON, A. J., PERICAK-VANCE, M. A., GREGORY, S. G., RIOUX, J. D., MCCAULEY, J. L., HAINES, J. L., BARCELLOS, L. F., CREE, B., OKSENBERG, J. R. & HAUSER, S. L. 2007. Risk alleles for multiple sclerosis identified by a genomewide study. *N Engl J Med,* 357**,** 851-62.

ITANO, A. A. & JENKINS, M. K. 2003. Antigen presentation to naive CD4 T cells in the lymph node. *Nat Immunol,* 4**,** 733-9.

JAFARI, N., VAN NIEROP, G. P., VERJANS, G. M., OSTERHAUS, A. D., MIDDELDORP, J. M. & HINTZEN, R. Q. 2010. No evidence for intrathecal IgG synthesis to Epstein Barr virus nuclear antigen-1 in multiple sclerosis. *J Clin Virol,* 49**,** 26-31.

JAQUIERY, E., JILEK, S., SCHLUEP, M., MEYLAN, P., LYSANDROPOULOS, A., PANTALEO, G. & DU PASQUIER, R. A. 2010. Intrathecal immune responses to EBV in early MS. *Eur J Immunol,* 40**,** 878-87.

JI, Q., CASTELLI, L. & GOVERMAN, J. M. 2013. MHC class I-restricted myelin epitopes are cross-presented by Tip-DCs that promote determinant spreading to CD8(+) T cells. *Nat Immunol,* 14**,** 254-61.

JI, Q., PERCHELLET, A. & GOVERMAN, J. M. 2010. Viral infection triggers central nervous system autoimmunity via activation of CD8+ T cells expressing dual TCRs. *Nat Immunol,* 11**,** 628-34.

JILEK, S., SCHLUEP, M., HARARI, A., CANALES, M., LYSANDROPOULOS, A., ZEKERIDOU, A., PANTALEO, G. & DU PASQUIER, R. A. 2012. HLA-B7-

restricted EBV-specific CD8+ T cells are dysregulated in multiple sclerosis. *J Immunol,* 188**,** 4671-80.

JILEK, S., SCHLUEP, M., MEYLAN, P., VINGERHOETS, F., GUIGNARD, L., MONNEY, A., KLEEBERG, J., LE GOFF, G., PANTALEO, G. & DU PASQUIER, R. A. 2008. Strong EBV-specific CD8+ T-cell response in patients with early multiple sclerosis. *Brain,* 131**,** 1712-21.

JUNKER, A., KRUMBHOLZ, M., EISELE, S., MOHAN, H., AUGSTEIN, F., BITTNER, R., LASSMANN, H., WEKERLE, H., HOHLFELD, R. & MEINL, E. 2009. MicroRNA profiling of multiple sclerosis lesions identifies modulators of the regulatory protein CD47. *Brain,* 132**,** 3342-52.

KAECH, S. M. & AHMED, R. 2001. Memory CD8+ T cell differentiation: initial antigen encounter triggers a developmental program in naive cells. *Nat Immunol,* 2**,** 415-22.

KAPPOS, L., LI, D., CALABRESI, P. A., O'CONNOR, P., BAR-OR, A., BARKHOF, F., YIN, M., LEPPERT, D., GLANZMAN, R., TINBERGEN, J. & HAUSER, S. L. 2011. Ocrelizumab in relapsing-remitting multiple sclerosis: a phase 2, randomised, placebo-controlled, multicentre trial. *Lancet,* 378**,** 1779-87.

KIVISAKK, P., MAHAD, D. J., CALLAHAN, M. K., SIKORA, K., TREBST, C., TUCKY, B., WUJEK, J., RAVID, R., STAUGAITIS, S. M., LASSMANN, H. & RANSOHOFF, R. M. 2004. Expression of CCR7 in multiple sclerosis: implications for CNS immunity. *Ann Neurol,* 55**,** 627-38.

KOINI, M., FILIPPI, M., ROCCA, M. A., YOUSRY, T., CICCARELLI, O., TEDESCHI, G., GALLO, A., ROPELE, S., VALSASINA, P., RICCITELLI, G., DAMJANOVIC, D., MUHLERT, N., MANCINI, L., FAZEKAS, F., ENZINGER, C. & GROUP, M. F. S. 2016. Correlates of Executive Functions in Multiple Sclerosis Based on Structural and Functional MR Imaging: Insights from a Multicenter Study. *Radiology,* 280**,** 869-79.

KOSTIC, M., DZOPALIC, T., ZIVANOVIC, S., ZIVKOVIC, N., CVETANOVIC, A., STOJANOVIC, I., VOJINOVIC, S., MARJANOVIC, G., SAVIC, V. & COLIC, M. 2014. IL-17 and glutamate excitotoxicity in the pathogenesis of multiple sclerosis. *Scand J Immunol,* 79**,** 181-6.

KOSTIC, M., STOJANOVIC, I., MARJANOVIC, G., ZIVKOVIC, N. & CVETANOVIC, A. 2015. Deleterious versus protective autoimmunity in multiple sclerosis. *Cell Immunol,* 296**,** 122-32.

KOZOVSKA, M. E., HONG, J., ZANG, Y. C., LI, S., RIVERA, V. M., KILLIAN, J. M. & ZHANG, J. Z. 1999. Interferon beta induces T-helper 2 immune deviation in MS. *Neurology,* 53**,** 1692-7.

KRAMETTER, D., NIEDERWIESER, G., BERGHOLD, A., BIRNBAUM, G., STRASSER-FUCHS, S., HARTUNG, H. P. & ARCHELOS, J. J. 2001. Chlamydia pneumoniae in multiple sclerosis: humoral immune responses in serum and cerebrospinal fluid and correlation with disease activity marker. *Mult Scler,* 7**,** 13-8.

KURTZKE, J. F. 2013. Epidemiology in multiple sclerosis: a pilgrim's progress. *Brain,* 136**,** 2904-17.

KURTZKE, J. F., BEEBE, G. W. & NORMAN, J. E., JR. 1985. Epidemiology of multiple sclerosis in US veterans: III. Migration and the risk of MS. *Neurology,* 35**,** 672-8.

KURTZKE, J. F. & HELTBERG, A. 2001. Multiple sclerosis in the Faroe Islands: an epitome. *J Clin Epidemiol,* 54**,** 1-22.

KVISTAD, S., MYHR, K. M., HOLMOY, T., BAKKE, S., BEISKE, A. G., BJERVE, K. S., HOVDAL, H., LOKEN-AMSRUD, K. I., LILLEAS, F., MIDGARD, R., NJOLSTAD, G., PEDERSEN, T., BENTH, J. S., WERGELAND, S. & TORKILDSEN, O. 2014. Antibodies to Epstein-Barr virus and MRI disease activity in multiple sclerosis. *Mult Scler,* 20**,** 1833-40.

LANG, D., VORNHAGEN, R., ROTHE, M., HINDERER, W., SONNEBORN, H. H. & PLACHTER, B. 2001. Cross-reactivity of Epstein-Barr virus-specific immunoglobulin M antibodies with cytomegalovirus antigens containing glycine homopolymers. *Clin Diagn Lab Immunol,* 8**,** 747-56.

LANG, H. L., JACOBSEN, H., IKEMIZU, S., ANDERSSON, C., HARLOS, K., MADSEN, L., HJORTH, P., SONDERGAARD, L., SVEJGAARD, A., WUCHERPFENNIG, K., STUART, D. I., BELL, J. I., JONES, E. Y. & FUGGER, L. 2002. A functional and structural basis for TCR cross-reactivity in multiple sclerosis. *Nat Immunol,* 3**,** 940-3.

LANZAVECCHIA, A. & SALLUSTO, F. 2001. The instructive role of dendritic cells on T cell responses: lineages, plasticity and kinetics. *Curr Opin Immunol,* 13**,** 291-8.

LARSEN, J. M., STEEN-JENSEN, D. B., LAURSEN, J. M., SONDERGAARD, J. N., MUSAVIAN, H. S., BUTT, T. M. & BRIX, S. 2012a. Divergent pro-inflammatory profile of human dendritic cells in response to commensal and pathogenic bacteria associated with the airway microbiota. *PLoS One,* 7**,** e31976.

LARSEN, M., SAUCE, D., ARNAUD, L., FASTENACKELS, S., APPAY, V. & GOROCHOV, G. 2012b. Evaluating cellular polyfunctionality with a novel polyfunctionality index. *PLoS One,* 7**,** e42403.

LARSEN, M., SAUCE, D., DEBACK, C., ARNAUD, L., MATHIAN, A., MIYARA, M., BOUTOLLEAU, D., PARIZOT, C., DORGHAM, K., PAPAGNO, L., APPAY, V., AMOURA, Z. & GOROCHOV, G. 2011. Exhausted cytotoxic control of Epstein-Barr virus in human lupus. *PLoS Pathog,* 7**,** e1002328.

LARSEN, P. D., BLOOMER, L. C. & BRAY, P. F. 1985. Epstein-Barr nuclear antigen and viral capsid antigen antibody titers in multiple sclerosis. *Neurology,* 35**,** 435-8.

LASSMANN, H., NIEDOBITEK, G., ALOISI, F., MIDDELDORP, J. M. & NEUROPROMISE, E. B. V. W. G. 2011. Epstein-Barr virus in the multiple sclerosis brain: a controversial issue--report on a focused workshop held in the Centre for Brain Research of the Medical University of Vienna, Austria. *Brain,* 134**,** 2772-86.

LAY, M. L., LUCAS, R. M., TOI, C., RATNAMOHAN, M., PONSONBY, A. L. & DWYER, D. E. 2012. Epstein-Barr virus genotypes and strains in central nervous system demyelinating disease and Epstein-Barr virus-related illnesses in Australia. *Intervirology,* 55**,** 372-9.

LAYDON, D. J., BANGHAM, C. R. & ASQUITH, B. 2015. Estimating T-cell repertoire diversity: limitations of classical estimators and a new approach. *Philos Trans R Soc Lond B Biol Sci,* 370.

LEUNG, C. S., HAIGH, T. A., MACKAY, L. K., RICKINSON, A. B. & TAYLOR, G. S. 2010. Nuclear location of an endogenously expressed antigen, EBNA1, restricts access to macroautophagy and the range of CD4 epitope display. *Proc Natl Acad Sci U S A,* 107**,** 2165-70.

LEVIN, L. I., MUNGER, K. L., O'REILLY, E. J., FALK, K. I. & ASCHERIO, A. 2010. Primary infection with the Epstein-Barr virus and risk of multiple sclerosis. *Ann Neurol,* 67**,** 824-30.

LEVIN, L. I., MUNGER, K. L., RUBERTONE, M. V., PECK, C. A., LENNETTE, E. T., SPIEGELMAN, D. & ASCHERIO, A. 2005. Temporal relationship between elevation of epstein-barr virus antibody titers and initial onset of neurological symptoms in multiple sclerosis. *JAMA,* 293**,** 2496-500.

LEVITSKAYA, J., CORAM, M., LEVITSKY, V., IMREH, S., STEIGERWALD-MULLEN, P. M., KLEIN, G., KURILLA, M. G. & MASUCCI, M. G. 1995. Inhibition of antigen processing by the internal repeat region of the Epstein-Barr virus nuclear antigen-1. *Nature,* 375**,** 685-8.

LEW, A. M., PARDOLL, D. M., MALOY, W. L., FOWLKES, B. J., KRUISBEEK, A., CHENG, S. F., GERMAIN, R. N., BLUESTONE, J. A., SCHWARTZ, R. H. & COLIGAN, J. E. 1986. Characterization of T cell receptor gamma chain expression in a subset of murine thymocytes. *Science,* 234**,** 1401-5.

LI, R., REZK, A., MIYAZAKI, Y., HILGENBERG, E., TOUIL, H., SHEN, P., MOORE, C. S., MICHEL, L., ALTHEKAIR, F., RAJASEKHARAN, S., GOMMERMAN, J. L., PRAT, A., FILLATREAU, S., BAR-OR, A. & CANADIAN, B. C. I. M. S. T. 2015. Proinflammatory GM-CSF-producing B cells in multiple sclerosis and B cell depletion therapy. *Sci Transl Med,* 7**,** 310ra166.

LI, X. & ZHENG, Y. 2015. Regulatory T cell identity: formation and maintenance. *Trends Immunol,* 36**,** 344-53.

LICHTY, J. J., MALECKI, J. L., AGNEW, H. D., MICHELSON-HOROWITZ, D. J. & TAN, S. 2005. Comparison of affinity tags for protein purification. *Protein Expr Purif,* 41**,** 98-105.

LIEDTKE, W., MALESSA, R., FAUSTMANN, P. M. & EIS-HUBINGER, A. M. 1995. Human herpesvirus 6 polymerase chain reaction findings in human immunodeficiency virus associated neurological disease and multiple sclerosis. *J Neurovirol,* 1**,** 253-8.

LIN, J. X. & LEONARD, W. J. 1997. Signaling from the IL-2 receptor to the nucleus. *Cytokine Growth Factor Rev,* 8**,** 313-32.

LINDSEY, J. W., DEGANNES, S. L., PATE, K. A. & ZHAO, X. 2016. Antibodies specific for Epstein-Barr virus nuclear antigen-1 cross-react with human heterogeneous nuclear ribonucleoprotein L. *Mol Immunol,* 69**,** 7-12.

LINDSEY, J. W. & HATFIELD, L. M. 2010. Epstein-Barr virus and multiple sclerosis: cellular immune response and cross-reactivity. *J Neuroimmunol,* 229**,** 238-42.

LINDSEY, J. W., HATFIELD, L. M., CRAWFORD, M. P. & PATEL, S. 2009. Quantitative PCR for Epstein-Barr virus DNA and RNA in multiple sclerosis. *Mult Scler,* 15**,** 153-8.

LINDSEY, J. W., HATFIELD, L. M. & VU, T. 2010. Epstein-Barr virus neutralizing and early antigen antibodies in multiple sclerosis. *Eur J Neurol,* 17**,** 1263-9.

LINDSEY, J. W., PATEL, S. & ZOU, J. 2008. Epstein-Barr virus genotypes in multiple sclerosis. *Acta Neurol Scand,* 117**,** 141-4.

LINK, J., LORENTZEN, A. R., KOCKUM, I., DUVEFELT, K., LIE, B. A., CELIUS, E. G., HARBO, H. F., HILLERT, J. & BRYNEDAL, B. 2010. Two HLA class I genes independently associated with multiple sclerosis. *J Neuroimmunol,* 226**,** 172-6.

LISAK, R. P., BENJAMINS, J. A., NEDELKOSKA, L., BARGER, J. L., RAGHEB, S., FAN, B., OUAMARA, N., JOHNSON, T. A., RAJASEKHARAN, S. & BAR-OR, A. 2012. Secretory products of multiple sclerosis B cells are cytotoxic to oligodendroglia in vitro. *J Neuroimmunol,* 246**,** 85-95.

LONG, H. M., CHAGOURY, O. L., LEESE, A. M., RYAN, G. B., JAMES, E., MORTON, L. T., ABBOTT, R. J., SABBAH, S., KWOK, W. & RICKINSON, A. B. 2013. MHC II tetramers visualize human CD4+ T cell responses to Epstein-Barr virus infection and demonstrate atypical kinetics of the nuclear antigen EBNA1 response. *J Exp Med,* 210**,** 933-49.

LONG, H. M., ZUO, J., LEESE, A. M., GUDGEON, N. H., JIA, H., TAYLOR, G. S. & RICKINSON, A. B. 2009. CD4+ T-cell clones recognizing human lymphoma-associated antigens: generation by in vitro stimulation with autologous Epstein-Barr virus-transformed B cells. *Blood,* 114**,** 807-15.

LOUVEAU, A., SMIRNOV, I., KEYES, T. J., ECCLES, J. D., ROUHANI, S. J., PESKE, J. D., DERECKI, N. C., CASTLE, D., MANDELL, J. W., LEE, K. S., HARRIS, T. H. &

KIPNIS, J. 2015. Structural and functional features of central nervous system lymphatic vessels. *Nature,* 523**,** 337-41.

LUCAS, R. M., PONSONBY, A. L., DEAR, K., VALERY, P., PENDER, M. P., BURROWS, J. M., BURROWS, S. R., CHAPMAN, C., COULTHARD, A., DWYER, D. E., DWYER, T., KILPATRICK, T., LAY, M. L., MCMICHAEL, A. J., TAYLOR, B. V., VAN DER MEI, I. A. & WILLIAMS, D. 2011. Current and past Epstein-Barr virus infection in risk of initial CNS demyelination. *Neurology,* 77**,** 371-9.

LUND, O., NIELSEN, M., KESMIR, C., PETERSEN, A. G., LUNDEGAARD, C., WORNING, P., SYLVESTER-HVID, C., LAMBERTH, K., RODER, G., JUSTESEN, S., BUUS, S. & BRUNAK, S. 2004. Definition of supertypes for HLA molecules using clustering of specificity matrices. *Immunogenetics,* 55**,** 797-810.

LUNEMANN, J. D., EDWARDS, N., MURARO, P. A., HAYASHI, S., COHEN, J. I., MUNZ, C. & MARTIN, R. 2006. Increased frequency and broadened specificity of latent EBV nuclear antigen-1-specific T cells in multiple sclerosis. *Brain,* 129**,** 1493-506.

LUNEMANN, J. D., HUPPKE, P., ROBERTS, S., BRUCK, W., GARTNER, J. & MUNZ, C. 2008a. Broadened and elevated humoral immune response to EBNA1 in pediatric multiple sclerosis. *Neurology,* 71**,** 1033-5.

LUNEMANN, J. D., JELCIC, I., ROBERTS, S., LUTTEROTTI, A., TACKENBERG, B., MARTIN, R. & MUNZ, C. 2008b. EBNA1-specific T cells from patients with multiple sclerosis cross react with myelin antigens and co-produce IFN-gamma and IL-2. *J Exp Med,* 205**,** 1763-73.

LUNEMANN, J. D., TINTORE, M., MESSMER, B., STROWIG, T., ROVIRA, A., PERKAL, H., CABALLERO, E., MUNZ, C., MONTALBAN, X. & COMABELLA, M. 2010. Elevated Epstein-Barr virus-encoded nuclear antigen-1 immune responses predict conversion to multiple sclerosis. *Ann Neurol,* 67**,** 159-69.

LUZURIAGA, K. & SULLIVAN, J. L. 2010. Infectious mononucleosis. *N Engl J Med,* 362**,** 1993-2000.

MACKENZIE, I. S., MORANT, S. V., BLOOMFIELD, G. A., MACDONALD, T. M. & O'RIORDAN, J. 2014. Incidence and prevalence of multiple sclerosis in the UK 1990-2010: a descriptive study in the General Practice Research Database. *J Neurol Neurosurg Psychiatry,* 85**,** 76-84.

MACLENNAN, I. C., TOELLNER, K. M., CUNNINGHAM, A. F., SERRE, K., SZE, D. M., ZUNIGA, E., COOK, M. C. & VINUESA, C. G. 2003. Extrafollicular antibody responses. *Immunol Rev,* 194**,** 8-18.

MAGLIOZZI, R., HOWELL, O., VORA, A., SERAFINI, B., NICHOLAS, R., PUOPOLO, M., REYNOLDS, R. & ALOISI, F. 2007. Meningeal B-cell follicles in secondary progressive multiple sclerosis associate with early onset of disease and severe cortical pathology. *Brain,* 130**,** 1089-104.

MAKRYGIANNAKIS, D., HERMANSSON, M., ULFGREN, A. K., NICHOLAS, A. P., ZENDMAN, A. J., EKLUND, A., GRUNEWALD, J., SKOLD, C. M., KLARESKOG, L. & CATRINA, A. I. 2008. Smoking increases peptidylarginine deiminase 2 enzyme expression in human lungs and increases citrullination in BAL cells. *Ann Rheum Dis,* 67**,** 1488-92.

MAMELI, G., COSSU, D., COCCO, E., MASALA, S., FRAU, J., MARROSU, M. G. & SECHI, L. A. 2014. Epstein-Barr virus and Mycobacterium avium subsp. paratuberculosis peptides are cross recognized by anti-myelin basic protein antibodies in multiple sclerosis patients. *J Neuroimmunol,* 270**,** 51-5.

MASSA, J., MUNGER, K. L., O'REILLY, E. J., FALK, K. I. & ASCHERIO, A. 2007. Plasma titers of antibodies against Epstein-Barr virus BZLF1 and risk of multiple sclerosis. *Neuroepidemiology,* 28**,** 214-5.

MASTRONARDI, F. G., NOOR, A., WOOD, D. D., PATON, T. & MOSCARELLO, M. A. 2007. Peptidyl argininedeiminase 2 CpG island in multiple sclerosis white matter is hypomethylated. *J Neurosci Res,* 85**,** 2006-16.

MAURER, M. A., RAKOCEVIC, G., LEUNG, C. S., QUAST, I., LUKACISIN, M., GOEBELS, N., MUNZ, C., WARDEMANN, H., DALAKAS, M. & LUNEMANN, J. D. 2012. Rituximab induces sustained reduction of pathogenic B cells in patients with peripheral nervous system autoimmunity. *J Clin Invest,* 122**,** 1393-402.

MAYO, L., TRAUGER, S. A., BLAIN, M., NADEAU, M., PATEL, B., ALVAREZ, J. I., MASCANFRONI, I. D., YESTE, A., KIVISAKK, P., KALLAS, K., ELLEZAM, B., BAKSHI, R., PRAT, A., ANTEL, J. P., WEINER, H. L. & QUINTANA, F. J. 2014. Regulation of astrocyte activation by glycolipids drives chronic CNS inflammation. *Nat Med,* 20**,** 1147-56.

MAZZANTI, B., HEMMER, B., TRAGGIAI, E., BALLERINI, C., MCFARLAND, H. F., MASSACESI, L., MARTIN, R. & VERGELLI, M. 2000. Decrypting the spectrum of antigen-specific T-cell responses: the avidity repertoire of MBP-specific T-cells. *J Neurosci Res,* 59**,** 86-93.

MCMAHON, E. J., BAILEY, S. L., CASTENADA, C. V., WALDNER, H. & MILLER, S. D. 2005. Epitope spreading initiates in the CNS in two mouse models of multiple sclerosis. *Nat Med,* 11**,** 335-9.

MECHELLI, R., MANZARI, C., POLICANO, C., ANNESE, A., PICARDI, E., UMETON, R., FORNASIERO, A., D'ERCHIA, A. M., BUSCARINU, M. C., AGLIARDI, C., ANNIBALI, V., SERAFINI, B., ROSICARELLI, B., ROMANO, S., ANGELINI, D. F., RICIGLIANO, V. A., BUTTARI, F., BATTISTINI, L., CENTONZE, D., GUERINI, F. R., D'ALFONSO, S., PESOLE, G., SALVETTI, M. & RISTORI, G. 2015. Epstein-Barr virus genetic variants are associated with multiple sclerosis. *Neurology,* 84**,** 1362-8.

MELCHERS, F., TEN BOEKEL, E., SEIDL, T., KONG, X. C., YAMAGAMI, T., ONISHI, K., SHIMIZU, T., ROLINK, A. G. & ANDERSSON, J. 2000. Repertoire selection by pre-B-cell receptors and B-cell receptors, and genetic control of B-cell development from immature to mature B cells. *Immunol Rev,* 175**,** 33-46.

MILLER, A., SHAPIRO, S., GERSHTEIN, R., KINARTY, A., RAWASHDEH, H., HONIGMAN, S. & LAHAT, N. 1998. Treatment of multiple sclerosis with copolymer-1 (Copaxone): implicating mechanisms of Th1 to Th2/Th3 immune-deviation. *J Neuroimmunol,* 92**,** 113-21.

MILLER, D., BARKHOF, F., MONTALBAN, X., THOMPSON, A. & FILIPPI, M. 2005. Clinically isolated syndromes suggestive of multiple sclerosis, part 1: natural history, pathogenesis, diagnosis, and prognosis. *Lancet Neurology,* 4**,** 281-288.

MINAMI, Y., KONO, T., MIYAZAKI, T. & TANIGUCHI, T. 1993. The IL-2 receptor complex: its structure, function, and target genes. *Annu Rev Immunol,* 11**,** 245-68.

MOND, J. J., LEES, A. & SNAPPER, C. M. 1995. T cell-independent antigens type 2. *Annu Rev Immunol,* 13**,** 655-92.

MOON, U. Y., PARK, S. J., OH, S. T., KIM, W. U., PARK, S. H., LEE, S. H., CHO, C. S., KIM, H. Y., LEE, W. K. & LEE, S. K. 2004. Patients with systemic lupus erythematosus have abnormally elevated Epstein-Barr virus load in blood. *Arthritis Res Ther,* 6**,** R295-302.

MOSMANN, T. R., CHERWINSKI, H., BOND, M. W., GIEDLIN, M. A. & COFFMAN, R. L. 2005. Two types of murine helper T cell clone. I. Definition according to profiles of lymphokine activities and secreted proteins. 1986. *J Immunol,* 175**,** 5-14.

MOSMANN, T. R. & COFFMAN, R. L. 1989. Heterogeneity of cytokine secretion patterns and functions of helper T cells. *Adv Immunol,* 46**,** 111-47.

MOUDGIL, K. D., SERCARZ, E. E. & GREWAL, I. S. 1998. Modulation of the immunogenicity of antigenic determinants by their flanking residues. *Immunol Today,* 19**,** 217-20.

MUMFORD, C. J., WOOD, N. W., KELLAR-WOOD, H., THORPE, J. W., MILLER, D. H. & COMPSTON, D. A. 1994. The British Isles survey of multiple sclerosis in twins. *Neurology,* 44**,** 11-5.

MUNGER, K. L., CHITNIS, T. & ASCHERIO, A. 2009. Body size and risk of MS in two cohorts of US women. *Neurology,* 73**,** 1543-50.

MUNGER, K. L., LEVIN, L. I., HOLLIS, B. W., HOWARD, N. S. & ASCHERIO, A. 2006. Serum 25-hydroxyvitamin D levels and risk of multiple sclerosis. *JAMA,* 296**,** 2832-8.

MUNGER, K. L., LEVIN, L. I., O'REILLY, E. J., FALK, K. I. & ASCHERIO, A. 2011. Anti-Epstein-Barr virus antibodies as serological markers of multiple sclerosis: a prospective study among United States military personnel. *Mult Scler,* 17**,** 1185-93.

MURAT, P., ZHONG, J., LEKIEFFRE, L., COWIESON, N. P., CLANCY, J. L., PREISS, T., BALASUBRAMANIAN, S., KHANNA, R. & TELLAM, J. 2014. G-quadruplexes regulate Epstein-Barr virus-encoded nuclear antigen 1 mRNA translation. *Nat Chem Biol,* 10**,** 358-64.

MURATA, T. 2014. Regulation of Epstein-Barr virus reactivation from latency. *Microbiol Immunol,* 58**,** 307-17.

MURRAY, T. J. 2009. The history of multiple sclerosis: the changing frame of the disease over the centuries. *J Neurol Sci,* 277 Suppl 1**,** S3-8.

NIELSEN, L., LARSEN, A. M., MUNK, M. & VESTERGAARD, B. F. 1997. Human herpesvirus-6 immunoglobulin G antibodies in patients with multiple sclerosis. *Acta Neurol Scand Suppl,* 169**,** 76-8.

NITTA, T., MURATA, S., UENO, T., TANAKA, K. & TAKAHAMA, Y. 2008. Thymic microenvironments for T-cell repertoire formation. *Adv Immunol,* 99**,** 59-94.

NIZZOLI, G., KRIETSCH, J., WEICK, A., STEINFELDER, S., FACCIOTTI, F., GRUARIN, P., BIANCO, A., STECKEL, B., MORO, M., CROSTI, M., ROMAGNANI, C., STOLZEL, K., TORRETTA, S., PIGNATARO, L., SCHEIBENBOGEN, C., NEDDERMANN, P., DE FRANCESCO, R., ABRIGNANI, S. & GEGINAT, J. 2013. Human CD1c+ dendritic cells secrete high levels of IL-12 and potently prime cytotoxic T-cell responses. *Blood,* 122**,** 932-42.

NOSTER, R., RIEDEL, R., MASHREGHI, M. F., RADBRUCH, H., HARMS, L., HAFTMANN, C., CHANG, H. D., RADBRUCH, A. & ZIELINSKI, C. E. 2014. IL-17 and GM-CSF expression are antagonistically regulated by human T helper cells. *Sci Transl Med,* 6**,** 241ra80.

OLIVAL, G. S., LIMA, B. M., SUMITA, L. M., SERAFIM, V., FINK, M. C., NALI, L. H., ROMANO, C. M., THOMAZ, R. B., CAVENAGHI, V. B., TILBERY, C. P. & PENALVA-DE-OLIVEIRA, A. C. 2013. Multiple sclerosis and herpesvirus interaction. *Arq Neuropsiquiatr,* 71**,** 727-30.

OLSON, J. K., CROXFORD, J. L., CALENOFF, M. A., DAL CANTO, M. C. & MILLER, S. D. 2001. A virus-induced molecular mimicry model of multiple sclerosis. *J Clin Invest,* 108**,** 311-8.

ORTON, S.-M., HERRERA, B. M., YEE, I. M., VALDAR, W., RAMAGOPALAN, S. V., SADOVNICK, A. D., EBERS, G. C. & CANADIAN COLLABORATIVE STUDY, G. 2006. Sex ratio of multiple sclerosis in Canada: a longitudinal study. *Lancet Neurology,* 5**,** 932-936.

PAKPOOR, J., DISANTO, G., GERBER, J. E., DOBSON, R., MEIER, U. C., GIOVANNONI, G. & RAMAGOPALAN, S. V. 2013. The risk of developing multiple sclerosis in individuals seronegative for Epstein-Barr virus: a meta-analysis. *Mult Scler,* 19**,** 162-6.

PAKPOOR, J. & RAMAGOPALAN, S. 2015. Evidence for an Association Between Vitamin D and Multiple Sclerosis. *Curr Top Behav Neurosci,* 26**,** 105-15.
PARDRIDGE, W. M. 2012. Drug transport across the blood-brain barrier. *J Cereb Blood Flow Metab,* 32**,** 1959-72.
PEARSON, G. R. 1988. ELISA tests and monoclonal antibodies for EBV. *J Virol Methods,* 21**,** 97-104.
PENDER, M. P., CSURHES, P. A., BURROWS, J. M. & BURROWS, S. R. 2017. Defective T-cell control of Epstein-Barr virus infection in multiple sclerosis. *Clin Transl Immunology,* 6**,** e126.
PENDER, M. P., CSURHES, P. A., LENARCZYK, A., PFLUGER, C. M. & BURROWS, S. R. 2009. Decreased T cell reactivity to Epstein-Barr virus infected lymphoblastoid cell lines in multiple sclerosis. *J Neurol Neurosurg Psychiatry,* 80**,** 498-505.
PENDER, M. P., CSURHES, P. A., PFLUGER, C. M. & BURROWS, S. R. 2014a. Deficiency of CD8+ effector memory T cells is an early and persistent feature of multiple sclerosis. *Mult Scler,* 20**,** 1825-32.
PENDER, M. P., CSURHES, P. A., SMITH, C., BEAGLEY, L., HOOPER, K. D., RAJ, M., COULTHARD, A., BURROWS, S. R. & KHANNA, R. 2014b. Epstein-Barr virus-specific adoptive immunotherapy for progressive multiple sclerosis. *Mult Scler,* 20**,** 1541-4.
PETRIE, H. T., LIVAK, F., SCHATZ, D. G., STRASSER, A., CRISPE, I. N. & SHORTMAN, K. 1993. Multiple rearrangements in T cell receptor alpha chain genes maximize the production of useful thymocytes. *J Exp Med,* 178**,** 615-22.
PFUHL, C., OECHTERING, J., RASCHE, L., GIESS, R. M., BEHRENS, J. R., WAKONIG, K., FREITAG, E., PACHE, F. C., OTTO, C., HOFMANN, J., EBERSPACHER, B., BELLMANN-STROBL, J., PAUL, F. & RUPRECHT, K. 2015. Association of serum Epstein-Barr nuclear antigen-1 antibodies and intrathecal immunoglobulin synthesis in early multiple sclerosis. *J Neuroimmunol,* 285**,** 156-60.
PLOTKIN, S. A. 2001. Immunologic correlates of protection induced by vaccination. *Pediatr Infect Dis J,* 20**,** 63-75.
POHL, D., KRONE, B., ROSTASY, K., KAHLER, E., BRUNNER, E., LEHNERT, M., WAGNER, H. J., GARTNER, J. & HANEFELD, F. 2006. High seroprevalence of Epstein-Barr virus in children with multiple sclerosis. *Neurology,* 67**,** 2063-5.
POHL, D., ROSTASY, K., JACOBI, C., LANGE, P., NAU, R., KRONE, B. & HANEFELD, F. 2010. Intrathecal antibody production against Epstein-Barr and other neurotropic viruses in pediatric and adult onset multiple sclerosis. *J Neurol,* 257**,** 212-6.
POLMAN, C. H., O'CONNOR, P. W., HAVRDOVA, E., HUTCHINSON, M., KAPPOS, L., MILLER, D. H., PHILLIPS, J. T., LUBLIN, F. D., GIOVANNONI, G., WAJGT, A., TOAL, M., LYNN, F., PANZARA, M. A., SANDROCK, A. W. & INVESTIGATORS, A. 2006. A randomized, placebo-controlled trial of natalizumab for relapsing multiple sclerosis. *N Engl J Med,* 354**,** 899-910.
POSER, C. M., HIBBERD, P. L., BENEDIKZ, J. & GUDMUNDSSON, G. 1988. Analysis of the 'epidemic' of multiple sclerosis in the Faroe Islands. I. Clinical and epidemiological aspects. *Neuroepidemiology,* 7**,** 168-80.
PRECOPIO, M. L., SULLIVAN, J. L., WILLARD, C., SOMASUNDARAN, M. & LUZURIAGA, K. 2003. Differential kinetics and specificity of EBV-specific CD4+ and CD8+ T cells during primary infection. *J Immunol,* 170**,** 2590-8.
QI, H. 2016. T follicular helper cells in space-time. *Nat Rev Immunol,* 16**,** 612-25.
QUACH, Q. L., METZ, L. M., THOMAS, J. C., ROTHBARD, J. B., STEINMAN, L. & OUSMAN, S. S. 2013. CRYAB modulates the activation of CD4+ T cells from relapsing-remitting multiple sclerosis patients. *Mult Scler,* 19**,** 1867-77.

RACKE, M. K., LOVETT-RACKE, A. E. & KARANDIKAR, N. J. 2010. The mechanism of action of glatiramer acetate treatment in multiple sclerosis. *Neurology,* 74 Suppl 1**,** S25-30.

RADBRUCH, A., MUEHLINGHAUS, G., LUGER, E. O., INAMINE, A., SMITH, K. G., DORNER, T. & HIEPE, F. 2006. Competence and competition: the challenge of becoming a long-lived plasma cell. *Nat Rev Immunol,* 6**,** 741-50.

RADTKE, F., MACDONALD, H. R. & TACCHINI-COTTIER, F. 2013. Regulation of innate and adaptive immunity by Notch. *Nat Rev Immunol,* 13**,** 427-37.

RAINEY-BARGER, E. K., BLAKELY, P. K., HUBER, A. K., SEGAL, B. M. & IRANI, D. N. 2013. Virus-induced CD8+ T cells accelerate the onset of experimental autoimmune encephalomyelitis: implications for how viral infections might trigger multiple sclerosis exacerbations. *J Neuroimmunol,* 259**,** 47-54.

RAMMENSEE, H., BACHMANN, J., EMMERICH, N. P., BACHOR, O. A. & STEVANOVIC, S. 1999. SYFPEITHI: database for MHC ligands and peptide motifs. *Immunogenetics,* 50**,** 213-9.

RAMROODI, N., NIAZI, A. A., SANADGOL, N., GANJALI, Z. & SARABANDI, V. 2013. Evaluation of reactive Epstein-Barr Virus (EBV) in Iranian patient with different subtypes of multiple sclerosis (MS). *Braz J Infect Dis,* 17**,** 156-63.

RANSOHOFF, R. M. & ENGELHARDT, B. 2012. The anatomical and cellular basis of immune surveillance in the central nervous system. *Nat Rev Immunol,* 12**,** 623-35.

RASMUSSEN, H. B., GENY, C., DEFORGES, L., PERRON, H., TOURTELOTTE, W., HELTBERG, A. & CLAUSEN, J. 1997. Expression of endogenous retroviruses in blood mononuclear cells and brain tissue from multiple sclerosis patients. *Acta Neurol Scand Suppl,* 169**,** 38-44.

RASOULI, J., CIRIC, B., IMITOLA, J., GONNELLA, P., HWANG, D., MAHAJAN, K., MARI, E. R., SAFAVI, F., LEIST, T. P., ZHANG, G. X. & ROSTAMI, A. 2015. Expression of GM-CSF in T Cells Is Increased in Multiple Sclerosis and Suppressed by IFN-beta Therapy. *J Immunol,* 194**,** 5085-93.

REBOLDI, A., COISNE, C., BAUMJOHANN, D., BENVENUTO, F., BOTTINELLI, D., LIRA, S., UCCELLI, A., LANZAVECCHIA, A., ENGELHARDT, B. & SALLUSTO, F. 2009. C-C chemokine receptor 6-regulated entry of TH-17 cells into the CNS through the choroid plexus is required for the initiation of EAE. *Nat Immunol,* 10**,** 514-23.

RECH, A. J., MICK, R., MARTIN, S., RECIO, A., AQUI, N. A., POWELL, D. J., JR., COLLIGON, T. A., TROSKO, J. A., LEINBACH, L. I., PLETCHER, C. H., TWEED, C. K., DEMICHELE, A., FOX, K. R., DOMCHEK, S. M., RILEY, J. L. & VONDERHEIDE, R. H. 2012. CD25 blockade depletes and selectively reprograms regulatory T cells in concert with immunotherapy in cancer patients. *Sci Transl Med,* 4**,** 134ra62.

REICH, A., ERLWEIN, O., NIEWIESK, S., TER MEULEN, V. & LIEBERT, U. G. 1992. CD4+ T cells control measles virus infection of the central nervous system. *Immunology,* 76**,** 185-91.

RHODES, G., RUMPOLD, H., KURKI, P., PATRICK, K. M., CARSON, D. A. & VAUGHAN, J. H. 1987. Autoantibodies in infectious mononucleosis have specificity for the glycine-alanine repeating region of the Epstein-Barr virus nuclear antigen. *J Exp Med,* 165**,** 1026-40.

RODSTROM, K. E., ELBING, K. & LINDKVIST-PETERSSON, K. 2014. Structure of the superantigen staphylococcal enterotoxin B in complex with TCR and peptide-MHC demonstrates absence of TCR-peptide contacts. *J Immunol,* 193**,** 1998-2004.

ROSE, J. W., WATT, H. E., WHITE, A. T. & CARLSON, N. G. 2004. Treatment of multiple sclerosis with an anti-interleukin-2 receptor monoclonal antibody. *Ann Neurol,* 56**,** 864-7.

ROWE, M., FITZSIMMONS, L. & BELL, A. I. 2014. Epstein-Barr virus and Burkitt lymphoma. *Chin J Cancer,* 33**,** 609-19.

ROWE, M., LEAR, A. L., CROOM-CARTER, D., DAVIES, A. H. & RICKINSON, A. B. 1992. Three pathways of Epstein-Barr virus gene activation from EBNA1-positive latency in B lymphocytes. *J Virol,* 66**,** 122-31.

ROWE, M., YOUNG, L. S., CADWALLADER, K., PETTI, L., KIEFF, E. & RICKINSON, A. B. 1989. Distinction between Epstein-Barr virus type A (EBNA 2A) and type B (EBNA 2B) isolates extends to the EBNA 3 family of nuclear proteins. *J Virol,* 63**,** 1031-9.

RUMPOLD, H., RHODES, G. H., BLOCH, P. L., CARSON, D. A. & VAUGHAN, J. H. 1987. The glycine-alanine repeating region is the major epitope of the Epstein-Barr nuclear antigen-1 (EBNA-1). *J Immunol,* 138**,** 593-9.

RUPRECHT, K., WUNDERLICH, B., GIESS, R., MEYER, P., LOEBEL, M., LENZ, K., HOFMANN, J., ROSCHE, B., WENGERT, O., PAUL, F., REIMER, U. & SCHEIBENBOGEN, C. 2014. Multiple sclerosis: the elevated antibody response to Epstein-Barr virus primarily targets, but is not confined to, the glycine-alanine repeat of Epstein-Barr nuclear antigen-1. *J Neuroimmunol,* 272**,** 56-61.

SALZER, J., HALLMANS, G., NYSTROM, M., STENLUND, H., WADELL, G. & SUNDSTROM, P. 2013. Smoking as a risk factor for multiple sclerosis. *Mult Scler,* 19**,** 1022-7.

SANADGOL, N., RAMROODI, N., AHMADI, G. A., KOMIJANI, M., MOGHTADERI, A., BOUZARI, M., REZAEI, M., KARDI, M. T., DABIRI, S., MORADI, M. & SANADGOL, E. 2011. Prevalence of cytomegalovirus infection and its role in total immunoglobulin pattern in Iranian patients with different subtypes of multiple sclerosis. *New Microbiol,* 34**,** 263-74.

SANTIAGO, O., GUTIERREZ, J., SORLOZANO, A., DE DIOS LUNA, J., VILLEGAS, E. & FERNANDEZ, O. 2010. Relation between Epstein-Barr virus and multiple sclerosis: analytic study of scientific production. *Eur J Clin Microbiol Infect Dis,* 29**,** 857-66.

SANTON, A., CRISTOBAL, E., APARICIO, M., ROYUELA, A., VILLAR, L. M. & ALVAREZ-CERMENO, J. C. 2011. High frequency of co-infection by Epstein-Barr virus types 1 and 2 in patients with multiple sclerosis. *Mult Scler,* 17**,** 1295-300.

SARGSYAN, S. A., SERKOVA, N. J., RENNER, B., HASEBROOCK, K. M., LARSEN, B., STOLDT, C., MCFANN, K., PICKERING, M. C. & THURMAN, J. M. 2012. Detection of glomerular complement C3 fragments by magnetic resonance imaging in murine lupus nephritis. *Kidney Int,* 81**,** 152-9.

SARMA, J. V. & WARD, P. A. 2011. The complement system. *Cell Tissue Res,* 343**,** 227-35.

SCHNEIDER, A., LONG, S. A., CEROSALETTI, K., NI, C. T., SAMUELS, P., KITA, M. & BUCKNER, J. H. 2013. In active relapsing-remitting multiple sclerosis, effector T cell resistance to adaptive T(regs) involves IL-6-mediated signaling. *Sci Transl Med,* 5**,** 170ra15.

SCHOENBORN, J. R. & WILSON, C. B. 2007. Regulation of interferon-gamma during innate and adaptive immune responses. *Adv Immunol,* 96**,** 41-101.

SEGAL, B. M., CONSTANTINESCU, C. S., RAYCHAUDHURI, A., KIM, L., FIDELUS-GORT, R., KASPER, L. H. & USTEKINUMAB, M. S. I. 2008. Repeated subcutaneous injections of IL12/23 p40 neutralising antibody, ustekinumab, in patients with relapsing-remitting multiple sclerosis: a phase II, double-blind, placebo-controlled, randomised, dose-ranging study. *Lancet Neurol,* 7**,** 796-804.

SERAFINI, B., ROSICARELLI, B., FRANCIOTTA, D., MAGLIOZZI, R., REYNOLDS, R., CINQUE, P., ANDREONI, L., TRIVEDI, P., SALVETTI, M., FAGGIONI, A. & ALOISI, F. 2007. Dysregulated Epstein-Barr virus infection in the multiple sclerosis brain. *J Exp Med,* 204**,** 2899-912.

SERAFINI, B., SCORSI, E., ROSICARELLI, B., RIGAU, V., THOUVENOT, E. & ALOISI, F. 2017. Massive intracerebral Epstein-Barr virus reactivation in lethal multiple sclerosis relapse after natalizumab withdrawal. *J Neuroimmunol,* 307**,** 14-17.

SHECHTER, R., LONDON, A. & SCHWARTZ, M. 2013. Orchestrated leukocyte recruitment to immune-privileged sites: absolute barriers versus educational gates. *Nat Rev Immunol,* 13**,** 206-18.

SHEEHAN, J. K., KESIMER, M. & PICKLES, R. 2006. Innate immunity and mucus structure and function. *Novartis Found Symp,* 279**,** 155-66; discussion 167-9, 216-9.

SHENG, W., YANG, F., ZHOU, Y., YANG, H., LOW, P. Y., KEMENY, D. M., TAN, P., MOH, A., KAPLAN, M. H., ZHANG, Y. & FU, X. Y. 2014. STAT5 programs a distinct subset of GM-CSF-producing T helper cells that is essential for autoimmune neuroinflammation. *Cell Res,* 24**,** 1387-402.

SHLOMCHIK, M. J. 2008. Sites and stages of autoreactive B cell activation and regulation. *Immunity,* 28**,** 18-28.

SIMON, K. C., O'REILLY, E. J., MUNGER, K. L., FINERTY, S., MORGAN, A. J. & ASCHERIO, A. 2012. Epstein-Barr virus neutralizing antibody levels and risk of multiple sclerosis. *Mult Scler,* 18**,** 1185-7.

SINCLAIR, A. J. 2013. Epigenetic control of Epstein-Barr virus transcription - relevance to viral life cycle? *Front Genet,* 4**,** 161.

SKARE, J., EDSON, C., FARLEY, J. & STROMINGER, J. L. 1982. The B95-8 isolate of Epstein-Barr virus arose from an isolate with a standard genome. *J Virol,* 44**,** 1088-91.

SMYK, D. S., ALEXANDER, A. K., WALKER, M. & WALKER, M. 2014. Acute disseminated encephalomyelitis progressing to multiple sclerosis: are infectious triggers involved? *Immunol Res,* 60**,** 16-22.

SPARKS-THISSEN, R. L., BRAATEN, D. C., KREHER, S., SPECK, S. H. & VIRGIN, H. W. T. 2004. An optimized CD4 T-cell response can control productive and latent gammaherpesvirus infection. *J Virol,* 78**,** 6827-35.

SRIRAM, S., STRATTON, C. W., YAO, S., THARP, A., DING, L., BANNAN, J. D. & MITCHELL, W. M. 1999. Chlamydia pneumoniae infection of the central nervous system in multiple sclerosis. *Ann Neurol,* 46**,** 6-14.

SUMAYA, C. V., MYERS, L. W., ELLISON, G. W. & ENCH, Y. 1985. Increased prevalence and titer of Epstein-Barr virus antibodies in patients with multiple sclerosis. *Ann Neurol,* 17**,** 371-7.

SUNDSTROM, P., JUTO, P., WADELL, G., HALLMANS, G., SVENNINGSSON, A., NYSTROM, L., DILLNER, J. & FORSGREN, L. 2004. An altered immune response to Epstein-Barr virus in multiple sclerosis: a prospective study. *Neurology,* 62**,** 2277-82.

SWAIN, S. L., MCKINSTRY, K. K. & STRUTT, T. M. 2012. Expanding roles for CD4(+) T cells in immunity to viruses. *Nat Rev Immunol,* 12**,** 136-48.

T HART, B. A., HINTZEN, R. Q. & LAMAN, J. D. 2009. Multiple sclerosis - a response-to-damage model. *Trends Mol Med,* 15**,** 235-44.

TAYLOR, G. S., LONG, H. M., BROOKS, J. M., RICKINSON, A. B. & HISLOP, A. D. 2015. The immunology of Epstein-Barr virus-induced disease. *Annu Rev Immunol,* 33**,** 787-821.

TAYLOR, G. S., LONG, H. M., HAIGH, T. A., LARSEN, M., BROOKS, J. & RICKINSON, A. B. 2006. A role for intercellular antigen transfer in the recognition of EBV-

transformed B cell lines by EBV nuclear antigen-specific CD4+ T cells. *J Immunol,* 177**,** 3746-56.

TELLAM, J. T., LEKIEFFRE, L., ZHONG, J., LYNN, D. J. & KHANNA, R. 2012. Messenger RNA sequence rather than protein sequence determines the level of self-synthesis and antigen presentation of the EBV-encoded antigen, EBNA1. *PLoS Pathog,* 8**,** e1003112.

TERASAKI, P. I., PARK, M. S., OPELZ, G. & TING, A. 1976. Multiple sclerosis and high incidence of a B lymphocyte antigen. *Science,* 193**,** 1245-7.

THACKER, E. L., MIRZAEI, F. & ASCHERIO, A. 2006. Infectious mononucleosis and risk for multiple sclerosis: a meta-analysis. *Ann Neurol,* 59**,** 499-503.

THOMPSON, M. R., KAMINSKI, J. J., KURT-JONES, E. A. & FITZGERALD, K. A. 2011. Pattern recognition receptors and the innate immune response to viral infection. *Viruses,* 3**,** 920-40.

TRACY, S. I., KAKALACHEVA, K., LUNEMANN, J. D., LUZURIAGA, K., MIDDELDORP, J. & THORLEY-LAWSON, D. A. 2012. Persistence of Epstein-Barr virus in self-reactive memory B cells. *J Virol,* 86**,** 12330-40.

TSAI, J. C. & GILDEN, D. H. 2001. Chlamydia pneumoniae and multiple sclerosis: no significant association. *Trends Microbiol,* 9**,** 152-4.

TZARTOS, J. S., FRIESE, M. A., CRANER, M. J., PALACE, J., NEWCOMBE, J., ESIRI, M. M. & FUGGER, L. 2008. Interleukin-17 production in central nervous system-infiltrating T cells and glial cells is associated with active disease in multiple sclerosis. *Am J Pathol,* 172**,** 146-55.

TZARTOS, J. S., KHAN, G., VOSSENKAMPER, A., CRUZ-SADABA, M., LONARDI, S., SEFIA, E., MEAGER, A., ELIA, A., MIDDELDORP, J. M., CLEMENS, M., FARRELL, P. J., GIOVANNONI, G. & MEIER, U. C. 2012. Association of innate immune activation with latent Epstein-Barr virus in active MS lesions. *Neurology,* 78**,** 15-23.

VAN NIEROP, G. P., JANSSEN, M., MITTERREITER, J. G., VAN DE VIJVER, D. A., DE SWART, R. L., HAAGMANS, B. L., VERJANS, G. M. & HINTZEN, R. Q. 2016a. Intrathecal CD4(+) and CD8(+) T-cell responses to endogenously synthesized candidate disease-associated human autoantigens in multiple sclerosis patients. *Eur J Immunol,* 46**,** 347-53.

VAN NIEROP, G. P., MAUTNER, J., MITTERREITER, J. G., HINTZEN, R. Q. & VERJANS, G. M. 2016b. Intrathecal CD8 T-cells of multiple sclerosis patients recognize lytic Epstein-Barr virus proteins. *Mult Scler,* 22**,** 279-91.

VAN NOORT, J. M., BSIBSI, M., GERRITSEN, W. H., VAN DER VALK, P., BAJRAMOVIC, J. J., STEINMAN, L. & AMOR, S. 2010. Alphab-crystallin is a target for adaptive immune responses and a trigger of innate responses in preactive multiple sclerosis lesions. *J Neuropathol Exp Neurol,* 69**,** 694-703.

VAN NOORT, J. M., BSIBSI, M., NACKEN, P. J., VERBEEK, R. & VENNEKER, E. H. 2015. Therapeutic Intervention in Multiple Sclerosis with Alpha B-Crystallin: A Randomized Controlled Phase IIa Trial. *PLoS One,* 10**,** e0143366.

VAN NOORT, J. M., VAN SECHEL, A. C., BAJRAMOVIC, J. J., EL OUAGMIRI, M., POLMAN, C. H., LASSMANN, H. & RAVID, R. 1995. The small heat-shock protein alpha B-crystallin as candidate autoantigen in multiple sclerosis. *Nature,* 375**,** 798-801.

VAN SECHEL, A. C., BAJRAMOVIC, J. J., VAN STIPDONK, M. J., PERSOON-DEEN, C., GEUTSKENS, S. B. & VAN NOORT, J. M. 1999. EBV-induced expression and HLA-DR-restricted presentation by human B cells of alpha B-crystallin, a candidate autoantigen in multiple sclerosis. *J Immunol,* 162**,** 129-35.

VAN STIPDONK, M. J., LEMMENS, E. E. & SCHOENBERGER, S. P. 2001. Naive CTLs require a single brief period of antigenic stimulation for clonal expansion and differentiation. *Nat Immunol,* 2**,** 423-9.

VANHEUSDEN, M., STINISSEN, P., T HART, B. A. & HELLINGS, N. 2015. Cytomegalovirus: a culprit or protector in multiple sclerosis? *Trends Mol Med,* 21**,** 16-23.

VELDHOEN, M., HOCKING, R. J., ATKINS, C. J., LOCKSLEY, R. M. & STOCKINGER, B. 2006. TGFbeta in the context of an inflammatory cytokine milieu supports de novo differentiation of IL-17-producing T cells. *Immunity,* 24**,** 179-89.

VENKEN, K., HELLINGS, N., THEWISSEN, M., SOMERS, V., HENSEN, K., RUMMENS, J. L., MEDAER, R., HUPPERTS, R. & STINISSEN, P. 2008. Compromised CD4+ CD25(high) regulatory T-cell function in patients with relapsing-remitting multiple sclerosis is correlated with a reduced frequency of FOXP3-positive cells and reduced FOXP3 expression at the single-cell level. *Immunology,* 123**,** 79-89.

VERBEEK, R., VAN DER MARK, K., WAWROUSEK, E. F., PLOMP, A. C. & VAN NOORT, J. M. 2007. Tolerization of an established alphaB-crystallin-reactive T-cell response by intravenous antigen. *Immunology,* 121**,** 416-26.

VINUESA, C. G., TANGYE, S. G., MOSER, B. & MACKAY, C. R. 2005. Follicular B helper T cells in antibody responses and autoimmunity. *Nat Rev Immunol,* 5**,** 853-65.

VOGEL, D. Y., KOOIJ, G., HEIJNEN, P. D., BREUR, M., PEFEROEN, L. A., VAN DER VALK, P., DE VRIES, H. E., AMOR, S. & DIJKSTRA, C. D. 2015. GM-CSF promotes migration of human monocytes across the blood brain barrier. *Eur J Immunol,* 45**,** 1808-19.

VOLPE, E., BATTISTINI, L. & BORSELLINO, G. 2015. Advances in T Helper 17 Cell Biology: Pathogenic Role and Potential Therapy in Multiple Sclerosis. *Mediators Inflamm,* 2015**,** 475158.

VON BUDINGEN, H. C., BAR-OR, A. & ZAMVIL, S. S. 2011. B cells in multiple sclerosis: connecting the dots. *Curr Opin Immunol,* 23**,** 713-20.

VYSE, A. J., HESKETH, L. M. & PEBODY, R. G. 2009. The burden of infection with cytomegalovirus in England and Wales: how many women are infected in pregnancy? *Epidemiol Infect,* 137**,** 526-33.

WAGNER, H. J., MUNGER, K. L. & ASCHERIO, A. 2004. Plasma viral load of Epstein-Barr virus and risk of multiple sclerosis. *Eur J Neurol,* 11**,** 833-4.

WAGNER, M., SOBCZYNSKI, M., KARABON, L., BILINSKA, M., POKRYSZKO-DRAGAN, A., PAWLAK-ADAMSKA, E., CYRUL, M., KUSNIERCZYK, P. & JASEK, M. 2015. Polymorphisms in CD28, CTLA-4, CD80 and CD86 genes may influence the risk of multiple sclerosis and its age of onset. *J Neuroimmunol,* 288**,** 79-86.

WAISMAN, A., HAUPTMANN, J. & REGEN, T. 2015. The role of IL-17 in CNS diseases. *Acta Neuropathol,* 129**,** 625-37.

WALKER, K. M., OKITSU, S., PORTER, D. W., DUNCAN, C., AMACKER, M., PLUSCHKE, G., CAVANAGH, D. R., HILL, A. V. & TODRYK, S. M. 2015. Antibody and T-cell responses associated with experimental human malaria infection or vaccination show limited relationships. *Immunology,* 145**,** 71-81.

WALLIN, M. T., PAGE, W. F. & KURTZKE, J. F. 2004. Multiple sclerosis in US veterans of the Vietnam era and later military service: Race, sex, and geography. *Annals of Neurology,* 55**,** 65-71.

WANG, H. H., DAI, Y. Q., QIU, W., LU, Z. Q., PENG, F. H., WANG, Y. G., BAO, J., LI, Y. & HU, X. Q. 2011a. Interleukin-17-secreting T cells in neuromyelitis optica and multiple sclerosis during relapse. *J Clin Neurosci,* 18**,** 1313-7.

WANG, L. M., ZHANG, D. M., XU, Y. M. & SUN, S. L. 2011b. Interleukin 2 receptor alpha gene polymorphism and risk of multiple sclerosis: a meta-analysis. *J Int Med Res,* 39**,** 1625-35.

WANG, Z., SADOVNICK, A. D., TRABOULSEE, A. L., ROSS, J. P., BERNALES, C. Q., ENCARNACION, M., YEE, I. M., DE LEMOS, M., GREENWOOD, T., LEE, J. D., WRIGHT, G., ROSS, C. J., ZHANG, S., SONG, W. & VILARINO-GUELL, C. 2016. Nuclear Receptor NR1H3 in Familial Multiple Sclerosis. *Neuron,* 92**,** 555.

WESNES, K., RIISE, T., CASETTA, I., DRULOVIC, J., GRANIERI, E., HOLMOY, T., KAMPMAN, M. T., LANDTBLOM, A. M., LAUER, K., LOSSIUS, A., MAGALHAES, S., PEKMEZOVIC, T., BJORNEVIK, K., WOLFSON, C., PUGLIATTI, M. & MYHR, K. M. 2015. Body size and the risk of multiple sclerosis in Norway and Italy: the EnvIMS study. *Mult Scler,* 21**,** 388-95.

WHITELEGG, A. M., BIRTWISTLE, J., RICHTER, A., CAMPBELL, J. P., TURNER, J. E., AHMED, T. M., GILES, L. J., FELLOWS, M., PLANT, T., FERRARO, A. J., COBBOLD, M., DRAYSON, M. T. & MACLENNAN, C. A. 2012. Measurement of antibodies to pneumococcal, meningococcal and haemophilus polysaccharides, and tetanus and diphtheria toxoids using a 19-plexed assay. *J Immunol Methods,* 377**,** 37-46.

WIENDL, H. & GROSS, C. C. 2013. Modulation of IL-2Ralpha with daclizumab for treatment of multiple sclerosis. *Nat Rev Neurol,* 9**,** 394-404.

WILLER, C. J., DYMENT, D. A., RISCH, N. J., SADOVNICK, A. D., EBERS, G. C. & CANADIAN COLLABORATIVE STUDY, G. 2003. Twin concordance and sibling recurrence rates in multiple sclerosis. *Proc Natl Acad Sci U S A,* 100**,** 12877-82.

WILLING, A., LEACH, O. A., UFER, F., ATTFIELD, K. E., STEINBACH, K., KURSAWE, N., PIEDAVENT, M. & FRIESE, M. A. 2014. CD8(+) MAIT cells infiltrate into the CNS and alterations in their blood frequencies correlate with IL-18 serum levels in multiple sclerosis. *Eur J Immunol,* 44**,** 3119-28.

WING, A. C., HYGINO, J., FERREIRA, T. B., KASAHARA, T. M., BARROS, P. O., SACRAMENTO, P. M., ANDRADE, R. M., CAMARGO, S., RUEDA, F., ALVES-LEON, S. V., VASCONCELOS, C. C., ALVARENGA, R. & BENTO, C. A. 2016. Interleukin-17- and interleukin-22-secreting myelin-specific CD4(+) T cells resistant to corticoids are related with active brain lesions in multiple sclerosis patients. *Immunology,* 147**,** 212-20.

WUNSCH, M., HOHMANN, C., MILLES, B., ROSTERMUND, C., LEHMANN, P. V., SCHROETER, M., BAYAS, A., ULZHEIMER, J., MAURER, M., ERGUN, S. & KUERTEN, S. 2016. The Correlation between the Virus- and Brain Antigen-Specific B Cell Response in the Blood of Patients with Multiple Sclerosis. *Viruses,* 8**,** 105.

YAO, Q. Y., TIERNEY, R. J., CROOM-CARTER, D., DUKERS, D., COOPER, G. M., ELLIS, C. J., ROWE, M. & RICKINSON, A. B. 1996. Frequency of multiple Epstein-Barr virus infections in T-cell-immunocompromised individuals. *J Virol,* 70**,** 4884-94.

YATES, J. L., WARREN, N. & SUGDEN, B. 1985. Stable replication of plasmids derived from Epstein-Barr virus in various mammalian cells. *Nature,* 313**,** 812-5.

YEA, C., TELLIER, R., CHONG, P., WESTMACOTT, G., MARRIE, R. A., BAR-OR, A., BANWELL, B. & CANADIAN PEDIATRIC DEMYELINATING DISEASE, N. 2013. Epstein-Barr virus in oral shedding of children with multiple sclerosis. *Neurology,* 81**,** 1392-9.

YEO, T. W., DE JAGER, P. L., GREGORY, S. G., BARCELLOS, L. F., WALTON, A., GORIS, A., FENOGLIO, C., BAN, M., TAYLOR, C. J., GOODMAN, R. S., WALSH, E., WOLFISH, C. S., HORTON, R., TRAHERNE, J., BECK, S., TROWSDALE, J., CAILLIER, S. J., IVINSON, A. J., GREEN, T., POBYWAJLO, S., LANDER, E. S.,

PERICAK-VANCE, M. A., HAINES, J. L., DALY, M. J., OKSENBERG, J. R., HAUSER, S. L., COMPSTON, A., HAFLER, D. A., RIOUX, J. D. & SAWCER, S. 2007. A second major histocompatibility complex susceptibility locus for multiple sclerosis. *Ann Neurol,* 61**,** 228-36.

ZIVADINOV, R., ZORZON, M., WEINSTOCK-GUTTMAN, B., SERAFIN, M., BOSCO, A., BRATINA, A., MAGGIORE, C., GROP, A., TOMMASI, M. A., SRINIVASARAGHAVAN, B. & RAMANATHAN, M. 2009. Epstein-Barr virus is associated with grey matter atrophy in multiple sclerosis. *J Neurol Neurosurg Psychiatry,* 80**,** 620-5.

ZOGHI, S., AMIRGHOFRAN, Z., NIKSERESHT, A., ASHJAZADEH, N., KAMALI-SARVESTANI, E. & REZAEI, N. 2011. Cytokine secretion pattern in treatment of lymphocytes of multiple sclerosis patients with fumaric acid esters. *Immunol Invest,* 40**,** 581-96.

ZOU, J., HANNIER, S., CAIRNS, L. S., BARKER, R. N., REES, A. J., TURNER, A. N. & PHELPS, R. G. 2008. Healthy individuals have Goodpasture autoantigen-reactive T cells. *J Am Soc Nephrol,* 19**,** 396-404.

ZUMER, K., SAKSELA, K. & PETERLIN, B. M. 2013. The mechanism of tissue-restricted antigen gene expression by AIRE. *J Immunol,* 190**,** 2479-82.